DNA Repair and Response to Therapy: Exploring their Relation in Epithelial Ovarian Cancer Models

Thesis

DNA REPAIR AND RESPONSE TO THERAPY: EXPLORING THEIR RELATION IN EPITHELIAL OVARIAN CANCER MODELS

Thesis submitted for the degree of Doctor of Philosophy

The Open University, UK

Discipline of Life and Biomolecular Sciences

by

Federica Guffanti

Master Degree in Biology Applied to Biomedical Research

Istituto di Ricerche Farmacologiche Mario Negri IRCCS, Milan, Italy

October 2020

DNA REPAIR AND

RESPONSE TO THERAPY: EXPLORING THEIR RELATION

IN EPITHELIAL OVARIAN CANCER MODELS

Thesis submitted for the degree of Doctor of Philosophy

The Open University, UK

Discipline of Life and Biomolecular Sciences

by Federica Guffanti

Istituto di Ricerche Farmacologiche Mario Negri IRCCS, Milan, Italy

October 2020

ABSTRACT

Epithelial ovarian cancer (EOC) is often characterized by defects in DNA repair pathways, which partially explain its sensitivity to platinum compounds and to poly (ADP-ribose) polymerase inhibitors (*PARPi*). However, EOC almost invariably relapses with a drug resistant, incurable disease. Biomarkers able to predict the response to therapy could ameliorate the management of EOC patients.

The studies herein reported aimed to elucidate the role of different DNA repair pathways as possible determinants of cisplatin (DDP) and olaparib (a *PARPi*) response in a collection of patient-derived xenografts (PDXs) characterized for their response to both drugs. We analysed the expression of 35 different DNA repair genes involved in DDP and olaparib response, and found *CDK12, XPF, PALB2, USP28, ARTEMIS, ARID1A* and *MDR1* associated with DDP response. In particular, *CDK12* expression was significantly higher in

DDP resistant PDXs and associated with higher recurrence rate in EOC patients with low residual tumour. We analysed the basal level of RAD51 foci in proliferating cells of formalin-fixed paraffin-embedded PDX tumours, as possible readout of homologous recombination pathway, and found that the percentage of RAD51 foci-positive cells predicted olaparib, but not DDP response.

As DDP adducts can be repaired by multiple pathways including nucleotide excision repair (NER) and base excision repair (BER), we studied POLB, ERCC1, XPF and ERCC1/XPF complex as read out of NER and BER activity, but no correlation with DDP response was found.

These findings support the role of CDK12 and RAD51 foci expressed in untreated tumours in the response to DDP and olaparib, respectively, in our EOC PDX models and warrant the setup of DNA repair functional assays able to capture the complexity of factors determining DDP and PARPi response, that could be easily translated in the clinical practice to prioritize treatment choice in EOC patients.

"Considerate la vostra semenza:

fatti non foste a viver come bruti

ma per seguir virtute e canoscenza"

"Consider well the seed that gave you birth:

you were not made to live as brutes,

but to follow virtue and knowledge"

Dante Alighieri, Hell, poem XXVI

AKNOWLEDGEMENTS

I have a long list of marvellous persons to thank, who helped and supported me along these latest four years.

My sincere gratitude to the Istituto di Ricerche Farmacologiche Mario Negri IRCCS that gave me the opportunity to obtain the PhD.

The first thank to my internal supervisor Giovanna Damia, and Massimo Broggini, Head of the Molecular Pharmacology Laboratory at the Mario Negri Institute, my first mentors, that every day along these years, gave me the passion for this incredible job.

I would like to thank my external supervisors, Prof Simon Langdon and Dr Helen Coley, for their guidance, professionalism and competence demonstrated through these years.

A special thanks to all my colleagues, especially Elisa, Francesca, Roberta and Sara, for their friendship, the support received in any moments, and their incredible capacity to make easier any difficulties, I wish all of them the brilliant future that they deserve.

To my family, all my gratitude for having supported me in any moment and decision.

To Vincenzo, the love of my life.

To my grandfather Renato, who is looking at me above in the sky, to him it is dedicated this thesis.

PREFACE

The work described herein was performed at the Istituto di Ricerche Farmacologiche Mario Negri IRCCS in Milan, Italy from 2016 to 2020.

This work was performed under the supervision of Dr Giovanna Damia (director of studies), and Dr Helen Coley and Dr Simon Langdon (external supervisors).

DECLARATION

This thesis has not been submitted in whole or in part for a degree or diploma or other qualifications to any other university.

The experimental work described herein was performed by myself, Federica Guffanti. Collaborations to perform specific parts of the project (xenobank characterization, histopathological analyses, statistical analyses and genomic studies) are clearly indicated in the “Materials and Methods” and “Results” chapters.

TABLE OF CONTENTS

LIST OF FIGURES AND TABLES

1. INTRODUCTION

1.1 OVARIAN CANCER

Ovarian cancer, also named the “silent killer”, is the most lethal gynaecological malignancy in the Western countries and the fifth most lethal cancer worldwide among women (Bray et al., 2018). The adjective “silent” is due to the absence of specific symptoms in its early phases of development leading to late diagnosis and a dismal prognosis. Depending on the cells of origin, ovarian cancers can be classified into ovarian carcinomas, deriving from epithelial cells, sex cord-stromal tumours, originating from the hormone-producing cells in the cortex of the ovary, or germ cell tumours, deriving from the granulosa cells localized inside the ovarian follicles.

Epithelial ovarian carcinoma (EOC) is the most common type, accounting for 90% of tumours (Cho and Shih, 2009). It is clinically and pathologically distinct from the non-epithelial ovarian cancers and will be the subject of this thesis. EOC is a broad term gathering heterogeneous types of cancers, sharing the same anatomical position (all disseminate to the ovaries and related pelvic organs), but few molecular features. In fact, they have different origins, mutational profiles and sensitivity to pharmacological therapies. Based on histopathology and genomic analyses and on the cells of origin (all these aspects will be discussed in the following chapters), the four most relevant and currently identified EOC sub-types are serous carcinoma (divided into high grade serous (HGSOC, ~70% of total EOC) and low grade serous (LGSOC, ~3%) carcinomas), endometrioid carcinoma (divided into high grade endometrioid (HGEOC, ~3%) and low grade endometrioid (LGEOC, ~10%) carcinomas), mucinous carcinoma (MC, ~3%) and clear cell carcinoma (CCC, ~10%) (Duska and Kohn, 2017) (**figure 1.1**).

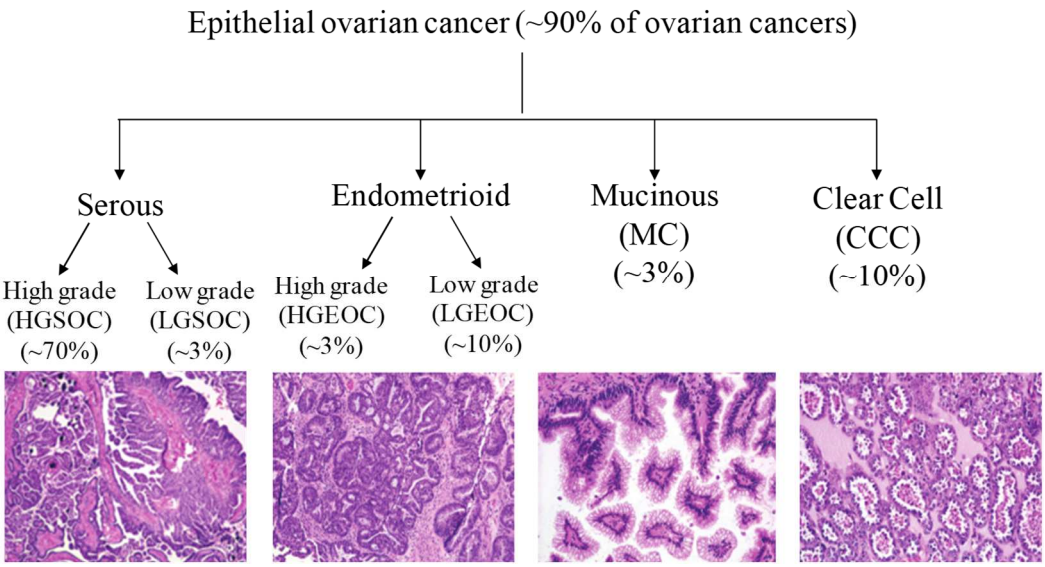

Figure 1.1 The most diffuse histological subtypes of epithelial ovarian cancer

In this schematic figure are reported the incidence rate (in percentage) and histological representative images for each of the most diffuse subtypes of epithelial ovarian cancer (adapted from (Karst and Drapkin, 2010)).

1.1.1 Incidence and mortality rates in epithelial ovarian cancer

Globally, 295,414 new cases of ovarian carcinoma were diagnosed in 2018, while 184,799 women died from this disease in the same year (Bray et al., 2018; Gaona-Luviano et al., 2020). Based on these statistics, ovarian carcinoma is the seventh most common cancer diagnosed among women (3.4% of oncology diagnosis) and the fifth cause of death from cancer in women in the world (4.4% of the entire cancer-related mortality) (Bray et al., 2018). Reported incidence and mortality rates slightly differ depending on geographical areas and ethnic origins (Momenimovahed et al., 2019). African and Asiatic populations register a mild lower incidence, in part due to the variability of cancer registration that could lead to an underestimation of the incidence rate, while the mortality rate in African women is higher than in women in Europe and in Asia, who tend to have the better survival (La Vecchia, 2017). Worldwide differences in mortality rates can be attributed to disparities in the access of sanitary care and treatments, and in part due to a different incidence of the

ovarian carcinoma histotypes across ethnic groups (i.e. clear cell carcinoma is more diffuse in Asia

than in Europe and USA, where more aggressive histotypes, such as high grade serous and endometrioid cancers are more frequent) (Jemal et al., 2017). Considering incidence and mortality trends of ovarian carcinoma in Italy, as an example of a Western country, the Italian Association of Oncology Medicine (AIOM) estimated a slow decreasing in incidence for the period 2003-2018 (-0.9%), while the mortality rate was stable (-0.1%) (**figure 1.2**) (Cancer Genome Atlas Research Network, 2011; "https://www.aiom.it/wp-content/uploads/2018/10/2018_NumeriCancro-operatori.pdf," n.d.). It has been reported that the incidence rate would decrease in parallel with the increasing use of contraceptive pill, which seems to reduce the risk of ovarian carcinoma (Collaborative Group on Epidemiological Studies of Ovarian Cancer et al., 2008), while the lack of new effective therapies may be one explanation for the un-improved mortality rate.

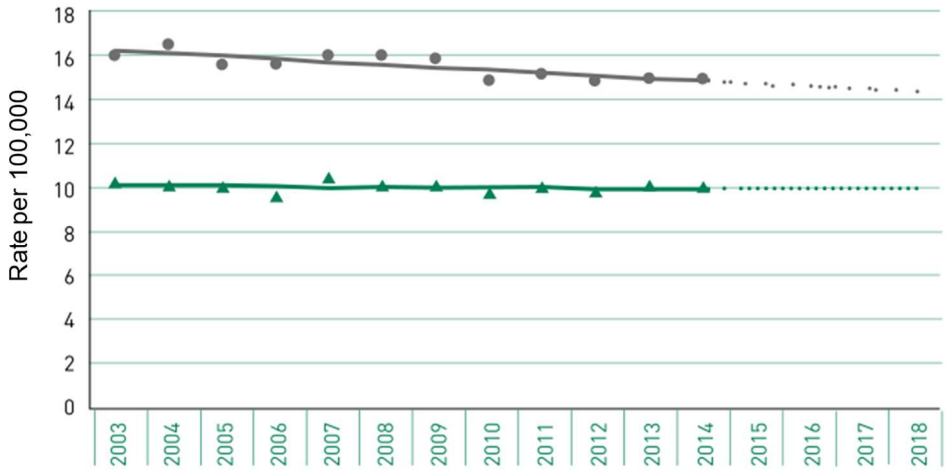

Figure 1.2 EOC incidence (grey curve) and mortality (green curve) estimated trends (period 2003-2018)

Rates are normalized for the European population in 2013.

At the time of diagnosis, almost 75% of patients show distant/metastatic disease and this is associated with a 5-year survival rate of 29% (Reid et al., 2017). On the contrary, when diagnosed as local disease, ovarian carcinoma patients have a 5-year survival rate of 92%

(Reid et al., 2017). These statistics highlight the lack of pre-symptomatic diagnostic tools and effective early detection strategies, that should have an important role in a much earlier diagnosis. Furthermore, a better understanding of the biology of EOC is warranted to find new biomarkers and new therapeutic strategies.

1.1.2 Risk and preventive factors for epithelial ovarian cancer

The estimated lifetime risk of developing ovarian carcinoma is 1 in 80 women ("https://www.aiom.it/wp-content/uploads/2019/09/2019_Numeri_Cancro-operatori-web.pdf," n.d.; Torre et al., 2018). EOC may affect all women, but especially those who have already had their menopause; in fact, the incidence rate rises after 40-years of age, the peak of diagnosis is in women aged 55 to 64 and the curve drops slowly over 80-years old, suggesting an age-related risk (Doubeni et al., 2016).

Epidemiological research has identified several hormonal factors implicated in the pathogenesis of EOC. The "incessant ovulation hypothesis" proposes that after the ovulation process, the rupture of the ovarian surface epithelium undergoes rounds of repair and cellular proliferation processes that might facilitate the onset of spontaneous mutations (Fathalla, 1971). Consequently, situations that increase the number of lifetime ovulations (i.e. nulliparity, post-menopausal hormone therapies for more than 5 years, early age at menarche or late age at menopause) favor the risk of developing cancer. On the contrary, oral-contraceptive pill use for at least 10 years, has a significant protective effect on the risk of ovarian carcinoma, as well as multiparity, fallopian tubal ligation, late age at menarche and early age at menopause (Mallen et al., 2018). Some environmental and life-style risk factors have been reported, but the risk correlated with EOC is less evident and still controversial. The most discussed factors are obesity, high body mass index, smoking and the prolonged use of genital talcum powder (Cannistra, 2004; Penninkilampi and Eslick, 2018). Endometriosis, polycystic ovary syndrome and pelvic inflammatory disease are benign gynecological conditions may degenerate in the development of ovarian tumours. In

particular, during endometriosis, which is a chronic-inflammatory condition, the retrograde menstrual flux causes the deposition of endometrioid cells in other areas, like the ovaries and pelvic peritoneum, that may evolve to malignant lesions (especially endometrioid and clear cell ovarian carcinomas (Reid et al., 2017).

Even if sporadic tumours are the majority of cases, genomic predisposition and familiar history are the strongest risk factors associated with EOC, especially for the high grade serous/endometrioid ovarian carcinoma (HGOC) histotype, the most aggressive and diffuse ovarian cancer subtype. It was observed that 15% to 20% of patients with HGOC have germline mutations in the breast cancer-associated genes (*BRCA1* or *BRCA2*) (Jones et al., 2017). *BRCA1* and *BRCA2*-mutated genes are high-penetrant susceptibility genes that encode for tumour suppressor proteins and their mutational status is actually used as a biomarker to detect women with high-risk to develop EOC and breast cancer. *BRCA1* or *BRCA2* mutation carriers have an overall risk of developing EOC by the age of 70 of 39% and 11% respectively, while the cumulative risk for breast cancer is 65% for *BRCA1* mutation carriers and 45% for *BRCA2*, depending on the type and location of the mutations along the gene sequence (Antoniou et al., 2003). Several studies focusing on hereditary gynaecologic tumours and *BRCA1/2* mutation carriers have led to the identification of the Hereditary Breast and Ovarian Cancer (HBOC) syndrome. It is an autosomal dominantly inherited disease characterized by a three-fold lifetime risk of developing breast and/or ovarian carcinomas before 40-years of age. *BRCA1* and *BRCA2* have a causative role in ~70% of hereditary EOC and other intermediate-risk susceptibility genes have been identified. These include Fanconi anemia (FA) pathway (*FANCD2, FANCC, FANCA, FANCM*), *RAD51C, RAD51D, BRIP1, ATM* and *ATR*, all involved in the DNA repair cluster. Also mutated DNA mismatch repair (MMR) genes (*MLH1, MSH2, MSH6, PMS2*) are associated with the autosomal dominant hereditary syndrome, Lynch syndrome, which accounts for 10-15% of inherited EOC, typically endometrioid and clear cell ovarian

carcinomas (Kobayashi et al., 2013; Mallen et al., 2018). The identification of women with high risk of developing EOC may help to prevent or delay the cancer onset through different strategies. Patients should be supported by personalized programs of medical screening and genetic counseling, according to their cancer risk type. The use of the oral-contraceptive pill should be supported when pregnancy is not demanded, since it reduces the risk of ovarian cancer also in *BRCA1/2* mutation carriers. Prophylactic surgery is the most preventive treatment option. Prophylactic bilateral salpingo-oophorectomy (BSO) (surgical removal of fallopian tubes and ovaries) lowers the ovarian cancer risk by 80% and, if performed before age of 50, exhibits a 50% reduction in subsequent breast cancer risk, leading to reduction of mortality-risk related to cancer. On the other hand, BSO causes an anticipated menopause and consequently exposes women to higher risk for osteoporosis and cardiovascular diseases. These side effects should be taken into consideration to decide when BSO is suggested (Chang and Bristow, 2012; Clarke-Pearson, 2009; Collaborative Group on Epidemiological Studies of Ovarian Cancer et al., 2008). For these reasons, clinical trials are evaluating if a two-step prophylactic surgery could delay the onset of anticipated menopause. The two-step strategy consists of bilateral salpingectomy followed by oopherectomy after some years, based on more recent pathogenesis studies that point to the fallopian tubes as the primary site of origin for HGOC (Pérez-López and Chedraui, 2016). A personalized and routine screening program in *BRCA1/2* mutated patients might help to postpone the BSO as much as possible, and at the same time, lead to an early detection of ovarian malignancy. For sporadic EOC, the knowledge of risk and preventive factors, especially those related to life-style habits and hormonal therapies, may help to lower the lifetime risk to develop EOC, even if at the moment there are no effective screening procedures.

1.1.3 Pathology of ovarian carcinoma

1.1.3.1 Anatomy of the ovaries and Fallopian tubes

The ovaries are the female gonads whose main functions are the production of gametes and the secretion of hormones estrogen and progesterone. Each ovary has an ovoid structure, sized 4 cm x 2 cm. They are located one on each side of the uterus, in the pelvic cavity and are linked to the uterus by peritoneal ligaments. The ovaries surface is covered by flat epithelial cells, which form a layer named the germinal epithelium or ovarian surface epithelium (OSE). Above the epithelium, a fibrotic connective tissue, named the cortex includes the follicular structures. Each follicle contains a single oocyte and cooperates for its development. The inner part of the ovary is the medulla, a dense connective tissue full of blood and lymphatic vessels and nerve fibers.

The fallopian tubes or uterine tubes are part of the reproductive tract together with the uterus, cervix and vagina. Each tube is directly associated with each ovary and, even if there is no direct contact between these two parts, the last part of the tube (infundibulum) expands through finger-like structures named fimbriae and surrounds the ovary. After the ovulation, the mature oocyte is released from the ovary in the pelvic cavity and enters into the Fallopian tube to get into the uterus, facilitated by cilia that cover the inner surface of the tubes and by peristaltic movements.

The anatomy of the female reproductive tract with the two ovaries is illustrated in **figure 1.3**.

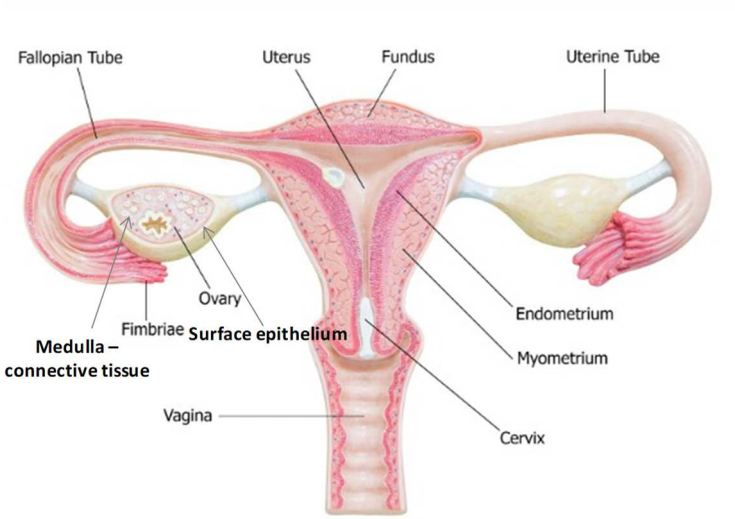

Figure 1.3 Anatomy of the female reproductive apparatus

Ovaries are connected to the uterus by ligaments and are surrounded by the terminal parts of Fallopian tubes, named fimbriae. These structures collect the mature oocytes after ovulation conducting it towards the uterus (modified from https://edition.cnn.com/2016/12/20/health/salpingectomy-ovarian-cancer-fallopian-tubes/index.html).

1.1.3.2 EOC: origin and pathogenesis

The development of effective early-screening strategies, new therapeutic options and in general, improvements in understanding the biology of ovarian carcinoma, have long been hampered by the lack of knowledge of the site of origin and carcinogenesis process of these tumours.

The ovarian surface epithelium (OSE) has been traditionally considered the site of origin of all EOC histotypes. OSE originates from the coelomic epithelium and is composed of cells morphologically similar to the mesothelium, lining the peritoneal cavity. The OSE was assumed to invaginate into the underlying stroma forming the so-termed cortical inclusion cysts (CICs). CICs are thought to acquire by metaplastic change a Müllerian phenotype, resembling the epithelia of fallopian tubes, endometrium, endocervical or gastrointestinal tract (Park et al., 2018). Ultimately, these epithelial cells may degenerate into a neoplastic formation giving rise to borderline malignancies that may evolve into high-grade and low-

grade carcinomas, according to the cellular phenotype acquired previously (**figure 1.4**) (Fleszar et al., 2018; Okamura and Katabuchi, 2005). This theory was supported by the "theory of incessant ovulation" suggested by Fathalla in 1971 (Fathalla, 1971) in which the OSE, exposed to repeated damage and repair processes during the ovulatory cycles, could undergo metaplastic transformation and form CICs. The Müllerian epithelium lining the CICs is exposed to hormones and inflammatory factors present in the ovarian stroma, which may facilitate the onset of deleterious mutations resulting in neoplastic transformation (Fathalla, 1971).

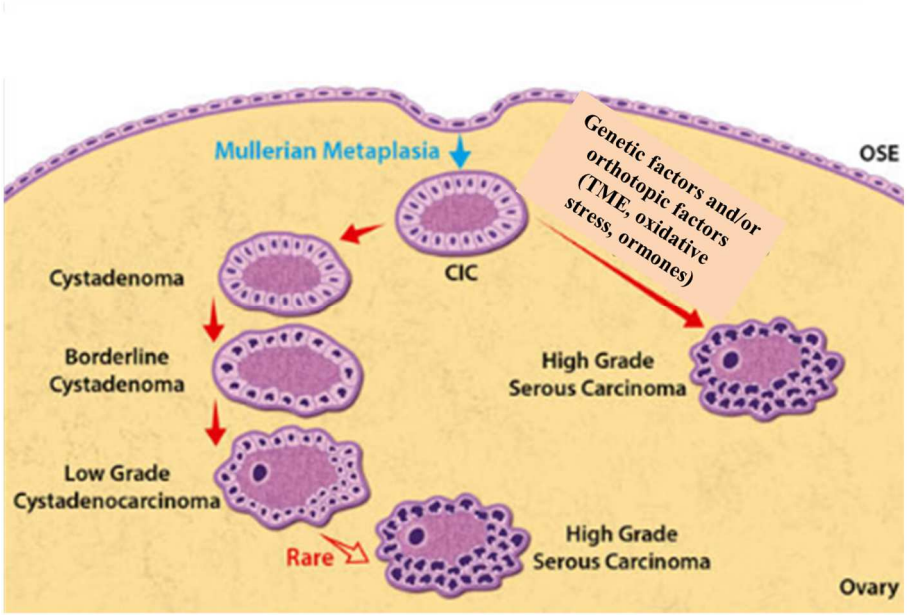

Figure 1.4 EOC origin: the theory of OSE

Epithelial cells forming the ovarian surface epithelium (OSE), may invaginate into the stroma of the ovary forming cortical inclusion cysts (CICs). CICs are lined by epithelial cells with a Müllerian phenotype acquired through a metaplastic process that resembles epithelia of fallopian tubes or that of other Müllerian tissues. Under hormonal or inflammatory factors present in the stroma, CICs could then undergo malignant transformation forming low grade and high grade EOCs, whose histology reflects the previously acquired phenotype (schematic illustration modified from (Aggarwal et al., 2016)).

Some limitations in the "theory of OSE" have been put forward, since none of the constitutive elements of EOCs, nor biomarkers, such as PAX8 or CA125 extensively

expressed in carcinomas, have ever been found in the normal ovaries. Moreover, EOC subtypes are more similar to other tumours of extra-ovarian tissues in the female gynaecologic apparatus. For example, serous, endometrioid and mucinous carcinomas histologically reflect fallopian tube, endometrium or endocervical tumours, respectively. Considering also the embryonic development, the doubts against the "theory of OSE" were reinforced since tissues and organs deriving from the Müllerian ducts (i.e. fallopian tubes and endometrium) are notably distinct and separate from those like ovaries, deriving from the mesothelial layer of the peritoneum, which lines all the pelvic and abdominal organs (Li et al., 2012; Prat, 2012). The Müllerian ducts, also named paramesonephric ducts, are paired ducts of the embryo parallel to the lateral side of the urogenital ridge. In the female they develop to form the fallopian tubes, uterus, cervix and the upper one-third of the vagina.

Although the model described for the "theory of OSE" could be sustained by features associated with the onset of some borderline, endometrioid, clear cell and mucinous ovarian tumours (Kroeger and Drapkin, 2017; Levanon et al., 2008), the third argument against the traditional theory of EOC pathogenesis is the fact that no precancerous lesions of EOCs have been found in a reproducible manner in normal ovaries. In fact, the transition from the CICs to high-grade EOC has never been reported and gene expression studies have revealed that the majority of EOCs (serous, endometrioid and mucinous) little resemble the genomic profile of the proposed cells of origin (the OSE) (Kurman and Shih, 2010).

With the aim to explain the origin of tumours not directly involving the OSE, a second theory was proposed in 1972, named "secondary Müllerian system theory" (Lauchlan, 1972). The secondary Müllerian system refers to those Müllerian-type epithelia like CICs, paraovarian and paratubal cysts, endometriosis, endosalpingiosis and endocervicosis, outside the primary Müllerian system (i.e. uterus, cervix and fallopian tubes). According to this theory, tumours with a Müllerian phenotype found in the pelvis probably derived from these secondary structures, either directly or by metaplastic transformation (**figure 1.5**). As the tumour enlarges, it comprises the ovary resulting in an adnexal ovarian tumour, that appears to

develop from the ovary itself. This theory provides a clear explanation for the presence of ovarian-like cancers arising outside the primary Müllerian system and could also explain why women who have already undergone prophylactic surgery, might develop peritoneal carcinomas later on (Aggarwal et al., 2016). However, this theory does not explain why the majority of mucinous tumours morphologically reflect the gastrointestinal tract rather than the endocervical epithelium and consequently they cannot be considered part of the Müllerian-type tumours (Kurman and Shih, 2010).

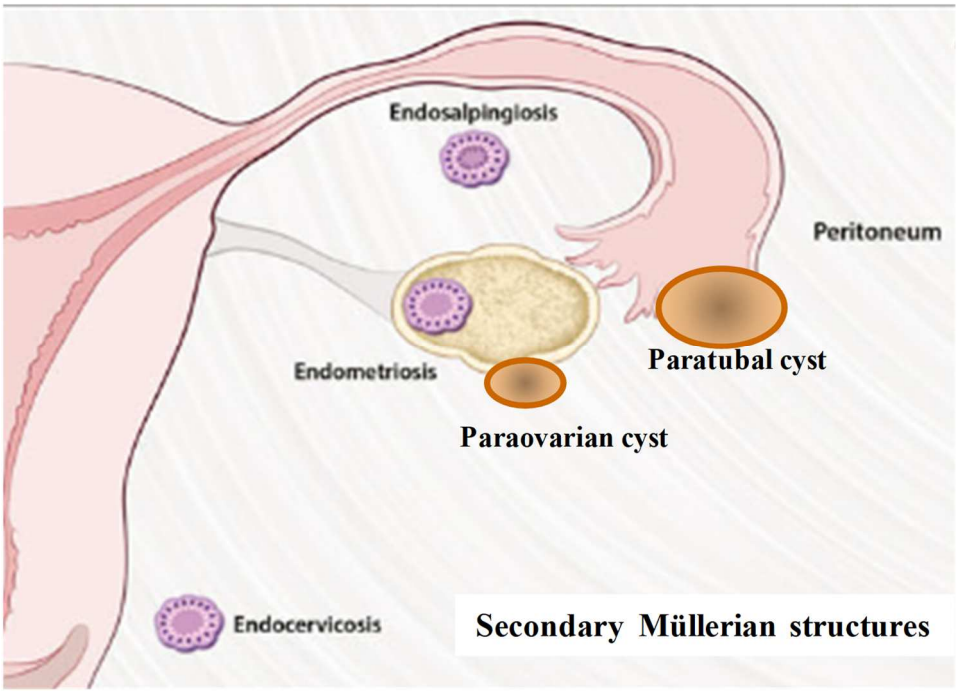

Figure 1.5 EOC origin: the theory of secondary Müllerian system

In addition to the primary Müllerian system (i.e. fallopian tubes, uterus and cervix) it is possible to observe in the pelvis secondary Müllerian epithelia, such as paratubal and paraovarian cysts, endometriosis, endosalpingiosis and endocervicosis formations that could directly or through metaplastic process give rise to tumours with a Müllerian phenotype like serous, endometrioid and clear cell carcinomas (adapted from (Aggarwal et al., 2016)).

The most relevant point against the "theory of OSE" and the "secondary Müllerian system theory" is that precancerous lesions have never been found in OSE, nor in the paratubal or paraovarian cysts.

In the late 1990s and early 2000s, prophylactic salpingo-oopherectomy was recommended for women with familiar history of ovarian cancer and/or germline mutations in *BRCA* or *BRCA2* genes and pathologists began to evaluate these specimens more carefully. They did not find any precancerous lesion in the ovary, but, interestingly, they found occult non-invasive or invasive neoplastic lesions in the fimbria of the fallopian tubes with a frequency ranging from 42% to 100% in patients BRCA-mutated diagnosed with HGSOC (Reade et al., 2014). In 1999, Dubeau firstly suggested that serous ovarian carcinoma might originate from the Müllerian system, including the fallopian tubes (Dubeau, 1999). He reported that the vast majority of epithelial ovarian cancer specimens histologically recapitulated the tubal epithelium, but not that of normal ovaries, where no precancerous lesions had ever been observed (Dubeau, 1999). Afterwards, in 2003, it was proposed that occult lesions localized in the tubal fimbriated ends might spread their benign or malignant epithelial cells to the ovary, then these cells could implant on the OSE and start to growth into the ovarian stroma as CICs (Kuhn et al., 2012). Corroborating this so-called "theory of imported disease", several studies identified and named these precancerous lesions as tubal intraepithelial cancers (TICs) and subsequently serous tubal intraepithelial cancers (STICs) since they were observed in specimens deriving from both women having a great familiar risk to develop HGSOC and from women affected by sporadic (non-hereditary) HGSOC (Morrison et al., 2015; Rabban et al., 2014). STICs were described as the precancerous lesions localized in the fallopian tubes able to give origin to HGSOC, the most diffuse and aggressive subtype. Even if STICs have not been associated with endometrioid carcinomas (EMCs), clear cell (CCCs) and mucinous cancers (MCs), this theory was adapted to explain the origin of EMCs and CCCs, where endometrial-type cells coming from endometriosis would be able to move

from the uterus through the fallopian tubes, to form endometriotic cysts, whose cells could shed and implant on the close ovary (**figure 1.6**) (Giudice, 2010; Piek et al., 2003). According to the "theory of imported disease" EOC does not originate from the ovary, but represents an "imported disease", distinct from the real primary ovarian cancer (i.e. the sex cord-stromal tumours and germ cell ovarian cancer).

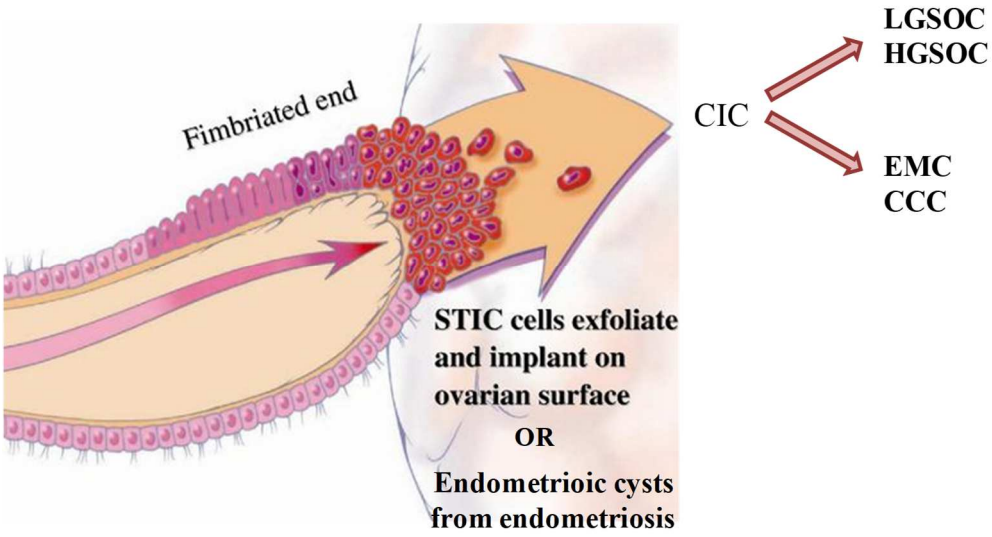

Figure 1.6 EOC origin: the theory of imported disease

The terminal part of fallopian tube (fimbria) is the site of origin of serous tubal intraepithelial carcinomas (STICs) and endometrioic cysts (in women affected by endometriosis). Cells from these lesions are hypothesized to spread to the ovary, implant on the OSE and then forming cortical inclusion cysts (CICs) from which may derive low grade or high grade serous ovarian carcinomas (LGSOC/HGSOC) from STICs or endometrioid or clear cell carcinomas (EMC/CCC) from endometrioic cysts (modified from (Kurman and Shih, 2011)).

In the ensuing years, different morphologic and molecular genetic studies elucidated that EOC is not a single disease, but is a heterogeneous group of different entities having peculiar clinic-pathologic features and biological behaviours. This concept led to a paradigm shift regarding the EOC carcinogenesis based on a new "dualistic model". It divides the ovarian surface epithelial tumours into two categories termed "type I" and "type II", first described in 2008 and then reviewed in 2016 by Kurman and Shih (Kurman and Shih, 2016, 2008).

The Type I group includes low grade serous, low grade endometrioid, clear cell and mucinous carcinomas, Müllerian-mixed tumours, also named sero-mucinous carcinomas (they comprise cystadenomas, atypical proliferative (borderline) tumours and carcinomas), and malignant Brenner tumours. They usually appear as a large, cystic malignant mass, confined in one ovary, and are typically diagnosed at an early stage and low grade, with the exception of CCCs which are considered high grade. The detection of low-grade tumours is generally accompanied with a favourable prognosis, but when type I tumours are diagnosed in an advanced stage, they have a poor outcome due to their poor sensitivity to the standard chemotherapy. The Type II group is largely composed of high grade serous and endometrioid carcinomas and in a minor part, of carcinosarcomas and undifferentiated carcinomas. They account for 90% of EOC-related deaths, because their early detection is still challenging as they are usually diagnosed at advanced stage, evolve rapidly and are highly aggressive. Type II tumours usually involve both the ovaries and extra-ovarian sites, like omentum and mesentery, and ascites formation is common. However, cytoreductive surgery and standard chemotherapy based on platinum agents combined with paclitaxel provide lengthened progression free survival because initially most patients respond. Unfortunately, 70% of cases will recur with drug resistant disease (Kurman and Shih, 2016, 2010, 2008; Vang et al., 2013).

One of the main features of the dualistic model was the relation of the different histologic subtypes to their precursor lesion. Type I tumours were found to develop from benign precursor lesions, notably atypical proliferative (borderline) tumours (APTs), characterized by specific mutations (the mutational profiles will be broadly discussed in the chapter 1.3.5 "*Molecular profile associated to different EOC histotypes*") able to induce morphologic changes evolving in a step-wise fashion manner from benign to invasive low-grade tumours. In contrast, type II was thought to develop mostly from STICs in fallopian tubes and subsequently disseminating to the ovaries, and a minor percentage was thought to evolve

probably *de novo* from CICs deriving from tubal epithelium cells implanted on the OSE, that undergo metaplastic malignant transformation (Vang et al., 2013). Now, the revised and expanded dualistic model considers the new histopathologic classification integrating it with the emerging molecular/genetic studies and better elucidates the morphologic and molecular features of the precursor lesions proper for each subtype (**figure 1.7**) (Kurman and Shih, 2016).

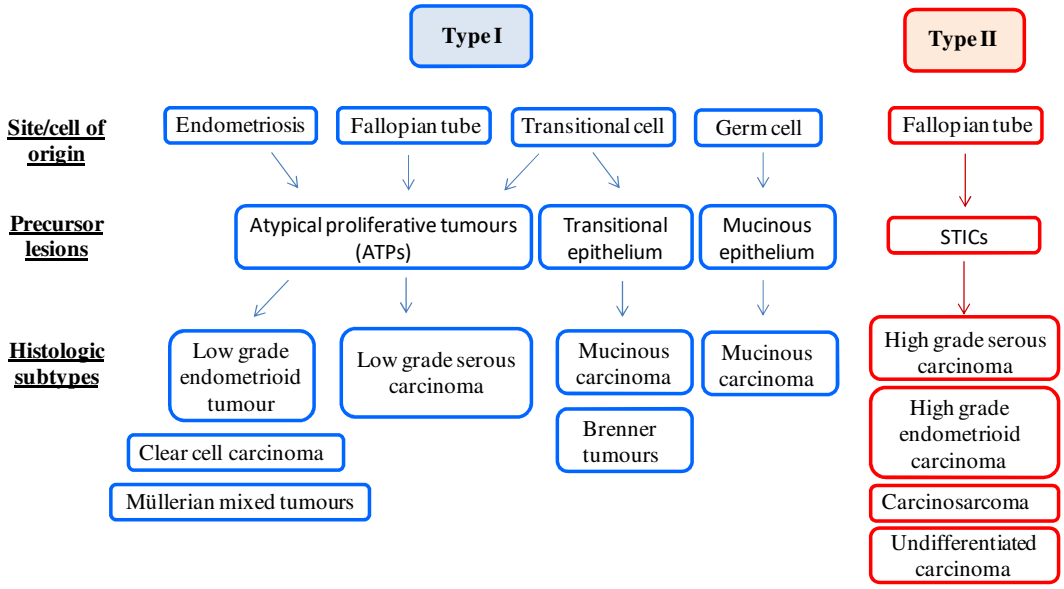

Figure 1.7 Dualistic model of EOC carcinogenesis

EOC include different histological subtypes that can be divided into type I and type II. Type I includes low grade serous (LGSOC), low grade endometrioid (LGEMC), mucinous (MC), clear cells carcinomas (CCC), Müllerian mixed and Brenner tumours. Their sites of origin as well as their precursor lesions, is different for each ovarian subtypes, ranging from endometriosis and fallopian tube epithelium for LGSOC, LGEMC, CCC and Müllerian mixed tumours, to transitional epithelium or germ cells for Brenner tumours and MC. Type II comprises high grade serous (HGSOC) and endometrioid (HGEMC), carcinosarcomas and undifferentiated tumours, all of which have a tubal origin and main of them derive directly from serous tubal intraepithelial cancers (STICs).

The site of origin of low grade serous tumour (LGSOC) is localized in the fallopian tubes, where its potential precursor lesion could be a hyperplastic formation named papillary tubal

hyperplasia, that evolves to APTs, often characterized by mutations affecting *KRAS*, *BRAF* and *ERBB2*, which constitutively activate the MAP-kinase pathway and drive neoplastic transformation. Endometrioid carcinoma (EMC), clear cell carcinoma (CCC) and Müllerian mixed carcinoma are defined endometriosis-related carcinomas, since they are derived from epithelial cells of endometrial origin, passed through the fallopian tubes and arrived at the ovary through endometriosis. This association, hypothesized for decades, has now been proven by genetic studies. Mutations in *ARID1A*, a tumour suppressor gene involved in switch/sucrose non-fermentable (SWI/SNF) chromatin remodelling, were detected in up to 50% of CCC, in 30% of EMC and in the epithelial cells forming the endometriomas, the APT that, as in LGSOCs, is often found adjacent to EMC and CCC, but not in the endometriotic cysts, which are located more distant from cancer. Somatic mutations in *PTEN*, another tumour suppressor gene, are observed in EMC and CCC and in endometriotic cysts, supporting these latter as possible precursor lesions for edometriosis-related carcinomas (Kurman and Shih, 2016) (**figure 1.8**). The origin of primary mucinous carcinomas (MC) is still unknown. MC typically displays foci of mucinous cystoadenoma, mixed with APTs and epithelial malignant cells. Mutational profiling of these sections revealed the same *KRAS* somatic mutations in all the three areas, supporting the idea of clonal evolution (Simons et al., 2020). Recently, it was hypothesized that MC might derive from either teratomas (cancers from germ cells) or Brenner tumours that give rise to different subtypes of MC. It was argued that Brenner tumours could derive from groups of epithelial cells, named Walthard cell nests, which can be found adjacent to the fallopian tubes and ovaries (tuboperitoneal junctions) and have been observed to undergo metaplasia processes. However, subsequent transformation pathways are similar regardless of the cell of origin and finally develop a gastrointestinal phenotype (Simons et al., 2020).

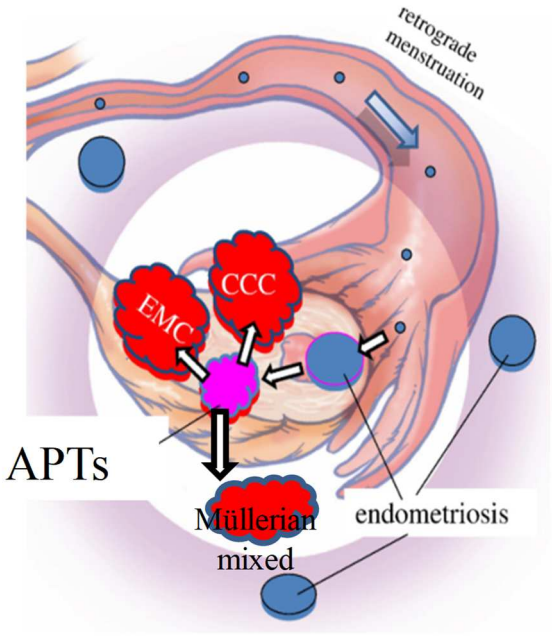

Figure 1.8 Model of endometriosis-related ovarian cancers formation

Endometriosis determines a retrograde menstrual flux from the uterus through fallopian tubes that leads the deposition on ovarian surface of endometrioid cells. These could form endometrioic cysts and atypical proliferative tumours, thought to be the precursor lesions for low grade EMC, CCC and Müllerian mixed tumours (adapted from (Kurman and Shih, 2011)).

Regarding HGSOC, the predominant histotype, many of these tumours may develop from STICs in the fimbriated ends of the fallopian tubes. STICs were found in *BRCA1/2* mutation carries, but also in 50% to 60% of women with sporadic HGSOC. Several data support their role as precursor lesions and now their clonal relationship has been reported. STICs are often found in the absence of carcinoma in women with higher familiar risk for EOC. When STIC and HGSOC are both present, they usually show the identical *TP53* mutation. In addition, STICs have shorter telomeres compared to the concomitant HGSOC, and this condition is one of the earliest events in carcinogenesis. In engineered mouse models, the inactivation of *TP53*, *PTEN* and *BRCA1/2* genes leads to the development of STICs and HGSOC (Karst and Drapkin, 2010). Because STIC is a carcinoma more or less confined to the fallopian tube

epithelium, it would be expected that the existence of a STIC's precursor lesion would be found there too. Serous tubal intraepithelial lesions in transition were found close to STICs and normal tube cells expressing higher levels of p53 (termed p53 signature) were reported, but their effective relation with STIC has yet clearly to be established. It is likely that the p53 signature cells undergo subsequent molecular events, such as loss of *BRCA* function, leading to malignant STICs. In a recent study (Wu et al., 2019), the genomic landscape of tubal precursor lesions including p53 signature, dormant or proliferative STICs, have been analysed in specimens from women without any cancer diagnosis using whole-exome sequencing and amplicon sequencing. The results showed that p53 signature and dormant STICs have less somatic mutations and allelic imbalance than tubal lesions associated with ovarian cancer, indicative of their earlier onset in tumour development process, and a low Ki-67 proliferative index (<10%), in line with the fact that it could take two or more decades to develop into STIC, whereas proliferative STIC could progress to carcinoma in a much shorter time (~6 years), suggesting an acceleration from this stage towards tumour formation (Wu et al., 2019). However, not all HGSOC are associated with STIC and directly to fallopian tubes. It has also been suggested that a small proportion of HGSOC may develop from LGSOC after the acquisition of additional mutations, such as p53 (Li et al., 2012) **(figure 1.9)**.

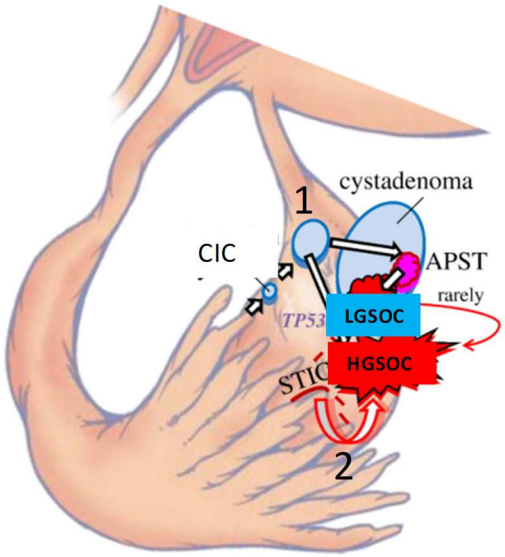

Figure 1.9 Model of low grade serous (LGSOC) and high grade serous (HGSOC) carcinoma formation

LGSOC and HGSOC can develop from cortical inclusion cysts (CICs) of tubal origin and cystadenomas (1) or from serous tubal intraepithelial cancers (STICs) implanting directly on ovarian surface and giving origin to HGSOC (2) (adapted from (Kurman and Shih, 2011)).

In aggregate, there is mounting evidence suggesting that HGSOC, LGSOC, EMC, MC and CCC should be considered different diseases, deriving from different sites of origin, with different molecular events during oncogenesis, and characterized by peculiar molecular profiles and patterns of spread.

1.1.3.3 Symptoms and diagnosis

EOC prodromic symptoms are shared by many common gynaecological and gastrointestinal conditions, such as irritable bowel syndrome, and include constipation, vague pelvic pressure, abdominal distension, early satiety, fatigue, nausea, change in bowel and urinary function, body weight loss and back pain (Lheureux et al., 2019b; Orr and Edwards, 2018a). They usually appear when the presence of the tumour mass produces abdominal distension,

pelvic pressure and when malignant nodules spread in the peritoneal cavity, affecting abdominal organs function. However, since the pain is minimal and symptoms are misleading, typically, EOC diagnosis is delayed by months from their onset (Goff et al., 2004). Symptom presentation and duration differ significantly by tumour histology. Women with serous tumours are significantly more likely to report bowel symptoms than women with other histological subtypes; women with endometrioid carcinoma are three times more likely to report abnormal bleeding, while MC are usually diagnosed as large primary tumours (>15cm in diameter) that cause symptoms when the disease is still confined to the ovary. Women with MC are likely to have a better prognosis since this subtype is easily detected in an early stage than women with HGSOC, whose symptoms have a short duration, but it is diagnosed at advanced stage (Morice et al., 2019).

Ovarian cancer, due its anatomic position, is characterized by pelvic dissemination, since small clusters of cells shed from fallopian tube epithelium and OSE into the intraperitoneal fluid, which transports cancer cells all over the abdomen, favouring a diffuse tumour peritoneal diffusion. In addition, tumour cells can move through lymphatic or blood vessels to form metastasis in distant organs, such as kidney, parenchyma of the liver or lungs (Bast et al., 2009).

Generally, when the diagnosis is suspected, the diagnostic pathway includes the measurement of cancer antigen 125 (CA125) blood concentration and transvaginal sonography (TVS). CA125 is a membrane-spanning mucin glycoprotein whose extracellular domain is cleaved, releasing CA125 in the extracellular environment and in blood, where it can be measured with an immunoassay. Increase of serum CA125 levels is strongly associated with ovarian cancer, being detected in 90% of patients with advanced stage (III-IV) and in 50%-60% with stage I disease (Elias et al., 2018). However, CA125 alone lacks sensitivity and specificity. Greater specificity can be achieved by the combination of CA125 and TVS. In the two-stage screening strategy, abnormal CA125 serum levels are followed

by pelvic ultrasound check and, if lesions are detected, by laparoscopy to assess the disease stage. Alternatively, CA125 assay and TVS can be performed concomitantly. The United Kingdom Collaborative Trial of Ovarian Cancer Screening (UKCTOCS) has been one of the latest clinical trials focused on the diagnostic value of the two-stage screening strategy (Jacobs et al., 2016). More than 200.000 postmenopausal women at average risk have been allocated in three groups: control (no screening), annual TVS, and the use of an ovarian cancer algorithm (ROCA) to interpret the impact of CA125 to prompt TVS. The primary end point was not reached (mortality reduction); however, subsequent analyses suggested a late survival advantage from the two-stage screening, but longer follow-up will be needed (Jacobs et al., 2016).

Effective screening tools are not yet available. In fact, owing to the relatively low incidence and prevalence of EOC, to achieve a good predictive value screening tests should have a very high specificity (>99%) and sensitivity (>75%), to be effective in detecting early curable stages, cost-effective and to improve the overall survival (Elias et al., 2018). Thus, early detection of EOC remains an unmet health need. The discovery and validation of novel biomarkers and cost-effective strategies should be explored in new randomized clinical trials, alone or in combination.

1.1.3.4 Classification and staging

When EOC has been diagnosed, histological classification and staging of the tumour are pivotal steps to provide the most appropriate clinical care and therapeutic strategy.

In 2014 the histologic and staging classifications of EOC has been reviewed and updated (Zeppernick and Meinhold-Heerlein, 2014). The World Health Organization (WHO) and the International Federation of Gynecology and Obstetrics (FIGO) revised their guidelines in light of the most recent scientific studies, that underscored the heterogeneous nature and biological behavior of ovarian carcinoma. The WHO Classification divides epithelial

ovarian tumours by cell type (serous, endometrioid, clear cell, mucinous and transitional tumours), by grade (I to IV), and by atypia (benign, borderline -atypical proliferation, low malignant potential- and malignant); malignant may be invasive or non-invasive) (Meinhold-Heerlein et al., 2016). In addition, high grade tumours with serous/endometrioid/transitional histology with p53 mutations are all considered high grade serous ovarian cancers (HGSOC), serous tumours are divided into low and high grade based on p53 lack (IHC assessment) or mutations, and the requirement for p53 testing for grade 2 tumours will appropriately re-classify a percentage of grade 2 tumours to high grade (Duska and Kohn, 2017).

The FIGO staging system is used to identify the spread of ovarian cancer (**table 1.1**). Stage I tumours are confined to the ovaries with different degrees of spread (IA, IB, IC) and no peritoneal involvement. Stage II defines tumours localized to one or both the ovaries and with some pelvic organ involvement. Stage II may include curable tumours as well as tumours that have seeded the pelvic peritoneum and, therefore, have a poor prognosis. Following recent advice, these tumours should undergo p53 immunostaining and if positive, they should be considered high grade (Duska and Kohn, 2017). The vast majority of HGSOC present at stage III with different degrees of spread (IIIA, IIIB, IIIC), and involve one or both the ovaries, with microscopic metastasis affecting pelvic and abdominal peritoneum surfaces and/or regional lymph node metastasis. Finally, tumours that involve distant metastasis beyond the peritoneal cavity, as liver/splenic parenchymal metastasis and extra-abdominal metastasis, are classified as stage IV (Mutch and Prat, 2014; Prat and FIGO Committee on Gynecologic Oncology, 2015). The presence of ascites is also an important factor in the FIGO classification. Ascites fluid in early-stage disease is a poor prognostic factor, with smaller tumour volume and absence of ascites in advanced disease are associated with a favourable outcome (Eitan et al., 2005).

Table 1.1 2014 FIGO ovarian cancer staging system

Stage I: Tumour is confined to the ovary.
IA: tumour confined to one ovary; capsule intact; no malignant cells in the ascites or peritoneal washing.
IB: tumour limited to both ovaries; capsule intact; no malignant cells in the ascites or peritoneal washing.
IC: tumour limited to one or both ovaries with any of the following: IC-1: surgical spill during intervention; IC-2: capsule ruptured before surgery or tumour on ovarian surface; IC-3: malignant cells present in the ascites or peritoneal washing.
Stage II: Tumour involves one or both ovaries with pelvic extension or primary peritoenal cancer.
IIA: extension and/or implants on the uterus/fallopian tubes/ovaries.
IIB: extension to other pelvic intraperitoneal tissues.
Stage III: Tumour spread to the peritoneum outside of the pelvis and/or metastasis to the retro-peritoneal lymph nodes.
IIIA-1: metastasis to retroperitoneal lymph nodes with or without microscopic peritoneal involvement beyond the pelvic.
IIIA-2: microscopic peritoneal involvement with or without nodes.
IIIB: macroscopic peritoneal <2 cm above the pelvic brim.
IIIC: macroscopic peritoneal >2 cm above the pelvic brim.
Stage IV: Distant metastasis excluding peritoneal metastases.
IVA: pleural effusion with malignant cells
IVB: metastases to extra-abdominal organs and lymph nodes outside abdomen and parenchymal metastases.

Adapted from (Mutch and Prat, 2014).

1.1.3.5 Molecular profile associated with different EOC histotypes

In the last decade, a deep knowledge of EOC-molecular characterization was obtained by advanced sequencing techniques. In particular, the identification of specific mutational profiles led to the division in two categories (type I and II) of ovarian carcinomas, and at the same time, revealed the heterogeneous nature of each single histotype.

Generally, type I tumours are relatively genetically stable, without *TP53* mutations (except for MC, where *TP53* mutations may occur as a late event (Palmirotta et al., 2017)). Type I tumours are often characterized by activating mutations of *KRAS*, *BRAF* and amplifications in *ERBB2*, all involved in the mitogen-activated protein kinase (MAPK) pathway, which regulates cellular proliferation, differentiation and survival mechanisms (Hunter et al., 2015; Jones et al., 2012). Somatic mutations of *KRAS* at codons 12 and 13 are the most common

(Dobrzycka et al., 2009) and lead to a constitutive activation of the GTPases, which phosphorylate its downstream targets and effectors (Burotto et al., 2014). The majority of *BRAF* mutations occur from a substitution of valine to glutamic acid at position 600 in the exome 15 (V600E) and seem to be mutually exclusive with *KRAS* mutations (Ilenkovan and Gourley, 2018; Romero et al., 2013). *KRAS* somatic mutations are the most frequent alterations in mucinous subtype (40% to 65% of MC (Morice et al., 2019)) and are found in >20% of LGSOC and EMC, while BRAFV600E is observed in less than 5% of type I EOC (Geyer et al., 2009; Romero et al., 2013). Amplification of *ERBB2* (gene encoding for HER2) has been revealed in 19% of MC and 14% of CCC (Anglesio et al., 2013). Other well-identified and diffused mutations include *PIK3CA*, *PTEN* and *ARID1A*. The *PIK3CA* gene encoding the catalytic subunit (p110α) of PI3K protein, is an oncogene whose phosphorylation activates AKT. The PI3K/AKT signaling pathway controls many cellular processes, such as cell proliferation, apoptosis and motility (Ediriweera et al., 2019). The region containing *PIK3CA* is amplified in 50% of ovarian carcinomas (Bader et al., 2005) but its mutations, mostly missense, are observed mainly in the small subset of EMC and CCC subtypes, in which their frequency is approximately of 20% (Levine et al., 2005; Wang et al., 2005). *PTEN* is an oncosuppressor gene and inactivating somatic mutations are uncommon in sporadic EOC. *PTEN* is inactivated by loss of heterozygosity (LOH), which means the loss of the second wild type allele containing the gene of interest when the first allele was already mutated, in only 3-8% of cancers largely EMC, CCC and LGSOC, while *PTEN* promoter hypermethylation causes loss of expression in >20% of CCC (Bast et al., 2009; Ilenkovan and Gourley, 2018). Another oncosuppressor gene is *ARID1A*, whose inactivating mutations (somatic truncating or missense mutations) are the most frequently observed in CCC subtype, accounting for 46% of cases and in 30% of EMC (Wiegand et al., 2010).

In 2011 The Cancer Genome Atlas (TCGA) Research Network employed whole exome sequencing and a variety of other high-throughput technologies to analyze 489 HGSOC

samples and catalog their exome sequences, DNA copy number, mRNA and microRNA expression, from which emerged the main HGSOC's molecular alterations (Cancer Genome Atlas Research Network, 2011). HGSOC, which is the predominant and most representative subtype for type II ovarian cancers, usually evolves rapidly and is characterized by aggressive biological behavior and genomic instability, which is clearly associated with the mutational profile. HGSOC shows a simple mutational profile: tumours harbor *TP53* mutations in almost all cases, making evident its role as an essential driver mutation in the pathogenesis of HGSOC (Ahmed et al., 2010; Cancer Genome Atlas Research Network, 2011; Cole et al., 2016). *TP53* mutations are usually missense and tend to cluster in the DNA binding domain region (exon 5 to 9), but also non- sense or frameshift mutations may be observed all over the coding region (Ahmed et al., 2010; Silwal-Pandit et al., 2014). Such mutations can cause both loss-of-function or gain-of-function effects on p53 protein (Silwal-Pandit et al., 2017).

Beside *TP53*, the TCGA study registered mutations in other genes albeit with a low prevalence, but which were statistically significant: *BRCA1, BRCA2, NF1, RB1, PTEN* and *CDK12*. In the TCGA cohort, *BRCA1* and *BRCA2* harbor germline mutations in 8% and 6% of samples respectively, and somatic mutations in an additional 3% of sporadic tumours, making them the second most mutated genes in HGSOC (Cancer Genome Atlas Research Network, 2011; Hennessy et al., 2010). *BRCA1* and *BRCA2* mutations are largely frameshift insertions or deletions in different genetic regions coding for the protein functional domains. In general, it has been assessed that 81% of *BRCA1* and 72% of *BRCA2* mutations are followed by LOH indicating a biallelic inactivation, while promoter hypermethylation constitutes an alternative mechanism also leading to loss of *BRCA1* expression (not *BRCA2*), observed in 10% to 20% of HGSOC (Cancer Genome Atlas Research Network, 2011; Ceccaldi et al., 2015). Of note, genetic or epigenetic silencing of *BRCA1* are mutually exclusive, both contributing to *BRCA* silencing (Konstantinopoulos et al., 2015). BRCA1 and BRCA2 proteins act in the homologous recombination (HR) pathway involved in the

DNA repair mechanism and later studies showed that more than a half of HGSOC presented HR deficiencies, a condition determined not only by *BRCA1/2* alterations, but also by mutations in FA genes (mainly *PALB2, FANCA, FANCI, FANCF, FANCD2* and *FANCC*), in core HR restriction site associated DNA (RAD) genes (*RAD50, RAD51* and *RAD51C*), and in DNA damage response genes involved in HR (*ATM, ATR, CHEK1*, and *CHEK2*) found mutated or silenced with a low prevalence in HGSOC (Ceccaldi et al., 2015; Mittempergher, 2016). Globally, all the alterations that affect HR genes or related genes induce a HR deficiency, a condition termed "*BRCAness"* phenotype, one of the hallmarks of HGSOC (Konstantinopoulos et al., 2015; Turner et al., 2004). However, other genes involved in different DNA repair pathways, such as nucleotide excision repair (NER) and MMR, can be found mutated in HGSOC, albeit with a low frequency (<10%) (Cancer Genome Atlas Research Network, 2011; Konstantinopoulos et al., 2015).

CDK12 has emerged as a possible new hit in ovarian cancer, where it has been found mutated in 3% of cases (Cancer Genome Atlas Research Network, 2011). CDK12 belongs to the cyclin-dependent kinases family, it is classified as an oncosuppressor and its role consists in the transcriptional regulation of several genes, included some involved in the HR, such as *ATM, ATR, CHK1, FANCI, MDC1* and *RAD51C* (Chilà et al., 2016). Cells expressing inactive CDK12 have been reported to contain functional defects in HR repair and display a tandem duplication phenotype (Vanderstichele et al., 2017).

High grade serous ovarian cancer is mostly characterized by chromosomal instability, in particular copy number alterations (CNA), gain or loss of DNA sequences. Heterozygous or homozygous loss are determinants for oncosuppressor inactivation. *PTEN* has been found deleted in 7% of HGSOC (Konstantinopoulos et al., 2015) with possible consequences on HR activity. Mendes-Pereira and colleagues proposed that *PTEN* deficiency could be linked to transcriptional downregulation of *RAD51* and therefore cause a HR defective (HRD) phenotype (Mendes-Pereira et al., 2009). Also, *RB1* and *NF1* are tumour suppressors located

in regions affected by homozygous deletions in at least 2% of HGSOC (Cancer Genome Atlas Research Network, 2011).

The most common amplified genes are *CCNE1, EMSY* and *MYC* in more than 20% of HGSOC (Cancer Genome Atlas Research Network, 2011). 14% of HGSOC shows an amplification of *CCNE1*, which is mutually exclusive with *BRCA1/2* loss (Cancer Genome Atlas Research Network, 2011). *CCNE1* overexpression promotes uncontrolled proliferation and increases genomic instability. Moreover, *CCNE1*-amplified tumours represent a well-studied group since they are associated with poor overall survival and primary treatment failure (Mittempergher, 2016). *EMSY* amplification is reported in 17% of HGSOCs and represents another mechanism of HR deficiency. This could be due to the interaction of EMSY with BRCA2, leading to inhibition of its transcriptional activity (Hughes-Davies et al., 2003). However, the exact role of *EMSY* alterations in HR deficiency is still controversial (Mittempergher, 2016).

Genomic instability in type II EOC reflects the global effect of *TP53* alterations and DNA-repair deficiency, which make the tumour more susceptible to DNA breaks and chromosomal rearrangements. Furthermore, aberrations that occur in type I tumours are not observed in type II and *vice versa*, and this may in part explain the deep differences between these groups, assessing even more the concept of EOC as a heterogeneous group of diseases. The mutational profile of each EOC histological subtype is summarized in **figure 1.10**.

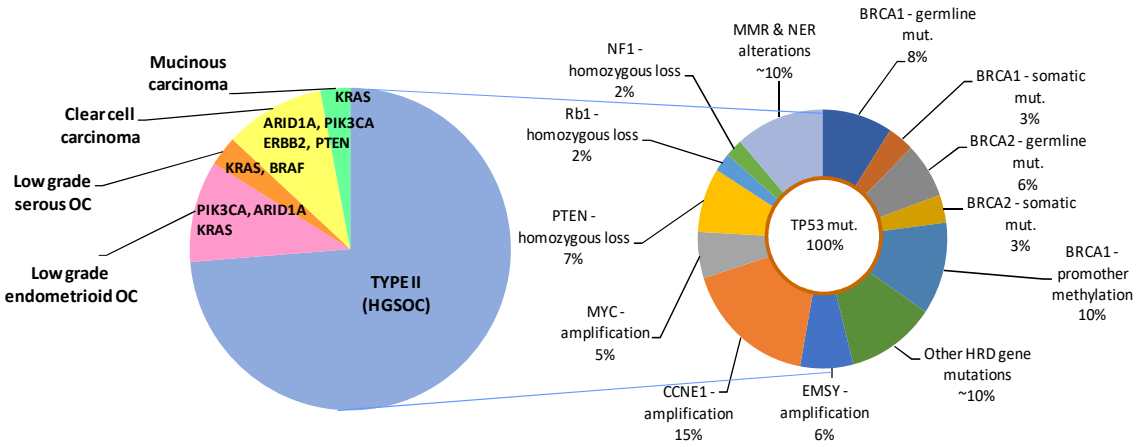

Figure 1.10 The most common genetic and epigenetic abnormalities occurring in the ovarian cancer subtypes

The graph on the left shows the main abnormalities occurring in the different type I tumour-subtypes. On the right side are highlighted the main alterations and their frequencies found in type II tumours (high grade serous and endometrioid carcinomas).

Other attempts to classify EOC took into consideration tumour gene expression profiles. Tothill *et al.* (Tothill et al., 2008), as well as Tan *et al.* (Tan et al., 2013) through microarray gene expression profiling identified distinct biological subtypes of ovarian carcinoma. In the first study 285 serous and endometrioid tumours of the ovary, fallopian tubes and peritoneum, low grade and high grade, were analysed and their expression profiles correlated with clinical outcomes. Six molecular signatures were identified and validated in an independent dataset; two mainly represented low grade serous and endometrioid tumours, respectively, while the other four subtypes included high grade serous and endometrioid tumours, confirming that high grade serous and endometrioid are molecularly similar. These subtypes were named: C1 (high stromal response), C2 (high immune signature), C4 (low stromal response) and C5 (mesenchymal, low immune signature). C1 showed a significant trend toward early relapse and short overall survival, and overexpression of stromal response biomarkers; C2 was particularly enriched in tumour infiltrating T-cells; C4, unlike C1, had higher

level of E-cadherin, an epithelial marker, and low stromal associated factors; C5 was firstly described, and particularly reflects epithelial to mesenchymal transition (EMT) tracts, such as low E-cadherin levels, activation of WNT/β catenin pathway and overexpression of vimentin and N-cadherin, markers of mesenchymal cells (Tothill et al., 2008). Subsequently, Tan *et al*. (Tan et al., 2013) using a cohort of 1538 EOC including all the histotypes, identified five molecular subtypes: Epithelia-A (Epi-A), Epithelia-B (Epi-B), Mesenchymal, Stem-like-A (Stem-A) and Stem-like-B (Stem-B), and correlated them with clinicopathological information. The aim of this study was to better explore the potential of gene expression profiles as predictive biomarker and to find specific vulnerabilities that could be exploited during treatment decision. For instance, the Stem-A subtype was associated with poor prognosis, but was sensitive to vincristine and vinorelbine, two microtubule polymerization inhibitor drugs, leading to the possibility of tailoring personalized treatment for ovarian cancer patients based on tumour genetic profile (Tan et al., 2013).

1.1.4 Management of EOC

1.1.4.1 Primary treatment

Primary treatment of newly diagnosed EOC has evolved over the last 50 years on an evidence-based approach and integrates surgical intervention with systemic chemotherapy (adjuvant and neoadjuvant, whether necessary), followed by an appropriate follow-up.

The main goal of surgical intervention besides establishing the FIGO stage, is to achieve complete resection, consisting in the removal of all visible macroscopic disease, with no residual tumour (R0). In fact, residual tumour after cytoreductive surgery is one of the most important determinants of long-term survival, with the amount of residual tumour being inversely proportional to patient survival (du Bois et al., 2009; Griffiths, 1975). Du Bois *et al.* reported that even if the preoperative tumour burden (as indicated by different FIGO stages) maintained an important prognostic role, complete surgical debulking significantly improved prognosis in any FIGO stage in HGSOC. In particular, the median survival in the group of complete debulking surgery was 99.1 months (95% CI, 83.5 to 100) compared to those of small residual tumour burden after surgery (1-10mm) group (36.2 months, 95% CI, 34.6 to 39.4) and macroscopic residual tumour burden (>1cm diameter) group (29.6 months, 95% CI, 27.4 to 32.2) (du Bois et al., 2009).

Surgery includes, whenever possible, complete hysterectomy, bilateral salpingo-oophorectomy, complete tumour debulking, omentectomy, diaphragm resection and bulky lymph node removal (Jayson et al., 2014). It is important to distinguish surgical approaches used in early stage and those for advanced disease. Once optimal staging laparoscopy assesses the presence of low-risk early EOC (FIGO stage IA-IB, non-clear cell carcinoma or borderline tumours, grade 1) and does not detect occult disease, fertility conservative surgery is indicated in young women, with the aim of preserving the remaining ovary and uterus (Komiyama et al., 2016; Trimbos, 2017). For early stage disease, there is no indication for adjuvant chemotherapy, since it does not improve overall survival (OS) or progression free

survival (PFS) (Trimbos, 2017). On the contrary, maximal debulking surgery is always recommended for advanced EOC, even if not always feasible. It has been estimated that in 30% to 60% of high-grade EOC, it is possible to obtain an optimal debulking surgery, with a residual tumour ≤ 1 cm in diameter, or suboptimal surgery (residual tumours >1 cm) (Orr and Edwards, 2018b). Interval debulking surgery (IDS) should be considered as a treatment option if primary surgery is not possible due to extensive disease, metastasis or poor patient condition (Komiyama et al., 2016). IDS has the same aim of complete resection and is generally performed after 3 or 6 cycles of neoadjuvant chemotherapy (NACT), and followed by additional adjuvant chemotherapy cycles (Lheureux et al., 2019a). EORTC 55971 and CHORUS randomized clinical trials have demonstrated a non-inferior prognosis for patients treated with NACT + IDS, respect those treated with primary debulking surgery followed by chemotherapy (Kehoe et al., 2015; Vergote et al., 2010) leading to increased use of NACT + IDS over the past decade in EOC patients.

Together with surgery, adjuvant chemotherapy has a central role in the treatment of advanced EOC (FIGO stages II-IV). The standard frontline therapy is a combination of platinum and taxane doublet, typically administered both intravenously, every 3 weeks, for 6 cycles of treatment, even if over the last decades, several variations have been explored (Marth et al., 2017). The introduction of cisplatin (DDP) in 1976 as front-line therapy significantly improved PFS in the first clinical trial (Wiltshaw and Kroner, 1976). In 1979 FDA approved the use of DDP for the treatment of EOC, but only in the late ‘80s, when anti-emetic drugs were introduced, DDP became the treatment of choice (Muggia, 2009). Clinical trials by the Gynaecologic Oncology Group (GOG) later explored DDP in combination with cyclophosphamide, which became the reference regimen for subsequent trials until the randomized trial GOG111, comparing DDP/paclitaxel regimen with the standard DDP/cyclophosphamide, showed a superior survival outcome in the new combination arm (McGuire et al., 1996). Afterwards, GOG158 trial reported less toxicity and the same efficacy using carboplatin than DDP, with paclitaxel (Ozols et al., 2003), defining

carboplatin/paclitaxel as the best tolerated doublet and that has been the standard regiment for first-line treatment in advanced EOC over the last 20 years.

During this period, several studies have tried to address some questions on different platinum/taxane schedule, dose density, mode of administration (intravenous and/or intraperitoneal), role of hyperthermia, and additional chemotherapeutic agents. GOG132 and ICON3 trials investigated the potential of platinum monotherapy, showing that platinum had the dominant effect on outcome, but subsequent treatment with paclitaxel upon recurrence, extended survival (International Collaborative Ovarian Neoplasm Group, 2002; Muggia et al., 2000). When paclitaxel was combined with a platinum compound, the combination extended PFS longer than monotherapy (Parmar et al., 2003). Platinum monotherapy has not been completely excluded, and is recommended for frail and elderly patients, who may not tolerate the combination regimen (Komiyama et al., 2016). Alternative schedules of administration of platinum and paclitaxel include the dose-dense carboplatin/paclitaxel regimen, based on the Norton-Simon hypothesis, in which shorter interval between doses of cytotoxic agents should be more effective in reducing tumour burden than dose escalation (Simon and Norton, 2006). Dose-dense therapy has been applied in EOC patients receiving paclitaxel (1h intravenous, at 80 mg/ml on days 1, 8, and 15) plus carboplatin (1h intravenous, at an AUC of 6 on day 1), every 3 weeks for 6 cycles (Lheureux et al., 2019a). The Japanese trial JGOG3016 revealed a significant improvement in survival outcomes in patients who received dose-dense regimen than the standard ones (Harano et al., 2014), but the ICON8 study, performed in a European population, did not confirm any PFS improvement and reported several cases of toxicity, which led to premature trial stop (Clamp et al., 2019). In the absence of confirmatory data, dose-dense administration of paclitaxel currently can be considered an option, but not a standard of care.

Intraperitoneal (IP) chemotherapy uses an intra-abdominal device to locally administer, usually platinum agents, directly into the abdominal cavity leading to a higher drug exposure in cancer cells than after intravenous injection. It has been found to significantly prolong

PFS and OS in three studies (GOG104, 114 and 172) (Alberts et al., 1996; Armstrong et al., 2006; Markman et al., 2001): however, the regimen was poorly tolerated, due to toxicity related to chemotherapy itself, infections and abdominal discomfort, as only 42% of patients were able to finish all 6 cycles. For these reasons, IP chemotherapy has not been adopted as a standard of care in the majority of countries.

A second complementary therapeutic strategy is Hyperthermic Intraperitoneal Chemotherapy (HIPEC), already applied with efficacy in other peritoneal diseases, such as peritoneal carcinomatosis from colon and gastric cancer (Esquivel, 2016). HIPEC is done at the completion of cytoreductive surgery. No clear-cut efficacy data exist for HIPEC in EOC; HIPEC was used in different regimens and in heterogeneous patients, with discordant results in terms of survival improvement (Chiva and Gonzalez-Martin, 2015; van Driel et al., 2018).

The role of other cytotoxic drugs in combination with DDP and/or the doublet DDP/paclitaxel has been investigated. Pegylated liposomal formulation of doxorubicin (PLD) is a new formulation of doxorubicin characterized by a better toxicological profile, in particular with less cardiotoxicity, and improved efficacy. PLD in combination with carboplatin was evaluated in first-line chemotherapy for women with advanced EOC in a large randomized clinical trial MITO-2 (Pignata et al., 2011) and in a subsequent large Cochrane meta-analysis (Lawrie et al., 2013). These studies reported that PLD/carboplatin was as effective as the standard doublet regimen regarding PFS and OS outcomes in first-line chemotherapy; however, women treated with PLD experienced more toxicity (anemia and thrombocytopenia) leading to a higher % of treatment discontinuation (Lawrie et al., 2013). Based on these results, the platinum/PLD combination cannot be considered among the best therapeutic options, but it may be used in patients who do not tolerate or are allergic to paclitaxel. Topotecan and gemcitabine treatments, which have reproducible activity and reasonable therapeutic index, have been tested in EOC frontline treatment in combination with DDP/paclitaxel; however, their addition to DDP/paclitaxel (triplet regimen) in the five-arm phase III randomized trial GOG182-ICON5 was not better than the standard doublet

(Bookman et al., 2009), confirming doublet carboplatin/paclitaxel chemotherapy as the optimal therapeutic option, despite its side effects (nausea, vomiting, myelosuppression, peripheral neuropathy, and alopecia) (Lheureux et al., 2019a).

It is important to note that treatment guidelines are mainly driven by response rates of high-grade serous carcinoma, the predominant advanced EOC subtype and the most sensitive to this chemotherapy regimen. Nevertheless, rarer tumours like low-grade serous carcinoma, clear cell carcinoma, mucinous carcinoma and undifferentiated cancers are much less responsive to the platinum-based chemotherapy (Lheureux et al., 2019a). Based on EOC cumulating biological knowledge, the management of ovarian cancer is evolving from a one-size-fits all approach towards a personalized one, that considers both histology and molecular characteristics. For example, based on LGSOC's biology, MEK-inhibitor treatment has been evaluated in recurrent tumours and hormonal therapy in LGSOC frontline treatment, as well as immunotherapy is being assessed in CCC (Lheureux et al., 2019a).

Treatment response after first-line therapy is monitored through follow-up visits, in which pelvic examination and CA125 measurement are considered [113]. Even single evaluation of elevated CA125 levels did not demonstrate the capacity to predict the onset of tumour recurrences, CA125 levels considered together with clinical pelvic examination through radiological evaluation improve the monitoring of patients during the follow-up (Katabuchi, 2017).

1.1.4.2 Treatment of relapses

Despite ~80% of women with advanced ovarian carcinoma having a good response to first-line treatment, more than 70% of them will experience recurrent disease within the first 3 years (Bowtell et al., 2015). Recurrent ovarian cancer (ROC) is rarely, if ever, curable so the main treatment aim in this setting is to prolong patient survival maintaining a good quality of life. While the leading approach is chemotherapy, as surgery is indicated for few selected patients, actually there is no standard treatment. Even if the number of available therapies has increased, the selection of the most appropriate regimen remains challenging. Considerable efforts have been undertaken to find biomarkers able to predict tumour sensitivity to therapy and to overcome treatment failure.

The prognosis and probability of ROC's response are based on progression-free interval (PFI), the interval from the last dose of platinum-based chemotherapy and the onset of ROC, which defines different platinum sensitive patients, and guides the subsequent therapy. Ten to 15% of patients are considered "platinum-refractory", when they experience progression or stable disease during first-line chemotherapy, or when ROC appears within one months from the end of first-line chemotherapy. In these cases, the tumour is considered intrinsically resistant and the median survival is < 9 months (Lheureux et al., 2019a). "Platinum-resistant" disease responds to primary treatment, but recurrence occurs within 6 months, and this condition affects 20% to 30% of patients (Lheureux et al., 2019a). Platinum-refractory/resistant population has a poor prognosis and a null or poor response rate to platinum-based chemotherapy (<10%), even if some attempts to overcome platinum resistance have evaluated dose-dense chemotherapy or a dose-fractionated weekly therapy (Armbruster et al., 2018). Platinum-refractory and resistant EOC are usually treated with a single-agent chemotherapy based on topotecan, paclitaxel, PLD or gemcitabine, which have different objective response rate (ORR) and toxicity (Armbruster et al., 2018). Treatment of platinum-refractory or resistant EOC should be mainly focused on maintaining quality of

life and controlling symptoms, since the efficacy of pharmacological treatments decreases after each line.

Patients with a durable response to first-line platinum therapy are a heterogeneous group, which includes platinum-partially sensitive patients with a PFI between 6 and 12 months and platinum-sensitive patients, who experience a PFI ≥12 months. Partially sensitive and sensitive patients show a better response to a second platinum-containing regimen than to alternative non-platinum therapies (Lheureux et al., 2019a). Several therapeutic options are available for this group: platinum can be combined with paclitaxel, PLD or gemcitabine, and all these combinations are associated with better outcomes, so the choice will rely on side effects and hypersensitivity to the selected drugs. Treatment is usually administered for many cycles, until resistance or toxic side-effects appear.

An important "evolution" regarding the PFI concept is underway starting from the proposal during the fifth Ovarian Cancer Consensus Conference in Tokyo to reflect a wider range of treatments by replacing PFI with "treatment free interval" (TFI), which takes into consideration the period starting from the last dose of any treatment, not only platinum (TFIp), but also non-platinum agents (TFInp) or other biological agents (TFIb) (Wilson et al., 2017).

1.1.4.3 Targeted therapies and new drugs

The standard of care of EOC takes into little consideration the histological subtype or the genomic profile of the single case, but in the era of precision medicine, there is mounting interest for molecular-targeted therapies able to hit driver mutations or molecular targets, such as angiogenic mechanisms, DNA repair and signal transduction pathways (Rojas et al., 2016). At the moment, only two targeted therapies are approved by the U.S. Food and Drug Administration (FDA) and the European Medicines Agency (EMA) for the maintenance therapy of EOC and treatment of ROC. These are anti-angiogenic agents, such as

bevacizumab, and poly-adenosine diphosphate (ADP)-ribose polymerase (PARP) inhibitors (PARPi), such as olaparib, niraparib and rucaparib.

Bevacizumab is a humanized monoclonal antibody specifically directed against vascular endothelial growth factor A (VEGF-A) and the most studied anti-angiogenic agent. VEGF is a family of key regulators of angiogenesis, involved in endothelial cell survival, proliferation and vascular permeability. Increasing levels of VEGF in EOC promote tumour vascularization and vascular permeability which favor metastatic spread and ascites formation (Garcia et al., 2020). The rational for the use of anti-angiogenic therapy is based on evidence, where increased levels of VEGF in EOC were associated with poor prognosis and platinum resistance (Siddiqui et al., 2011). Bevacizumab in combination with chemotherapy, was studied in several phase III trials in platinum-sensitive and platinum-resistant recurrence settings. The OCEANS and GOG213 phase III randomized studies investigated the association of standard chemotherapy (carboplatin/gemcitabine or carboplatin/paclitaxel, respectively) in patients with platinum-sensitive ROC, who received one prior line of therapy. These studies compared chemotherapy with or without bevacizumab, followed by maintenance with or without bevacizumab (Aghajanian et al., 2012; Coleman et al., 2017). Both reported a significant increment in PFS in the arm treated with bevacizumab (12.4 vs 8.4 months in OCEANS and 13.8 vs 10.4 months in GOG213), and GOG213 also reported a higher OS (42.2 vs 37.3 months in chemotherapy + bevacizumab versus chemotherapy alone) (Coleman et al., 2017). The AURELIA phase III open-label trial demonstrated higher efficacy in terms of PFS of bevacizumab associated with single-agent chemotherapy (PTX or PLD or topotecan) than chemotherapy alone, in women with platinum-resistant ROC (PFS: 6.7 vs 3.4 months, respectively). Bevacizumab also improved quality of life in these patients and a retrospective analysis of AURELIA trial showed that the sub-group of patients with ascites had a major benefit from bevacizumab treatment, suggesting ascites as a phenotypic marker for anti-angiogenic therapy (Rojas et al., 2016). All these results were recently confirmed with cediranib, a tyrosine kinase

inhibitor that specifically target VEGF receptor (VEGFR) (Rojas et al., 2016). Cediranib and bevacizumab displayed similar efficacy and similar side effects (Lheureux et al., 2019a; Monk et al., 2016). However, benefits derived from anti-angiogenic therapy in EOC should be balanced with toxicity and related-costs, and although these agents are widely used, the lack of molecular biomarkers is a drawback in their use (Monk et al., 2016).

PARPi, whose mechanisms of action and determinants of response will be discussed in detail in the following chapters, are the most active and interesting class of agents recently approved for the treatment of EOC. Briefly, PARP is a large family of multifunctional proteins, where PARP1 is the prevalent isoform. PARP1 is involved in the base excision repair (BER) pathway, able to repair DNA single-strand breaks (SSBs). PARP1 inhibition causes an accumulation of un-repaired SSBs and stalled replication fork (RF), which in turn degenerate into the most lethal DNA double-strand breaks (DSBs). Cancer cells with defects in the DBS-repair pathways, such as HR, accumulate a great number of DSBs which determine the block of RF and enhance genomic instability, leading to cancer cell death. The rationale of the use of PARPi relies on the concept of synthetic lethality that was firstly introduced in biology by C. Bridges during his studies on *Drosophila Melanogaster*, then taken forward for the development of new cancer therapeutic approaches by Hartwell and colleagues (reviewed by (Ashworth and Lord, 2018; Hartwell et al., 1997)). The concept of "synthetic lethality" describes the situation whereby a combination of two defective genes or proteins induce severe effects or death, whereas the single defective gene/protein is not dangerous *per se*. This concept was further applied to explain the results reported in 2005 in two preclinical seminal studies, which demonstrated the extreme sensitivity of *BRCA1* and *BRCA2* mutated tumours to PARPi (Bryant et al., 2005; Farmer et al., 2005), laying the foundations for their clinical development. In the case of EOC, where half of the HGSOCs are HRD, the synthetic lethality approach aims to hit a second DNA repair pathway (i.e. BER) on which the HRD cancer cells rely on to repair DNA damage and survive. Olaparib was the first PARPi introduced into clinical practice and from 2014 and the end of 2017,

other PARPi, rucaparib and niraparib respectively, were approved in Europe and USA for the treatment of EOC, but with different clinical indications. Briefly, the most recent guidelines released from EMA ("www.esmo.org/guidelines/gynaecological-cancers/newly-diagnosed-and-relapsed-epithelial-ovarian-carcinoma/eupdate-ovarian-cancer-treatment-recommendations," n.d.) indicate the use of all the PARPi (olaparib, rucaparib and niraparib) as monotherapy in the maintenance setting, following platinum-based chemotherapy in relapsed, platinum sensitive, HGSOC adult patients, who are in complete or partial response to platinum-based therapy, regardless of *BRCA* status. Moreover, EMA approved monotherapy with rucaparib for patients with germline or somatic *BRCA1/2*-mutations who have received at least two lines of platinum-based chemotherapy, but are unable to receive again platinum due to toxicity (Oza et al., 2017).

Currently, FDA has approved olaparib, rucaparib and niraparib as monotherapy in the maintenance setting of advanced recurrent HGSOC patients, in complete or partial response to platinum-based therapy. Olaparib was also extended to 4th line monotherapy in germline or somatic *BRCA*-mutated patients and rucaparib as 3rd line monotherapy also in germline or somatic *BRCA*-mutated carriers. Even in the USA the tendency is to extend as much as possible the population of patients that could benefit from PARPi therapy, also in HRD not established patients.

The time scale approvals of PARPi by EMA and FDA, and their clinical indications are summarized in **table 1.2**.

Table 1.2 Time scale of PARPi approvals in Europe and USA and therapeutic indications

Drug	Year of approval	Agency	Patient requirements	*BRCA* status	Clinical setting
Olaparib (capsules)	2014	EMA	DDP sensitive, relapsed HGSOC, in CR or PR to DDP therapy	g/s *BRCA1/2* mut	Monotherapy maintenance
		FDA	Advanced OC	g *BRCA1/2* mut	4th line monotherapy treatment
	2017	FDA	Recurrent OC, in CR or PR to DDP therapy	g *BRCA1/2* mut	Monotherapy maintenance
Olaparib (tablets)	2018/19	EMA	DDP sensitive, relapsed HGSOC, post CR or PR to DDP therapy	g/s *BRCA1/2* mut	Monotherapy maintenance
			Advance OC, in CR or PR to DDP therapy		
		FDA	Advance OC, in CR or PR to DDP therapy	g/s *BRCA1/2* mut	Monotherapy maintenance
Rucaparib	2016	FDA	Advanced OC / progressive disease	g/s *BRCA1/2* mut	3rd line monotherapy treatment
	2018		Recurrent OC, in CR or PR to DDP therapy	-	Monotherapy maintenance
	2018	EMA	DDP sensitive, relapsed or progressive HGSOC	g/s *BRCA1/2* mut	3rd line monotherapy treatment
	2019		DDP sensitive, relapsed HGSOC, in CR or PR to DDP therapy	-	Monotherapy maintenance
Niraparib	2017	FDA	Recurrent OC, post CR or PR to DDP therapy	-	Monotherapy maintenance
		EMA	DDP sensitive, relapsed HGSOC, in CR or PR to DDP therapy	-	Monotherapy maintenance

Abbreviations: FDA= Food and Drug Administration; EMA= European Medicine Agency; EOC= epithelial ovarian cancer; Advanced= FIGO stage III or IV; DDP= platinum; CR= complete response; PR= partial response; g= germline; s= somatic; mut= mutation.

The use of PARPi in the maintenance setting was investigated in phase II and phase III trials. STUDY19 and SOLO-2 (phase II and III respectively) for olaparib, NOVA for niraparib and ARIEL-3 for rucaparib (Coleman et al., 2017; Ledermann et al., 2012, 2014; Mirza et al., 2016a; Pujade-Lauraine et al., 2017). Survival has been evaluated in treated arms compared with placebo arm, in recurrent, platinum-sensitive HGSOC patients. PFS was significantly improved in PARPi-treated arms (median PFS ranging from 16.6 to 21.0 months considering the different trials) than in the placebo arm (median PFS ranging from 5.4 to 5.5 months) (**table 1.3**). *BRCA*-mutated patients had the major benefit in terms of median PFS (hazard ratio (HzR) ranging from 0.18 to 0.27 in the different trials), respect those classified as HRD-positive (HzR ranging from 0.38 to 0.44). However, analyses of PFS in intention to treat population or in BRCA-wild type patients have demonstrated a significant increase in PFS in treated patients irrespective of *BRCA* or HRD status. In particular, niraparib in non-germline *BRCA*-mutated group showed a median PFS of 9.3 vs 3.9 months in placebo (HzR 0.45, 95% CI, 0.34-0.61) (Mirza et al., 2016a); in rucaparib trial the intention-to-treat population had a median PFS of 10.8 vs 5.4 months of placebo (HzR 0.36, 95% CI, 0.30-0.45) (Coleman et al., 2017); data obtained analyzing a subgroup of non-*BRCA* mutated tumours in STUDY 19 treated with olaparib, showed a median PFS of 7.4 vs 5.5 months in placebo (HzR 0.54, 95% CI, 0.34-0.85) (Friedlander et al., 2018; Ledermann et al., 2014; Pujade-Lauraine et al., 2017) (**table 1.3**). Taken together these results lead to the latest EMA approval for PARPi regardless of the BRCA status of tumours.

Data regarding OS are not yet completed apart for the first STUDY 19, where patients treated with olaparib did not experience a significant increment in OS (HzR 0.73, 95% CI, 0.55-0.95). It has been reported in this study 11% of long-term survival (PFS >6 years) of treated patients which include both BRCA-mutated and wild type carriers (Friedlander et al., 2018).

Table 1.3 Results of PARPi maintenance therapy in HGSOC

			PFS depending on specific biomarkers considered in each trial			
Clinical trial	Patient Population	Study design	*BRCA*-mutated	*BRCA*-wild type	HRD +	HRD –
Olaparib/Study 19 [*Ledermann et al., 2012, 2014; Friedlander, et al., 2018*]	Platinum-sensitive, recurrent HGSOC	Randomized 1:1, double blind, placebo controlled, phase II.	PFS: 11.2 months vs 4.3; HzR= 0.18	PFS: 7.4 months vs 5.5; HzR=0.54	Not considered	Not considered
Olaparib/SOLO2 [*Pujade-Lauraine et al., 2017*]		Randomized 2:1, double blind, placebo controlled, phase III.	PFS: 19.1 months vs 5.5; HzR= 0.3	Not included	Not considered	Not considered
Niraparib/NOVA [*Mirza, et al., 2016*]		Randomized 2:1, double blind, placebo controlled, phase III.	PFS: 21.0 months vs 5.5; HzR= 0.27	PFS: 9.3 months vs 3.9; HzR= 0.45	PFS: 12.9 months vs 3.8; HzR= 0.38 **HRD defined by Myriad assay*	PFS: 6.9 months vs 3.8; HzR= 0.58
Rucaparib/ARIEL3 [*Coleman et al., 2017*]		Randomized 2:1, double blind, placebo controlled, phase III.	PFS: 16.6 months vs 5.4; HzR= 0.23	*PFS: 10.8 months vs 5.4; HzR= 0.36	PFS: 9.7 months vs 5.4; HzR= 0.44 **HRD defined by Foundation Medicine 's T5 NGS assay*	PFS: 6.7 months vs 5.4; HzR= 0.58

Abbreviations: EOC= epithelial ovarian cancer; PFS= median progression free survival; HzR= hazard ratio; LOH= loss of heterozygosity; HRD= homologous recombination deficiency.

*PFS in intention to treat population, including all patients recruited in ARIEL3.

1.2 DNA REPAIR

1.2.1 DNA repair and cancer

In normal cells, genomic integrity is the result of high-fidelity replication processes associated with mechanisms that recognize and actively repair DNA lesions induced by endogenous or exogenous insults (Ganai and Johansson, 2016). The articulated signalling network responsible for DNA integrity is defined as DNA damage response (DDR) and DNA repair pathways are part of this network (Carrassa and Damia, 2017). DDR actively monitors the genomic integrity, and, in the presence of DNA lesions, it suspends cell cycle progression and activates the appropriate DNA repair pathway to solve each kind of lesion to preserve genomic integrity. Different types of DNA lesions are known: single base modifications, mismatches, intra- or inter-strand cross links (ICLs) and DNA single- (SSB) or double-strand breaks (DSB), and for each kind of damage detected on DNA, one or more specific DNA repair pathways are activated by DDR sensors in order to remove the lesion and replace the original sequence (Abbotts and Wilson, 2017; Hashimoto et al., 2016; Kinsella, 2009; Wright et al., 2018). Once the lesion has been repaired, the cell cycle progresses, or, in the alternative, DDR activates apoptosis to avoid an accumulation of dangerous DNA alterations (Carrassa and Damia, 2017). In fact, genetic or epigenetic alterations affecting DDR activity enhance the number of genomic mutations, and if they affect oncogenes or oncosuppressor genes, may induce malignant transformation and drive tumorigenesis (Kiwerska and Szyfter, 2019). Impaired DDR is one of the hallmarks of cancer (Hanahan and Weinberg, 2000), but also a “double-edged sword” because besides favouring carcinogenesis, DDR deficiency generally makes cancer cells more sensitive to DNA damaging chemotherapies (Ceccaldi et al., 2015; Kiwerska and Szyfter, 2019). In fact, DNA repair activity is able to modulate the effect of chemotherapy, since one of the main mechanisms of action of standard anti-tumour agents is the induction of severe inter-strand cross-links (ICLs), and/or double-strand breaks (DSBs) (Kitao et al., 2018) that if not

repaired, increase replication stress, mutational burden and chromosomal instability, finally inducing apoptosis (Kiwerska and Szyfter, 2019).

The progressive characterization of DNA repair pathways and proteins involved in DDR elucidated how these pathways interplay with each other and led to identifying targets for therapy and new therapeutic strategies. For instance, inhibition of critical genes can be exploited to improve responsiveness to standard chemotherapy, or in DDR defective tumours target the alternative remaining pathway, which the mutated cell relies on to survive has demonstrated the selective efficacy of the synthetic lethality approach. For instance, the extreme sensitivity of *BRCA1/2* mutated tumours, which have a defective HR pathway, to inhibition of PARP1/2 enzymes, involved in the SSB repair, became the paradigm of synthetic lethality concept applied to cancer therapy (Bryant et al., 2005; Farmer et al., 2005).

Moreover, several DNA repair genes, including *ATM, ATR, CHK1* and *WEE1* are interesting proteins acting between DDR and downstream activation of DNA repair, and are studied as therapeutic targets (Carrassa and Damia, 2017). Briefly, ATM and ATR are two kinases leading to activation of DDR once DNA damage has been created. In particular, ATM is activated in the presence of DSBs, activating then the deputy DNA repair pathway through BRCA1/53BP1 proteins to repair the DSB, which promote HR and non-homologous end joining (NHEJ) respectively, and regulates the checkpoint in G1/S phase. ATR is activated following DNA single-strand breaks (SSB), often a pre-lesion before DSB formation, and mediates its activity through CHK1, its downstream effector, which can be phosphorylated also by ATM. ATR/CHK1 regulate the checkpoint during the S phase, and in G2/M, regulating access in mitosis, and phosphorylate a number of proteins involved in HR and ICL repair (Carrassa and Damia, 2017; Maréchal and Zou, 2013). WEE1 is a kinase, which also regulates the checkpoint in G2/S cell cycle phases and may activates HR (Carrassa and Damia, 2017). *ATM, ATR, CHK1* and *WEE1* genes can be found mutated in approximately

2% of HGSOC, with consequences on DNA repair efficiency (Cancer Genome Atlas Research Network, 2011).

Due to their early and critical activity in inducing the activation of DNA repair, in particular HR, regulating the cell cycle phases and apoptosis, several inhibitors are currently being tested, alone exploiting the synthetic lethality approach in HR-deficient tumours, or in combination with chemotherapy (Carrassa and Damia, 2017; Cleary et al., 2020).

1.2.2 DNA repair pathways

Usually, all the DNA pathways are multistep processes, with many proteins involved in the same pathways (Abbotts and Wilson, 2017; Hashimoto et al., 2016; Kinsella, 2009; Wright et al., 2018).

DNA repair activity is generally structured in three phases regardless of the type of damage or pathway activated: 1) recognition of the damage by specific sensor proteins; 2) activation of the suitable effectors to remove DNA damage; 3) restoration of DNA strand integrity.

The mechanism of action and proteins involved in the seven major cellular DNA repair pathways will be described here. In particular, they participate to various extent in the removal of platinum adducts (i.e. NER, HR, FA, translesion synthesis (TLS) and MMR) or can influence PARPi activity (i.e. HR, FA, non-homologous end joining (NHEJ), BER) with consequences on EOC therapy and patient outcome.

1.2.2.1 Base excision repair

The base excision repair (BER) is responsible for the repair of aberrant bases on DNA, caused by a wide range of endogenous and exogenous insults and it is involved in repair of single strand breaks (SSB) (Dianov and Hübscher, 2013) (**figure 1.11**). The BER process consists of different enzymatic steps and is able to repair one or up to 12 nucleotides. In the presence of a single damaged nucleotide (the most frequent condition), the short patch BER pathway is generally activated, or alternatively, the long patch BER, which mainly involved

different glycosylases with respect to the short patch pathway (Kim and Wilson, 2012). The damage is recognized and removed by a damage-specific DNA glycosylase, which creates an apurinic or apyrimidinic (AP) site, then is processed by AP endonuclease (APE1), with the generation of SSB. Replacement of the damaged base and re-ligation of the DNA involve binding of poly(ADP-ribose) polymerases (PARP), DNA polymerase β (POLB) and ligase I or III (Damia and D'Incalci, 2007). PARP1, following auto-modification, can interact with other BER proteins such as XRCC1 and POLB, enabling their recruitment to the damage site (El-Khamisy et al., 2003; Mortusewicz and Leonhardt, 2007). In addition, PAR polymers formed by PARP-1 at the damaged site have a net negative charge which promotes chromatin loosening and facilitates the access to DNA of repair proteins (Weaver and Yang, 2013). POLB is a small polymerase, which replaces the single damaged nucleotide (Beard and Wilson, 2019). Completion of the BER pathway can be performed by either DNA ligase I or the DNA ligase IIIα/XRCC1 complex, where XRCC1 acts as a fundamental scaffold to bridge polymerase and ligase activity (Sleeth et al., 2004). Proteins acting at different levels in the BER pathway have been found dysregulated in different tumours (germline and somatic mutations, polymorphisms) (Broustas and Lieberman, 2014).

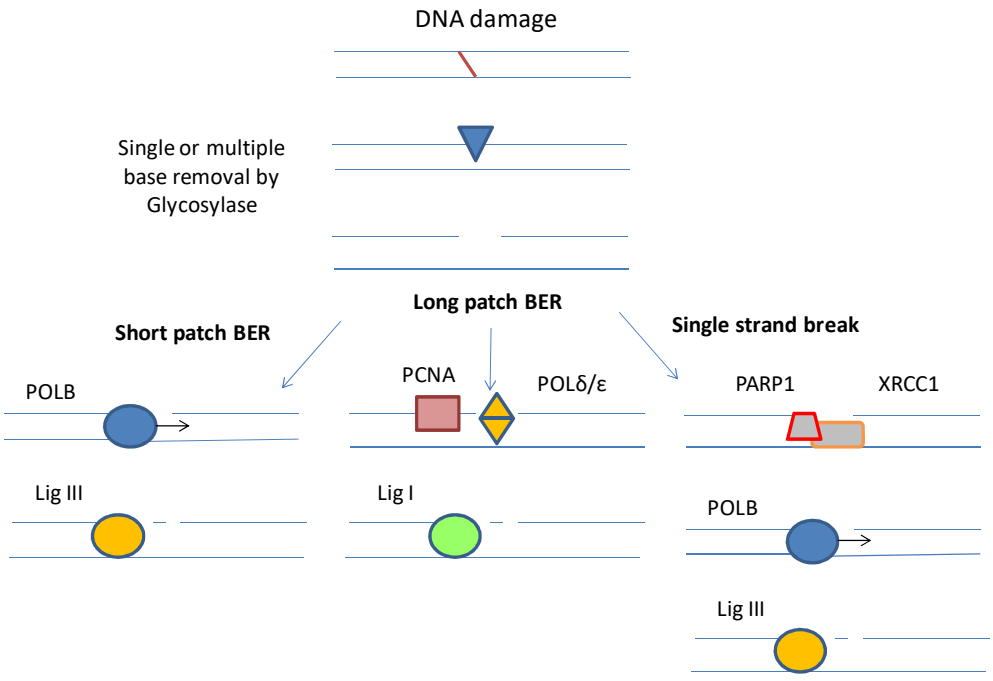

Figure 1.11 Schematic representation of base excision repair pathway.

Short patch BER removes and substitutes single damaged nucleotide; long patch BER removes and substitutes up to 12 nucleotides; BER through PARP enzyme repairs DNA single strand breaks.

1.2.2.2 Mismatch repair

The mismatch repair (MMR) (**figure 1.12**) recognizes and corrects the wrong incorporation of single nucleotide (mismatch), or erroneous insertion and deletion loops occurring during DNA replication (Kunkel and Erie, 2015). MMR involves different well-conserved proteins, that detect the mismatches (MSH2-MSH6) forming the heterodimer complex hMutSα, or the indel loops (MSH2-MSH3) forming the heterodimer complex hMutSβ. When hMutS slides along the newly replicated strand and finds a mismatch to repair, it recruits PMS2 and MLH1 proteins, together forming the hMutLα complex. The next steps are not completely elucidated in eukaryotic cells, but DNA is unwound, excised by the exonuclease I (Exo1), that removes the short sequence (up to 4 nucleotides) containing the error, correctly re-synthesizes the DNA sequence by polymerase δ or polymerase ε and finally ligates the nick (Hsieh and Zhang, 2017; Kunkel and Erie, 2015). MMR can also induce apoptosis recruiting ATM/ATR by hMutLα (Gee et al., 2018). Mutations in MMR genes can destabilize the genome increasing the mutational rate and inducing microsatellite instability, which favour cancer development (Curtin, 2012). Inherited mutations in MMR represent the second most common cause of hereditary ovarian cancer, after *BRCA1/2* mutations, and are the cause of Lynch Syndrome that predisposes to colorectal, endometrial and ovarian cancer (Backes and Cohn, 2011). However, MMR alterations can occur in sporadic cancers, usually through epigenetic mechanism, such as hypermethylation of hMLH1 promoter leading to lack of protein expression (Leskela et al., 2020).

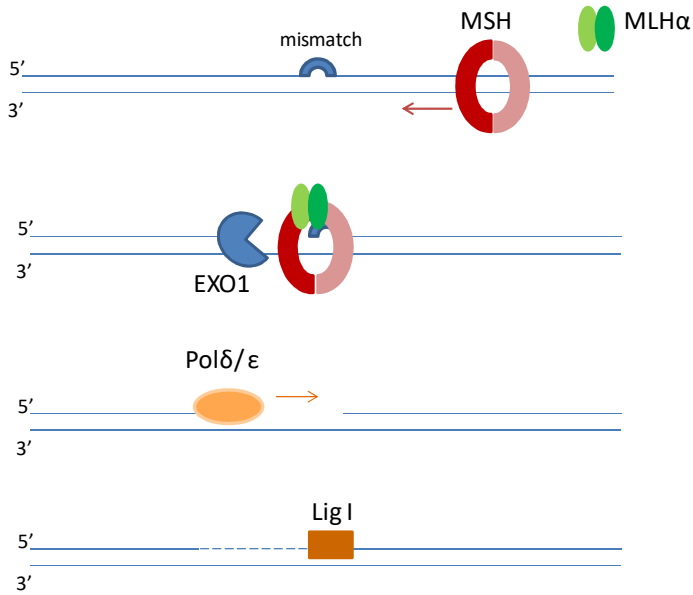

Figure1.12 Schematic representation of mismatch repair pathway

MSH complex slides along the newly replicate DNA strand looking for eventually mismatches or indel loops. In proximity of the mismatch, MSH recruits the complex MLHα (MLH1+PMS2), unwinding the DNA and activating the nuclease EXO1 for the 5' to 3' excision of the sequence including the mismatch (up to 4 pb). Finally, the high-fidelity polymerase δ or ε re-synthesizes the correct sequence and ligase I completes the ligation.

1.2.2.3 Nucleotide excision repair

Nucleotide excision repair (NER) is a highly conserved and versatile pathway that repairs a broad range of helix-distorting and bulky DNA lesions, mostly induced by exogenous sources. This system is one of the major players involved in the removal of all cisplatin DNA lesions, including intra-strand and inter-strand crosslinks (ICLs), and is almost entirely responsible for the removal of pyrimidine dimers caused by UV radiation (Damia and D'Incalci, 2007). It is a multistep process in which at least 20-30 proteins are involved. Two major NER pathways can be recognized: the global genome repair (GGR) pathway, which participates in the context of a non-replicating DNA and slowly controls and repairs the entire genome, preventing mutations to be passed on to the next generation and keeping genomic integrity; the transcription coupled repair (TCR), which efficiently acts on transcribed DNA, when RNA

polymerase is stalled for the presence of DNA damage (Tian et al., 2015). The basic steps of NER are: damage recognition; excision and release of the 24-32 nucleotides oligomer; synthesis of the excised sequence and ligation. DNA damage is recognized by the co-operation of replication protein A (RPA), Xeroderma pigmentosum group A (XPA), XPC and TFIIH, which assemble at the damaged site. TCR-NER requires also Cockayne syndrome WD repeat protein A (CSA) and CSB to detect the damage, while in GGR-NER XPC-RAD23B and DNA damage-binding protein (DDB) participate in the process. Therefore, while the two sub-pathways differ in the initial steps of recognition of DNA lesions, they converge into a common molecular mechanism. The complex formed at the damaged site unwinds the double helix by 25 nucleotides around the lesion (thanks to XPB and XPD helicases of TFIIH complex). The 3' endonuclease XPG then replaces XPC in the complex, which gains more stability and recruits the 5' nuclease XPF-ERCC1. These two enzymes are responsible for the incision of DNA around the lesion and for the removal of the damaged sequence, the limiting step of the process. The gap is then filled by POL δ or POL ε, with the aid of the accessory proteins proliferating cell nuclear antigen (PCNA) and replication factor C (RFC), and by DNA ligase III (**figure 1.13**) (Dijk et al., 2014).

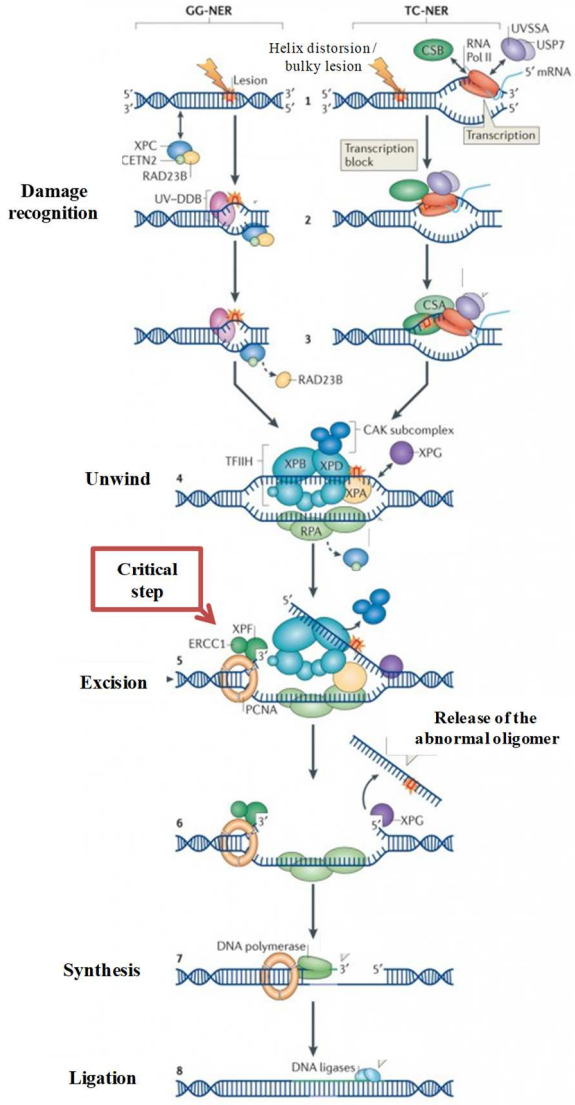

Figure 1.13 Schematic view of nucleotide excision repair pathway

Global NER (GG-NER) repairs overall the genome, while transcription-coupled NER (TC-NER) quickly acts during transcription. The recognition players are different between GG-NER and TC-NER. In the first, XPC–RAD23B and DDB are required, while TC-NER involves CSA and CSB. XPA, RPA and TFIIH are involved in both pathways. Thereafter the steps are common, with unwinding of DNA helix, excision of the damaged oligonucleotide by XPG and ERCC1–XPF nuclease, which represent the critical step of the process, then synthesis of the oligonucleotide by POLs δ/ε and ligation by DNA ligase III (adapted from (Schwertman et al., 2012)).

1.2.2.4 Homologous recombination

The homologous recombination (HR) pathway is a multistep, error-free mechanism (**figure 1.14)** involved in DNA double strand breaks (DSB), acting during the S and G2 phases of the cell cycle (**figure 1.15**). It relies on the presence of the sister chromatid as a template for the DNA sequence to be repaired. First, the MRE11, RAD50 and NSB1 (MRN) complex detects and binds the broken ends of DSBs (**step 1**, **fig 1.14**), recruiting ataxia telangiectasia kinase (ATM). ATM phosphorylates and activates BRCA1 on the DSB site, promoting end resection through the MRN-BRCA1–CtIP complex, after CtIP cyclin-dependent-kinase (CDK)-mediated phosphorylation leading to the exposure of two ssDNA regions, which overhang on either side of the DSB (**step 2**, **fig 1.14**). Following, the BRCA2 protein is then recruited at the damaged site by BRCA1 and their interaction is mediated by PALB2, which is the essential link between BRCA1 and BRCA2 (**step 3**, **fig 1.14**). The central player of HR repair, the single strand binding protein RAD51, which forms visible nuclear foci, is loaded onto the 3'single-strand overhangs by BRCA2 and RAD51, and guides strand invasion and copying to homologous sequences in the intact sister chromatid to repair the lesion without lack of genetic material (**step 3 and 4, fig 1.14**). DNA polymerase uses the homologous sister chromatid as a template, and uses the ssDNA as a primer to synthesize new DNA sequence (**step 5, fig 1.14**). The final steps involve endonuclease MUS81 and ligase IV to solve this complex structure (**step 6, fig 1.14**) and complete the solution of DSB (**step 7, fig 1.14**) (Lord and Ashworth, 2016).

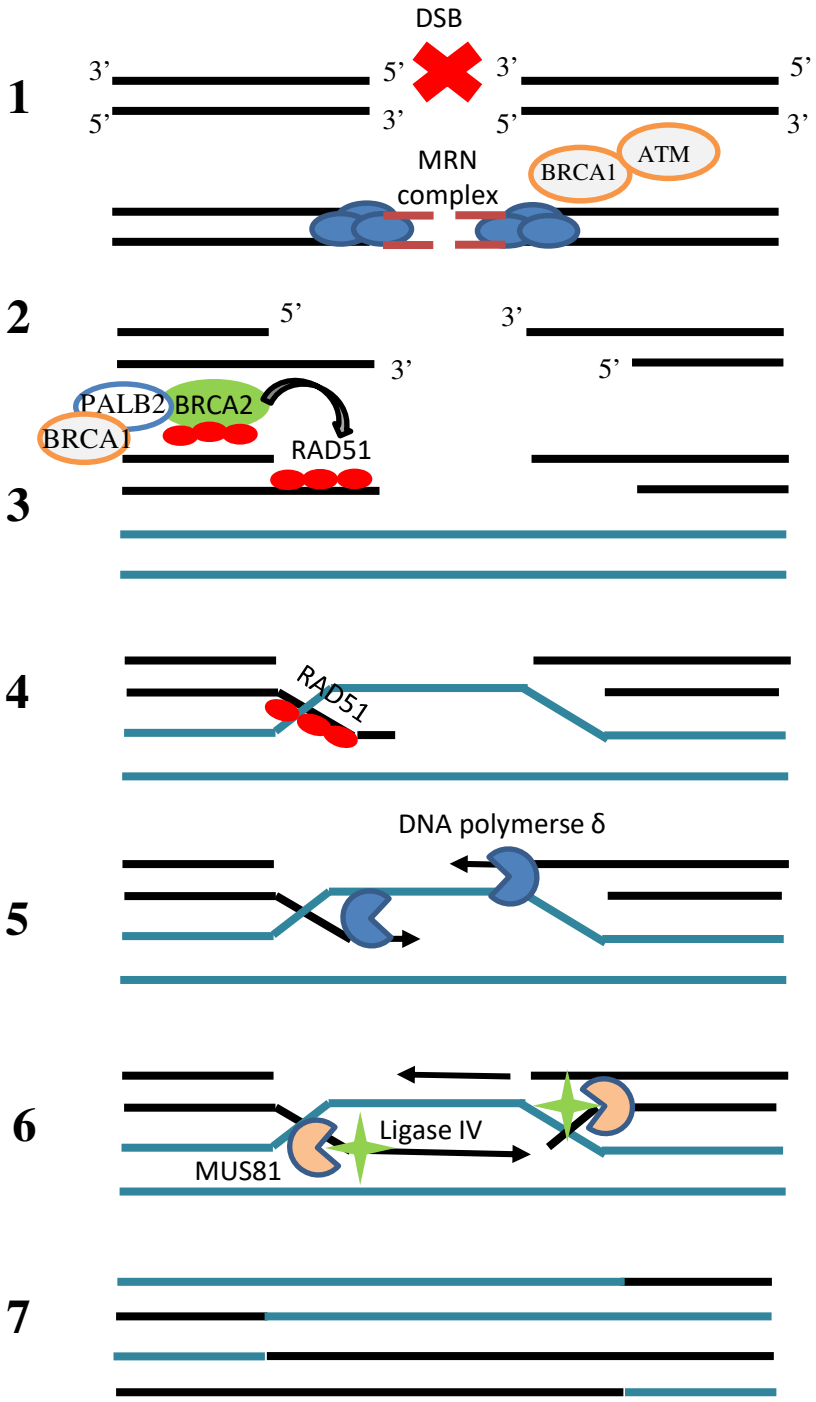

Figure 1.14. Schematic view of homologous recombination repair

1.2.2.5 Non-homologous end joining

Classical non-homologous end joining (NHEJ) is also involved in DSB repair predominantly during G0/G1 phases or as an alternative to HR when defective. It solves DSBs with minimal end processing in an error-prone manner (Chang et al., 2017). Its name is derived from the mechanism of action, through which the two breaks end are directly ligated, without using the homologous template. This explain the low fidelity of NHEJ products. NHEJ needs the activation of KU70/KU80 heterodimer, a ring-like structure which binds DNA at DSB site with high affinity and recruits the serine-threonine kinases DNA-PKs, stabilizing them on DNA. If the ends of DNA are not compatible, then "overhangs" of DNA need to be removed creating a microhomology necessary to guide the process, then re-synthesized by nucleases and DNA polymerases such as Artemis. Artemis can form both 3' and 5' endonuclease when complexed with DNA-PK (Ma et al., 2002). Once the ends are compatible, they can be ligated by ligase IV and XRCC4 co-factor (Assis et al., 2013) (**figure 1.15**).

A sub-pathway of NHEJ is the alternative-end joining (Alt-EJ), which is activated when NHEJ and HR are inhibited or absent, a sort of spare DNA repair pathway, suggesting the importance of solving the deleterious DSB for the cell. It can be activated throughout all the cell cycle phases and is independent from the KU complex. Alt-EJ uses microhomologies distant from DSB, frequently creating deletions or other mutagenic lesions. The key players of Alt-EJ are PARP1, XRCC1 and DNA ligase III, and it is promoted by DNA polymerase θ (POLQ) (Kent et al., 2015). PARP1 recognizes and binds the DSB competing with KU proteins, then XRCC1 and LigIII form a complex to ligate the broken strand (Audebert et al., 2004) (**figure 1.15**).

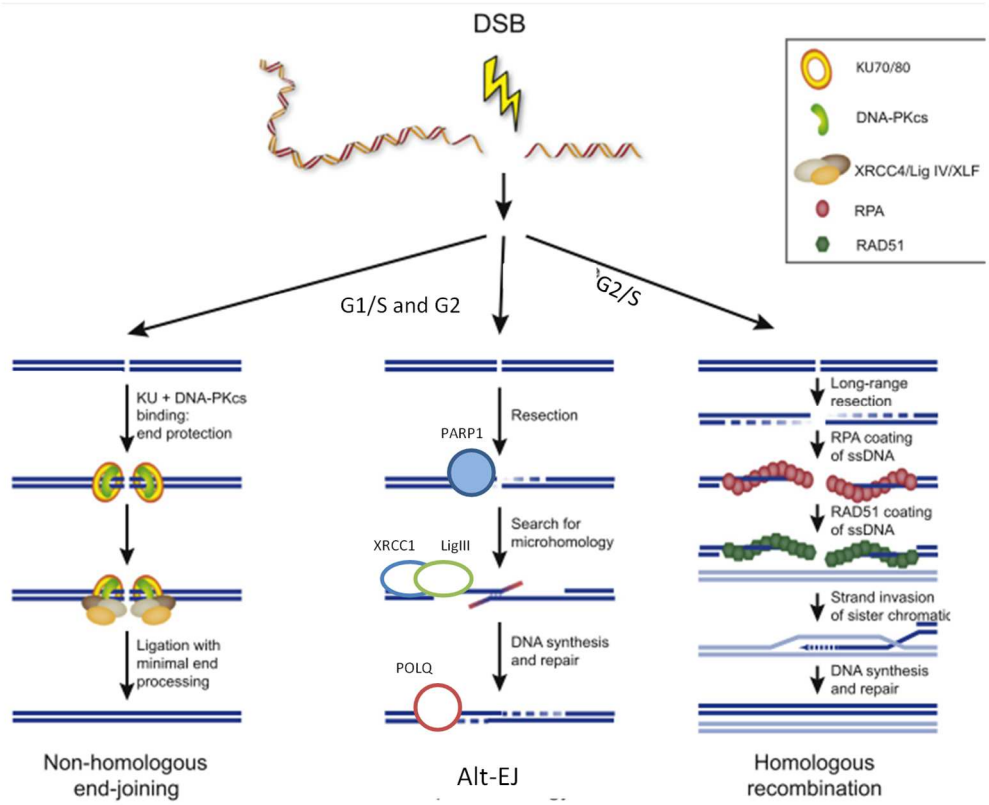

Figure 1.15 Overview of DNA repair pathways involved in the repair of DNA double strand breaks (DSBs)

NHEJ and Alt-EJ are available during all the cell cycle phases, are quick but error-prone mechanisms, while HR acts during replication phase and is a high-fidelity repair system (image adapted from (Noordermeer and van Attikum, 2019)).

1.2.2.6 Fanconi anemia

Fanconi anemia is a rare inherited syndrome, characterized by congenital defects, progressive bone marrow failure and elevated risk of haematological and squamous cell carcinomas (Soulier, 2011). The 19 genes of FA encoded for proteins involved in the same pathway, which determine ICL repair during the G2/S phase of the cell cycle, orchestrating the recognition of the ICL, incision, bypass of the lesion and repair (Kottemann and Smogorzewska, 2013) (**figure 1.16**). When the replication fork meets the ICL, the replication stalls and ATR mediate the phosphorylation of FANCM, the first FA protein that binds the ICLs, together with two histone fold proteins (MHF1, MHF2). FANCM is a scaffold protein for the FA core complex, composed of 14 components including FANCA, B, C, E, F, G and L. The core complex on DNA forms nuclear foci visible during G2/S phase and functions as a large ubiquitin ligase for two other FA proteins, FANCD2 and FANCI (Ceccaldi et al., 2016). Phosphorylation and monoubiquitylation modify the FANCD2-I complex and are reverted by the USP28 protein at the end of the process. Post-translational modifications are necessary for the correct interaction of FANCD2-I with foci and other DNA repair proteins, including BRCA1, BRCA2, RAD51, XPF-ERCC1 and PCNA to execute ICL repair (Ceccaldi et al., 2016). The XPF-ERCC1 nuclease complex, as described above, has a central role in NER and is necessary to unhook the ICL lesions (Hodskinson et al., 2014). Unhooking the DNA leaves the crosslinked nucleotide link to the complementary strand, which is bypassed by TLS polymerases REV1 or (REV3–REV7) (Sarkar et al., 2006). Ligation restores an intact DNA duplex, which functions as a template for HR-mediated repair of the DSB, further processed by nucleases such as MRN complex or EXO1, reducing DSB to a single-stranded DNA overhang. This single-stranded DNA coated with RPA is a substrate for RAD51-mediated strand invasion promoted by BRCA2 and subsequently the HR pathway completes the repair (Prakash et al., 2015). So, ICL repair needs the cooperation of FA, with NER, TLS and HR pathways (Ceccaldi et al., 2016).

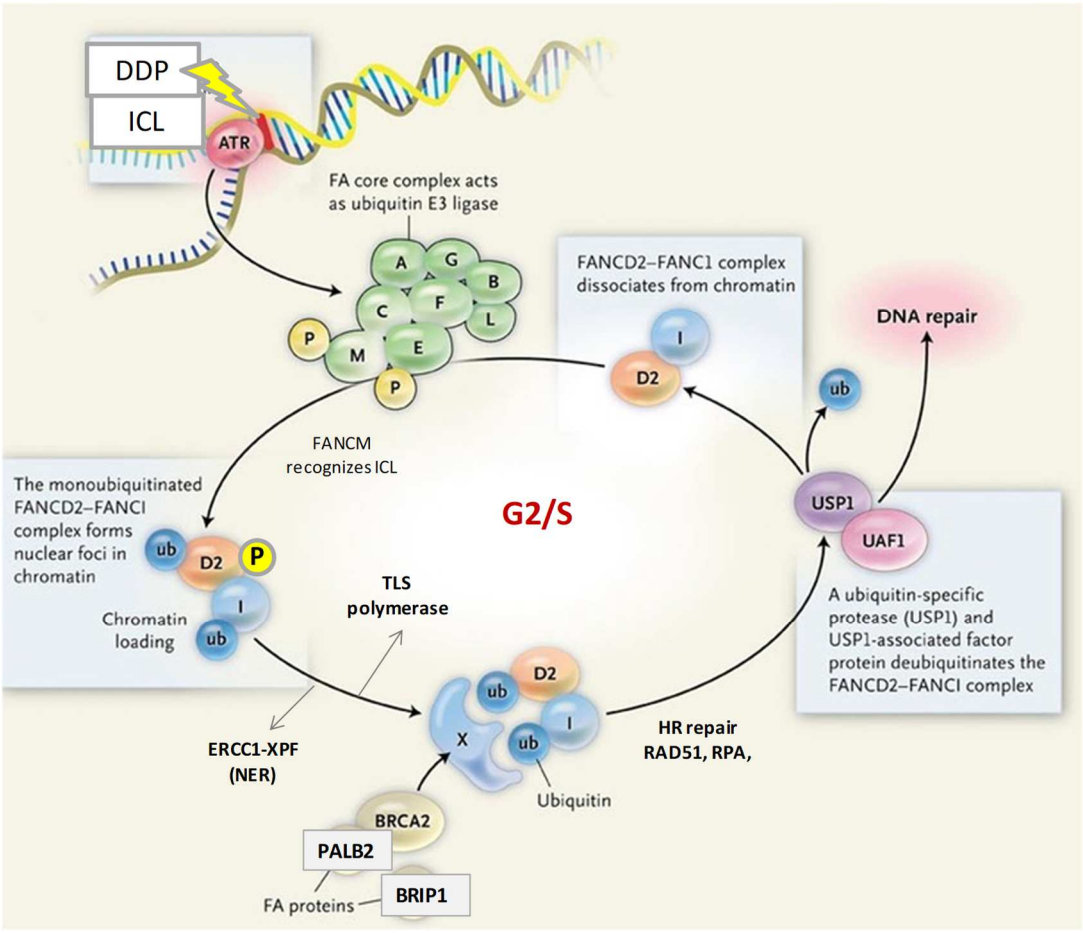

Figure 1.16 Schematic overview of Fanconi anemia pathway

Fanconi anemia pathway is activated during G2/S phase to repair ICLs in cooperation with NER, HR and TLS (adapted from (Cai et al., 2020)).

1.2.2.7 Translesion synthesis repair

If damaged DNA bases are not repaired or in presence of ICLs, replication stalls because the DNA strands cannot be separated. Stalled replication forks are most frequently resolved using error-free mechanisms such as HR. However, replication may proceed by switching out regular DNA polymerases for alternative polymerases, such as DNA polymerase η (POLH) which is able to use the damaged strand as a template in an error-prone process known as translesion DNA synthesis (TLS), triggered by PCNA protein mono-ubiquitylation. Such a mechanism contributes to survival, but should be considered a DNA damage tolerance mechanism, rather than a DNA repair mechanism (Zhao and Washington, 2017).

1.3 MECHANISM OF ACTION OF PLATINUM AGENTS

1.3.1 Cisplatin and carboplatin

Cisplatin (Cis-diamminedichloroplatinum (II)) (DDP), was synthesized for the first time at the end of 19th century by the Italian chemist Michele Peyrone (Dilruba and Kalayda, 2016). Its anti-proliferative effect was observed by Rosenberg in the late 1960s during his studies on the effect of electricity on *E. coli* growth using a platinum electrode (Rosenberg et al., 1965). Then, the characterization of cisplatin cytostatic/cytotoxic properties was extended through *in vivo* studies in hematologic and solid tumour xenograft models (Rosenberg et al., 1969). These experiments led to clinical trials and to cisplatin approval in 1979. Cisplatin is the oldest member of a wide family of anti-neoplastic drugs borne in the second half of the 20th century, which contain in their structure a platinum atom that coordinates different complexes and named for this reason platinum-based agents or platins. Carboplatin (cis-diammine-cyclobutanedicarboxylate-platinum (II)) is a cisplatin analogue developed in the early 1980s, belonging to the second generation of platinum compounds. It was approved by FDA in 1989, with the aim of reducing the collateral effects of cisplatin (Ho et al., 2016). Cisplatin and carboplatin represent the two most effective platinum-agents used for the treatment of patients affected by solid malignancies including gynecologic and testicular tumours, thoracic malignancies, sarcomas, head and neck, gastric and bladder cancers (Ho et al., 2016). The core of their planar chemical structure includes the presence of a doubly-charged platinum atom surrounded by four ligands: two *cis*-diammine carrier ligands and two specific leaving groups also in *cis* position, responsible for the covalent binding between platinum ion and DNA bases (**figure 1.17**) (Makovec, 2019). Structurally, carboplatin differs from cisplatin for the presence of a bidentate dicarboxylate ligand instead of two chloride ligands (**figure 1.17**), but in terms of activity, it forms the same reaction products at the equivalent dose of cisplatin, although with different kinetics (Dasari and Tchounwou, 2014).

Carboplatin displays a lower reactivity, a slower kinetic, but also a lower excretion rate, that translated in a retention half-life of 30 hours compared to 1.5/ 3.6 hours for cisplatin and is less potent, requiring a higher dose to reach the same effectiveness of cisplatin (Dasari and Tchounwou, 2014). The toxicological profile of the two drugs is different: carboplatin limiting toxicity being myelosuppression, while nephrotoxicity, neurotoxicity and ototoxicity are the most frequent side effects of cisplatin (Dasari and Tchounwou, 2014).

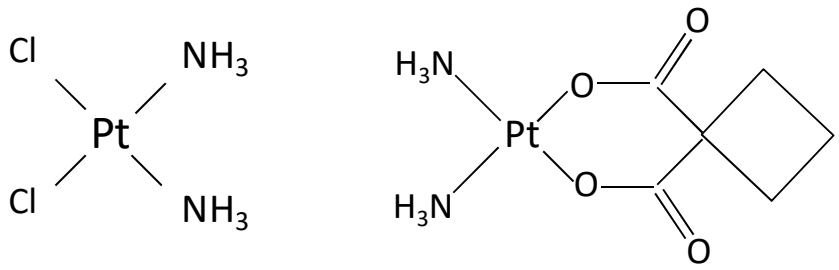

Figure 1.17 Chemical structures of cisplatin (left) and carboplatin (right)

1.3.2 Mechanism of action

Platinum agents are administered intravenously and from the blood stream they have to enter the cells to exert their therapeutic/cytotoxic effect, but the mechanisms of platinum intake are not fully elucidated (Makovec, 2019). Platinum enter the cells mainly by passive diffusion or facilitated diffusion, thanks to some membrane transporters of the solute carrier super-family. Cisplatin is a substrate of the cation transporters OCT1 and OCT2, primarily expressed in liver and kidney respectively (Makovec, 2019), while the role of copper transporters CTR1 and CTR2 is still debated. In fact, recent studies seem to exclude these trans-membrane proteins directly transporting cisplatin and carboplatin into the cells, as they do with copper (Makovec, 2019). Probably, copper transporters bind platinum and this interaction leads to a vesicular internalization by pinocytosis that also prevents drug inactivation by glutathione (GSH) and metallothioneins (MTs) (Arnesano et al., 2007). In parallel, platinum molecules can exit the cell both passively and, in an energy-dependent

manner. Another two copper transporters ATP7A and ATP7B are localized on Golgi membranes and on cytosolic vesicles. They internalize platinum molecules in an ATP-dependent way into vesicles, facilitating the efflux of the drug throughout the cell and keeping it outside the nucleus (Zhou et al., 2020). Platinum efflux is catalyzed by multidrug resistance-associated proteins (MRP, ABCC), especially MRP2 and MRP4 for cisplatin, functioning as ATP-dependent efflux pumps. The balance between these import and export mechanisms is such that only 1% of the administered drug will reach the therapeutic target (Makovec, 2019).

Cisplatin and carboplatin can be considered prodrugs, since they need to be transformed into the pharmacologically active drug (Gheorghe-Cetean et al., 2017) through a reaction of "aquation" that occurs in the cytoplasm and consists in the substitution of one or both the leaving groups with molecules of water, leading to a very reactive, positively charged molecule. The "aquation" reaction happens spontaneously, probably due to the lower intracellular concentration of chlorides than in the extra-cellular environment for cisplatin; for carboplatin, the biotransformation in its active form requires an active cleavage of the cyclobutane-decarboxylate groups by an esterase (Ho et al., 2016). However, the active species derived from cisplatin and carboplatin are the same (Dasari and Tchounwou, 2014). The hydrolyzed platinum-derived products are strongly reactive electrophile molecules, which bind with any nucleophilic species like proteins enriched in cysteine and methionine aminoacids, (i.e. glutathione and metallothioneins), or nitrogen donor atoms on nucleic acids (i.e. RNA and DNA). Hence, platinum agents are able to form covalent bindings with both DNA or non-DNA targets.

All platinum targets are responsible for their cytotoxic effect on normal (toxic effects) and tumour cells (antitumour effects) (Gheorghe-Cetean et al., 2017). It was estimated that even if DNA platination is the main mechanism through which platinum drugs induce cell death, only 5-10% of platinum adducts are found in genomic DNA, while the remaining involve non-DNA targets (Gheorghe-Cetean et al., 2017) (**figure 1.18**). The active forms of cisplatin

and carboplatin also trigger reactive oxygen species (ROS) production and induce cellular oxidative stress, blocking mitochondrial respiration (Aggarwal, 1993) and calcium uptake in mitochondria. Excessive accumulation of ROS, damaged mitochondria and imbalance of calcium homeostasis can reduce ATPase activity and induce apoptosis besides DNA damage (Dasari and Tchounwou, 2014; Kleih et al., 2019). Furthermore, platinum can bind the zinc-finger motif present in several protein DNA-binding domains, such as DNA polymerase α, one of the major players involved in DNA replication (Makovec, 2019). Another non-DNA target of cisplatin and carboplatin with lethal consequences for the cell is tubulin. Tubulin requires guanosine-5'-triphosphate (GTP) to assembly into microtubule filaments forming part of the cytoskeletal structure, but platinum drugs bind to the N7-atom in guanine of GTP preventing the exchange of energy between GTP and tubulin, slowing microtubule formation and interfering with mitosis, causing cell-cycle arrest and possibly cell death (Makovec, 2019). GSH represents the main non-DNA target of platinum drugs, due to the amount of thiol groups in GSH with which platins strongly interact. This interaction is fundamental in the platinum drugs pharmacodynamic, because the intracellular GSH-level and the rate by which the enzyme glutation S-transferase (GST) conjugates GSH to the drug determine the amount of drug inactivated through cellular excretion (Mistry and Harrap, 1991; Sawers et al., 2014).

The interactions of platinum agents with cellular proteins and DNA, their activation and transformation are summarized in **figure 1.18**.

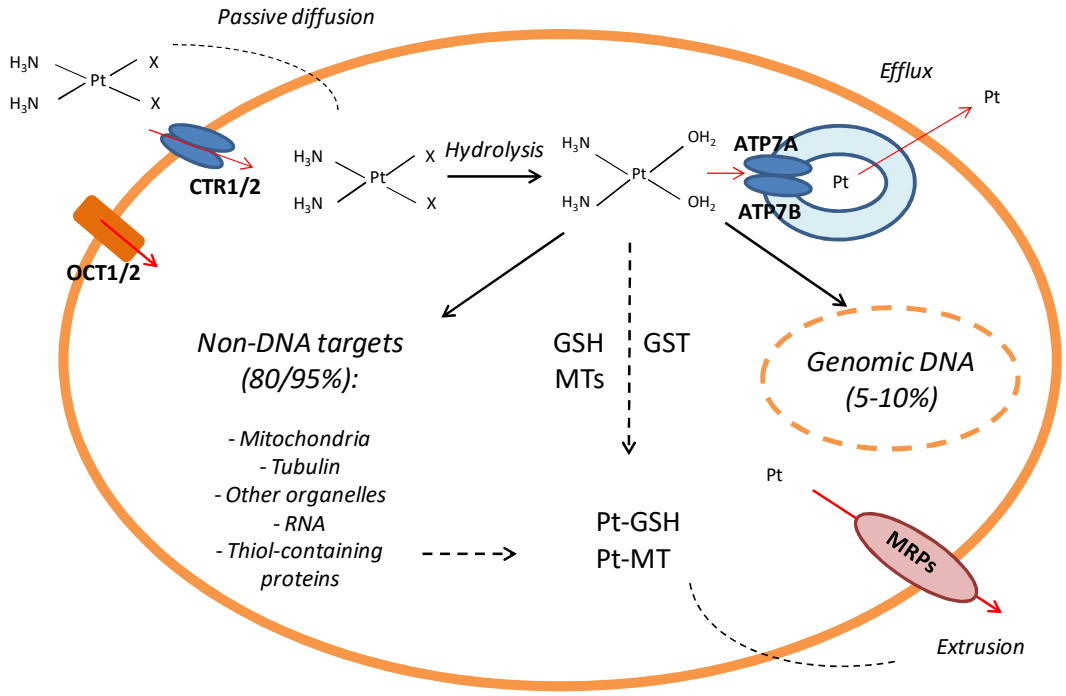

Figure 1.18 Intracellular trafficking of platinum compounds (cisplatin and carboplatin)

Platinum drugs may enter the cell by passive diffusion, cation transporters (OCT1, OCT2) or copper transporter proteins–CTR1, CTR2. Once in the cytoplasm, platinum drugs are activated by a hydrolysis reaction, where the leaving groups are substituted with one or two water molecules. The active form is an electrophilic species which interact with DNA, RNA, organelles (lysosomes, endoplasmatic reticulum) and proteins enriched in sulfhydryl or thiol groups, especially glutathione (GSH) and metallothioneins (MTs). Platinum bound to MTs or GSH by the enzyme glutathione S-transferase (GST) is actively extruded from the cell by multidrug resistance-associated proteins (MRPs) or another P-glycoprotein ATPases (ATP7A, ATP7B).

Despite the presence of multiple non-DNA targets, genomic DNA is the principal target of platinum agents responsible for the pharmacological activity (Chaney et al., 2005; Dasari and Tchounwou, 2014). In particular, cisplatin and carboplatin form the same irreversible DNA-adducts (different from those generated by oxaliplatin) that from here on will be named Pt-DNA adducts (Chaney et al., 2005; Schoch et al., 2020). Cisplatin and carboplatin bind the nucleophilic N7 atom on the purine bases, the most reactive and accessible atom in the nucleotides, forming mono-adducts, which can evolve, forming a second covalent binding with another purine base, into two structurally different kind of crosslinks: intra-

strand crosslinks when platinum binds two adjacent purine bases within the same DNA strand or inter-strand crosslinks (ICLs), if the two bases are on opposite strands (Chaney et al., 2005). Among the Pt-DNA adducts, the most diffuse are the intra-strand crosslinks, especially 1,2-intrastrand p(GpG) crosslinks (~65%) between two guanines (**figure 1.19, A**), and 1,2- intra-strand p(ApG) crosslinks (~25%) (**figure 1.19, B**); inter-strand p(GpG) crosslinks (~10%) (**figure 1.19, C**) are the most cytotoxic lesions, as they interfere with DNA transcription and lead to apoptosis if not removed; 1,3-intrastrand p(GpXpG) crosslinks (~3%) between guanine and cellular proteins (**figure 1.19, D**) described to contribute to platinum effect, even if to a lower extent (Dasari and Tchounwou, 2014; Eastman, 1987).

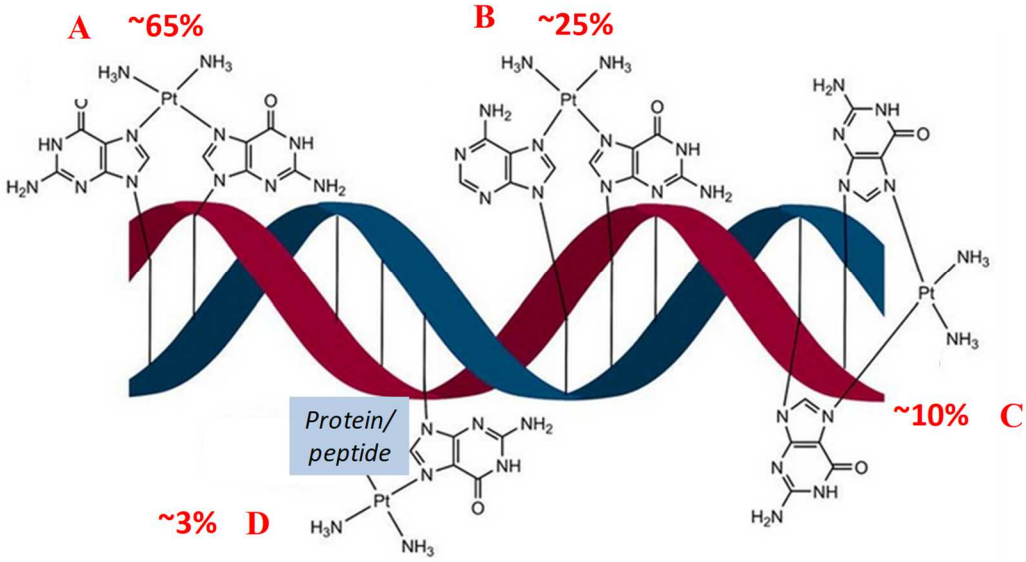

Figure 1.19 The most common intra-strand and inter-strand Pt-DNA adducts on DNA and their frequency

A) 1,2-intrastrand p(GpG) crosslink, the most diffuse (~65%) Pt-DNA adduct. **B)** 1,2 intrastrand p(ApG) crosslink. **C)** interstrand p(GpG) crosslink, the most cytotoxic lesion. **D)** 1,3-intrastrand p(GpXpG) crosslink, between guanine and intracellular proteins. (Modified from Łomzik M.'s PhD thesis (2016)).

The pathway leading to cell death by unrepairable platinum-induced DNA damages is complex and involves several proteins, cascades of signaling pathways, and is triggered by the block of DNA transcription and duplication (Dasari and Tchounwou, 2014; Jung and Lippard, 2006). Pt-DNA adducts can result in DNA SSBs or the more severe DNA DSBs, which are recognized by DNA damage sensors, in particular two kinases ataxia telangiectasia mutated protein (ATM) and the ATM- and RAD3-related protein (ATR), which act as mediators between DNA damages and the checkpoint regulators checkpoint kinase 1 (CHK1) and 2 (CHK2), each substrates and downstream effectors of ATR and ATM, respectively (Damia et al., 2001; Galluzzi et al., 2012). Their activation initially causes a transient block of the cell cycle, typically in phase G2/M, the stabilization through phosphorylation on Serine 20 of the tumour suppressor protein p53 (Galluzzi et al., 2014), and activation of specific DNA repair pathways. Typically, Pt-DNA adducts involved NER, BER, MMR, HR and TLS (Galluzzi et al., 2014; Martin et al., 2008; Slyskova et al., 2018; Zhou et al., 2020).

If the damage caused by Pt-DNA adducts is too high and cannot be removed in a short frame, the cellular balance between survival and apoptosis moves towards the second option and different cascade signaling pathways are activated to induce cell death (Galluzzi et al., 2014). Besides p53, the master regulator of intrinsic and extrinsic apoptotic pathways, also other secondary pro-apoptotic signaling pathways related to mitogen-activated protein kinase (MAPK) pathway, such as extracellular signal-related kinase (ERK), c-Jun N-terminal kinase (JNK) and stress activated protein kinase (p38-MAPK) can be activated after platinum exposure. Activation of these circuitries and their consequences following cisplatin treatment are still debated, however, it seems that ERK activation may contribute to cell cycle arrest to favour DNA repair, while JNK and p38-MAPK pathways may contribute to the activation of apoptosis via p53 and p73 activation, respectively (Achkar et al., 2018).

1.4 MECHANISM OF ACTION OF PARP INHIBITORS

1.4.1 PARP inhibitors

The introduction of PARP inhibitors (PARPi) in clinical practice has represented a recent revolution in the management of advanced ovarian carcinoma, since the time of approval of platinum agents more than forty years ago, both in terms of efficacy and for the novelty of its rationale. As previously described, the "synthetic lethality" approach fits well with the genomic profile of HGSOCs, that have defects in HR DNA repair pathway in half of the cases (Konstantinopoulos et al., 2015). In fact, PARPi have been shown to be extremely active in cells lacking HR and their use in HR deficient tumours represents the direct translation of these results. However, it has been shown that PARPi clinical activity may be extended also to HR-proficient tumours (Franzese et al., 2019).

At present, olaparib, rucaparib and niraparib are approved for the treatment of ovarian cancer in different therapeutic settings (chapter 1.4), while veliparib and talazoparib are under study in late phase clinical trials, in patients with newly diagnosed ovarian cancer, as well as in other advanced cancer, as single agent or in combination with other chemotherapies (Pilié et al., 2019). Currently, there are no clinical trials comparing head-to-head different PARPi, but preclinical studies showed pharmacological differences in terms of activity and side effects among single compounds. However, PARPi have shown an overall safe-profile, with fatigue, gastrointestinal symptoms and myelosuppression being the more common toxicities (Jiang et al., 2019).

Despite the promise and encouraging results obtained with the introduction of PARPi in oncology practice, several aspects need to be clarified to improve their clinical use, as the identification of PARPi response, beyond tumour HR status and mechanism underlying PARPi resistance observed in patients treated with these agents.

1.4.2 Mechanism of action

The poly (ADP-ribose) polymerase (PARPs) family includes 18 nuclear highly conserved proteins. PARP1 is the most characterized enzyme within this family and is involved in a broad spectrum of cellular mechanisms, in particular DNA repair and DNA damage response, but also chromatin remodeling, replication, transcription, and cell death signaling. PARP2 has similar functions and is believed to be able to compensate for the loss of PARP1 in vivo, but its role in DNA repair is less prominent (Kamaletdinova et al., 2019). The PARP1 structure includes four domains: one N-terminal DNA binding domain including two zinc-finger motifs, a C-terminal catalytic domain, a central auto-modification domain, and a caspase-cleaved domain (Liu and Tewari, 2016). The enzymatic function of PARP enzymes is named poly ADP-ribosylation (PARylation) and consists in transferring one or more ADP-ribose groups (up to 200) to glutamate, aspartate, serine, arginine or lysine residues on PARP1 itself or other acceptor proteins, using NAD+ as cofactor (Gavande et al., 2016). PARylation is a post-translational modification where PAR chains typically provide interaction scaffolds for other binding proteins. Among targets of PARP1 PARylation there are DNA repair proteins, whose recruitment is facilitated at the site of DNA damage, accelerating DNA repair. At the end of the process, PAR chains are rapidly erased by PAR-degrading enzymes, such as poly (ADP-ribose) glycohydrolase (PARG) (Kamaletdinova et al., 2019).

PARP1 can PARylate core histone H1 proteins causing relaxation of chromatin structures leaving DNA more accessible to replication machinery, transcriptional factors, and DNA repair proteins (Weaver and Yang, 2013). However, PARP1 is mostly studied in relation to its role in the repair of DNA SSBs and alkylating agent-induced DNA damages, since 90% of its PARylating activity is done in response to DNA damage (Kamaletdinova et al., 2019). In particular, PARP1 has a critical role in

different DNA repair pathways, such as BER, HR and NHEJ contributing to maintenance of genomic stability (Franzese et al., 2019). The enzyme is activated in the presence of SSB, which recognizes and links by means of its zinc finger binding motifs. The interaction with DNA causes a conformational change and its activation, leading to PARylation of proteins effectors of BER (i.e. XRCC1, DNA ligase III and DNA polymerase beta), which are recruited close to SSB to form a multi-complex that executes SSB repair (Franzese et al., 2019) (**figure 1.11**). The second target of PARP1 PARylation is PARP1 itself. The auto-PARylation happens in its central auto-modification domain, causing structure modification allowing the formation of a scaffold necessary for the recruitment of other proteins, and subsequently leading to its own release from DNA, restoring the catalytic site in the inactive state (Eustermann et al., 2015).

Globally, PARP1 prevents genomic instability by supporting also the repair of DSB, by activating the cell cycle regulator ATM during G1-M cell cycle phases, and recruiting the HR factors NBS1 and MRE11 to the damaged site, leading to activation of HR (Cook and Tinker, 2019). Simultaneously, PARP1 down-regulates the DSB error-prone pathway NHEJ, by inhibiting Ku70 and Ku80 (Patel et al., 2011). It is noteworthy that in the presence of high levels of DNA damage, the intracellular pool of NAD^+ may significantly reduce due to hyper-activity of PARP1. This situation, common in high proliferative, genomic unstable cancer cells, may determine an energy crisis which, if not reestablished, can induce cell death through the activation of JNK and release of pro-apoptotic proteins, such as Bax (Franzese et al., 2019).

In two seminal papers, it was shown that PARP inhibition caused disruption of DNA repair at different levels, mainly blocking SSB repair and inducing collapse of replication fork, thus generating DSBs. An overwhelming amount of DSB and inability to repair them by HR increased genomic instability and led to cell death. (Bryant et al., 2005; Farmer et al., 2005).

The PARPi currently used in the clinic, are small molecules able to inhibit the catalytic function of PARP1 and PARP2 by competing with NAD+ thanks to the nicotinamide moieties present in their structure (Mateo et al., 2019). This was the first mechanism of action described, and it was believed that prevention of PARylation was sufficient to impact the repair of SSB, leading to the activation of NHEJ in cancer cells with defective HR. The increased error-prone activity of NHEJ ultimately caused replication stress, chromosomal ruptures and finally apoptosis (Lord and Ashworth, 2016; Lupo and Trusolino, 2014). Subsequently, a second and more critical mechanism of action of PARPi was described in which an allosteric conformational change due to PARPi stabilizes PARP1/2 association with DNA at the damaged site, preventing enzyme release. This mechanism was defined "trapping" and the block of PARP proteins on damaged site prevents the recruitment of DNA repair machinery and also determines stall or, alternatively, the irreversible block of replication with subsequent collapse of the fork, resulting in DSB formation, and in replication stress (Murai et al., 2012). This mechanism was firstly described in preclinical models, where PARP1 was trapped on DNA damaged sites forming stable PARP-DNA complexes, that were not observed in cells lacking PARP1, suggesting also the importance of PARP expression for this mechanism (Murai et al., 2012). The efficacy of each PARPi better associated with their PARP-trapping ability than with the catalytic inhibition. For instance, talazoparib exhibits the greatest cytotoxicity and higher PARP-trapping potency, 100-fold higher than olaparib and rucaparib; niraparib has higher trapping activity than olaparib and rucaparib (about 10-fold), while veliparib is the least potent (100-fold lower than olaparib and rucaparib) (Murai et al., 2012). Ultimately, the combination effect of catalytic inhibition, which prevents auto-PARylation of PARP and trapping determine a substantial accumulation of PARP on DNA, close to the damage sites. PARP-DNA complexes are stable and prevent by steric hindrance the binding of DNA repair effectors and cause stalled replication fork that during the S

phase of the cell cycle lead to DSBs. This situation in healthy/HR proficient cells can be bypassed by activating HR to repair the DSBs, while in HR deficient cells NHEJ will take over. Being an error-prone pathway, there will be less efficient and less accurate DBS repair leading to DNA damage accumulation and cell death (Franzese et al., 2019) (**figure 1.20**).

Although, this is the dominant mechanism explaining the activity of PARPi in HRD tumours, alternative mechanisms have been proposed to explain the efficacy of PARPi in HR-proficient tumours, which rely on the consequences of PARP inhibition in other biological processes, such as energy metabolism and chromatin modification (Gavande et al., 2016).

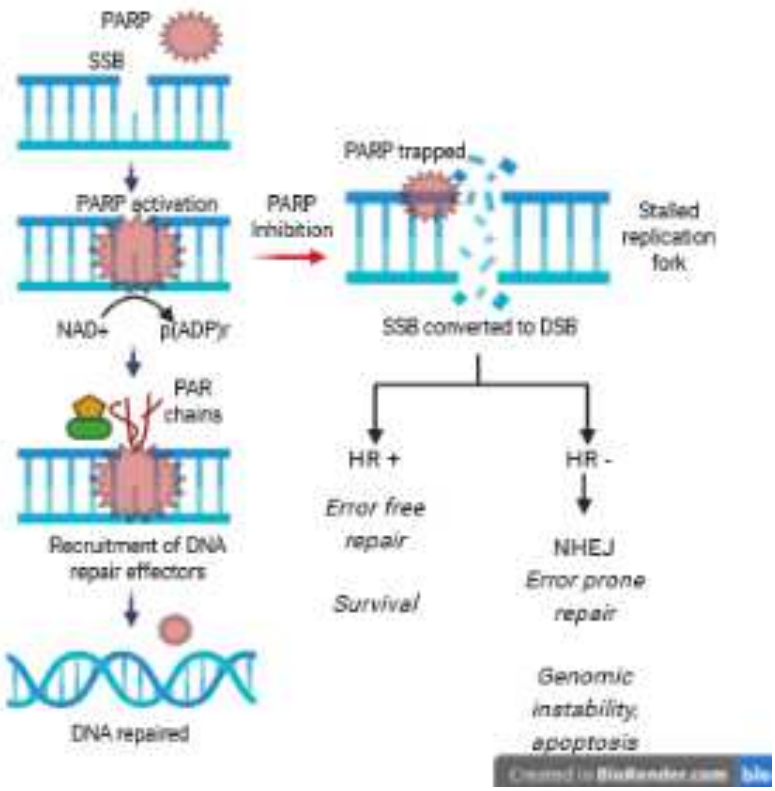

Figure 1.20 PARP activity and role of PARP inhibition in DNA repair and synthetic lethality

Left panel: PARP1 (red) binding to an induced single-strand break (SSB) results in activation of auto and trans poly ADP-ribosylation, forming PAR chains with scaffold function on PARP1 itself and on target proteins. This function aims at recruiting DNA repair effectors (i.e. XRCC1, DNA polβ, DNA ligase III) (yellow and green) and promotes DNA damage resolution. In the presence of PARP inhibitors (right panel),

PARP1is trapped on DNA damaged site, PARylation activity is blocked and replication fork stalled and then collapses generating double-strand breaks (DSB). In healthy/Homologous Recombination proficient (HR+) cells, HR is activated, DSB are repaired and cell cycle proceeds. While, in HR deficient cells (HR-), the error-prone DSB repair pathway non-homologous end-joining (NHEJ) is the only pathway available, but its activity alone induces DNA fragmentation, genomic instability and finally apoptosis (image created using BioRender ((“https://biorender.com/,”).

1.5 DETERMINANTS OF RESPONSE TO PLATINUM AGENTS AND PARP INHIBITORS THERAPY IN EOC

Ovarian cancer responsiveness to first-line standard therapy and eventually, to subsequent lines in case of tumour relapse, is still an unpredictable and urgent clinical question. Several possible predictive biomarkers and assays have been studied for precision medicine, but, at present, strong and accurate clinical tests to predict therapy response are still missing. As previously mentioned, "platinum-free interval" (PFI) is the reference marker of response currently used to choose the best therapeutic regimen in relapsed HGSOC (Milanesio et al., 2020). In addition, *BRCA* mutational status, histology, adverse symptoms to previous treatments and outcome after surgery are the other criteria considered in clinic to address patients to platinum and/ or PARPi-based therapy (Wilson et al., 2017). However, preclinical and clinical research are actively searching more accurate determinants of response.

Considering the importance of DNA repair in the mechanism of action of platinum agents and PARPi and the fact that more than 50% of HGSOC have defects in HR, I will summarize which are the data available on possible DNA repair-associated biomarkers of response to both platinum agents and PARPi in dedicated chapters. In addition, a brief summary of other mechanisms and pathways not related to DNA repair, but described to be important for the cellular response to these drugs will also be described.

1.5.1 Determinants of response to platinum compounds

Starting from the discovery of platinum compounds, different cellular or cancer conditions have been described able to modulate platinum cytotoxic effects. Mechanisms summarized in **figure 1.21** have been studied in relation with resistance or sensitivity to platinum, in preclinical models and in the clinic to find possible predictors of response. However, at the present, there are not yet specific molecular biomarkers validated in the clinic.

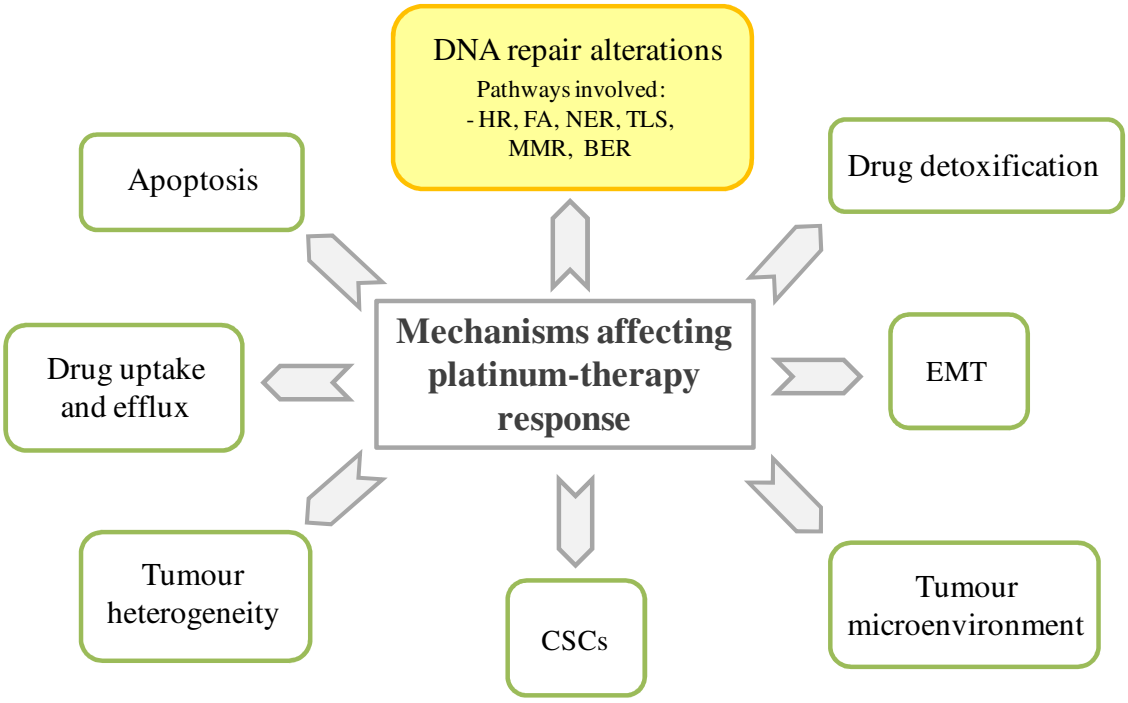

Figure 1.21 Schematic summary of the most studied pathways and tumour conditions able to influence the anti-tumour effect of platinum compounds in ovarian carcinoma

1.5.1.1 DNA repair as determinant for platinum-response

The cytotoxic effect of platinum chemotherapy mainly depends on the activity of several DNA repair pathways activated by the cell to cope with the different kinds of DNA damages generated by the drugs. It can be stated that monoadducts are repaired by BER, intra-strand crosslinks by NER, MMR and TLS, while the more severe ICLs and DSBs are repaired

through a coordinate interplay of different pathways: HR, FA, NER and NHEJ (Haynes et al., 2015). While preclinical evidence suggests that cells lacking NER, HR/FA and NHEJ pathways are extremely sensitive to platinum agents (Galluzzi et al., 2014), the inverse correlation is not always clear and sometimes discrepancies have been reported in experiments aimed to verify if up-regulation of different proteins/ DNA repair systems are associated with drug resistance (Galluzzi et al., 2014).

As described above, ICLs and DNA DSBs induced by platinum compounds, are mostly repaired by the HR and FA pathways during G2/S phases of the cell cycle (Deans and West, 2011; Michl et al., 2016). In addition, at least 50% of HGSOC has been shown to be deficient of HR, probably accounting for its extreme sensitivity to platinum drugs. The HR deficiency in HGSOC relies mainly on mutations/altered expression of genes involved in the above-mentioned pathways. Indeed, loss of function germline mutations (~14% of HGSOC) or somatic mutations in *BRCA1/2* genes (~3% of HGSOC) or in *FANCD2* (~1% HGSOC), are the most frequently mutated genes involved in HR and FA pathways, respectively (Cancer Genome Atlas Research Network, 2011). These patients are extremely sensitive to therapy (Garsed et al., 2018; Rocha et al., 2018), because impaired HR/FA function affects the ability of cancer cells to cope with platinum-induced ICL (Hoppe et al., 2018). *BRCA*-mutated patients also have a better prognosis than *BRCA*-wild type/HR proficient carriers, in part due to the enhanced sensitivity to chemotherapy (Hoppenot et al., 2018).

Beside *BRCA*-mutations, HGSOC may harbour genetic or epigenetic alterations in HR-related non-*BRCA* genes, which are involved directly in HR pathways (i.e. core *RAD51* genes), or regulate HR (i.e. *CDK12*) or are involved in other DNA repair pathways that collaborate with HR in the solution of platinum-induced damages (i.e. FA family genes) (Konstantinopoulos et al., 2015). Mutations in HR-related non-*BRCA* genes determine the so-called *BRCA*ness phenotype, a synonymous of HRD and a concept defined in 2004 to describe this subgroup of sporadic cancers with HRD and a phenotype similar to *BRCA*-mutated tumours (Turner et al., 2004).

Among them, interestingly, CDK12 is a transcription dependent kinase involved in the regulation of transcription of several DNA repair genes, such as *ATM, ATR, Chk1, FANCI*, and *RAD51C* (Ekumi et al., 2015), and *CDK12* amplifications or mutations affecting its catalytic domain account for 4% of HGSOC cases (Cancer Genome Atlas Research Network, 2011). Preclinical evidence showed that knock-down of *CDK12* sensitizes cells to both platinum drugs and PARPi, due to the downregulation of HR and FA genes, making CDK12 a possible target for therapy in cancer and an interesting possible marker of response to therapy (Chilà et al., 2016; Naidoo et al., 2018). The HRD phenotype is shown in HGSOC with *PTEN* suppressor homozygous loss (7% of HGSOC), which interferes with *RAD51* transcription, or with *EMSY* amplification (6% of HGSOC), whose role has yet to be defined (Konstantinopoulos et al., 2015).

Despite the emerging role of several genes and proteins as potential predictive biomarkers in EOC, so far, the presence of germline or sporadic *BRCA1/2* mutations is considered the best clinical determinant of response to platinum agents, even if the existence of variants of uncertain significance (VUS) and the onset of secondary somatic mutations able to restore the HR proficient status need to be taken into consideration to avoid false classification of HRD tumours (Hoppe et al., 2018). In fact, the most diffuse mechanism inducing platinum and PARPi resistance in *BRCA1/2* mutated carriers, consists in re-activation of HR function, caused by secondary reversion mutations or intragenic deletions. Such mutations are able to restore the protein reading frame, recovering the functional protein and consequently, the HR proficient phenotype (Galluzzi et al., 2014; Weigelt et al., 2017). These secondary mutations were observed in relapsing HGSOC, that have been previously treated with platinum agents, confirming their role in acquired drug resistance (Colombo et al., 2014). Recently, these mutations have been detected in tumour circulating free DNA (cfDNA) in patients with *BRCA1/2* germline mutations with breast or ovarian cancers, refractory and resistant to platinum or pre-treated with platinum and/or PARPi (Lin et al., 2019; Weigelt et al., 2017). In addition, mutations have been also reported in other HR genes, such as

RAD51C, RAD51D and *PALB2* (Lin et al., 2019). Analysis of *BRCA*-mutations in cfDNA by next-generation sequencing (NGS) is an extremely interesting and explored method, since liquid biopsies could be a useful clinical companion technique. The ability to identify in "real-time", one or multiple reversion mutations simultaneously long before the clinical manifestation of resistance to platinum or PARPi, and with minor discomfort for the patient, could help oncologists to re-direct therapeutic regimens (Milanesio et al., 2020). Reacquisition of HR activity can also rely on epigenetic changes, such as demethylation of *BRCA1/2* or *FANCF* promoters, often hypermethylated in tumours, with regaining of protein expression (D'Andrea, 2003; Patch et al., 2015). Such genetic and epigenetic modifications may be the results of genomic instability and chromosomal rearrangements, which usually characterizes HR-deficient tumours (Colombo et al., 2014).

As said, in ovarian cancer patients, germline-*BRCA*-mutations as well as germline or somatic mutations in HR-related genes (included somatic mutations in *BRCA1/2*) predicted response to DDP (p=0.0002) (Pennington et al., 2014). In addition, a better prognosis has been reported in germline-*BRCA*/HR-mutated patients with increased OS compared to *BRCA*/HR-wild type patients (HzR 0.6, CI 95% 0.4–0.8, p>0.0006). In particular, germline-*BRCA*-mutated patients had a median OS of 66 months, HR-mutated carriers 59 months, and HR-wild type 41 months, without significant difference between *BRCA*-mutated and HR-mutated patients (p=0.09) (Pennington et al., 2014). Using a targeted capture and massively parallel genomic sequencing method Pennington *et al* pinpoint the role of "omics" techniques in identifying genomic alterations. In fact, the identification of *BRCAness*/DDP sensitive tumours remains one of the major challenges in cancer management (Lord and Ashworth, 2016), and tests able to accurately predict this condition would have also a double positive effect, since these patients may eventually benefit by use of PARPi therapy (Ceccaldi et al., 2015).

Deep sequencing methods allowed identification of cancers with altered DNA repair pathways large scale disarray in chromosomal structures (Hasty and Montagna, 2014).

Specifically, it is now possible to evaluate through a combination of genomic profiling techniques (i.e. complementary genomic hybridization (CGH), single nucleotide polymorphisms (SNP) genotyping and next generation sequencing) such "genomic scars" originating from loss of HR function. Genomic scars are a sort of footprints left in the genome after exposure to DNA damage in a repair deficient background, and are generally characterized by loss of heterozygosity (LOH) and copy number changes (Hoppe et al., 2018; Watkins et al., 2014). The comparison between genomic scars in *BRCA*-mutated and *BRCA*-wild type tumours has shown common profiles associated with HR defects, suggesting the presence of a *BRCA*ness phenotype (Stover et al., 2016). Not only defects in HR can determine genomic signatures. For instance, also microsatellite instability can be detected in the presence of mismatch repair defects (Akbari et al., 2017; Fusco et al., 2018). Specific assays have been developed as companion diagnostic tools to identify HRD and platinum sensitive tumours (Watkins et al., 2014). Methods that will be described were developed to identify peculiar genomic signatures associated with a DNA repair defective to be possibly used as biomarker of HRD. CGH array detects copy number variations (CNV), which are gains or losses of genomic material, affecting gene expression (Hehir-Kwa et al., 2015); it has been applied to identify *BRCA*ness breast cancers and a CGH signature was also associated with better responsiveness to platinum therapy (Vollebergh et al., 2014). Using SNP array data, two commercial genomic scar assays have been tested in clinical trials to identify tumours with HRD. The "myChoice HRD" assay by Myriad evaluates the presence of LOH, telomeric allelic imbalance (TAI) and large-scale transitions (LST) overall the genome, and based on these signatures an "HRD score" can be calculated, which classifies as HRD-positive tumours with score ≥42, and HRD-negative those with a score <42 (Pellegrino et al., 2019; Stronach et al., 2018). The "FoundationFocus CDx (*BRCA* LOH)" test by Foundation Medicine, Inc. is based on the presence of *BRCA1/2* mutations and percentage of the genome affected by LOH, and based on these factors a LOH-score has been defined, considering HRD-positive ≥16 and negative <16 (Coleman et al., 2017;

Pellegrino et al., 2019). Considered singularly, LOH is frequently found in HGSOC and Wang and colleagues estimated LOH and CNV in ovarian cancer patients finding that high-LOH group patients also include *BRCA*-mutated patients and was associated with increased platinum-sensitivity and PFS, both considering or excluding *BRCA*-mutated patients from this group (Wang et al., 2012). The TAI score quantifies allelic loss or CNV extended from the damaged site to the telomere, without crossing the centromere (De Picciotto et al., 2016) and a high TAI score was shown to predict platinum-response in ovarian and breast cancer, in vitro and in patients, and was associated with *BRCA1/2* mutations (Birkbak et al., 2012). The LST identifies large chromosomal breaks between adjacent regions (at least 10Mb), and a high LST score was found to predict *BRCA1/2* inactivation in basal-like breast cancer (Popova et al., 2012). Marquard *et al*. studied the pan-cancer distribution of single LOH/TAI/LST-associated signatures and quantified for each a relative score in 5371 tumours, derived from 15 different tumour types (Marquard et al., 2015). They found that the single scores positively correlated with one other, and the distribution of the three signatures in the same tumour type had a similar trend, suggesting that LOH, TAI and LST depend on tumour biology. Moreover, tumours that received DDP shared higher median scores relative to LOH, TAI and LST, suggesting the platinum treatment determines reproducible genomic alterations that can be detected with these methods (Marquard et al., 2015). These data suggested that considering LOH, TAI and LST signatures together could be a method to assess a predictive assay, laying the foundation for "myChoice HRD" assay development, whose predictive potential for platinum therapy was validated in a retrospective analysis on data deriving from three single-arm clinical trials in neoadjuvant setting of triple negative breast cancer. The analysis showed that an HRD-positive score (≥42) associated with increased possibility to achieve a complete response to therapy or minimal residual disease after neoadjuvant therapy, regardless of *BRCA*-mutational status (Telli et al., 2016). In ovarian cancer it was validated as companion diagnostic test in the niraparib clinical trial (chapter 1.5.4) (Mirza et al., 2016b).

Besides the identification of point mutations in HR genes and CGH and SNP-based arrays evaluating genomic scars, mutational signatures can be detected and analysed through NGS as distinctive mutational patterns of the single tumours, determined by specific mutagenic exposures and processes of repair along the life course of the cell (Hoppe et al., 2018).

The BROCA test is a targeted capture and massively parallel sequencing assay, that identifies mutations in key HR genes and predicts increased primary treatment platinum sensitivity and longer overall survival in EOC (Morse et al., 2019; Pennington et al., 2014). *BRCA*-mutated tumours are typically characterized by enhanced mutational burden, which can be considered by combining somatic mutation count with CNV. The analysis of these genomic alterations led to identify peculiar mutational signatures (Hoppe et al., 2018). Signature 3 is a mutational signature described by Alexandrov *et al*. and was associated with the HRD phenotype, in particular with *BRCA*-mutations (Alexandrov et al., 2013). This signature has been recognized in different tumour types including pancreatic, breast and other cancers, and used as predictive biomarker for DDP response (Alexandrov et al., 2013), and more recently, for rucaparib in triple negative breast cancer (Chopra et al., 2020).

The HRDetect mutational-signature-based algorithm is a weighted model of mutational signatures, including a score of microhomology-mediated deletions, base substitutions and rearrangement signatures and HRD score, based on genomic scars. The HRDetect test has demonstrated good performance in predicting *BRCA*ness phenotype in breast, ovarian and pancreatic cancer, identifying *BRCA*-deficient tumour in FFPE samples with a narrow edge of error (Davies et al., 2017). Interestingly, this assay also considers epigenetic alterations in *BRCA1* promoter, and it has been able to identify a *BRCA*ness phenotype in one-third of the tumours analysed *BRCA* wt and without known HR-gene mutations (Davies et al., 2017), suggesting its potential use as companion diagnostic in clinical trials. Very recently, the HRDetect assay has been tested in a triple negative breast cancer trial aimed to investigate the activity of PARP inhibitors. The HRDetect test successfully identified HRD tumours (Chopra et al., 2020).

However, the predictive value of genomic scar and mutational signature-based tests needs to be improved, since they do not reflect the dynamic of tumour evolution. In fact, they lose part of their predictive potential in the advanced cancer setting, where metastatic or relapsing tumours after treatment may acquire secondary mutations, that restore HR functionality leading to drug resistance, without modifying the original genomic scars and mutational signatures of HRD (Pellegrino et al., 2019). This is of particular importance in ovarian cancer, where secondary mutations restoring *BRCA*-function occur in approximately half of HGSOC with acquired resistance to platinum (Norquist et al., 2018). A possible solution to overcome these limitations is the development of assays to evaluate the functional proficiency/deficiency of HR repair (chapter 6).

2% of HGSOC show mutations affecting FA genes, such as *PALB2, FANCA, FANCI, FANCL*, and these tumours are considered HR-deficient, sharing the same hyper-sensitivity to platinum-based chemotherapy and PARPi (Konstantinopoulos et al., 2015). The FA pathway is activated during S phase to repair ICLs cooperating with HR; however, it has been shown that several FA proteins act in NER and TLS, and alt-EJ, regardless of the cell cycle phase (Ceccaldi et al., 2016).

One mechanism of resistance to ICL-inducing agents is the accelerated removal of DNA bulky adducts, as observed in ovarian cancer after prolonged exposure to cisplatin, and this has been associated also with high level of FANCF (Dabholkar et al., 1994, 1992; Taniguchi et al., 2003). The *FANCF* promoter is often subjected to hyper-methylation in EOC causing a reduced protein expression. It was reported that platinum-treatment caused a hyper-methylation of *FANCF* promoter and is associated with resistance to DDP and to mytomicin C, another ICL-inducer drug (Patch et al., 2015; Taniguchi et al., 2003). Besides ICL-repair, the other major function of FA is protection of the replication fork, also in *BRCA1/2*-deficient tumours and suppression of the error-prone NHEJ during the replication phase (Ceccaldi et al., 2016; Kais et al., 2016), suggesting its importance not only as determinant of platinum-chemotherapy, but also to other DNA damaging agents.

The NHEJ pathway is the alternative pathway of HR in DSB repair. Contrary to HR, NHEJ is active along all phases of the cell cycle and is an error-prone mechanism (Chang et al., 2017). Recent evidence suggests that it may influence platinum-therapy. DNA-PKs involved in classical NHEJ are commonly found upregulated in HGSOC, and high expression is associated with advanced stage, poor survival and platinum resistance (Abdel-Fatah et al., 2014), while alterations in NHEJ have been associated with resistance to rucaparib in ex vivo models, and this opens interesting questions, since approximately 50% of EOC present defects in NHEJ, independently from HR-activity (McCormick et al., 2017).

Together with HR, the NER pathway has a key role in the removal of DDP induced DNA damage. The NER pathway is responsible for the resolution of platinum-induced inter-strand crosslinks and for recognition of ICLs, cooperating with HR, FA and TLS for their removal (Spivak, 2015). Patients affected by Xeroderma Pigmentosum, an autosomal recessive disease characterized by the loss of NER suffer hyper-photosensitivity and have a high risk of developing skin cancer in early age (Black, 2016), suggesting a key role of NER in UV-induced damage. Cells defective in NER were 100-fold more sensitive to cisplatin than the parental line (Damia et al., 1996), and conversely, higher levels of NER were associated with platinum-resistance in ovarian cancer cells (Dabholkar et al., 1994, 1992). Recently, data from TCGA reported that approximately 8% of EOC harbour homozygous deletions, non-synonymous or splice mutations in NER genes (Cancer Genome Atlas Research Network, 2011), and Ceccaldi *et al.* identified a subgroup of HGSOC characterized by NER alterations, which showed enhanced survival (similar to patients harbouring *BRCA*-mutations) compared to tumours without NER defects, suggesting that NER deficiency could induce platinum-sensitivity and better outcomes (Ceccaldi et al., 2015). Excision repair cross-complementation group 1 (ERCC1) and xeroderma pigmentosum complementation group A and F (XPA, XPF) are the NER proteins most studied in relation to platinum response, both in preclinical and in clinical studies (Spivak, 2015). ERCC1 and XPF form a nuclease complex with a central role in NER activity, but also in recombination,

DSB and ICL repair (Kirschner and Melton, 2010). The role of ERCC1 in platinum resistance has been largely studied in different tumour types, but still not completely elucidated and controversial results have been reported in ovarian cancer (Bahamon et al., 2016; Cimino et al., 2013). In non-small cell lung, two studies showed that high *ERCC1* mRNA and protein levels correlated with poor patient outcome (Olaussen et al., 2006; Simon et al., 2005), and even in ovarian cancer patients similar results were observed, where high ERCC1 protein levels correlated with decreased survival and platinum resistance (Steffensen et al., 2009). Recently, evaluating 331 EOC cases, a low level of ERCC1 protein was identified as a predictor of platinum response and correlated also with increased PFS (Mesquita et al., 2019). However, other studies reported opposite findings, where no correlation or even a negative correlation between ERCC1 and platinum-response was observed (Ganzinelli et al., 2011; Rubatt et al., 2012; Scurry et al., 2018; Zhao et al., 2018). At present, clinical data have not yet validated ERCC1 as a biomarker for platinum-response, and possible explanations for the lack of concordant results pinpoint the heterogeneity of clinical studies (different design, heterogeneous clinical-pathological features of the patients), as well as the presence of different ERCC1 isoforms, of which only one is able to complex with XPF (Friboulet et al., 2013b). In addition, a big problem is the lack of a validated antibody specific for the active isoform, as reported by Friboulet *et al.* that could not corroborate the predictive potential of ERCC1 in a previously tested cohort of lung cancer patients, likely due to the different quality among 8F1 anti-ERCC1 primary antibody batches used (Friboulet et al., 2013a).

ERCC1 polymorphisms were also evaluated as possible biomarkers for response, but up to now without success (Caiola et al., 2014, 2013; Tang et al., 2017; Yan et al., 2012). XPF expression has been evaluated in relation to platinum response and clinical-pathological features in cancer patients, but clear results and clinical validation are still lacking. Partial positive results were observed in ovarian tumours, where combined low ERCC1 and XPF expression levels, evaluated by IHC, discriminate platinum sensitive patients with a

favourable PFS (Mesquita et al., 2019). Other NER genes, such as XPA, XPD, have been studied, but none of them correlated with DDP response in ovarian cancer (Amable, 2016; Caiola et al., 2014; Ganzinelli et al., 2011). NER is currently an interestingly mechanism with large potential to be exploited as a predictive biomarker, but further studies are required.

TLS is a pathway involved in bypassing the bulky adducts, including GpG intra-strand crosslinks generated by cisplatin (Roy and Schärer, 2016), leading DNA polymerases to continue the DNA synthesis in spite of unrepaired DNA, and to progress through the cell cycle without arrest (Bassett et al., 2002). DNA polymerases involved in TLS (i.e. DNA polymerase β (POLB), polymerase η (POLH), REV3 and REV7 (Shachar et al., 2009)), were found upregulated (both as expression and activity) in several platinum-resistant cell lines and tumours (Albertella et al., 2005; Bassett et al., 2003; Gomes et al., 2019; Zhao et al., 2012). POLB activity is most error-prone among all DNA polymerases involved in TLS, since it incorporates erroneous nucleotides with high frequency in the presence of cisplatin-adducts (Bassett et al., 2003). POLB overexpression correlated with DDP resistance; however, the use of POLB antagonists resulted in controversial results, as in some experiments increased cisplatin efficacy was observed, but not in others (Stewart, 2007; Wojtaszek et al., 2019). Defects in POLH and REV3 correlated with increased cisplatin sensitivity, while overexpression was associated with resistance (Albertella et al., 2005; Knobel et al., 2011).

The MMR recognizes mismatched and unmatched DNA base pairs, and insertion-deletion loops, including the ones caused by both cisplatin and carboplatin treatment and activates apoptosis (Martin et al., 2008). MMR genes have been found down-regulated through genetic or epigenetic mechanisms in association with DDP-acquired resistance (Lin and Howell, 1999; Samimi et al., 2000). Functional inactivation of MMR has been associated with the inability to induce apoptosis after DDP treatment, causing drug resistance (Martin et al., 2008). Less than 10% of HGSOC present hMLH1 promoter hypermethylated (Leskela et al., 2020) and this condition has been associated with platinum resistance (Strathdee et al.,

1999; Watanabe et al., 2007). Treatment of platinum-resistant, hMLH1 hypermethylated ovarian cancer cells with 5-azacytidine reverted the resistant phenotype (Cameron et al., 1999). The most frequently mutated or silenced MMR genes are MutL Homolog 1 (hMLH1), whose promoter appears hypermethylated in ovarian cancer, endometrial, gastric and colorectal carcinoma (Bignami et al., 2003; Peltomäki, 2003), MutS homolog 2 (hMSH2) and MutS homolog 6 (hMSH6) (Galluzzi et al., 2014; Stewart, 2007). Defects in hMLH1, hMSH3 and hMSH6 have been shown to correlate with DDP resistance by activating TLS (Vaisman et al., 1998).

BER is responsible for both removing small single base lesion and for repair of SSB via a sub-pathway involving PARP1. BER involvement in ICL repair has been recently postulated (Wilson and Seidman, 2010) suggesting that targeting BER enhances sensitivity to cisplatin and other ICL-inducer agents (Wang et al., 2009). POLB is the most studied component of BER, and its expression has been evaluated as a prognostic marker (Alvisi et al., 2020; Horton et al., 2015), or in response to DDP therapy in lung and ovarian cancer models reporting contrasting findings (Caiola et al., 2015; Guffanti et al., 2020).

1.5.1.2 Determinants of response to platinum-based therapy beyond DNA repair pathways

Responsiveness to platinum relies also on uptake and/or extrusion of the drug, drug detoxification, and cell death induction, all factors able to influence the response to the drug. In addition, there is mounting evidence on the role of tumour microenvironment, or phenotypic transformations, including epithelial to mesenchymal transition (EMT) and the onset of undifferentiated-stemness tumour phenotype, in determining sensitivity/resistance to platinum-based therapy (Chen and Chang, 2019; Colombo et al., 2014; Galluzzi et al., 2012; Singh and Settleman, 2010).

A reduction of cisplatin effective concentration from 20 to 70% was observed in several DDP resistant cancer cell lines (Kelland, 1993). This reduction was explained by a fall in drug uptake and/or an augmented efflux of the drug outside nucleus and/or cytoplasm (Zhou

et al., 2020). DDP exploits the active membrane copper transporter CTR1 to enter the cell and CTR1 expression can be down-regulated by elevated intracellular copper concentration or cisplatin treatment. Interestingly, CTR1 low levels were associated with DDP resistance in vitro (Ishida et al., 2010). As observed in sensitive and in resistant cell lines of small cell lung carcinoma, DDP resistant cells display lower CTR1 expression than the sensitive ones and reduced DDP and carboplatin cytoplasmic concentrations (Song et al., 2004). Combination therapy with carboplatin and the copper lowering agent trientine has been tried in five patients with resistant HGSOC, who showed a partial reversion of resistance in 4 out of 5 of them (partial remission or stable disease) (Fu et al., 2012). However, other conflicting results were reported on the role of CTR1 in platinum resistance and the clinical potential of modulating CTR1 is under study (Zhou et al., 2020).

ATP7A and ATP7B, responsible for keeping cisplatin outside the nucleus confined into cytosolic vesicles, have been investigated in platinum resistance with contrasting results in different tumour types (Martinez-Balibrea et al., 2009; Stewart, 2007). The most investigated proteins responsible for platinum efflux and drug-resistance are those belonging to the multidrug resistance family (MRP, ABCC), ATP-binding cassette membrane transporters, whose targets are several physiological molecules and drugs (Keppler, 2011). The *ABCB1* gene encodes for the MRP1 or MDR1 protein. Recently, 114 ovarian cancer samples deriving from 92 HGSOC patients were analyzed through whole genome sequencing to characterize genomic profile associated with primary or acquired platinum resistance (Patch et al., 2015). In this study, one of the four mechanisms identified linked to acquired resistance, involved structural variants (SVs) of the *ABCB1* gene, which determined a fusion gene, resulting in upregulation of *ABCB1*. All patients with this fusion had been previously treated with DDP and/or other substrates of the P-glycoprotein MDR1 (Patch et al., 2015). Further studies are required to definitively establish the role different transporters in platinum efflux, as well as validated methods to assess their expression and/or function; this

is an active field of research for the possibility to pharmacologically modulate the transporters activity, providing another treatment option to delay/overcome resistance.

Platinum agents, once entered the cell, undergo possible detoxification by glutathione-S-transferase to GSH, and by metallothioneins (MTs). Increased GSH and glutathione-S-transferase (GST) levels has been observed in different platinum resistant tumours (Byun et al., 2005; Kelland, 1993; Siddik, 2003). Silencing of GST with shRNA demonstrated to re-sensitize platinum resistant cells (Möltgen et al., 2020). Therapeutic strategies preventing the formation of GS-platinum complexes using GSH competitive inhibitors (Cadoni et al., 2017) or interfering with GSH synthesis have been evaluated, but were not tumour-specific and caused severe toxicity in normal tissues (Estrela et al., 2006). In a similar way, also MTs have been investigated, since cytosolic binding of platinum to MT interferes with platinum uptake into the nucleus. shRNA against MT could reverse resistance (Lee et al., 2015) and some miRNAs have been shown to be involved in the regulation of MT transcription (Pekarik et al., 2013).

Platinum agents can activate apoptosis by both extrinsic and intrinsic pathways, the first starting from binding of tumour necrosis factors to cell membrane receptors and subsequent activation of caspases, while the intrinsic pathway is activated by switching the balance from anti-apoptotic (BCL family proteins) to pro-apoptotic proteins (Bax, Bak), leading to enhanced mitochondrial outer membrane permeabilization, release of cytochrome C and activation of the caspase signalling (Zhou et al., 2020). Platinum resistant cancer cells have problems in activating apoptosis, due to alterations involving key-apoptotic regulators, such as p53. HGSOC is one of the tumours presenting the highest prevalence of *TP53* mutations, suggesting it is a critical tumour suppressor for this disease (Binju et al., 2019; Cancer Genome Atlas Research Network, 2011). Typically, anticancer agents act by inducing apoptosis, and in case of not functioning or absent p53, the cell is not able to trigger apoptosis and cell cycle proceeds, determining continuous proliferation and drug resistance (Vazquez et al., 2008). However, nearly 99% of HGSOC are mutated in *TP53*, but this cancer type is

also one of the most responsive tumour types to platinum, pinpointing that apoptosis is a complex mechanism modulated by many cellular pathways (Binju et al., 2019). Several studies focused on the role of different mutations affecting *TP53* function (mostly sited in the DNA binding site), in relation with platinum response or survival, but conflicting findings do not allow a definitive conclusion (Bischof et al., 2019; Mandilaras et al., 2019). Cisplatin resistance may be also affected by extra-tumour conditions such as tumour microenvironment (TME). The TME is a complex system of non-malignant cells, which actively interact with cancer cells regulating tumour development, metastatic process and drug response (Chen and Chang, 2019). The TME includes cancer associated fibroblasts (CAFs), vascular cells, extracellular matrix components and immune cells, able to release proliferative factors, pro-inflammatory cytokines, chemokines and other molecules, which favour cancer survival in hypoxic conditions, escape from the immune system and dedifferentiation of epithelial cancer cells towards a mesenchymal phenotype, less responsive to therapy (Fiori et al., 2019; Hinshaw and Shevde, 2019; Vaupel and Multhoff, 2018).

The TME can physically obstruct platinum drug delivery and diffusion, in the presence of poor tumour vascularisation and/or a dense extracellular matrix (Chen and Chang, 2019). On the other hand, cellular components of TME, such as tumour associated macrophages (TAMs) polarized in a M2 status, favour tumour proliferation and platinum-resistance by secreting pro-inflammatory, pro-angiogenic and stimulating cytokines (Coward et al., 2011). CAFs secrete growth factors like EGF and IGF-1, which contribute to tumour development, and IL-8 that has been reported to induce cisplatin-resistance in gastric cancer (Zhai et al., 2019), and are able to induce dense stroma surrounding the tumour and limit drug diffusion (Erez et al., 2010).

With the advent of “omics” technologies, it became evident that each tumour, even of the same histotype, is different from the others and also areas of the same tumour may change over time in terms of proliferation, differentiation and invasion rate (Brabletz et al., 2018).

Specifically, HGSOC is characterized by genomic instability and heterogeneity. Different studies focused on the impact of genomic heterogeneity on prognosis and chemo-resistance (Tothill et al., 2008). The presence of subpopulations of cancer cells with different sensitivity to therapy and subjected to a "Darwinian" selective pressure by chemotherapy itself have been described. Chemotherapy hits sensitive cells, leaving alive those resistant ones leading to resistant recurrence through clonal expansion (Marusyk et al., 2020).

The complex relationship among EMT, cancer stem cells (CSCs) and platinum resistance (Fabregat et al., 2016; Tanabe et al., 2020) has been an active field of research. EMT is a physiological cellular program in which epithelial cells switch towards a mesenchymal phenotype, due to activation/downregulation of specific transcription factors (Snail, Slug, Zeb1, Zeb2), miRNAs (miRNA-200 family members, let-7) and signalling pathways, as WNT pathways and TGFβ (Brozovic, 2017). Alterations in these pathways often occur in carcinomas, in which cells acquire mesenchymal features becoming less differentiated, more aggressive, with an invasive, metastatic and apoptotic resistant phenotype (Brozovic, 2017). EMT is associated with resistance to different drugs, including cisplatin and carboplatin, even if the underlying mechanisms are still to be elucidated (Brozovic, 2017). Several studies have been performed evaluating differences in expression of EMT markers (low levels of E-cadherin, high levels of vimentin, fibronectin and EMT-transcriptional factors) in cancer cells upon treatment, or confronting parental cell lines with their counterpart made resistant to DDP (Brozovic, 2017). Upregulation of Snail and Slug discriminated primary sensitive EOC versus DDP resistant ones (Haslehurst et al., 2012), and these results were corroborated in a non-small cell lung cancer model of acquired resistance to DDP (Wang et al., 2014). Snail also associated with induction of stemness phenotype in HGSOC (Hojo et al., 2018). In fact, cells during EMT show features similar to those of CSCs and display the activation of the same pathways, including MAPK/ERK, TGFβ-SMAD, PI3K-AKT-NFkB and WNT/β-catenin (Loret et al., 2019). CSCs are able to self-renewal and to divide originating other differentiated cancer cells. They are thought to be in a dormancy state, refractory to

chemotherapy, and during certain conditions are able to exit from this state and to proliferate (Tanabe et al., 2020). The potential link between EMT and CSCs as a determinant for platinum-acquired resistance emerged from different studies. Ricci *et al.* evaluated the expression of several genes associated to both EMT and CSCs in platinum-acquired resistant models of ovarian cancer patient-derived xenografts (PDXs), where it was observed the higher expression of *TCF3, CAMK2N1, EGFR*, and *IGFBP4* (EMT associated genes) and *SMO, DLL1, STAT3*, and *ITGA6* (CSC associated genes) in DDP low-responsive PDXs than in the sensitive ones, and *MMP9, CD44, DLL4, FOXP1, MERTK*, and *PTPRC* genes were significantly more expressed in re-growing PDXs tumours after DDP treatment (Ricci et al., 2017), supporting the hypothesis that EMT process and CSC could be enhanced after the first cycle of DDP treatment.

A knowledge of tumour biology is of pivotal importance to better understand all the factors that could affect the prognosis and the efficacy of therapy. Even if it is possible to elaborate therapeutic approaches to prevent or reduce the negative effects of the above-mentioned mechanisms related to drug resistance, it is still challenging to recognize these aspects and to individualise them possibly before the onset of resistant recurrent tumours.

1.5.2 Determinants of response to PARPi

PARPi share with platinum compounds different mechanisms that influence their anti-tumour efficacy, such as HR defects, because both platinum and PARPi cytotoxic activity is mainly modulated by DNA repair activity. Moreover, drug resistance has been observed also for PARPi and the number of resistant cases is increasing in parallel with the expansion of their use in clinic, not only to treat ovarian and breast cancers, but also other cancers. For these reasons, the study of PARPi determinants of response, as for platinum, is an active field of research and the major findings will be described. Firstly, the role of DNA repair will be described as a determinant of response, then a series of miscellaneous mechanisms

not related to repair. In **table 1.4**, mechanisms investigated as possible determinants of response to PARPi are summarized, putting in evidence those common with platinum agents.

1.5.2.1 DNA repair as determinant of response to PARPi

Sensitivity of ovarian and breast cancer towards PARPi treatment has been observed in tumours with germline *BRCA1/2* mutations, whose inherent defects in HR pathway are amplified by PARP enzymes inhibition, leading to an overload of DSB, genomic instability and apoptosis (Bryant et al., 2005; Farmer et al., 2005). This is one of the first and more successful examples of synthetic lethality translated into clinical practice and which identified germline *BRCA1/2* mutations as the best clinical biomarker for response to PARPi therapy (Kaufman et al., 2015). The use of PARPi was further extended to sporadic tumours with somatic mutations in BRCA genes. Several studies demonstrated comparable response between germline and somatic *BRCA1/2* mutations. An exploratory analysis in Study 19 reported olaparib treatment was equally effective in HGSOC patients carrying somatic mutation in BRCA genes or germline mutations (PFS hazard-ratio 0.17 [95% CI 0.04-1.12] and 0.17 [95% CI 0.03-0.34] versus control, respectively) (Dougherty et al., 2017). Similar results were reported for rucaparib in an integrated efficacy data analysis of two different trials (SOLO10 and ARIEL2), where the objective response rates (ORR) were similar in somatic (55.6% [95% CI 30.8-78.5]) and germline *BRCA*-mutated patients (53.4% [95% CI 42.5-64.1]) (Oza et al., 2017).

Because PARPi sensibility mostly relies on HR defects, as well as for platinum agents, DDP sensitivity itself is currently a surrogate marker for HRD and clinical biomarker of response to olaparib and rucaparib in the presence of *BRCA1/2* mutations (Franzese et al., 2019; Rafii et al., 2017), or in the case of niraparib maintenance therapy, regardless of *BRCA1/2* mutations (Konstantinopoulos et al., 2020). The predictive value of platinum sensitivity was demonstrated in several studies in combination with *BRCA1/2* mutations, where HGSOC *BRCA*-mutated patients achieving complete or partial response to platinum first line therapy

had a better clinical response to olaparib than platinum-resistant and refractory *BRCA*-mutated tumours (Fong et al., 2010; Gelmon et al., 2011). Similar results have been reported analysing data from ARIEL2 trial, in which HGSOC platinum-resistant and refractory patients, with germline or somatic mutations in *BRCA1/2* treated with rucaparib, showed ORRs of 25% and 0%, respectively, compared to 43% and 70% in platinum-sensitive/responsive tumours (Dal Molin et al., 2018).

The predictive value of platinum sensitivity was also investigated in *BRCA* wild type (wt) tumours, where ovarian cancer patients sensitive to platinum retained a certain sensitivity to PARPi measured as objective response rate: ORR 33% in *BRCA* wt vs. 60% in *BRCA* mutated, platinum-sensitive, but significantly higher than in *BRCA* wt and platinum-resistant patients (ORR 4%) (Gelmon et al., 2011). However, the response to platinum agents does not always overlap with that to PARPi, as demonstrated by the evidence tumours sensitive to platinum drugs can be resistant to PARPi, and that some platinum-resistant patients were sensitive to PARPi (Gelmon et al., 2011). One explanation could be the presence of mutations in NER genes leading to inactivation of the pathway, that is responsible for the platinum sensitivity, but does not impact on PARPi efficacy, as recently reported in a subgroup of HGSOC platinum-sensitive, but resistant to PARPi (Ceccaldi et al., 2015).

In order to extend as much as possible, the number of beneficiaries of PARPi therapy, beyond platinum-sensitive and *BRCA*-mutated cases, sporadic tumours without apparent HR mutations were further investigated with the aim to identify PARPi responsive tumours. Despite the overall efficacy of PARPi treatment in well-established HRD tumours, not all sporadic cancers belonging to this group appeared to be as sensitive to PARPi as hereditary tumours (Mirza et al., 2016b). It was observed that approximately 30% of HGSOC patients that did not show HRD phenotype neither *BRCA1/2* mutations, were sensitive to PARPi (Konstantinopoulos et al., 2015). This apparently contrasting evidence can be explained by the fact that HR is a complex and multi-step process, whose factors and regulators are still to be completely elucidated.

The wider use of whole genome sequencing (WGS), whole exome sequencing (WES) and accurate copy number alteration assessments were exploited to develop genomic assays to detect common genomic and mutational signatures in HRD tumours. As previously described, two genomic scar assays were introduced in clinical trials for PARPi therapy in ovarian cancer to assess their role as predictive biomarkers for PARPi sensitivity. The Foundation Medicine's LOH-based assay was the companion test to evaluate HRD in both ARIEL2 and ARIEL3 trials. In ARIEL2 trial, rucaparib was administered as monotherapy to relapsed, DDP-sensitive patients, and it was observed that PFS was significantly longer in patients *BRCA*-mutated (median PFS 12.8 months, HzR 0.27, 95% CI 0.16-0.44, p<0.0001) or *BRCA*-wt/high LOH score (≥16) (median PFS 5.7 months, HzR 0.62, 95% CI 0.42-0.90, p=0.011), compared with patients *BRCA*-wt/low LOH score (<16) (median PFS 5.2 months) (Swisher et al., 2017), suggesting that high LOH-score could identify patients DDP-sensitive without *BRCA*-mutations and sensitive to rucaparib. In ARIEL3 trial, the efficacy of rucaparib was assessed as maintenance monotherapy in platinum-sensitive recurrent ovarian cancers which achieved a complete or partial response to second or later line of platinum chemotherapy but that cannot tolerate further treatment lines with platinum. While positive LOH-score, associated with HRD condition, even predictive of treatment benefit, did not fully explain the increased PFS resulted in patients *BRCA*-wt and LOH-negative, where median PFS was 10.8 months in treated patients versus 5.4 months in untreated (HzR 0.36, 95% CI 0.30-0.45, p<0.0001) (Coleman et al., 2017). Similar results were observed using "myChoice HRD" assay in the ENGOT-OV16/NOVA clinical trial for niraparib in maintenance therapy for platinum-sensitive advanced ovarian cancer patients, where patients with high HRD score as well as *BRCA*-mutated patients had higher benefit from niraparib treatment than placebo treated patients. However, the genomic assay was sensitive enough to detect a subgroup of HRD-negative/*BRCA*-wt patients who partially respond to therapy, even if with a lower extent than *BRCA*-mutated/HRD high population (median PFS 9.3 months vs. 3.9 months in placebo group, hazard ratio 0.45; 95% CI, 0.34

to 0.61, p<0.001) (Mirza et al., 2016b). Based on these results, niraparib was approved as maintenance therapy for platinum-sensitive relapsing ovarian cancer, regardless of *BRCA* mutations or HRD status. Data from these clinical trials highlight some drawbacks of the available assays, such as the unlikelihood to capture dynamic changes in the tumour.

Unfortunately, resistance also affects tumours treated with PARPi and cases of *de novo* or acquired resistance have been reported both in preclinical and in clinical practice. At present, several potential mechanisms and proteins have been identified in preclinical models, even if most of them still requires clinical validation (Noordermeer and van Attikum, 2019). Notably, the presence of platinum-resistance often predicts resistance to PARPi therapy, suggesting that many mechanisms underlying these events may be the same (Fong et al., 2010; Konstantinopoulos et al., 2015) (**table 1.4**).

Restoration of functional *BRCA1/2* and *RAD51C/D* through secondary mutations represents a well described mechanism associated with PARPi-resistance in the clinic, in tumours with germline or somatic mutations in the above-mentioned genes (Domchek, 2017). As previously described for platinum, secondary somatic mutations (i.e. deletions, frameshift, nonsense mutations) can restore the open reading frame of the gene, forming a new, non-wild type, functional isoform, or can restore heterozygosity (Barber et al., 2013; Kondrashova et al., 2017; Norquist et al., 2011). Often tumours expressing *BRCA1* secondary mutations are characterized by alt-EJ signature, suggesting that secondary mutations may be the result of the error-prone repair of DSB operated by alt-EJ in HRD tumours and that *POLQ* could be a driver of PARPi-resistance (Ceccaldi et al., 2015). Secondary mutations were found in both solid and liquid biopsies, where *BRCA1/2* reversion mutations were present in recurrent HGSOC patients resistant to platinum or PARPi (Christie et al., 2017). Reverting mutations turned in frame *BRCA2* and *PALB2* sequences in patients with progressive prostate cancer, pretreated with olaparib (Goodall et al., 2017). As previously mentioned, also *RAD51C* and *RAD51D* are subjected to secondary reversion mutations, which have been described in association with acquired resistance to rucaparib in

a cohort of HGSOC patients from the ARIEL2 trial (Kondrashova et al., 2017; Liu et al., 2017).

As for platinum-resistance, HR restoration may be mediated also by epigenetic changes. This mechanism was observed in breast cancer PDXs with hypermethylation at diagnosis (Ter Brugge et al., 2016) and in ovarian cancer patients, where tumours with *BRCA1* promoter heterozygous methylation were less responsive to rucaparib than those with homozygous methylation (Kondrashova et al., 2018). In triple-negative breast cancer adding to mutational profile the information regarding homozygous *BRCA1*-methylation status ameliorated their predictive potential to identify patients who might benefit from olaparib/eribulin combination (Kawachi et al., 2020). Of note, *BRCA1* promoter methylation can be overturned by genomic rearrangements that place *BRCA1* expression under the control of a different promoter, as was found in PARPi-resistant PDX tumours (Ter Brugge et al., 2016). Alternative splicing variants of *BRCA1* with residual function can still influence the response to HRD target therapies (Bouwman et al., 2013). For instance, mice bearing $BRCA1^{\Delta 11/\Delta 11}$; $p53^{-/-}$ mammary tumour expressing the $BRCA1^{\Delta 11/\Delta 11}$ variant in which part of the exon 11 is lost, are DDP-resistant and partially resistant to olaparib, while tumours with a frameshift mutation in exon11 are not resistant (Wang et al., 2016). Breast cancer models with $BRCA1^{C61G}$ mutation located in the highly-conserved N-terminal RING domain necessary to bind BARD1, rapidly developed *in vivo* resistance to DDP and olaparib, since BRCA1 stabilization was enhanced (Drost et al., 2011). Interestingly, it was observed in in vitro experiments that under PARPi treatment, *BRCA1*-mutated protein levels increased and this can be explained by the fact that under treatment pressure some clones expressing *BRCA1*-mutated in the BRCT domain can be selected (Johnson et al., 2013). BRCT mutated proteins are able to recruit heat shock proteins 90 (HSP90), which stabilize BRCA1 preventing proteasomal degradation, increasing cytoplasmic accumulation and preventing BRCA1 interacting with PALB2, RAD51 and BRCA2, determining DDP and PARPi resistance

(Anantha et al., 2017; Johnson et al., 2013). Then, it was also demonstrated that this mechanism of resistance could be reverted with HSP90 inhibitors (Johnson et al., 2013).

Another way to restore HR function in *BRCA1*-deficient cells relies on the concomitant loss of NHEJ. The choice between HR or NHEJ pathway to repair DSB, depends on the availability of end resection, necessary to HR; on the contrary end protection is necessary to NHEJ (Ceccaldi et al., 2016). 53BP1 is a protein of NHEJ that blocks CtIP-mediated DNA end resection through different downstream effectors and mechanisms, and promotes NHEJ-mediated DSB repair (Konstantinopoulos et al., 2015; Noordermeer and van Attikum, 2019). Based on this knowledge, three studies using *in vitro* and *in vivo* models demonstrated that HR defects in a *BRCA1*-deficiency background could be partially reverted inhibiting *TP35BP1* which encodes for 53BP1 protein, thus blocking NHEJ, and reducing PARPi hyper-sensibility of these tumours (Bouwman et al., 2010; Bunting et al., 2010; Cao et al., 2009). Notably, only double knockout *BRCA1* and *TP53BP1* cells restores HR, while this effect was not observed in *BRCA2*-deficient cells, suggesting that restoration of end resection via loss of *53BP1* is independent of *BRCA1* (Bouwman et al., 2010; Bunting et al., 2010). Other experiments supported this hypothesis. In breast cancer mouse models, it was observed that *BRCA1*-deficient tumours and resistant to olaparib had low expression levels of *TP53BP1* (Jaspers et al., 2013). More recently, it was shown that human ovarian cancer specimens, deriving from a phase I trial of the PARP inhibitor ABT-767, *BRCA1*-deficient not responsive to treatment were negative for 53BP1 (stained with validated IHC assay) (Hurley et al., 2019). RIF1 and REV7, which are part of the Shieldin (SHLD) complex together with SHLD1/2/3 (Noordermeer et al., 2018; Setiaputra and Durocher, 2019), were identified as 53BP1 downstream effectors (Chapman et al., 2013; Zimmermann et al., 2013) and that again their loss induced PARPi resistance, through increasing resection and restoring HR activity (Feng et al., 2013; Mukherjee et al., 2019; Xu et al., 2015). Depletion of *REV7* was found in vitro to restore HR through CtIP-mediated end resection and cause PARPi resistance. Again, it was seen in *BRCA1* but not *BRCA2*-deficient cells, highlighting

the different activity of BRCA protein (Xu et al., 2015). SHLD complex which is recruited at DSB in a 53BP1- and RIF1-dependent manner, was also identified during genome-wide CRISPR/Cas9 screens aimed to identify new PARPi-resistance determinants (Dev et al., 2018; Gupta et al., 2018). From these screens a second interesting factor, whose loss leads to PARPi resistance in *BRCA1*-deficient cells was identified, DYNLL1 (Noordermeer et al., 2018). End resection starts with the recruitment of MRN complex and proceeds with nucleases (EXO1 and DNA2); DYNLL1 acts blocking MRE11, a component of the MRN complex, from access to DNA thus preventing end resection (He et al., 2018). As for the other factors, loss of *DYNLL1* allow the recruitment at DSB of proteins involved in end resection, thus restoring RAD51 foci formation and HR in *BRCA1*-deficient setting. *DYNLL1* loss/low levels was observed in a clinical cohort of primary *BRCA1* deficient HGSOC specimens and associated with fewer chromosomal abnormalities (He et al., 2018); in vitro *DYNLL1* loss in *BRCA1* deficient cell leads to PARPi resistance (Becker et al., 2018). NHEJ represents the counteracting pathway of HR, that, if suppressed, can cause PARPi resistance (McCormick et al., 2017). Alterations in other DNA repair pathways may affect drug response to PARPi, such as TLS repair. CHD4 is a chromatin remodelling factor involved in several cellular pathways (Zhang et al., 2019), whose loss in *BRCA2*-deficient ovarian cancer cell line correlated with restored cell cycle progression and enhanced DNA-damage tolerance, in line with activation of TLS repair. Its loss has been associated with cisplatin and olaparib resistance and reduced survival in *BRCA2*-deficient ovarian cancer patients (Guillemette et al., 2015). These data are important since previously it was observed that in HR proficient tumours, *CHD4* loss enhanced platinum and PARPi sensitivity (Pan et al., 2012), suggesting that TLS induction determines resistance independently of HR.

Beside the rational use of PARPi in *BRCA1/2*-mutated or HRD tumours (Lord and Ashworth, 2017), not all *BRCA*-deficient tumours are sensitive to PARPi (Gelmon et al., 2011), as well as PARPi demonstrated efficacy beyond HRD-status (Mirza et al., 2016b; O'Connor, 2015). In fact, several studies demonstrated the efficacy of PARPi in other

tumour types beyond HRD ovarian and breast cancer, such as small cell lung cancer (SCLC) (Murai et al., 2016) and Ewing sarcomas (Tang et al., 2015), which appear to be HR proficient suggesting that additional factors may contribute to increase PARPI sensitivity.

PARP1 protein expression levels was investigated as a possible biomarker of PARPi response. In ovarian cancer preclinical models PARP1 protein expression and enzymatic activity were measured using a radiotracer, and it was observed that protein expression and PARP1 activity positively correlated with the response of olaparib and talazoparib alone or in combination with radiotherapy, both in *BRCA1*-mutated and wild type tumours (Makvandi et al., 2016; Sander Effron et al., 2017). Gan *et al.* observed in a cohort of 174 sporadic HGSOC a significantly negative correlation between PARP1 expression and patient survival, regardless of BRCA1 levels (Gan et al., 2013). Hjortkjær and colleagues did not find any correlation between either PARP1 IHC-score and clinical outcome in 170 biopsies of primary ovarian cancer, taking also into account BRCA1 levels (high or low) (Hjortkjær et al., 2017). These contrasting results suggest that further studies are needed. Mutation in PARP1 has been shown to associate with resistance to PARPi. Pettitt *et al.* by different mutational screenings, identified PARP1 loss-of-function as a potent mechanism able to prevent trapping and induce acquired resistance to PARPi in normal and in human cancer cell lines (Pettitt et al., 2013). More recently the same authors identified close to full-length mutant forms of PARP1 that cause *in vitro* and *in vivo* PARPi resistance (Pettitt et al., 2018, 2013). Specifically, mutations affecting the zinc-finger domain of PARP1 were able to prevent trapping and cause resistance to talazoparib in vitro. For instance, PARP1 (R591C) mutation was found in a HGSOC patient with primary resistance to olaparib (Pettitt et al., 2018). Loss-of-function mutations that hit PARG protein could reduce PARPi trapping activity, and thus reduce their efficacy (Gogola et al., 2018).

Another critical consequence of PARPi therapy relies on dysregulation of replicative fork (RF) due to PARP-trapping, that, in HRD cells, enhances replicative stress, fork collapse, and eventually induces cell death (Franzese et al., 2019). *BRCA1/2* and *PARP1*, in addition

to their role in DNA repair, protect the RF under replicative stress conditions (Schlacher et al., 2012). In *BRCA*-deficient cells, RAD51 filaments are not stabilized and cannot block the nucleolytic activity of MRE11 nuclease that degrades the new ssDNA, thus forming a shorter new strand which determines the RF collapse and thus sensitivity to PARPi (Liptay et al., 2020; Schlacher et al., 2011). The unravelling of the mechanisms at the basis of RF protection lead to identification of *BRCA* downstream effectors having an independent role in protecting the RF, such as SMARCAL1/ZRANB3/HTLF (chromatin remodelling factors), PTIP, and EZH2. All these proteins are necessary to recruit MRE11; EZH2 recruits MUS81 at stalled RF, and mediate PARPi sensitivity in *BRCA*-deficient cells (Ray Chaudhuri et al., 2016; Rondinelli et al., 2017) (**figure 1.22**). SMARCAL1/ZRANB3/HTLF are necessary for MRE11 nucleolytic activity, and their loss in *BRCA*-deficient cells cause PARPi resistance (Taglialatela et al., 2017). Loss of PTIP protects the nascent ssDNA from degradation by MRE11, especially in *BRCA*-deficient cells, where also RAD51 protection was lost (Ray Chaudhuri et al., 2016). EZH2 usually recruits MUS81 by methylation of lys27 on histone 3 (H3K27me3) at stalled fork. In addition, EZH2 loss maintains stalled RF preventing its disruption and causing PARPi resistance, but contrary to PTIP, it has been observed only in *BRCA2*-deficient cells or in mouse models, where low EZH2 and MUS81 expression levels correlated with PARPi resistance (Rondinelli et al., 2017).

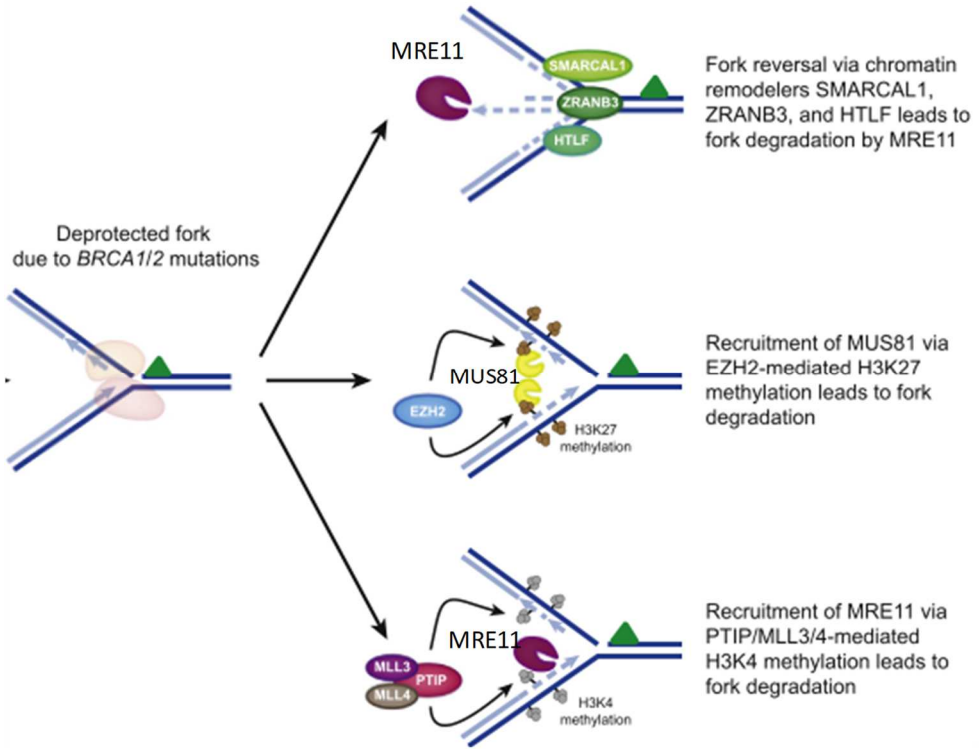

Figure 1.22 Schematic overview of the mechanisms leading to restoration of replication fork protection (adapted from (Noordermeer and van Attikum, 2019)).

There are also proteins, not directly involved in protecting the RF, but able to influence its dynamic and potentially to influence PARPi response. E2F7 is a transcription factor activated in the presence of DSB to arrest the cell cycle in G1/S phase and able to negatively regulate the expression of several HR genes, among them, *RAD51* and *BRCA1* (Mitxelena et al., 2018). E2F7 depletion in vitro led to increased RAD51 foci formation and activation of RAD51-mediated HR repair and RF stabilization, due to prevention of MRE11 activity. All this was associated with the onset of PARPi resistance in a *BRCA2*-deficient setting (Clements et al., 2018).

In 2012, SLFN11 was firstly discovered as a determinant of response to topoisomerases I and II inhibitors and platinum compounds (Zoppoli et al., 2012), then it has been extended also to PARPi (Murai et al., 2016) becoming the subject of several studies. The relation between *SLFN11* expression and response to PARPi was observed in a panel of 60 NCI lung cancer cell lines treated with talazoparib (a potent PARPi) and olaparib, where gene

expression analysis of the treated cells found a significant association between drug response and *SLFN11* expression levels, irrespective of *BRCA*-status, and these results have been further corroborated in isogenic xenografts for *SLFN11* (Murai et al., 2016). SLFN11 is a nuclear protein upregulated during replication stress, when it binds and permanently blocks the replication fork by opening the chromatin through its ATPase activity, promoting a prolonged arrest in S-phase (Noordermeer and van Attikum, 2019). Upon treatment with DNA-damaging agents, which induce replication stress, *SLFN11* is activated and the prolonged S-phase arrest mediated by *SLFN11* blocks replication and enhances apoptosis and determines hyper-sensibility to the treatment (Murai et al., 2016). Conversely, loss of *SLFN11* decrease the efficacy of these treatments because cells sustain replication even in the presence of DNA damage, enter G2 phase as observed, and thus lead to resistance regardless of HR status (Murai et al., 2018, 2016). Trying to elucidate whether *SLFN11*-mediated arrest of the cell cycle in S-phase depends from ATR-checkpoint regulation, Murai *et al.* combined talazoparib with an ATR-inhibitor, observing resistant cells recover their sensitivity to PARPi and suggesting the use of ATR inhibitors as a possible strategy to overcome resistance in *SLFN11*-deficient tumours (Murai et al., 2016). Since *SLFN11* upregulation or depletion are often observed in a wide range of tumours (Cancer Genome Atlas Research Network, 2011; Murai et al., 2019) and *SLFN11* expression could be considered a very promising biomarker for PARPi regardless of HRD status, these findings suggest also the potential use of PARPi in different tumours (Shee et al., 2019). For instance, the fusion protein EWS-FLI1, a marker of Ewing sarcoma, is a transcription factor constitutively activated, which upregulates *SLFN11* transcription and this could explain the sensitivity of this tumour to PARPi (Tang et al., 2015).

Thus, loss of PTIP, RADX, EZH2 and SLFN11 induce resistance to PARPi, without increasing HR activity in *BRCA*-deficient cells, suggesting that mechanisms which protect the RF and ensure cell cycle progression or sustain replication stress should be taken into consideration as possible determinants of PARPi clinical activity.

1.5.2.2 Determinants of response to PARPi beyond DNA repair

Induction and up-regulation of MET/HGFR signaling pathways contribute to PARPi resistance. MET/HGFR is a tyrosine kinase receptor found amplified or upregulated in almost 10% of EOC (Cancer Genome Atlas Research Network, 2011). Upregulation of MET directly phosphorylates PARP1, increasing its activity and affecting its binding site which reduces the interaction with PARPi causing resistance (Du et al., 2016). Preclinical studies have evaluated MET inhibitors in combination with PARPi in *BRCA*-mutated breast and HGSOC cancer models, where they showed a synergistic effect and determine cell growth inhibition, especially in tumours overexpressing MET, and interestingly, in tumours resistant to PARPi (Dong et al., 2019; Du et al., 2016; Han et al., 2019). Combination of MET inhibitors and PARPi could be a strategy to overcome PARPi resistance in MET overexpressing tumours as observed in preclinical models (Han et al., 2019). Clinical trials with MET inhibitors in solid tumours are underway, but none at the moment is testing the combination with PARPi (info updated at September 2020).

PARPi drug availability and intracellular concentrations are regulated by p-glycoprotein transporters such as ABCB1 in murine models. *ABCB1* upregulation was associated with decreased PARPi concentration within the cells (Rottenberg et al., 2008), as well as in an ovarian cancer cell line resistant to PARPi, the treatment with verapamil, inhibitor of MDR1, reverted the resistant phenotype to sensitive (Vaidyanathan et al., 2016). These results led to research of new PARPi molecules with less affinity to MDR1, and new therapeutic strategies aimed to combine PARPi and transporter inhibitors (McMullen et al., 2020).

Most of these findings derived from preclinical studies which have provided evidence for multiple mechanisms possibly related to PARPi resistance in *BRCA*-deficient tumours. However, only secondary mutations in HR genes have been validated as mechanism of resistance in the clinic to date, and loss of *53BP1* is under study in human tumours. The effective impact and frequency of each of these mechanisms are not established and

definitive studies are required to assess the relative impact of secondary mutations, loss of *53BP1*, and upregulation of *ABCB1* efflux transporters in *BRCA*-deficient tumours. It would be also interesting to assess if different *BRCA1/2* mutations may change the impact of these mechanisms on therapy response and considering the wide range of potential of different PARPi, how their trapping potency or other pharmacologic characteristics could be differently modulated by these processes.

Table 1.4 Mechanisms and molecular alterations associated with PARPi resistance and eventually, cross-resistance with cisplatin

Mechanisms of PARPi Resistance	*Detailed alterations*	*Impact on DDP resistance*
Restoration of functional HR	1) Reactivation of functional proteins: - BRCA & RAD51 reversion mutations - BRCA1 promoter de-methylation - BRCA hypomorphic mutated forms or splicing variants with residual activity - BRCA forms protected from degradation 2) Restoration of end-resection: - Loss of 53BP1 - Loss of REV7 - Loss of DYLLN	1) Cross resistance 2) DDP not affected
Alterations in PARP1 or PARG which decrease PARP-trapping	- Loss of function mutations affecting PARP1 or PARG - *PARP1/2* low expression levels - Hypomorphic mutated forms with residual activity	DDP not affected
Dysregulation of RF stability/	- Loss of SMARCAL1/ZRANB3/HTLF - Loss of PTIP - Loss of EZH2 - Loss of RADX - Loss of E2F7	Cross resistance
Sustained replication regardless of DNA damage	Loss of SLFN11	Cross resistance
Activation of TLS repair	- Loss of CHD4	Cross resistance
Activation of MET/HGFR and PI3K/AKT pathways	1) Amplification/up-regulation of MET/HGFR pathway 2) Up-regulation of pro-survival PI3K/AKT pathway	1) DDP not affected 2) Cross resistance
Increased efflux	- Overexpression of *ABCB1* gene	Cross resistance

1.6 DNA REPAIR FUNCTIONAL ASSAYS

Personalized medicine requires new methods to better stratify patients in order to receive the best therapy, which means for ovarian cancer patients, to select those patients who will benefit from platinum- and PARPi-based treatment. In this context great efforts have been made to find biomarkers and to set up tests able to determine the functional activity of some DNA repair pathways, especially those involved in DSB repair, to predict therapy response and/or the acquisition of drug-resistance.

Isogenic models and in vitro or ex vivo cell or tissue cultures have been largely used in preclinical experiments (Alkema et al., 2016; Clark et al., 2012; Liu et al., 2018; Walton et al., 2017); the first are suitable to study the role of a single gene as putative biomarker of response, while with the latter is possible to study the cellular response to a given drug. These experiments are useful to identify key drivers in DNA repair and possibly identify putative biomarkers of response. However, they suffer from poor translatability to clinical practice, since patient biopsies are not always available.

Due to the relevance of HR in determining DDP and PARPi response to therapy, several methods aimed to evaluate the expression of key HR genes and HR capacity to repair DSBs. In particular, formation of nuclear RAD51 foci is a downstream event in HR and occurs when the sister chromatid is available leading to recombination process (Hoppe et al., 2018). RAD51 foci formation is absent in *BRCA*-mutated cells and is generally considered a surrogate marker for HR (Bhattacharyya et al., 2000), detectable by common immunofluorescence (IF) and immunohistochemical (IHC) techniques. RAD51 foci levels have been quantified in ovarian cancer ex vivo models after ionizing radiation, which cause DSB repair by HR, and low induced levels correlated with PARPi response (Mukhopadhyay et al., 2010; Shah et al., 2014). The interest toward this test has been amplified by recent findings that demonstrated its capacity to predict PARPi resistance in *BRCA1/2*-mutated tumours, where revertant mutations had restored HR-proficiency (Waks et al., 2020). In

addition, it has also shown to predict PARPi sensitivity in *BRCA*-wild type tumours, identifying *BRCA*ness tumours *BRCA1/2* wild type (Castroviejo-Bermejo et al., 2018a).Very recently, Cruz *et al.* set up IF quantification of RAD51 foci in proliferative/geminin positive cells in untreated breast cancer FFPE samples, and determined a RAD51 score, which discriminated PARPi sensitive (low score) from resistant (high score) tumours (Cruz et al., 2018). Geminin is a marker of G2/S cell cycle phase, when HR is active, so, the evaluation of RAD51 foci in proliferating cells should enforce the test, as suggested also in other studies (Naipal et al., 2014). Given that HRD tumours are usually responsive both to PARPi and DDP agents, RAD51 assay should be predictive also for DDP therapy. A functional test to assign an HR-score based on RAD51 foci levels was established in ovarian cancer ex vivo cultures, only evaluating proliferating-G2/S phase cells, after DSB induction with radiation. Based on this score, tumours were divided into HR-deficient (HRD) or HR-proficient (HRP) and the assay significantly predicted DDP response (Tumiati et al., 2018b). This functional assay was also validated in triple negative breast cancer (Tumiati et al., 2018a). The assay also scored specimens derived from different sites of the same ovarian cancer patients (i.e. omentum, ovary, abdominal metastases), with different levels of HR proficiency being observed in samples from the different sites (Tumiati et al., 2018b), corroborating the idea that drug-resistance may derive from the selection of subclones and enforcing the role of intra-tumour heterogeneity as a possible cause of DDP-resistance.

A strong indicator of DSB not closely related with HR activity, is the protein H2AX, a component of the histone in nucleosome, which is phosphorylated by ATM and ATR kinases after DSB induction, necessary to start the recruitment and localization of other DNA repair proteins (Kuo et al., 2018). The new phosphorylated protein γH2AX is visible as nuclear foci sited close to DSB where repair activity is ongoing, but γH2AX foci are present not only during DNA repair, but also during apoptosis caused by DNA fragmentation, especially at the later time points after DNA damage induction, and distinguishing apoptosis from DNA

repair may be misleading (Rogakou et al., 2000). For this reason, γH2AX foci are considered biomarkers of DSB and globally of DDR, associated with cellular stress condition and genomic instability (Palla et al., 2017). Stefanou *et al.* described a method to test DDR induction through γH2AX foci quantification in peripheral blood monocyte cells from *BRCA*-mutated EOC patients and healthy donors observing a higher basal level of γH2AX foci in EOC patients, index of genomic instability, and γH2AX expression levels correlating with response to DDP-based therapy (Stefanou et al., 2015), but validation in a larger cohort of patients is needed.

Another strategy to improve specificity of foci-based tests to enforce their potential as predictor of therapy response, consists in evaluating different markers for DSB at the same time, for instance γH2AX, RAD51 and Nbs1, a component of MRN complex, phosphorylated by ATM in response to DSB and involved in recognition of the DSB (Wilsker et al., 2019). Time course and spatial quantification of the three proteins by quantitative multiplex IF assay, named IFA, aimed to assess the activation of DDR in colorectal cancer FFPE samples after exposure to different DNA damaging agents, cisplatin included. Preliminary results in PDXs tumours and human specimens were encouraging and an increased IFA-score suggested activation of DDR (Wilsker et al., 2019).

A functional test widely used in preclinical studies to directly evaluate the functionality of HR or NHEJ to solve DSB is a green fluorescent protein (GFP)-based plasmid assay, where two plasmids are co-transfected within the cells to be tested for HR or NHEJ proficiency. The first plasmid encodes for the restriction enzyme *I-SceI*, while the second reporter plasmid includes the restriction site for *I-SceI* and the substrate for the specific DNA repair pathway to be analyzed. Once co-transfected, *I-SceI* cleaves the reporter plasmid at the level of *GFP* coding plasmid, whose homologous sequence has been selected to be specifically detected and repaired by one of the main DSB end-joining pathways. If the cell is DNA repair proficient, the *GFP* gene will be repaired and the protein transcribed and the green fluorescent signal will be detected by fluorescence-activated cell sorting (FACS) analysis.

The percentage of positive/proficient cells will be quantified and normalized over a population transfected with plasmid containing the wild-type *GFP* gene. This assay, or similar based on the same principle, have been largely used in in vitro cells, peripheral blood lymphocyte cells and in ex vivo cultures to establish the effective DSB repair proficiency and to detect genotoxic carcinogens (Deniz et al., 2013; Ireno et al., 2014; Keimling et al., 2012). The potential of the GFP-based functional assay to correlate the efficacy of DSB repair to DNA-damaging agents response has been explored in breast cancer cells, where encouraging findings have been shown (Deniz et al., 2017).

Another assay has been recently described to correlate NHEJ activity with sensitivity to rucaparib in a panel of primary and commercial ovarian cancer cell lines (McCormick et al., 2017). It requires the cellular extracts to which linear plasmids are added. If the cells are NHEJ proficient, the plasmids will be end-joined and will acquire a multimer conformation (McCormick et al., 2017). The results showed a significant correlation between NHEJ deficiency (NHEJD) and resistance to rucaparib ($p=0.0022$), also in HRD tumours (NHEJD/HRD vs NHEJ/HRD cells, $p=0.0045$) (McCormick et al., 2017).

Defects in replication fork protection have been reported to correlate with sensitivity to carboplatin in 33 HGSOC short-term patient derived organoids (Hill et al., 2018). In these organoids, which well recapitulate the original human tumour characteristics, the DNA fiber assay was used to evaluate the replication fork stability. Stable RF was found in the majority of carboplatin resistant organoids (91%), while defects in stalled RF were observed in 61% of organoids and this condition correlated with sensitivity to carboplatin sensitive ones (Hill et al., 2018), suggesting that RF stability established by DNA fiber assay could be used to predict carboplatin response in HGSOC.

The NER pathway as previously mentioned, is a versatile mechanism and several data suggest it has a significant impact on DDP-based therapy, and emerging results sustained also its role in influencing PARPi treatment (Ceccaldi et al., 2015). ERCC1 and XPF form a heterodimer nucleasic complex, which can be considered a read-out of the NER activity

(Faridounnia et al., 2018). The proximity ligation assay (PLA) has been set up and applied to detect the ERCC1/XPF functional complex both in IHC on FFPE samples, and in IF (Friboulet et al., 2013a; Guffanti et al., 2020). The use of PLA by-passes the lack of validated primary antibodies to specifically detect the functional *ERCC1*-isoform 202, the only one out of four able to complex with XPF (Friboulet et al., 2013b). Preclinical evidence suggested that the ERCC1/XPF complex can be detected by PLA (Friboulet et al., 2013a), but the predictive potential of ERCC1 or ERCC1/XPF as a biomarker for DDP response need further validation (Guffanti et al., 2020).

1.7 PATIENT-DERIVED XENOGRAFT MODELS

Patient-derived xenografts (PDXs) are the most relevant EOC human models currently used in the field of preclinical EOC research (Ricci et al., 2014). EOC PDXs may be generated by heterotopic (i.e. subcutaneous) or orthotopic (i.e. intra-peritoneum or intra-bursal) transplantation of human cancer cell lines, or directly from fragments of patients' biopsies or cells from ascitic fluid into immunodeficient mice (Hidalgo et al., 2014). The rationale beside the establishment of PDXs aimed to create models recapitulating the complexity of EOC (Aparicio et al., 2015). In fact, PDXs retain the main histological and molecular characteristics of donor tumour as confirmed in several studies, even after some in vivo passages when the tumour is propagated, confirming their genomic stability (Liu et al., 2019; Ricci et al., 2014). PDXs have been obtained from all the EOC subtypes, especially from HGSOC, which is the most prevalent and clinic relevant histotype. Large collections of extensively characterized PDXs have been established reflecting the heterogeneity of EOC (Heo et al., 2017; Ricci et al., 2014). Another advantage offered by PDXs, especially orthotopic models, is the possibility to study the process of tumour progression, metastasis formation and dissemination, as well as the role of tumour microenvironment and vascularization on EOC therapy (Bizzaro et al., 2018; Ricci et al., 2014). The second most relevant application of PDXs relies in drug-response studies and in the preclinical development of novel therapies (Hidalgo et al., 2014; Karakashev and Zhang, 2021). Validation studies showed a good correlation between PDXs response to chemotherapy and what observed in the original donor patient (Topp et al., 2014), and the ability to recapitulate the clinical spectrum of sensitivity to established therapies (Ricci et al., 2014). The correlation suggests the PDXs may have a predictive value and thus a role in the field of personalized medicine and in the search of biomarkers (Hidalgo et al., 2014), as well as in the studies on chemoresistance (Guffanti et al., 2018; Nagaraj et al., 2015). Notably, it is also possible to induce in vivo acquired chemoresistance by prolonged exposure to the drug,

similar to what observed in the clinic (Ricci et al., 2017). These acquired-resistant models have been utilized to explore the molecular mechanisms at the basis of acquired chemoresistance and to test novel pharmacological strategies to overcome this important clinical issue. However, as all models, also PDXs suffer from some limitations. Differently from in vitro and ex vivo models, PDXs are not suitable for high-through put screening tests, due to different reasons: low engraftment rate; relative slow tumour growth rate; high costs associated with long term experiments and the necessity of specialized trained personal (Karakashev and Zhang, 2021). Moreover, PDXs cannot be genetically modified and the use of immunocompromised mice precludes the studies of novel immunotherapies, that may be investigated using alterative, but challenging, humanized immune system mice (Choi et al., 2018).

2. AIMS

Epithelial ovarian cancer (EOC) is a lethal malignancy and, even if the majority of patients are initially extremely sensitive to platinum-taxol based chemotherapy, most of the responding tumours will recur within five years after diagnosis with a platinum-resistant phenotype. Recently, the therapeutic approach of EOC has been revolutionised by the introduction of PARP inhibitors (PARPi), particularly effective in homologous recombination (HR) deficient tumours. However, also for PARPi, cases of intrinsic or acquired resistance have been observed. For these reasons, the ability to identify patients who will effectively respond to therapy and the possibility to predict the onset of resistance to both platinum and PARPi will help to address patients receive the most appropriate treatment and to delay the onset of resistance, avoiding unnecessary and toxic treatments.

50% of high grade serous ovarian cancers, the most diffuse subtype, harbour defects in the HR DNA repair pathway, involved in the repair of DNA double strand breaks and intra-strand crosslinks, making these tumours very sensitive to both platinum agents and PARPi. HR deficiency is an important determinant of platinum/PARPi sensitivity and the most studied one; however, considering that these drugs cause different kind of lesions, involving many different DNA repair pathways, such as FA, BER, NER, MMR and TLS, the study of other possible DNA repair key determinants is warranted. Due to the complexity and the inter-connection among the various DNA repair mechanisms, the role of each pathway and how their presence or absence determines the final cell response to therapy is still an open question. In addition, there are no validated functional tests correlating the tumour DNA repair status and response to therapy.

Starting from this background, we hypothesized that among DNA repair effectors could be possible to identify predictive biomarkers and finding functional tests able to measure the DNA repair activity of the tumour. The present PhD thesis aims to better elucidate the role of different DNA repair pathways in determining the response to cisplatin and olaparib (a PARPi) in a preclinical setting to find possible predictive biomarkers. This work has been carried out using ovarian cancer patient-derived xenograft (PDX) models established during

the last decade in the Department of Oncology at the Mario Negri's Institute, where I undertook the PhD course.

In particular, the present thesis is organized into the following parts:

- in the first part, an overview of the xenobank is presented. We demonstrated that our PDXs are robust models, recapitulating the original tumours from which they derived. They resemble well the heterogeneity of EOC, and the most frequent HR genetic alterations. Moreover, the PDXs show a spectrum of response to DDP and olaparib similar to what is observed in the clinic, making them a good model for our studies;
- the EOC-PDXs have been characterized at different molecular levels and these features have been correlated with tumour response to therapy. In particular, I analysed the expression levels of 35 genes involved in the main DNA repair pathways, described to be involved in cisplatin and olaparib mechanism of action, the promoter methylation status of selected DNA repair genes and the HR mutational profile of the PDXs. Then, these data have been correlated with response to DDP and olaparib;
- in the third part, I focused on the research of possible determinants of HR activity. The HRDetect assay was applied to ten PDXs to evaluate their HR status, and the expression of RAD51 nuclear foci was quantified using and comparing two different immunohistochemical approaches in FFPE untreated xenograft tumours and correlated with the response to DDP and olaparib;
- in the fourth section, ERCC1, ERCC1/XPF complex and POLB were studied at different levels (mRNA and protein expression), as surrogate markers for NER and BER activity in response to DDP therapy.

Taken together the studies presented in my PhD thesis had the overall aim to improve understanding of the role of DNA repair in ovarian cancer as a determinant of response to platinum and PARPi-based therapy and to find possible DNA repair functional tests able to predict response to therapy.

3. MATERIALS AND METHODS

3.1 IN VIVO STUDIES

3.1.1 Patient specimen collection and clinical data

Fresh clinical specimens (primary ovarian tumours, omental metastasis or ascitic fluid) were obtained from patients undergoing cytoreductive surgery for ovarian tumour by laparotomy or paracentesis at the San Gerardo Hospital (Monza, Italy) and at the European Institute of Oncology (IEO) (Milan, Italy). Clinical data were obtained from medical records. Primary surgery was performed to establish the diagnosis, staging and debulking. Surgical staging was based on the FIGO (International Federation of Gynaecology and Obstetrics) classification. The study protocol for tissue collection and clinical information was approved by the Institutional Review Board and patients provided written informed consent authorizing the collection and use of the tissue for biomedical research purposes.

3.1.2 Compliance with guidelines and laws regulating animal research

Procedures involving animals and their care were conducted in conformity with institutional guidelines at the Institute of Pharmacological Research Mario Negri IRCCS (Milan, Italy), which adheres to the principles set out in the following laws, regulations, and policies governing the care and use of laboratory animals: Italian Governing Law (D. lg 26/2014; Authorization n°.19/2008-A issued March 6, 2008 by Ministry of Health); Mario Negri Institutional Regulations and Policies providing internal authorization for persons conducting animal experiments (Quality Management System Certificate-UNI EN ISO 9001:2015–Reg, N°6121); the NIH Guide for the Care and Use of Laboratory Animals (2011 edition) and EU directive and guidelines (EEC Council Directive 2010/63/UE). All in vivo experiments complied with protocols approved by the Ethical Committee of the Institute of Pharmacological Research Mario Negri IRCCS and the Italian Ministry of Health (approval numbers 510-2016 and 296/2018-PR).

In addition, intensive in vivo training is required by Institute of Pharmacological Research Mario Negri IRCCS guidelines to ensure respect and compliance with the above-mentioned laws.

3.1.3 Animals and establishment of patient-derived xenografts

All the experiments involving animals were carried out using six- to eight-week old female NCr-nu/nu mice obtained from Envigo Laboratories (Italy). Mice were maintained under specific pathogen-free conditions, housed in isolated vented cages, and handled using aseptic procedures.

For the isolation of patient-derived xenografts, tumour specimens were engrafted in nude mice within 24 hours from the surgical intervention. Specifically, fragments from tumour masses (primary tumour or metastasis) were engrafted subcutaneously (s.c.), whereas ascitic fluid were injected intraperitoneally (i.p.) as cancer cell suspension.

To obtain s.c. models, mice were anesthetized using an automatic delivery system that provides a continuous flow of 3% isoflurane (Florane, Abbott Laboratories) in 1% oxygen. A fragment of fresh human tumour specimen, dissected free of necrotic tissue, was injected subcutaneously in the flank of animals by incision with sterile scissors and the use of a trocar. The animals were followed for appearance of the tumour once a week. Once tumour formation was observed, mice were monitored at least twice a week, and tumour weight (TW) and body weight (BW) were measured. TW was monitored with a Vernier calliper and the TW (1mg= $1mm^3$) was calculated as follows: [length (mm) x width $(mm)^2$]/2. When the TW reached 20% of mouse total BW (approximately, 1500 mg), mice were euthanized by CO_2 exposure. Skin was disinfected with ethanol and an incision was performed to access the tumour mass, which was collected using sterile surgical instruments. Then, tumours were fragmented, dissected from eventually necrotic areas and re-injected in animals for a new passage.

To obtain i.p. models, ascitic fluid from paracentesis was centrifuged, washed repeatedly, resuspended in phosphate buffered saline (PBS) solution, and injected intraperitoneally in mice at a dose of 10 $x10^6$ to $20x10^6$ cells in 200 uL of saline solution (0.9% NaCl). Criteria for growing tumours were abdominal distension and palpable tumour masses in the peritoneal cavity. Mice were monitored at least twice a week, and the animal BW were measured. Mice were euthanized when an increment of 10-15% of their BW was observed and the day of the autopsy was considered as survival time. Ascitic fluid and subsequent peritoneal washings (3 ml sterile saline solution) were harvested using a 5 ml syringe, collected in a 15 ml tube, and centrifuge at 1200 rpm for 10 min at 4°C. Pellet was washed 1 to 3 times with Red Blood Cell Lysis Buffer (Merk) to remove the erythrocytes following the manufacturer instructions. 1 ml of pellet was considered to contain $100x10^6$ cancer cells.

3.1.4 PDX samples storage

At the time of euthanizing, xenograft tumour specimens were in part immediately frozen in dry ice and stored at -80°C for molecular studies. For histopathological and immunohistochemical studies, part of the sample was fixed in formalin solution (10% phosphate-buffered formalin (BioOptica) for 24 hrs to avoid excessive crosslink formation and loss of antigens, and maintained in a solution of 70% of ethanol until to be paraffin-embedded (FFPE).

FFPE tumour samples from 60 EOC-PDXs were included in a tissue microarray (TMA), using a standard technique (Pilla et al., 2012). The pathologist selected two core biopsies from distinct areas of FFPE PDX samples and these were randomly included to generate a TMA. All the samples are included in duplicate. Besides PDXs tumour samples, the TMA also includes specimens of murine healthy ovaries, murine ovarian carcinomas and ovarian cancer xenografts from human ovarian cancer cell lines, as internal controls.

3.1.5 Antitumour pharmacological activities

Cisplatin (Sigma-Aldrich) diluted in saline solution was given intravenously (i.v.) at the dose of 5 mg/kg, every seven days for three times. Olaparib (Targetmol) was dissolved in 10% v/v dimethyl sulfoxide (DMSO) in 10% w/v HP-beta-ciclodestrine and diluted in sterile water, given per os at the dose of 100 mg/kg, daily for 28 days.

The tumour growth of EOC-PDXs was monitored, and when the s.c. PDXs reached approximately 120 mg of TW, mice were randomized to receive the treatment or in the control group to receive the vehicle of the drug. i.p. PDXs were randomized to treatment at an advanced stage (i.e. 25% of expected median survival time). Each group comprised 8-10 mice.

For s.c. PDXs, treatment efficacy was expressed as best tumour growth inhibition (T/C), calculated as follows:

$$\frac{T}{C}\% = \frac{median\ TW\ of\ treated\ mice}{median\ TW\ of\ control\ mice} \text{ x } 100$$

For i.p. PDXs, treatment efficacy was expressed as the best increase in lifespan (ILS), calculated as follows:

$$\textbf{ILS\%} = \frac{(median\ survival\ days\ of\ treated\ mice - median\ survival\ days\ of\ control\ mice)}{median\ survival\ days\ of\ control\ mice}\ x\ 100$$

Drug activity was defined as follows:

	s.c. PDXs	**i.p. PDXs**
Very sensitive	T/C% ≤10%	ILS% ≥100%
Sensitive	10%< T/C% <50%	40%< ILS% <100%
Resistant	T/C% ≥50%	ILS% ≤40%

The best T/C% parameter used to assess the response to antitumour treatments in s.c. PDXs was compared with the modified Response Evaluation Criteria in Solid Tumours (mRECIST) method, similar to that applied in the clinical setting (Castroviejo-Bermejo et al., 2018a; Cruz et al., 2018). To assess the best response for olaparib and cisplatin treated

PDXs, we considered the minimum value of % tumour volume change (min ΔVt %) sustained for at least 10 days. Antitumour response was classified into four groups:

Complete response (CR)	min ΔVt % ≤ -95%
Partial response (PD)	-95% < min ΔVt % < -30%
Stable disease (SD)	-30 < min ΔVt % < +20%
Progressive disease (PD)	ΔVt % ≥ 20%

3.2 HISTOPATHOLOGICAL ANALYSIS

Dr Patrizia Perego, Director of the Department of Surgical Pathology, Cytology and Medical Genetics, at the San Gerardo Hospital (Monza, Italy), performed all the immunohistochemical analyses. FFPE tissue slides (1μm) were dewaxed in xylene and rehydrated through decreasing ethanol concentrations, then washed in Tris Buffer Saline (TBS) pH 7.6 twice. Antigen retrieval was performed using Antigen Retrieval Buffer pH 6 for 30 min at 98°C. Endogenous peroxidases were inhibited by incubating the samples in 3% H_2O_2 for 5 min followed by washing in TBS. The slides were incubated for 30 min with primary anti-human antibody. In particular, anti- cytokeratin pool (65-67, 64, 59, 58, 56.5, 56, 54, 52, 50, 48, 40 KDa) and anti-CA125 (DAKO). Then samples were incubated for 20 min with a biotinylated link antibody and alkaline phosphatase-labelled streptavidin (Labeled Streptavidin Biotin (LSAB) + System-HRP, DAKO) and finally washed in TBS. The chromogen diaminobenzidine (provided by LSAB+ System-HRP, DAKO) was then applied for 5 min with Mayer's haematoxylin diluted 1:4 in distilled water, dehydrated, mounted using an automated instrument and visualized with a BX60 microscope (Olympus).

3.3 MOLECULAR ANALYSES

3.3.1 DNA extraction and purification

Genomic DNA was extracted from snap frozen xenograft tumours using the Maxwell® 16 System (Promega). The Maxwell® 16 DNA Purification Kit (Promega) was used to isolate genomic DNA in combination with the Maxwell® 16 Instrument. Maxwell® 16 Instruments are magnetic particle handlers that efficiently pre-process liquid and solid samples, transport the paramagnetic microbeads through purification reagents in the prefilled cartridges and mixes during processing.

Cells or tissue biopsy were directly added to the first well of the cartridge containing the lysis buffer. Then, the cartridge was loaded into the instrument, which was set up with the proper extraction protocol. DNA purification employed a guanidine thiocyanate-based procedure to disrupt cells and denature proteins and magnetic microbeads to separate DNA from other cellular components. After the automatic procedure, DNA is eluted in 300 µl of sterile H_2O and 2 µl was used to determine the concentration with a NANODROP nd-1000 spectrophotometer (Thermo Fisher Scientific). The absorbance of DNA or RNA samples was measured at 260 nm, 280 nm and 230 nm. The concentration was automatically established by the instrument using the Lambert-Beer formula, relating the absorbance measured by the instrument with the concentration of the absorbing molecule. Nucleic acid purity was controlled based on the 260/280 and 260/230 ratios (nucleic acids vs proteins and nucleic acids vs contaminants, respectively). Accepted ratios range from 1.7 to 2.1.

3.3.2 STR analysis

Short tandem repeats (STR) analysis was performed by Dr Mirko Marabese, Head of the Molecular Genetic Unit at the Institute of Pharmacological Research Mario Negri IRCCS, using a multiplex STR-specific PCR, based on the Powerplex® 16 HS system kit (Promega). This PCR was used to simultaneously amplify 16 STR loci across the human genome in each

sample: D3S1358, TH01, D21S11, D18S51, Penta-E, D5S818, D13S317, D7S820, D16S539, CSF1PO, PENTA_D, Vwa, D8S1179, TPOX, FGA, and the Amelogenin (AMEL) locus for sex determination. The PCR reaction was done following the manufacturer instructions provided with the Powerplex® 16 HS system kit (Promega) and 1 ng of purified DNA was required for the PCR. The multiplex-PCR was performed in a Veriti96-well Thermal Cycler (Applied Biosystem).

STR profiles were generated with GeneMarker HID (SoftGenetics).

3.3.3 Mutational status analysis

For the present thesis, I performed the mutational status analyses of *TP53* (exons 5 to 9), *BRAF* (exons 11 and 15), *KRAS* (exon 2) and *PI3Kα* (exons 10 and 21) using the Sanger method on the EOC-PDXs of the xenobank. Whole genome sequencing was conducted on 10 selected PDXs (detailed in chapter 4.2.3) in collaboration with Dr Nik-Zainal at the Wellcome Trust Sanger Institute (Hinxton, UK), who performed the WGS focusing on HR DNA repair pathway genes (Chopra et al., 2020; Davies et al., 2017). The NGS and RNA-seq analysis and subsequent validation with Sanger methods to detect aberrations and mutations in HR genes were described by Dr Francesca Bizzaro, PhD student in the Therapy of Tumor Metastases Laboratory at the Mario Negri's Institute (Bizzaro, Francesca, 2018).

3.3.3.1 Sanger method

PCR reaction

Genomic DNA was obtained from EOC-PDXs and amplified by PCR with primers designed *ad hoc* using "Primer3 Input" software ("http://primer3.ut.ee/," n.d.).

Primers sequences were the following:

Gene	Exons	Primer forward (5'-3')	Primer reverse (5'-3')
TP53	5-6	TTGCTTTATCTGTTCACTTGTGC	GCCACTGACAACCACCCTTA
	7	TGCTTGCCACAGGTCTCC	GGTCAGAGGCAAGCAGAGG
	8-9	CAAGGGTGGTTGGGAGTAGA	CCCCAATTGCAGGTAAAACA
KRAS	2	CTTAAGCGTCGATGGAGGAG	AGAATGGTAATGCACCAGTAA
BRAF	11	AAGGGGATCTCTTCCTGTATCC	GAAACTTTTGGAGGAGTCCTGA
	15	AACACATTTCAAGCCCCAAA	CTGATTTTTGTGAATACTGGGAACT
PI3Kα	10	TGAAAATGTATTTGCTTTTTCTGT	ACATGCTGAGATCAGCCAAA
	21	GCTTTGTCTACGAAAGCCTCT	ATGCTGTTCATGGATTGTGC

The mix for gene amplification (Promega) was prepared as follow:

PCR reaction mix components (Promega)	*Volume per single reaction*
BUFFER 5x FLEXI (without $MgCl_2$)	10 µl
$MgCl_2$ (25 mM)	5 µl
dNTP (10 mM)	1 µl
Primer Forward /Reverse (10µM)	2 µl + 2 µl
TaqHotStart enzyme	0.25 µl
DNA 5ng/ µl	10 µl
H_2O	10 µl
Final volume	50 µl

PCR amplification conditions were reported below:

Cycles	Duration	Temperature
1	2 min	94°C
35	15 sec	94°C
	30 sec	60°C
	45 sec	72°C
1	5 min	72°C

PCR product purification

PCR products were verified by detecting single band-amplicons with a 1.5% agarose gel. Amplified DNA was purified using the Illustra™ GFX PCR DNA and Gel Band Purification kit (GE Healthcare) following the kit instructions. 500 ul of capture buffer were added to each sample and transferred to a GFX column and centrifuged. After two washing steps, the elution buffer (20 ul) was added to each column and again centrifuged to recover purified DNA.

Sequencing of amplified DNA

Mycrosynth Seq Lab service (Germany) performed the sequencing. Results were shown as chromatograms and FinchTV software (Geospiza) was used to analyse them.

3.3.4 Promoter methylation status analysis

Promoter methylation status in the PDXs was assessed using two methods: pyrosequencing technique for *BRCA1, MLH1, ERCC1, XPA* genes, and MS-PCR for *BRCA1, FANCF* and *XPG* genes. In both cases, specific small promoter regions (<500 pb) including several CpG sites were analysed after conversion with sodium bisulfite.

3.3.4.1 Sodium bisulfite conversion

Sodium bisulfite treatment is used to convert cytosine in uracil, while 5-methylcytosines remain intact. Then, 1 μg of genomic DNA was converted with Epitect Plus DNA Bisulfite Kit (Qiagen) according to the manufacturer instructions. To verify successful sodium bisulfite conversion of the samples, a region of the *Calponin* promoter was amplified by MS-PCR in all the modified samples using the following primers (Sriraksa et al., 2010):

Gene	Primer forward (5'-3')	Primer reverse (5'-3')
Calponin	*GGAAGGTAGTTGAGGTTGTG*	*CCCAAACTCAAAACTCTAACCT*

The PCR mix and conditions are described in (Sriraksa et al., 2010) and are reported below:

PCR reaction mix components (Promega)	*Volume per single reaction*
BUFFER 5x FLEXI (without $MgCl_2$)	5 µl
$MgCl_2$ (25 mM)	3 µl
dNTP (10 mM)	5 µl
Primer Forward /Reverse (10µM)	1 µl + 1 µl
TaqHotStart enzyme	0.12 µl
DNA converted 20 ng/uL	1 µl
H_2O	8.9 µl
Final Volume	25 µl

Cycles	Duration	Temperature
1	5 min	95°C
35	30 sec	95°C
	30 sec	63°C
	1 min	72°C
1	5 min	72°C

3.3.4.2 Pyrosequencing technology

After bisulfite conversion, PCR is required to amplify the converted DNA samples. For *BRCA1, MLH1, ERCC1* and *XPA* pre-designed primers (Pyromark CpG Assays by Qiagen) were used (**table 3.1**), covering the following regions of the promoter (**figure 3.1**):

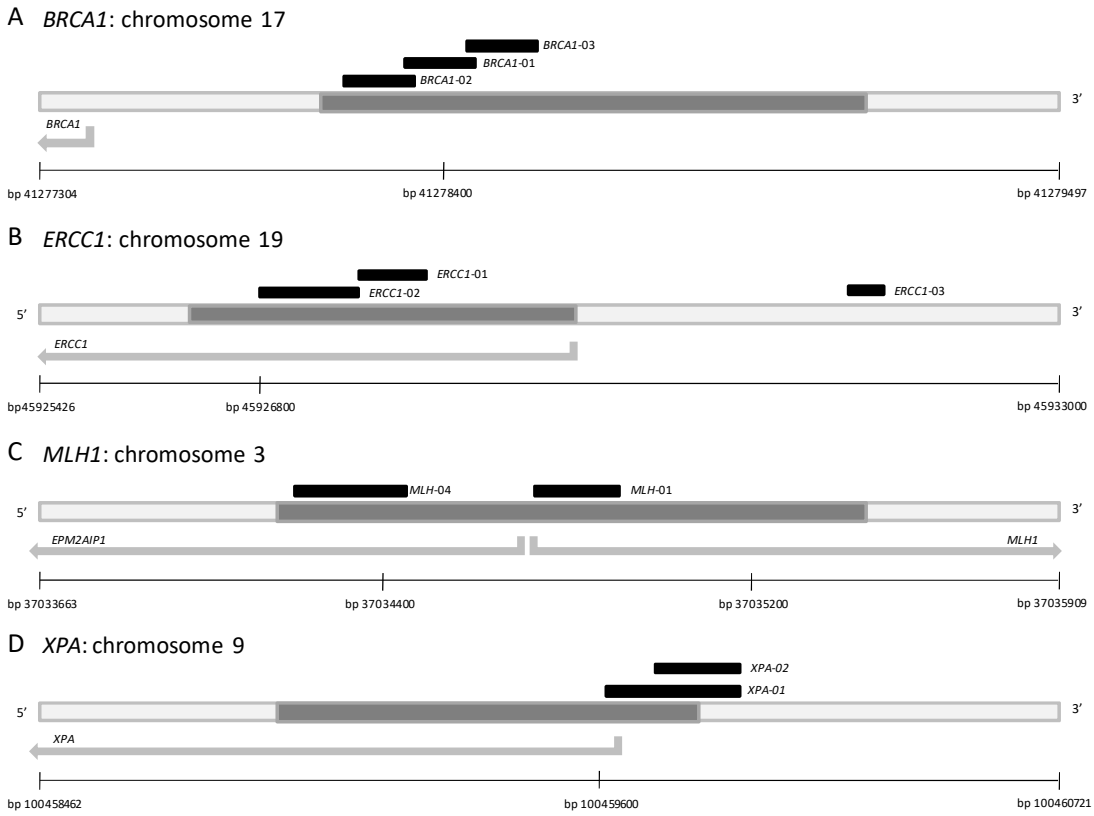

Figure 3.1 Chromosomal location of the PyromarkCpG assays (Qiagen) used to analyse the methylation status of *BRCA1*, *ERCC1*, *MLH1* and *XPA* through Pyromark PCR and Pyrosequencing (Qiagen)

Genomic coordinates are shown along with PyromarkCpG assays (in black) and promoters (dark grey).

Table 3.1 List of the PyromarkCpG Assays (Qiagen) used for Pyrosequencing

Gene	Assay name	Qiagen Assay Name	Number of CpG sites included
BRCA1	*BRCA1*-01	Hs_BRCA1_01_PM PyroMark CPG assay PM00064862	4
	BRCA1-02	Hs_BRCA1_02_PM PyroMark CPG assay PM00064869	3
	BRCA1-03	Hs_BRCA1_03_PM PyroMark CPG assay PM00064876	4
ERCC1	*ERCC1*-01	Hs_ERCC1_01_PM PyroMark CPG assay PM00071904	6
	ERCC1-02	Hs_ERCC1_02_PM PyroMark CPG assay PM00071911	4
	ERCC1-03	Hs_ERCC1_03_PM PyroMark CPG assay PM00185682	5
MLH1	*MLH1*-01	Hs_MLH1/EPM2AIP1_01_PM PyroMark CPG assay PM00104839	5
	MLH1-04	Hs_MLH1/EPM2AIP1_04_PM PyroMark CPG assay PM00104860	6
XPA	*XPA*-01	Hs_XPA_01_PM PyroMark CPG assay PM00142212	6
	XPA-02	Hs_XPA_02_PM PyroMark CPG assay PM00142219	5

20 ng of DNA converted were amplified by PCR using the Pyromark PCR kit (Qiagen) and following the kit instructions. The PCR conditions were the following:

Cycles	Duration	Temperature
1	15 min	95°C
45	30 sec	95°C
	30 sec	56°C
	30 sec	72°C
1	10 min	72°C

PCR products were checked by agarose gel analysis before Pyrosequencing.

The PyroMark ID96 platform, an in vitro nucleic acid sequence-based detection test based on pyrosequencing technology, and PyroMark ID96 software were used to sequence and analyse pyrograms of the promoter regions of the selected genes giving the % of CpG sites found methylated.

3.3.4.3 MS-PCR

For *BRCA1*, *FANCF* and *XPG*, the analysis of promoter methylation status was performed with methylation specific-PCR and primers designed *ad hoc* to distinguish the methylated (M) from the unmethylated (U) region, as detailed below:

Gene	Primer name	Primer forward (5'-3')	Primer reverse (5'-3')
BRCA1	BRCA1_M	TCGTGGTAACGGAAAAGCGC	AAATCTCAACGAACTCACGCCG
	BRCA1_U	TTGGTTTTTGTGGTAATGGAAAAGTG	CAAAAAATCTCAACAAACTCACACCA
FANCF	FANCF_M	TTTTTGCGTTTGTTGGAGAATCGGGTTTTC	ATACACCGCAAACCGCCGACGAACAAAACG
	FANCF_U	TTTTTGTGTTTGTTGGAGAATTGGGTTTTT	ATACACCACAAACCACCAACAAACAAAACA
XPG	XPG_M	GCGGATTTATTAGCGAAGGCGG	CACTAATAAAAACGCATTAAAACGAA
	XPG_U	TTTGTGGATTTATTAGTGAAGGTGGG	ATAAAAACACATTAAAACAAAAAAAC

The region in *BRCA1* promoter was different from those previously analysed and it ranges from 41277722 bp to 41277808 bp.

20 ng of bisulfite converted DNA were amplified with MS-PCR. Mixture (Promega) and conditions were those reported for *Calponin*, except for the temperature of annealing relative to each couple of primers: for *BRCA1* 62°C, for *FANCF* 58°C and for *XPG* 52°C.

MS-PCR products were then separated on 2% agarose gels and visualized with SYBR Green I Nucleic Acid Gel Stain (Thermo Fisher Scientific) and images were acquired with Odyssey Fc (Licor) system.

3.3.5 Gene expression analysis

3.3.5.1 RNA extraction and retrotranscription

Total RNA was extracted from snap frozen tumour tissues or tumour cells with Maxwell® RSC simplyRNA Tissue Kit (Promega). Similarly, for DNA extraction, the kit provided all the reagents and prefilled cartridges required for RNA extraction from as few as 10^6 cells. The extraction was then carried out automatically by the Maxwell® RSC Instrument (Promega).

The first step required is manual, and it is necessary before loading the sample into the cartridge. It required the incubation of cells with a mixture containing 20µl of thioglycerol in 200µl of Homogenization Solution per sample. Snap frozen tissue homogenization was facilitated with an automatic homogenizer (UltraTurrax-Ika). Then, 200µl of a guanidine thiocyanate containing solution (Lysis Buffer), which maintains the integrity of RNA while dissolving cell components, were added to the homogenate solution. The final solution was vortexed for 20 sec and the overall volume of 400µl was loaded into the first well of the cartridge (**figure 3.2**).

The Maxwell® RSC Instrument was set up for the protocol of RNA extraction from cells and it employs magnetic microbeads to separate RNA from the other cellular components, sequential ethanol-based washing steps and DNAse enzyme to digest the DNA. At the end

of the process, RNA was found eluted in 50µl of RNAse free water and then quantified using Nanodrop spectrophotometer. RNA samples were storage at -80°C until use.

Figure 3.2 Maxwell® RSC cartridge system (Promega) employed for automated RNA extraction from tissues or cells

Samples homogenized with Lysis Buffer were loaded into the first well of the cartridge. A plunger needs to be added into the last well and 5µl of DNAse containing solution into the fourth well. The Maxwell instrument automatically extracted RNA from the sample, washed it and eluted it in the tube in front of each cartridge.

High Capacity cDNA Archive kit (Life Technologies) was used to perform retrotranscription reaction. A range from 200ng to 1µg of total RNA was retrotranscribed to single-stranded cDNA using random hexamers.

The reaction protocol was: 25°C for 10 min followed by 2h at 37°C.

cDNA reaction products were kept at -20°C until the RT-PCR step.

3.3.5.2 Real time-PCR reaction

The absolute quantification of the mRNA copies of 35 DNA repair genes was determined using real time-PCR with SYBR green® technology.

Optimal primer pairs were chosen, spanning splice junctions, using Primer3 software as above mentioned. Synthesis of oligonucleotides used as primers was performed by Metabion (Germany). Primer specificity was verified by detecting single-band amplicons of the PCR products in agarose gel. They were also tested for the human specificity using murine cDNA.

All the DNA samples extracted from PDXs were also tested with PCR in order to assess the % of murine DNA contamination using primers specifically designed to distinguish between murine and human *ACTB*. We accepted for the experiments xenografts tumours having more than 70% of human DNA.

Experiments were run in triplicate, and absolute quantification of the number of mRNA molecules was determined by RT-PCR thermocycler (ABI-7900, Applied Biosystems), loading 384-well plates with an EpMotion 5075 robot (Eppendorf).

Expression data were normalized employing the geometric mean of two housekeeping genes: actin-β (*ACT*B) and cyclophilin (*CYP*), used as endogenous controls.

A detailed list of the primers used in the RT-PCR experiments is reported:

Gene function	Gene	Primer forward (5'-3')	Primer reverse (5'-3')
Housekeeping	*ACTB*	TCACCCACACTGTGCCCATCTACGA	CAGCGGAACCGCTCATTGCCAATGG
Housekeeping	*CYP*	GACCCAACACAAATGGTTCC	TTTCACTTTGCCAAACACCA
Homologous recombination (HR)	*BRCA1*	GAACGGGCTTGGAAGAAAAT	GTTTCACTCTCACACCCAGA
	BRCA2	TGTCACAACCGTGTGGAAGT	TGATGGACGCCAAATACTCA
	RAD51	CAGATGCAGCTTGAAGCAAA	TTCTTCACATCGTTGGCATT
	PALB2	CTTGGCAGTGGGAAAAACTT	TTCCCAAAGCTACACACACG
	RAD51C	GCCTTGCTTGTTCCTGCATT	TGGCTGGGTGACTTGTACAA
DNA DSB response	*53BP1*	TGGTTCCATCAGTCAGGTCA	ACAGCAGGAGCAGATTCCAC
	ARTEMIS	ACAGGAGACTTCAGATTGGCG	CACTCCTCCCGACTTGGAATT
	PTIP	AGGAAAGCCATGTTCACAGC	CACCTGCCAAATAAGCCATT
Base excision repair (BER)	*PARP1*	AAGAAATGCAGCGAGAGCAT	CCAGTGTGGGACTTTTCCAT
	POLB	TGCCTGGAGTAGGAACAAAAA	GGAAATTGATGGATGAACTCG
	OGG1	CTCCACTCCTGCCCTGTG	CCAGTGTGCAGGACTTTGC
Nucleotide excision repair (NER)	*XPA*	ATGCGAAGAATGTGGGAAAG	CTTGTTTTGCCTCTGTTTTGG
	XPD	GTGGCCATCAGCTCCAAAT	CAGCAGGAGGTTCCCATAGT
	XPF	TTGTGAGGAAACTGTATCTGTGG	AGCAAGCATGGTAGGTGTCA
	XPG	TCTGGAAGCTGCTGGAGTG	GACAAAAGGAATGGCAGGAG
	ERCC1 tot	CCAACAGCATCATTGTGAGC	TCTTGGCCCAGCACATAGTC
	ERCC1iso2	GACCACCGTGAAGTCAGTCA	GGGCATAAGGCCAGATCTTC
Fanconi anemia (FA)	*FANCA*	GAGACCAGTCACCCTGTGCT	CAGAAGGAAAGACGGGAGAA
	FANCC	GGCAAAAGCTTGTTGGAATC	CCAGGAGTTAAGTTTTGATTGTCC
	FANCF	GCTAGTCCACTGGCTTCTGG	GGTGGCGGCTAGTCACTAAA
	FANCD2	CCTCGACTCATTGTCAGTCAAC	GATGATGTCATGCTGCAGGT
Mismatch repair (MMR)	*MLH1*	AAGCCATGTGGCTCATGTTA	AGGGGCTTTCAGTTTTCCAT
Non-homologous end joining (NHEJ)	*KU70*	GCTTCTGCCTAGCGATACCA	CCCATGAGCATCAAACCTGG
	KU80	TGAGAAGACAGACACCCTTGA	CCGGGGATGTAAAGCTCTGT
	DNA-PK	GCACTTTCAGCCCTGGAATC	CTGCTCCATAAAGTACTGCAGT
Microhomology end joining (MMEJ)	*POLQ*	GCTGGAACTTTTGCTGACCA	TCATGCCAACGATTTGCACA
Translesion repair (TLS)	*POLH*	CTGGCACAAGTTCGTGAGTC	CGTTCAATCACAGCAAAACG
Regulator of DNA repair gene transcription	*CDK12*	TTGTCACAGATAAACAAGATGCAC	TGCACCAAACCAGATTCTAGC
DNA damage response	*SLFN11*	TGGGTAGGCATGATGACAGA	AAGGGGAGGCCCACTAGATA
Chromatin organizer	*ARID1A*	GTGTTGCTCAGTCTCGCTCA	ATTGGTTCATGGAAGGATGC
	CARM1	ATCCGGATCCTGATGGCCA	AGCAACGTCAAACCAGAAAGC
	CHD4	ACCCAAGAAAGTAGCTCCCC	ACTGGCATCATCGAAGTCAGA
Cell cycle regulators	*REV7*	AGTGGTGGTGGTGATTTTGG	AGCTGCTCCACATGAGACAA
	CCNE1	AATGCGAGCAATTCTTCTGG	CGCCATATACCGGTCAAAGA
Deubiquitination	*USP28*	AGTGCTGCCAACAAGGAAGT	TTGAATTTTGGGAGACTCCAG
Drug transporter	*MDR1*	CCCATCATTGCAATAGCAGG	GTTCAAACTTCTGCTCCTGA

The RT-PCR reaction mix was prepared as follow:

PCR reaction mix components	*Volume per single reaction*
2X Go Taq qPCR Master Mix (Promega)	5 µl
Primers F / R 10 µM	0.2 µl + 0.2 µl
H_2O	0.6 µl
cDNA 2,5 ng/µl	4 µl
Final Volume	10 µl

The reaction conditions were:

Cycles	**Duration**	**Temperature**
1	2 min	50°C
1	10 min	94°C
40	15 sec	94°C
	1 min	60°C
1	15 sec	95°C
1	15 sec	60°C

The last two steps were added when a dissociation curve protocol was needed.

Raw data were generated with SDS Relative Quantification Software (Applied Biosystems). Standard curves for each gene were included for the absolute quantification of mRNA copies. To generate the calibration curve of a specific gene, a RT-PCR was run with a cDNA sample (i.e. an ovarian cancer cell line, which expresses the gene of interest) at the condition described above. After RT-PCR, the amplification product was run in agarose gel and the sample band was then extracted and purified with Gel Band Purification kit (GE Healthcare) as previously detailed. Next, the PCR amplicon diluted in RNAase free water, was quantified with the Nanodrop instrument.

The calculation of the number of mRNA molecules for each PCR product was performed with the following formula:

$$\textbf{N° of mRNA copies=} \frac{6.023x10^{23}}{(330\ x\ amplicon\ lenght\ (n°\ bp)} \ x\ cDNA\ concentration\ \left(\frac{\mu g}{\mu L}\right) x10^{-6}$$

Next, the starting "mother dilution" corresponding to 10^8 mRNA copies was prepared in RNAse free water, and the subsequent dilution points were prepared by serial dilution from the first "mother", from 10^7 to 1 copy of mRNA (10^7, 10^6, 10^5, 10^4, 10^3, 10^2, 10^1, 10^0).

The calibration points were added into the definitive 384-well plate, 4 µL of each point, in triplicate, instead of sample.

The standard curve obtained in this way at the end of the RT-PCR run allowed me to extrapolate the exact quantity of mRNA starting from the number of Ct for each sample.

A robust standard curve must have a slope of -3.3 (±0.3) and Y-intercept ranging from 1 to 0.98.

3.3.6 HRDetect assay

The HRDetect assay was applied to ten of our PDXs in collaboration with Dr Nik-Zainal, who set up this assay and the relative algorithm, aimed to elaborate a score indicative of the HRD status of a tumour sample. The detailed method is described in (Chopra et al., 2020; Davies et al., 2017).

Briefly, genomic DNA was extracted from the snap frozen PDX tumours. We checked the amount of human *ACTB* vs murine *ACTB* contamination (only samples with >70% of human DNA were accepted) and 1000 ng of DNA in 30 ul of TE buffer was sent to the Wellcome Trust Sanger Institute to perform the whole genome sequence (WGS), in parallel with an aliquot of the germline DNA of the patient from which the PDX was derived from, extracted from blood sample, stored in the PANDORA Biobank at the Mario Negri Institute.

500-bp insert genomic libraries were constructed according to Illumina library protocols and 150 bp paired-end sequencing performed on an Illumina HiSeq X Ten using HCS (v3.5.0) for HiSeq X systems, to an average sequence depth of 38.5× for both tumour and normal. The resulting reads were aligned to the reference patient genome.

Mutation calling was performed as described in (Nik-Zainal et al., 2016), evaluating somatic substitutions, indels, structural variants, allele-specific copy number variations and loss of heterozygosity (LOH) across the *BRCA1, BRCA2* and *PALB2* genes.

Mutational signature contributions for substitution signatures 3 and 8, rearrangement signatures 3 and 5, deletions at microhomology and HRD LOH index were calculated for each sample as input into the weighted model, HRDetect.

The HRDetect algorithm is based on a lasso logistic regression model, which was used to identify the genomic features that could distinguish the two categories of samples: the HRD and HR proficient tumours, and to assign a probabilistic score to each sample. The HRDetect algorithm was run as described in (Davies et al., 2017).

The HRDetect score could be >0.7, suggesting an HRD tumour, and, vice versa, <0.7 indicative of HR proficiency.

3.3.7 Nuclear foci immunofluorescence-based assays

To detect and quantify RAD51 foci, we applied two immunofluorescence (IF)-based methods. The first was performed in collaboration with Dr Deborah Wilsker of the Frederick National Laboratory for Cancer Research (MD, USA), where RAD51 foci where detected on the TMA including 60 PDXs of our xenobank. The second method we applied was recently set up by the Experimental Therapeutics Group, at the Vall D'Hebron Institute (Barcelona, Spain) headed by Dr Violeta Serra (Castroviejo-Bermejo et al., 2018a; Cruz et al., 2018). This latter assay was employed on FFPE tissue samples of PDXs.

3.3.7.1 IF detection of RAD51 foci on TMA

5 μm TMA slice was deparaffinised, and prepared for the staining following the method described in (Wilsker et al., 2019).

IF co-staining was performed to detect RAD51 foci using a custom-conjugated Rad51-DNP primary antibody detected with the use of Alexa Fluor 488, conjugated anti-Dinitrophenyl-

KLH Rabbit IgG Antibody fraction, (DNP-488; Thermo Fisher Scientific) (FITC channel) and B-catenin, using a mouse primary antibody detected with the use of Alexa Fluor 546 (TRITC channel). B-catenin was used as marker of cancer cells and RAD51 foci was quantified in this population of cells.

Automatic images acquisition was performed with a Nikon 90i confocal microscope (20x) and over 2500 images were acquired.

A Quality Control process was followed according to (Marrero et al., 2016), excluding poor quality tissue (low number of cancer cells or no tumour tissue); aspecific FITC signal, due to RBCs, autofluorescence, or damaged tissue; high background due to microscope Gain; only β-catenin positive tissues were analysed.

Samples with a minimum of 2900 countable nuclei were considered significant and high confidence.

The quantitative analysis was performed by Definiens Tissue Studio® software (Definiens AG, Germany) for analysis of marker expression and nuclear segmentation and enumeration. RAD51 assay reported the % of cells per sample expressing ≥5 RAD51 foci per nucleus, in compliance with the Quality Control process.

3.3.7.2 IF detection of RAD51 foci on FFPE samples (PARPiPred test)

3 μm FFPE tissue sections were deparaffinised with xylene and hydrated with decreasing concentrations of ethanol solutions.

Antigen retrieval was performed boiling the tissue sections in a microwave for 4 min at 110°C in DAKO Antigen Retrieval Buffer pH 9.0.

Samples were cooled down in MilliQ water and ice, then permeabilized in PBST solution (PBS + Tween 20%) for 5 min and incubated with the blocking buffer solution (PBST + 1% bovine serum albumin fraction V (BSA)) for 1 hr.

The following primary antibodies were used for IF experiments:

- rabbit anti-RAD51 ab133534 (Abcam), diluted 1:1000

- mouse anti-geminin NCL-L (NovoCastra), diluted 1:100

- mouse anti-γH2AX monoclonal antibody clone JBW301 (Millipore), diluted 1:200

- mouse anti- BRCA1 c-terminus (D9) sc6954 (SantaCruz), diluted 1:50

- rabbit anti-geminin 10802-1-AP (ProteinTech Group), diluted 1:400.

Primary antibodies were diluted in blocking buffer solution, properly diluted, and incubated at room temperature for 1 hr. For the co-staining it was used the anti-body anti the foci-protein of interest and the antibody anti-geminin, according with the proper species.

After washing buffer with PBST, secondary antibodies were diluted in blocking buffer 1:500, using Alexa Fluor 488 (FITC) (usually for geminin) and Alexa Fluor 568 (m-Cherry) (usually for nuclear foci) (Life Technologies), and incubated at room temperature for 30 min, in dark chamber.

Again, two washing steps with PBST were repeated and tissue sections were put into distilled water for 5 min, before dehydration was performed with increasing concentration of ethanol. Nuclei were stained with 4',6-DiAmidino-2-PhenylIndole (DAPI) (30 ng/ml in PBS, Sigma-Aldrich) 10 min in dark chamber, following two washes in PBS and one in distilled water. Slides were mounted with Vectashield solution (VectorLab).

Slices were stored at -20°C, protected from light, until analysis.

Slices were observed using the ECLIPSE Ti2-E (Nikon) fluorescence microscope, with the objective 60x/1.27 WI Plan APO IR, ∞ 0.15/0.19 WD 0.18-0.16 Nikon.

RAD51 foci was quantified by scoring the % of geminin-positive tumour cells with ≥5 foci per nucleus (RAD51+/GEM+). Scoring was performed blind. At least hundred GEM+ cells in three different areas of the tissue section were analysed.

The same scoring was performed for BRCA1 foci (BRCA1+/GEM+ cells) and γH2AX (γH2AX+/GEM+).

We considered RAD51 positive tumours those samples, which included ≥10% RAD51+/GEM+ cells; BRCA1 positive tumours those with ≥35% BRCA1+/GEM+ cells

(calculated on the median of BRCA1+/GEM+ cells expressed in our EOC-PDXs); γH2AX positive tumours those with ≥25% γH2AX+/GEM+ cells.

3.3.8 Immunohistochemical analysis

ERCC1 and POLB immunohistochemical (IHC) analyses were performed in 5 μm TMA sections.

Sections were deparaffinised in xylene and hydrated with decreasing concentrations of ethanol solutions.

Antigen unmasking was done boiling the TMA section at 95°C for 30 min in MS-Unmasker tris (EDTA) pH 7.8 solution (Diapath, Italy), then endogenous peroxidases were quenched and the section was incubated with blocking solution (PBST+ 1% BSA) to block the aspecific sites.

For POLB, IHC used a rabbit anti-POLB primary antibody ab26343 (Abcam), diluted in blocking solution and incubated following datasheet instructions. Then it was incubated with a biotinylated secondary antibody (VC-BA-1000-MM15, Vector Laboratories, Burlingame, CA, USA). Sections were labelled by the avidin–biotin–peroxidase (ABC) procedure with a commercial immune-peroxidase kit (VC-PK-6100-KI01, Vector Laboratories). The immune-reaction was visualized with 3,3′-diaminobenzidine (DAB), (VC-SK-4100-KI01, Vector Laboratories) substrate.

For ERCC1, IHC used a rabbit anti-ERCC1 primary antibody Sc-10785 (Santa Cruz Biotechnology), diluted and incubated following datasheet instructions. Then, tumour sections were incubated with a secondary antibody poly-HRP (RE7200-K, Novo Castra). The immune reaction was visualized adding peroxidase 3,3′-diaminobenzidine (DAB) and its substrate (NovoCastra). Sections were then counterstained with Mayer's haematoxylin and cover slipped.

A semiquantitative score was assigned to each tumour by Prof Eugenio Scanziani, the pathologist who performed the analyses at the University of Milan.

For both ERCC1 and POLB the signal staining intensity was measured as follows:

Signal intensity	Intensity score
negative	0
faint	0.5
mild	1
moderate	2
marked	3

A second score was assigned to each tumour based on the % of positive cells.

- For POLB the score-scale was:

% of POLB positive cells	Positivity score
0%	0
0.1% - 25%	1
26% - 50%	2
51% - 75%	3
76% - 100%	4

- For ERCC1 the score-scale was:

% of ERCC1 positive cells	Positivity score
0%	0
1% - 9%	0.1
10% - 49%	0.5
> 50%	1

The final IHC score was calculated by multiplying the intensity score with the positivity score. If the two cores of the same tumour in the TMA were both evaluable, the final score was calculating on the average of the two single scores.

3.3.9 Proximity Ligation Assay

Proximity ligation assay (PLA), or Duolink® PLA technology, allows detection of endogenous protein-protein interactions in situ with high sensitivity and specificity. Briefly, cells or tissue were stained with two IHC or IF primary antibodies to target the two proteins

of interest (i.e. ERCC1 and XPF). The two primary antibodies must derive from different species (i.e. mouse and rabbit). Next, the Duolink® PLA PROBES kit (Merk) provided two secondary antibodies known as PLA probes (PLUS and MINUS) that bind to the constant regions of the primary antibodies and contains a unique DNA strand. If the proteins of interest interact and are close to each other (< 40 nm), the DNA probes hybridize making a circular DNA molecule. This DNA can be amplified and visualized by fluorescent complementary oligonucleotide probes (Duolink® Fluorescent Detection Reagent kit (Merk)) or by HRP-labelled probes and the substrate components (Duolink® Detection Reagents for Brightfield, Merk) required for HRP enzymatic reaction, that need to be incubated with the cells. The schematic diagram of Duolink® PLA (Merk) is shown in **figure 3.3**.

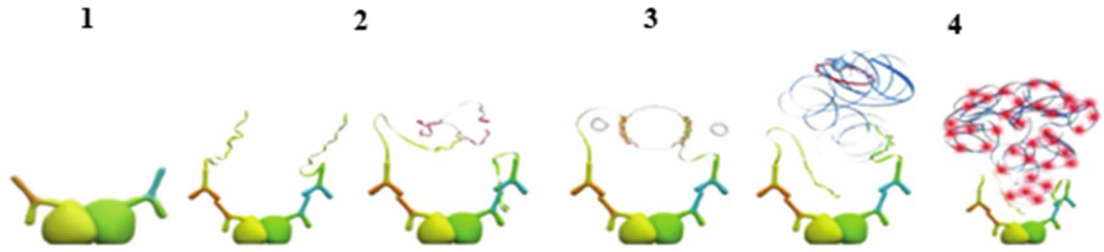

Figure 3.3 Duolink® PLA workflow

1) Two primary antibodies generated in different species bind the two proteins of interest on two epitopes of a single protein. 2) Secondary antibodies with MINUS and PLUS probes, which are species-specific, are added. 3) Two circle-forming DNA oligonucleotides and the ligase enzyme are added. 4) Polymerase enzyme amplifies the circular DNA. Fluorescent labelled, complementary oligonucleotides probes or HRP-labelled probes with its substrate are added and bind the amplified DNA, making visible the protein complex.

Protein-protein interactions were visualized as dots, and the number and intensity of the dots can be quantified by fluorescence or brightfield microscopy.

3.3.9.1 PLA on TMA (brightfield technology)

5 µm FFPE-TMA sections were put onto poly-lysine-coated glass slides. Sections were dewaxed and hydrated as usual, then, the first step requires antigen retrieval, leaving the

slides in the in MS-Unmasker Tris (EDTA) pH 7.8 solution (Diapath, Italy) and boiling at 95°C for 30 min. Once cooled down, the peroxidise quenching is required, incubating the tissues with H_2O_2 solution for 5 min. Then, blocking of aspecific sites was performed by adding the Blocking solution ready-to-use in the Duolink® PLA Probes kit (Merk) and leaving to incubate at 37°C in a wet chamber for 30min. Primary antibodies were used to detect ERCC1 (anti-rabbit, Sc-10785, Santa Cruz Biotechnology) and XPF (anti-mouse, MA56-12060, Thermo Fisher Scientific) diluted 1:100 and 1:200, respectively, in the same mixture with Antibody Diluent Solution of the same kit. Incubation was done at 4°C over-night, and a tissue slide was used as blank and it was left to incubate without primary antibodies. Next, PLA Probes MINUS and PLUS were added to the samples and left to incubate at 37°C for 1 hr and 30 min in a wet chamber, following manufacturer instructions, and allowing the formation of oligonucleotides. Then, the oligonucleotides were subsequently hybridized, ligated, amplified using the reagents and manufacturer instructions of the Duolink® Detection Reagents for Brightfield kit (Merk).

Slides were then counterstained with Vector® Nuclear Fast Red (VectaStain), dehydrated and mounted with Vectashield solution (VectorLab).

Images were acquired with the VS120-Virtual Slide microscope (Olympus) at 40X magnification and analysed with ImageJ software (ImageJ). In particular, the number of dots corresponding to the ERCC1/XPF complex were normalized by the number of nuclei visible in pink, evaluating at least three different areas of the tissue and counting at least 150 cancer cells for each tumour core. The final result was expressed as number of ERCC1/XPF foci per nucleus for each core. When two cores of the same PDXs were available the mean was calculated.

3.3.9.2 Cell culture conditions and in vitro treatment

Cell culture procedures were carried out aseptically in a class II laminar flow hood. Cells were maintained in a Heraeus CO 2 Auto-Zero incubator at 37°C in a humidified atmosphere

of 5% (v/v) CO_2 in air and routinely sub-cultured twice weekly. Cell lines were routinely tested for mycoplasma contamination by PCR and authenticated with the PowerPlex® 16 HS System (Promega) every 6 months by comparing the STR profiles to those deposited in the American Type Culture Collection (ATCC) and/or in the German Collection of Microorganisms and Cell Cultures (DSMZ) databases.

The human cancer cell line used in this project was the ovarian cancer cell line A2780, previously obtained from ATCC. The A2780 cell line was maintained in RPMI1640 with the addition of 10% foetal bovine serum (FBS) and 2 mM L-Glutamine (Lonza).

For the experiment, 40.000 cells/ml were seeded in 24-well plates. After 24 hrs, cells were treated with DDP (Sigma-Aldrich) at the IC_{50} dose of 10 μM (previously established in our laboratory) and 20 μM for 2 hrs. Then, DDP was removed and fresh medium was added into the wells. 24 hrs and 48hrs after the end of the treatment, cells were fixed with pure cold methanol at -20°C for 30 min, washed with PBS and storage in PBS at 4°C until PLA was performed.

3.3.9.3 PLA on A2780 DDP-treated cells (IF technology)

The PLA procedure was similar to that previously described for the brightfield conditions. The difference relies on the use of the Duolink® Fluorescent Detection Reagents Green (Merk) instead of the Duolink® Detection Reagents for Brightfield kit (Merk). The same primary antibodies were used for ERCC1 and XPF, at the same condition.

A2780 cells were incubated with DAPI solution (30 ng/ml in PBS, Sigma-Aldrich) for 10 min in a dark chamber, washed with PBS and then mounted.

The PLA signal was detected using the VS120-Virtual Slide microscope (Olympus) with FITC and DAPI channels at 40X magnification and imaging analysis was performed as previously described.

3.4 STATISTICAL METHODS

Statistical analyses were performed in collaboration with Dr Maria Francesca Alvisi and Dr Maddalena Fratelli, biostatisticians at the Mario Negri Institute, where this PhD thesis has been done. The agreement between T/C and mRECIST values used to establish the response of PDXs to chemotherapy, was assessed by Cohen's kappa index, as well as to verify the concordance between DDP and olaparib response.

The linear correlation between gene expression levels was measured by the Pearson test, while Spearman correlation coefficients were calculated for the correlation between continuous variables.

Response to therapy was analysed as categorical variable grouped in very sensitive (VS), sensitive (S) and resistant (R) based on the T/C and ILS values. For comparison of the three groups with different drug responses and the gene expression level, one-way ANOVA followed by a Tukey post-hoc test was applied. Microarray gene expression data of TCGA ovarian serous cystadenocarcinoma samples and *CDK12* co-expression analysis were retrieved from the cBioPortal platform ("http://www.cbioportal.org," n.d.). RNA sequencing v.2 expression data for a subset of the same database were retrieved from the TCGA data portal ("https://tcga-data. nci.nih.gov," n.d.).

The % of RAD51/BRCA1/γH2AX-foci positive cells were considered both as continuous variables and categorical variables by dichotomizing using these cut offs: 10% for RAD51, 35% for BRCA1 and 25% for γH2AX % foci. Non-parametric analyses were done if the assumption of normality was not satisfied. The Kruskall-Wallis test was used to analyse the association between the continuous % of RAD51/BRCA1-foci positive cells and response to DDP and olaparib, while Jonckheere-Terpstra per trend test was applied to analyse the statistical significance trend between % of RAD51/BRCA1 foci and response to DDP and olaparib. The Kruskall-Wallis test was also used to analyse the association between ERCC1/XPF foci, ERCC1 IHC score, POLB IHC score, ERCC1/XPF/POLB mRNA levels

and response to DDP. Spearman correlation index was calculated for the correlations between continuous variables. The unpaired t-test was used to analyse PLA foci number in untreated vs DDP-treated cells and the gene expression in hypermethylated PDXs vs non-hypermethylated.

P-values≤0.05 were considered statistically significant. SAS version 9.4 (SAS Institute, USA) and Prism software (Prism 7, GraphPad Software, USA) were used for the statistical analyses.

4. RESULTS

4.1 THE EOC XENOBANK

During the last decades in the Department of Oncology at the Institute for Pharmacological Research "Mario Negri" IRCCS, where this PhD project has been developed, great efforts have been carried out to establish a large platform of transplantable patient-derived EOC xenografts (EOC-PDXs). This platform, also named xenobank, is continuously updated and enlarged with new tumours deriving from our collaboration with the Gynaecological Division of San Gerardo Hospital in Monza (Italy) and the European Institute of Oncology (IEO) in Milan (Italy).

Clinical specimens (primary tumour, metastasis or ascitic fluid) are obtained from ovarian cancer patients undergoing surgical cytoreduction of the solid malignancy or paracentesis of ascitic fluid. Acceptance of the written informed consent gave the authorization for the collection and use of the tissue for research purposes. Clinical specimens are transplanted into nude immunodeficient mice subcutaneously or orthotopically/intraperitoneally to generate the PDXs (**figure 4.1**).

Currently, the xenobank includes more than sixty EOC-PDXs representing all the different EOC histotypes: serous, endometrioid, clear cell, mucinous, carcinosarcoma, müllerian mixed and undifferentiated carcinomas, at different grade and stage. Among them, 34 have been already described in Ricci *et al*. (Ricci et al., 2014), while the others have been recently introduced in the xenobank. These PDXs generally resemble well the original tumour from which they derived in terms of biological behaviour, histopathological and molecular features and they keep this consistency for several in vivo passages (Ricci et al., 2014). Our xenobank is a reliable tool to tackle various clinical unmet issues, such as the research of biomarkers and to evaluate functional assays to predict response to chemotherapy, which are the final aims of this thesis.

During my PhD, I contributed to the molecular profiling of the PDXs and their pharmacological characterization for the response to platinum/taxol, the standard drugs used

in the clinic for the management of EOC. Recently, given the importance of PARPi in ovarian carcinoma treatment, olaparib antitumor activity has also been tested. Furthermore, starting from PDXs sensitive to therapy, we have recently obtained three models of acquired resistance to cisplatin through repeated in vivo treatments, useful to study molecular determinants of acquired resistance to platinum therapy (Ricci et al., 2017) (**figure 4.1**).

In this first section, I will describe the PDXs selected for the experiments performed along my PhD project. In particular, the clinical-pathological features of the original tumours from which the PDXs derived, the mutational profile of the PDXs, the promoter methylation status of some DNA repair genes of interest, and PDXs response to cisplatin and olaparib will be reported. Parts of these data have been previously published (Guffanti et al., 2018; Ricci et al., 2014), others have been recently obtained, because the xenobank is a dynamic collection, which requires constant work in order to characterize the new established PDXs.

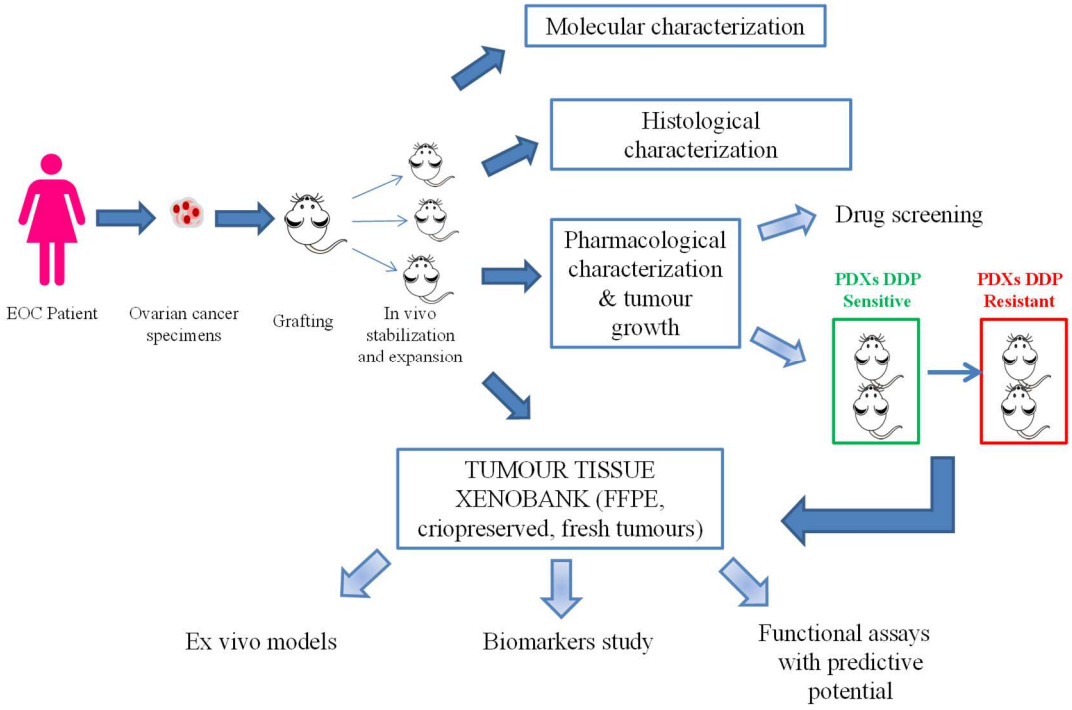

Figure 4.1 Establishment, characterization and application of the Mario Negri's EOC xenobank

Ovarian cancer specimens deriving from cytoreductive surgery or paracentesis interventions are received and transplanted within 24 hrs in athymic Foxn1^{nu} mice, subcutaneously or intraperitoneally. Once stabilized, the xenografts are histologically and molecularly characterized. The EOC-PDXs are characterized for their response to the standard drugs used in the clinic for the management of EOC (i.e. cisplatin, paclitaxel); recently, olaparib has been evaluated. Starting from cisplatin responsive PDXs, it was possible to induce resistance to therapy after repeated in vivo treatments, obtaining models with acquired resistance to cisplatin.

4.1.1 Clinical-pathological characteristics of the patient tumours from which the EOC-PDXs derived

The specimens used to generate the PDXs usually derive from cytoreductive surgery of primary tumours localized at the ovary, omentum, or from paracentesis at diagnosis or at relapse. The percentage of tumours successfully engrafted in vivo is around 25%, regardless of the histopathological characteristics of the tumour and the site of injection (Ricci et al., 2014). Currently, our xenobank consists of 68 models. Considering those PDXs whose histological subtype is known, the xenobank includes 44 high grade serous/endometrioid tumours, 2 low grade serous carcinomas, 3 clear cell carcinomas and 1 mixed clear cell/high grade endometrioid tumour, 2 mucinous, 1 mixed müllerian, 1 carcinosarcoma, 1 undifferentiated and 1 not classified tumour, while for the others the histological information is not currently available.

In **table 4.1** are summarized the main clinical-pathological characteristics of the original EOC specimens engrafted in nude mice to originate the PDXs we have available. The information includes: histotype, grade and stage of tumour at the diagnosis, first line treatment received and the origin (primary tumour or relapse) and source (ovary, omental metastasis or ascitic fluid) of the specimens used to establish the PDXs.

Except three patients (MNHOC18, MNHOC164 and MNHOC506) who received neoadjuvant therapy, all the PDXs from primary specimens are chemotherapy naïve, while those obtained from relapsing tumours have been almost all previously treated with platinum agents. The majority of patients received the standard treatment platinum-taxol doublet with the addition of bevacizumab in three cases (MNHOC263, MNHOC508, MNHOC513) or they received a therapeutic regimen containing cisplatin or carboplatin, except MNHOC182 and MNHOC258 who were not treated, and MNHOC18 and MNHOC78 who received epirubicin/cyclophosphamide in neoadjuvant therapy and cyclophosphamide in adjuvant treatment, respectively.

Table 4.1 Clinical-pathological characteristics of the original EOC from which PDXs derived

#ID EOC-PDXs	Tumour at diagnosis			Patient first line treatment§	Patient response	EOC-PDX tumours origin and source					Transplantation site	
						Primary			Relapse			
	Hystotype	Grade	Stage			Ov	Om	Asc	Om	Asc	ip	sc
MNHOC8	HGSOC	G3	IV	CBPT	PR			X			X	
MNHOC8Y	HGSOC	G3	IV	Epi-Dx	PD					X	X	
MNHOC8R	HGSOC	G4	IV	na	na							X
MNHOC10	HGSOC	G3	IIIC	DDP	PD			X			X	
MNHOC22	HGSOC	G3	IIII	DDP	PD					X	X	
MNHOC76	HGSOC	G3	IIIC	PAC	PD					X	X	
MNHOC84	HGSOC	G3	IIIC	DDP-PTX	na					X		X
MNHOC106	HGSOC	G3	IIIC	PAC	PR				X			X
MNHOC107	HGSOC	G3	IIIC	PAC	PR				X			X
MNHOC111/2C	HGSOC	G3	IIIC	DDP-PTX	PD					X	X	
MNHOC125	HGSOC	G3	IV	CBPT	PR	X						X
MNHOC239	HGSOC	G2	IV	CBPT-PTX	CR				X			X
MNHOC143	HGSOC	G3	IIIC	CBPT-PTX	NED	X						X
MNHOC149	HGSOC	G3	IIIC	CBPT-PTX	NED	X						X
MNHOC244	HGSOC	G2	IV	CBPT-PTX	CR	X						X
MNHOC250	HGSOC	G3	IIIC	CBPT-PTX	CR	X						X
MNHOC258	HGSOC	G3	IIIC	not treated		X						X
MNHOC263	HGSOC	G3	IIIC	CBPT-PTX-BEVA	CR	X						X
MNHOC266	HGSOC	G2	IIIC	CBPT-PTX	na			X			X	
MNHOC268	HGSOC	G2	IIIC	CBPT-PTX	PR	X						X
MNHOC270	HGSOC	G3	IIC	CBPT-PTX	CR	X						X
MNHOC271	HGSOC	G3	IIIC	CBPT-PTX	na	X						X
MNHOC276	HGSOC	G3	III	CBPT-PTX	na				X			X
MNHOC280	HGSOC	G3	IIC	CBPT-PTX	CR	X						X
MNHOC281	HGSOC	G3	IIIC	CBPT-PTX	PR	X						X
MNHOC289	HGSOC	G3	IIIC	CBPT-PTX	CR	X						X
MNHOC316	HGSOC	G3	IV	CBPT-PTX	na	X						X
MNHOC500	HGSOC	G3	IIIC	CBPT	NED	X						X
MNHOC506	HGSOC	G3	IIIC	CBPT-PTX (neoad.)	PD			X			X	
MNHOC508	HGSOC	G3	IIIC	CBPT-PTX-BEVA	NED		X					X
MNHOC511	HGSOC	na	na	CBPT-PTX	CR		X					X
MNHOC518	HGSOC	na	na	na	na						X	
MNHOC124	HGS/HGE OC	G2	IIIIC	CBPT-PTX	SD	X						X
MNHOC212	HGS/HGE OC	G2	IIIIC	CBPT-PTX	PR	X						X
MNHOC315	HGS/HGE OC	G2	IIIIC	CBPT	na	X						X
MNHOC18	HGEOC	G3	IV	Epi-CP (neoad.)	PD	X						X
MNHOC78	HGEOC	G2	IIIIC	CP	SD					X	X	
MNHOC154	HGEOC	G2	IIC	CBPT-PTX	CR				X			X
MNHOC218	HGEOC	G3	IIIC	CBPT-PTX	CR	X						X
MNHOC230	HGEOC	G3	IIB	CBPT-PTX	CR				X			X
MNHOC261	HGEOC	G2	IIIC	CBPT-PTX	CR	X						X
MNHOC503	HGEOC	G3	na	na	na							X
MNHOC513	HGEOC	na	na	CBPT-PTX-BEVA	NED		X					X
MNHOC520	HGSOC	na	na	na	na						X	
MNHOC241	LGSOC	G2	IC	CBPT-PTX	CR	X						X
MNHOC109	LGEOC	G2	IC	CBPT	CR				X			X
MNHOC79	HGEOC/CCC	G3	IIIC	DDP	SD					X	X	
MNHOC94/2C	CCC	G2	na	na	PD					X		X
MNHOC119	CCC	G3	IC	CBPT	CR	X						X
MNHOC142	CCC	G3	IIIC	CBPT-PTX	na			X			X	
MNHOC164	MC	G2	IV	CBPT-PTX (neoad.)	SD		X					X
MNHOC182	MC	G1	IC	not treated		X						X
MNHOC135	Mixed müllerian	G3	IIIB	TIP	CR	X						X
MNHOC88	Undifferentiated	G3	IIIC	DDP	na				X			X
MNHOC151	Carcinosarcoma	G3	IIB	na	na							X
MNHOC9	not classified	na	IIIC	CBPT-PEC	PR			X				X

Abbreviations: Ov: ovary; Om: omentum; Asc: ascite; i.p.: intraperitoneum; s.c.: subcutaneous; neoad: neoadjuvant chemotherapy; na: info. not available; CR: complete response; PR: partial response; SD: stable disease; PD: progressive disease; NED: not evident disease. §First line treatment: CBPT= carboplatin; DDP= cisplatin; PTX= paclitaxel; BEVA: bevacizumab; Epi: epirubicin; Dx: doxorubicin;CP= cyclophosphamide; TIP: PTX, DDP, isofosphamide; PAC: DDP, adriamicin, CP; PEC: DDP, Epi, CP.

4.1.2 The EOC-PDXs well resemble the tumour of origin

To exclude any possible phenotypic drift of the PDXs from the tumour of origin and after repeated in vivo passages, the histology of xenograft tumours has been compared by Dr Patrizia Perego of the Surgical Pathology Department of San Gerardo Hospital (Monza, Italy) with the tumour of the patient it derived from.

All the cases analysed retained the morphology and architecture of the tissue of origin, also after several in vivo passages, as demonstrated by haematoxylin/eosin (HE) staining. Two representative EOC-PDXs are shown in **figure 4.2**, where the patient's tissue was compared with the first in vivo passage of the PDX and after 7 and 10 passages, respectively. Besides the HE staining, the pathologist also evaluated the expression of pan-cytokeratin and CA125, markers generally used for the EOC diagnosis. All the EOC-PDXs expressed these markers and retained the positivity also after several in vivo passages, even if a slight decreased positivity has been observed (Ricci et al., 2014) (representative PDXs in **figure 4.2**).

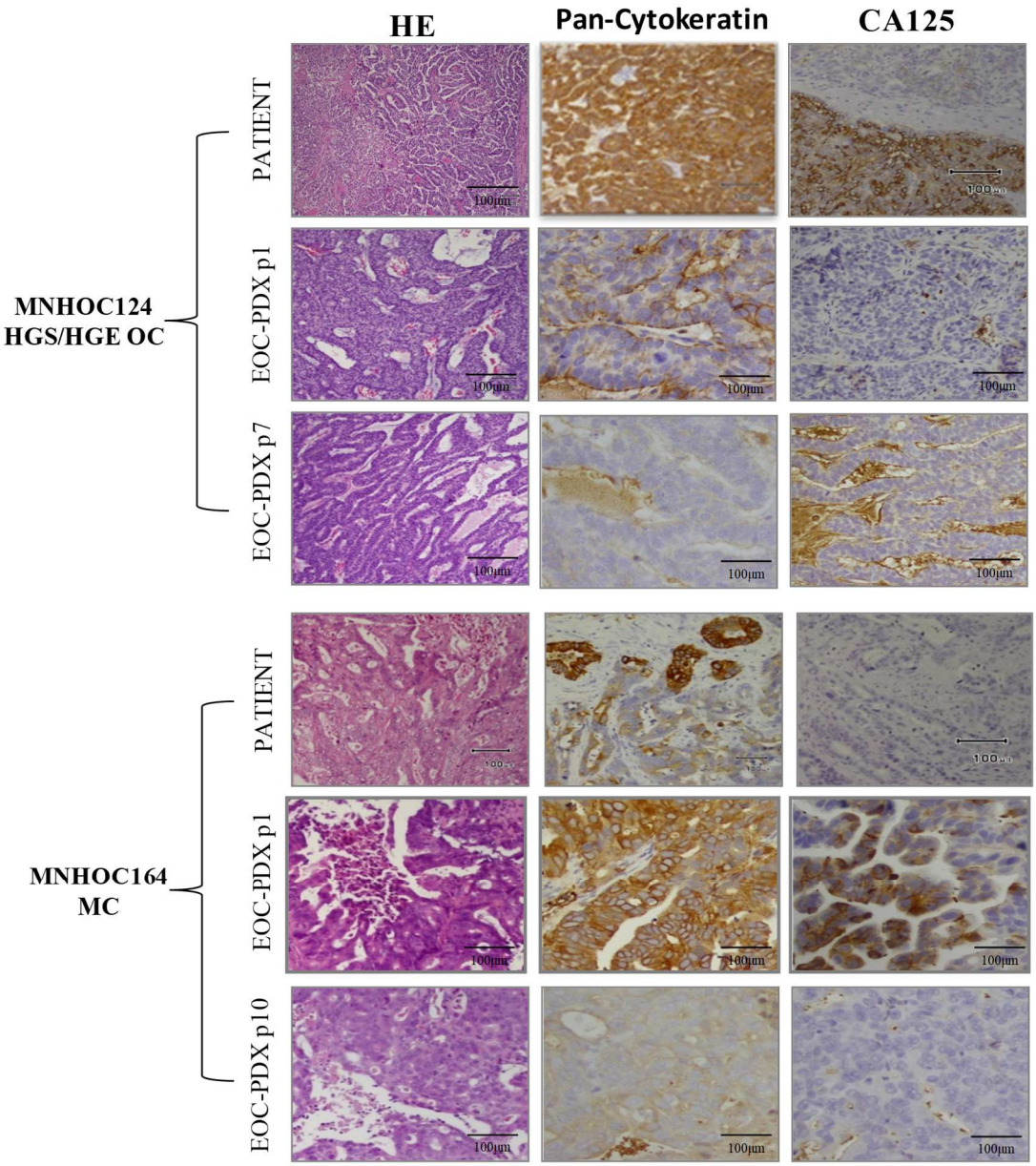

Figure 4.2 Comparative histological and immunohistochemical (IHC) analyses of tumours deriving from EOC-PDXs at different in vivo passages and the original patient tumour it derived from

Two EOC-PDXs are shown as representative cases, MNHOC124 (upper panel) is a mixed high grade serous/endometrioid tumour (HGS/HGEOC), while MNHOC164 (lower panel) is a mucinous carcinoma (MC). Three different staining have been performed for the comparison among patient and early and late in vivo passages of the PDXs: haematoxylin/eosin (HE) to evaluate the tissue structure and IHC analysis for pan-cytokeratin and CA125, markers of EOC.

We have also analysed the short tandem repeat (STR) sequences of the original patient tumours with those of the derived PDXs at different passages, to verify the origin of the tissue sample.

STR analysis is an informative approach widely used to verify tissue sample of origin and it is based on the comparison of allelic repeats at specific loci in DNA of different samples. STR are microsatellites with repetitive sequences of 3-7 base pairs diffuse along the human genome, whose number of repeats varies among individuals. We used this method to check that the STR sequences of the patients were preserved in the established PDXs. 16 different loci of the genome were analysed in half of the PDXs (at the first and later in vivo passages) of the xenobank and all of them maintained the same or significantly similar STR sequences, confirming the genetic stability of the PDXs also at later passages. **Figure 4.3** shows the allele report of the STR analysis in MNHOC124, as a representative PDX of the xenobank, where the STR sequences were compared between patient DNA (pt) and PDX at different in vivo passages (MNHOC124 p3 and p15).

Allele Report
SoftGenetics
GeneMarker HID V2.6.0

#ID EOC-PDXs	STR Marker															
	D3S1358	TH01	D21S11	D18S51	Penta_E	D5S818	D13S317	D7S820	D16S539	CSF1PO	Penta_D	AMEL	vWA	D8S1179	TPOX	FGA
124 pt	15, 18	6,8	29.2	13	12	10,11	11,12	7,8	9,13	10,13	11	X	17,18	8,12	8,11	10,21
MNHOC124 p3	15, 18	6	29.2	13	12	10,11	11,12	7,8, 222.22	9,13	10,13	11	X	17,18	8,12	8,11	10,21
MNHOC124 p15	15, 18	6,8	29.2	13	12	10,11	11,12	8, 222.22	9,13	10,13	11	X	17,18	8	8,11	10,21

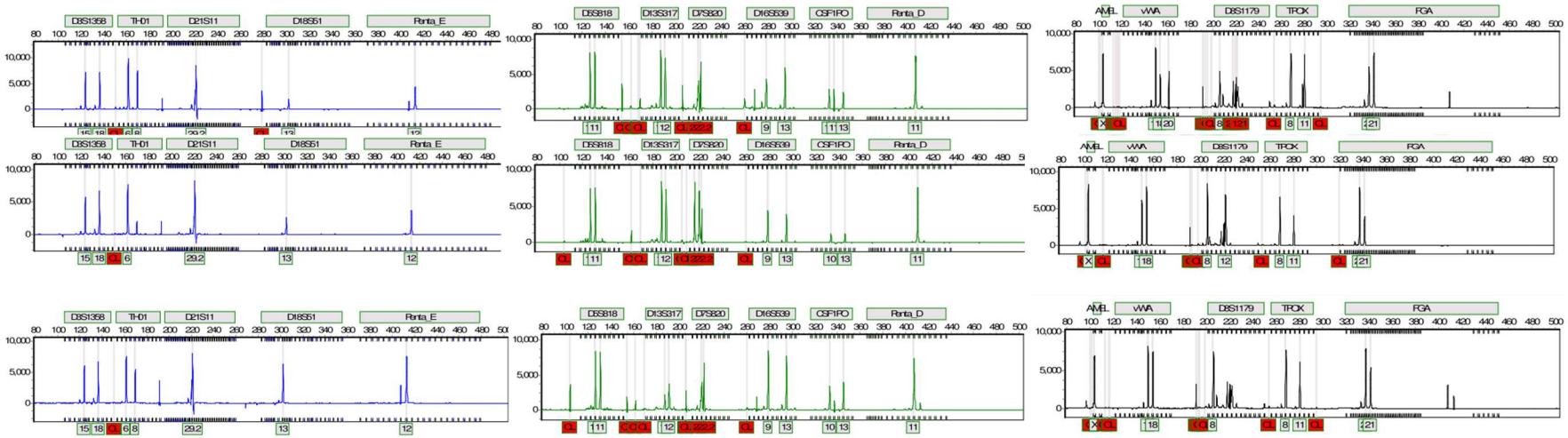

Figure 4.3 Allele report of MNHOC124 STR analysis

DNA from tumour patient (pt) 124 and from PDX after 3 and 15 passages in vivo (MNHOC124 p3 and MNHOC124 p15) were analysed for the STR profile in 16 different STR sites. In the upper table are summarized for each of the three samples the STR profile. The lower graphs show the STR peaks which mostly correspond among the samples, showing that the PDX retain the STR profile of the original tumour.

4.1.3 Mutational profile of the EOC-PDXs

The molecular characterization of EOC-PDXs included the analysis of the mutational status of genes involved in the pathogenesis of EOC (i.e. *TP53, KRAS, PIK3C, PTEN* and *BRAF*) and HR genes (i.e. *BRCA1, BRCA2, ATM, ATR, PALB2, FA* genes).

All the high grade serous and endometrioid PDXs analysed harbour non-synonymous *TP53* mutations. All the *TP53* mutations found in the PDXs localize in the exons 5-9 encoding for the DNA binding domain of the protein and are almost all pathogenic missense substitution mutations. Conversely, the clear cell (MNHOC94/2C, MNHOC119), mucinous (MNHOC164, MNHOC182) and low grade serous (MNHOC109, MNHOC241) PDXs have a wild type *TP53* or synonymous mutation (MNHOC109), consistent with data from the literature (Ahmed et al., 2010; Cancer Genome Atlas Research Network, 2011).

Among the other genes frequently mutated and involved in the pathogenesis of EOC, we found *KRAS* heterozygous mutations in exon 2 in MNHOC84 (p.G12A) and in the mucinous MNHOC182 (heterozygous mutation, p.G12D), while MNHOC18 shows an amplification of KRAS, and a *PTEN* nonsense mutation was found in the CCC MNHOC94/2C.

No mutations were found in the other analysed genes (*BRAF* and *PIK3C*).

While the previously described genes were analysed mostly by the Sanger technique, mutational data of the HR genes was derived from sequencing experiments (whole genome sequencing, next generation sequencing or RNA-seq) performed on selected PDXs in collaboration with other laboratories (i.e. Dr Nik-Zainal lab., Wellcome Trust Sanger Institute) or companies (i.e. Astra Zeneca). Most of the reported mutations were subsequently validated in Sanger and these results are reported in the PhD thesis of Dr Francesca Bizzaro (Bizzaro, Francesca, 2018).

14 EOC-PDXs (13 HGOC, 1 MC) are mutated in *BRCA1* and/or *BRCA2*. *BRCA1* frequently harbours substitution/missense and truncation/frameshift mutations, all described to be pathogenic ("ClinVar, https://www.ncbi.nlm.nih.gov/clinvar/," n.d.), except that observed in

MNHOC276, even if it is likely to be pathogenic. MNHOC513 contains a complete deletion of exon 23 of *BRCA1*, which determines the loss of function of the protein.

BRCA2 has a heterogeneous spectrum of mutations: MNHOC508 harbours a pathogenic frameshift deletion, MNHOC511 an unknown missense mutation; MNHOC18 carries a neutral, non-pathogenic missense mutation, while the MNHOC182 harbours a pathogenic mutation, without site specific LOH, rare in this histological subtype (Pennington et al., 2014). However, in these two latter cases, one of the alleles is wild type, so *BRCA2* should be transcribed and the protein be present, and so it is considered wild type.

The mutational status of other investigated HR genes is detailed in **table 4.2**. However, the majority of these mutations are described to be not pathogenic or of uncertain significance.

Table 4.2. Mutational profile of the most common mutated genes in EOC

#ID EOC-PDXs	Hystotype	*TP53*	*KRAS, B-RAF, PI3Ka*	*BRCA1, BRCA2*	Other HR genes
MNHOC8	HGSOC	c.514G>T p.V172F		WT	
MNHOC8Y	HGSOC	c.514G>T p.V172F		WT	
MNHOC8R	HGSOC	MUT			
MNHOC10	HGSOC	c.659A>G p.Y220C		WT	
MNHOC22	HGSOC	g.14755 G:C>T:A splice site c.993+1 G>A		BRCA1 (nonsense mutation)	PALB2: heterozygous mut. (unknown/missense, non pathogenic)
MNHOC76	HGSOC	c.723delC p.S241fs*5		WT	
MNHOC84	HGSOC	g.14451 G:C>T:A splice site c.783-1 G>T	KRAS WT/ c.35G>C p.G12A	WT	
MNHOC106	HGSOC	g.13999 G:C>T:A splicing site c.673-1 G>C		BRCA1 truncation frameshift (fs del)	
MNHOC107	HGSOC	c.517G>A p.V173M		BRCA1 truncation frameshift (fs del)	
MNHOC111/2C	HGSOC	c.839G>A p.R280K		WT	
MNHOC125	HGSOC	c.517G>A p.V173M		BRCA1 (missense mut.)	
MNHOC239	HGSOC	c.776A>T p.D259V		WT	
MNHOC143	HGSOC	MUT		WT	ATM and FANCA heterozygous mut. (unknown/missense)
MNHOC149	HGSOC	MUT			
MNHOC244	HGSOC	c.537G>A p.C135Y			
MNHOC250	HGSOC	c.844C>T p.R282W			
MNHOC258	HGSOC	c.125G>A p.C42Y			
MNHOC263	HGSOC	c.854delT p.S241fs*22			
MNHOC266	HGSOC	c.818G>A p.R273H		BRCA1: p.R1699Q LOH	ATR c.2228_2262del35 (del fs) NOT in ClinVar
MNHOC268	HGSOC	c.164_165delGT p.G55fs*21			
MNHOC270	HGSOC	c.421T>C p.C141R			
MNHOC271	HGSOC	c.556delC p.C141fs*28			
MNHOC276	HGSOC	c.396G>T p.K132N		BRCA1 c.2332dupT (fs, very likely pathogenic, not in ClinVar)	
MNHOC280	HGSOC	c.609C>T p.A159V			
MNHOC281	HGSOC	c.1048C>T p.R306C			
MNHOC289	HGSOC	c.660G>T p.C176F		WT	
MNHOC316	HGSOC	mutc.557G>A p.R175H			
MNHOC500	HGSOC	MUT		BRCA1 truncation frameshift (fs del)	ATM mut (unknown/missense) + FANCB (known/missense)
MNHOC506	HGSOC	MUT		WT	
MNHOC508	HGSOC	MUT		BRCA2 truncation frameshift (fs del)	
MNHOC511	HGSOC	c.523C>G p.R175G		BRCA1 mut (missense); BRCA2 mut (unknown/ missense)	
MNHOC518	HGSOC				
MNHOC124	HGS/HGE OC	c.524G>A p.R175H		WT	
MNHOC212	HGS/HGE OC	c.951G>A p.R273H		WT	
MNHOC315	HGS/HGE OC	c.569G>A p.146(W/*); c.909A>G p.D258N			
MNHOC18	HGEOC	c.527G>T p.C176F	KRAS amplification	BRCA2 mut (missense, non pathogenic)	
MNHOC78	HGEOC	c.518T>G p.V173G		BRCA1 truncation frameshift (fs del)	
MNHOC154	HGEOC	c.844C>T p.R282W		BRCA1.p.C61G LOH	ATM C>G wt/p.A235G and ATR: c.2595C>G p.H865Q
MNHOC218	HGEOC	c.841G>A p.D281N			
MNHOC230	HGEOC	c.927T>C p.L265P		WT	
MNHOC261	HGEOC	p.258_261 del		WT	
MNHOC503	HGEOC				
MNHOC513	HGEOC	MUT		BRCA1 exon 23 deletion (Loss of function)	FANCA mut (unknown/missense)
MNHOC520	HGEOC				
MNHOC241	LGSOC	WT			
MNHOC109	LGEOC	c.639A>G p.wt (R213R)		WT	
MNHOC79	HGEOC/CCC	g.14755 G:C>T:A		WT	
MNHOC94/2C	CCC	WT	PTEN nonsense mut.	WT	
MNHOC119	CCC	WT		WT	
MNHOC142	CCC				
MNHOC164	MC	WT			
MNHOC182	MC	WT	KRAS WT/ c.35G>C p.G12D	BRCA2 pathogenic, without site specific LOH	ATM mut (unknown/missense)
MNHOC135	Mixed müllerian	c.527G>T p.C176F		WT	
MNHOC88	Undifferentiated	p.A189fs*58			
MNHOC151	Carcinosarcoma				
MNHOC9	Not classified	p.C275G			

Abbreviations: wt= wild type; mut= mutated/mutation; LOH= loss of heterozygosity; del= deletion; fs= frameshift.

4.1.4 Promoter methylation status

The promoter methylation status of some DNA repair genes has been investigated in *BRCA1, FANCF*, *ERCC1, MLH1, XPA* and *XPG* genes, and described to be hypermethylated in ovarian cancer and associated with decreased gene transcription (Cancer Genome Atlas Research Network, 2011; D'Andrea, 2003; Sabatino et al., 2010).

For these analyses, two different methods were used: pyrosequencing with pre-custom assays (Qiagen) and methylation specific-PCR (MS-PCR) with primers designed *ad hoc*.

For pyrosequencing analysis, three promoter regions in *BRCA1* and *ERCC1* have been analysed including 11 and 15 CpG sites, respectively, and corresponding to the three assays provided by manufacturer. For *MLH1* and *XPA* two pre-custom assays for pyrosequencing were used for both genes, covering regions including 11 and 6 CpG sites, respectively.

From pyrosequencing analyses, *BRCA1* was the most hypermethylated gene, where 51% of the PDXs analysed had all three regions with more than 10% (threshold suggested by manufacturer) of the CpG sites hypermethylated, and 86% with almost one region hypermethylated. One of the two regions of *XPA* promoter was hypermethylated in five PDXs (MNHOC212, MNHOC239, MNHOC76, MNHOC8Y and MNHOC506). *MLH1* appeared strongly hypermethylated in MNHOC19 (96% and 87% of CpG sites methylated in both regions analysed), while MNHOC500 presented 11% of methylation in only one region. In **table 4.3** are reported the % of CpG islands found methylated, detailed for each PDX.

In EOC patients *BRCA1* promoter hypermethylation associates with low protein levels and occurs in 10% of HGSOC (Cancer Genome Atlas Research Network, 2011), so the high frequency found in our PDXs let us to hypothesize that the regions analysed were not those responsible for the transcription of the gene. To clarify this point, we set up a MS-PCR to analyse a different region of *BRCA1* promoter, whose hypermethylation has been described to correlate with low transcriptional levels of *BRCA1* in breast cancer PDXs (Ter Brugge et al., 2016). 55 of our EOC-PDXs have been analysed and 4 had a % methylation range from

84% to 100% (MNHOC212, MNHOC8Y, MNHOC8, MNHOC518), while MNHOC520 had 49% of CpG sites methylated. None of the other PDXs were hypermethylated from MS-PCR results (**figure 4.4** and **table 4.3**).

MS-PCR has also been used to analyse *FANCF* and *XPG*. None of the PDXs analysed showed methylation in *XPG* promoter (**figure 4.5 panel A**), while *FANCF* was found moderately methylated in MNHOC18 (70%) and slightly in MNHOC119 (6%) (**figure 4.5 panel B**).

Table 4.3 Quantification of the % of CpG islands methylated in different promoter regions of six DNA repair genes in the EOC-PDXs

	PYROSEQUENCING										MS-PCR		
	XPA_01	XPA_02	ERCC1_01	ERCC1_02	ERCC1_03	MLH1_01	MLH1_04	BRCA1_01	BRCA1_02	BRCA1_03	BRCA1_04	FANCF	XPG
MNHOC8	1%		0%	2%	15%	2%	3%	39%		73%	84%	0%	0%
MNHOC8Y	3%	13%	3%	3%	7%	5%	0%	96%	81%	83%	100%	0%	0%
MNHOC10											0%		
MNHOC22											0%		
MNHOC76	2%	20%	2%	3%	4%	2%	5%	58%	23%	83%	0%	0%	0%
MNHOC84		6%	2%	2%	5%	3%	1%	71%	7%	77%	0%	0%	0%
MNHOC106	5%	6%	3%	3%	4%	3%	5%	94%	70%	84%	0%	0%	0%
MNHOC107	2%	5%	2%	2%	3%	2%	8%	89%	8%	91%	0%	0%	0%
MNHOC111/2C	3%	3%	2%	3%	5%	3%	1%	93%	73%	82%	0%	0%	0%
MNHOC125	4%	5%	3%	3%	5%	3%	4%	96%	69%	94%	0%	0%	0%
MNHOC239	5%	13%	1%	2%	4%	5%	5%	5%	8%	13%	0%	0%	0%
MNHOC143	3%	0%	2%	1%	8%	2%	0%	3%	2%	5%	0%	0%	0%
MNHOC149	3%	3%	2%	2%	3%	2%	2%	6%	4%	29%	0%	0%	0%
MNHOC244	6%	3%	3%	3%	6%	4%	1%	94%	70%	95%	0%	0%	0%
MNHOC250	5%	7%	3%	3%	4%	4%	3%	92%	35%	93%	0%	0%	0%
MNHOC258	4%	5%	3%	2%	5%	3%	1%	93%	58%	96%	0%	0%	0%
MNHOC266	4%	5%	3%	4%	6%	4%	5%	5%	5%	9%	0%	0%	
MNHOC270											0%		
MNHOC271											0%		
MNHOC276											0%		
MNHOC280											0%		
MNHOC281											0%		
MNHOC289											0%		
MNHOC316											0%		
MNHOC500	4%	4%	3%	2%	5%	3%	11%	86%	55%	79%	0%	0%	0%
MNHOC506	2%	22%	1%	4%	6%	5%		79%		90%	0%	0%	0%
MNHOC508	2%	4%	2%			2%		95%		84%	0%	0%	0%
MNHOC511	3%	3%	2%	2%	3%	2%	1%	5%	3%	13%	0%	0%	0%
MNHOC518											100%		
MNHOC124	5%	7%	3%	3%	19%	4%	3%	95%	82%	90%	0%	0%	0%
MNHOC212	4%	12%	3%	3%	6%	5%	2%	95%	71%	92%	100%	0%	0%
MNHOC315											0%		
MNHOC18	3%	1%	1%	2%	3%	2%	1%	4%	5%	7%	0%	70%	0%
MNHOC78	4%	3%	2%	2%	4%	3%	2%	3%	3%	6%	0%	0%	0%
MNHOC154	4%	4%	3%	2%	5%	3%	2%	90%	33%	91%	0%	0%	0%
MNHOC218											0%	0%	
MNHOC230	5%	4%	3%	2%	4%	3%	3%	94%	41%	90%	0%	0%	0%
MNHOC261	4%	5%	4%	2%	5%	3%	2%	64%	30%	72%	0%	0%	0%
MNHOC503	2%	1%	1%	1%	4%	2%	2%	15%		53%	0%	0%	0%
MNHOC513											0%		
MNHOC520											49%		
MNHOC241	4%	5%	3%	2%	5%	3%	2%	8%	6%	22%	0%	0%	0%
MNHOC109	4%	0%	3%	2%	8%	96%	87%	6%	5%	31%	0%	0%	0%
MNHOC79	3%	0%	1%	1%	0%	1%	2%	90%	46%	91%	0%	0%	0%
MNHOC94/2C	4%	1%	2%	2%	4%	2%	1%	1%	3%	5%	0%	0%	0%
MNHOC119	3%	3%	2%	1%	4%	3%	0%	93%	6%	82%	0%	10%	0%
MNHOC142	2%	2%	4%	3%	5%	3%	3%	47%	35%	80%	0%	0%	0%
MNHOC164	4%	8%	4%	5%	5%	4%	1%	92%	37%	77%	0%	0%	0%
MNHOC182	2%	3%	1%	1%	5%	4%	3%	41%	12%	77%	0%	0%	0%
MNHOC135	6%	8%	4%	3%	8%	4%	3%	83%	46%	82%	0%	0%	0%
MNHOC88											0%		
MNHOC9	3%	3%	4%	3%	4%	3%	2%	14%	10%	50%	0%	0%	0%
MNHOC124 DDPR											0%	0%	
MNHOC239 DDPR											0%		
MNHOC266 DDPR											0%		

In light blue are highlighted those regions considered hypermethylated, having >10% of CpG sites methylated.

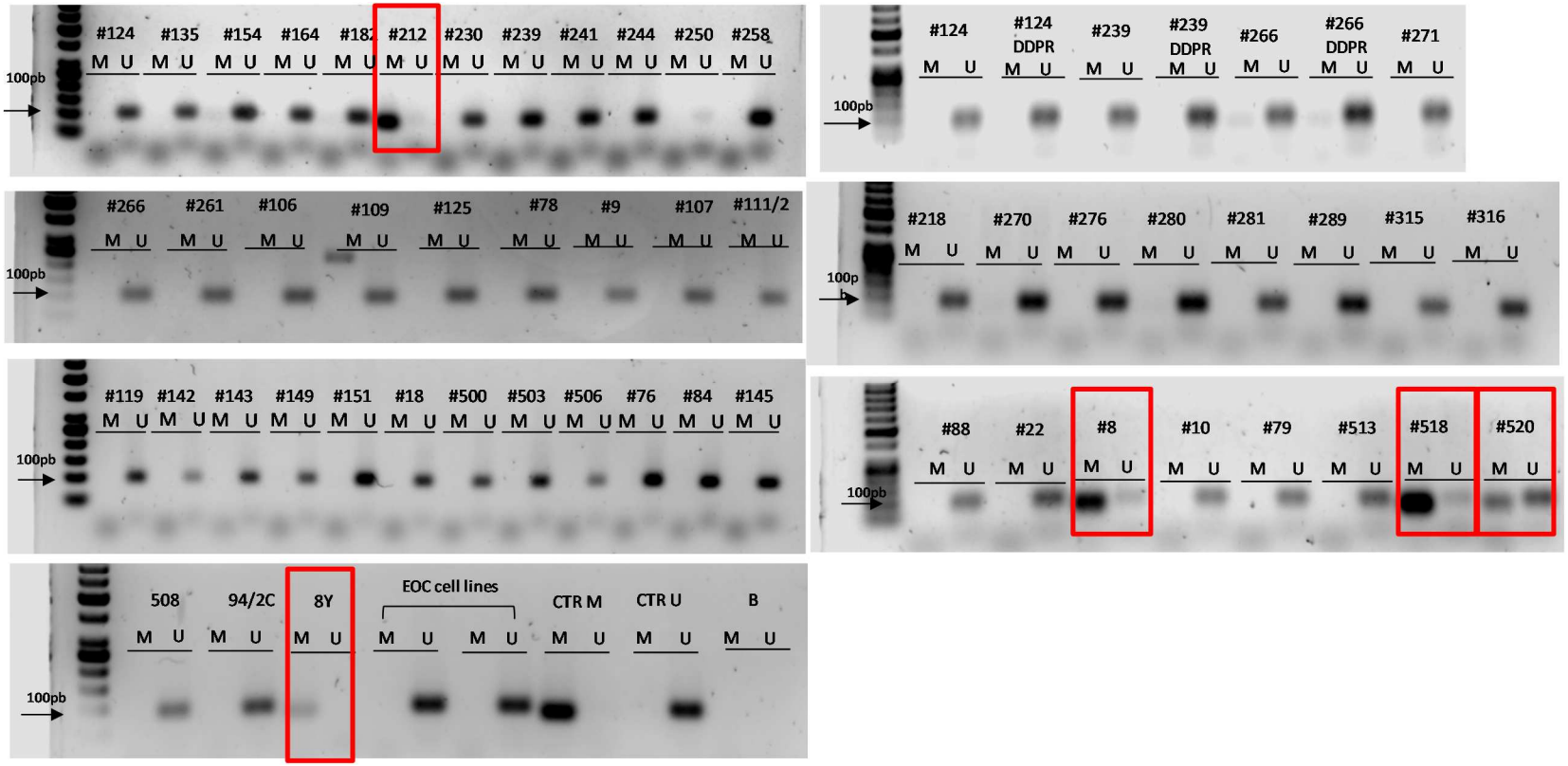

Figure 4.4 Methylation status of *BRCA1* promoter in the EOC-PDXs

55 PDXs of our xenobank have been analysed by MS-PCR using primers specifically designed to amplify the methylated (M) or unmethylated (U) region of interest. Two EOC cancer cell lines (A2780 and IGROV) were used as internal controls. EpiTect PCR Control DNA set (Qiagen) was used as PCR internal control (CTR M: methylated DNA and CTR U: unmethylated DNA). B: blank. In red are highlighted the PDXs resulted methylated.

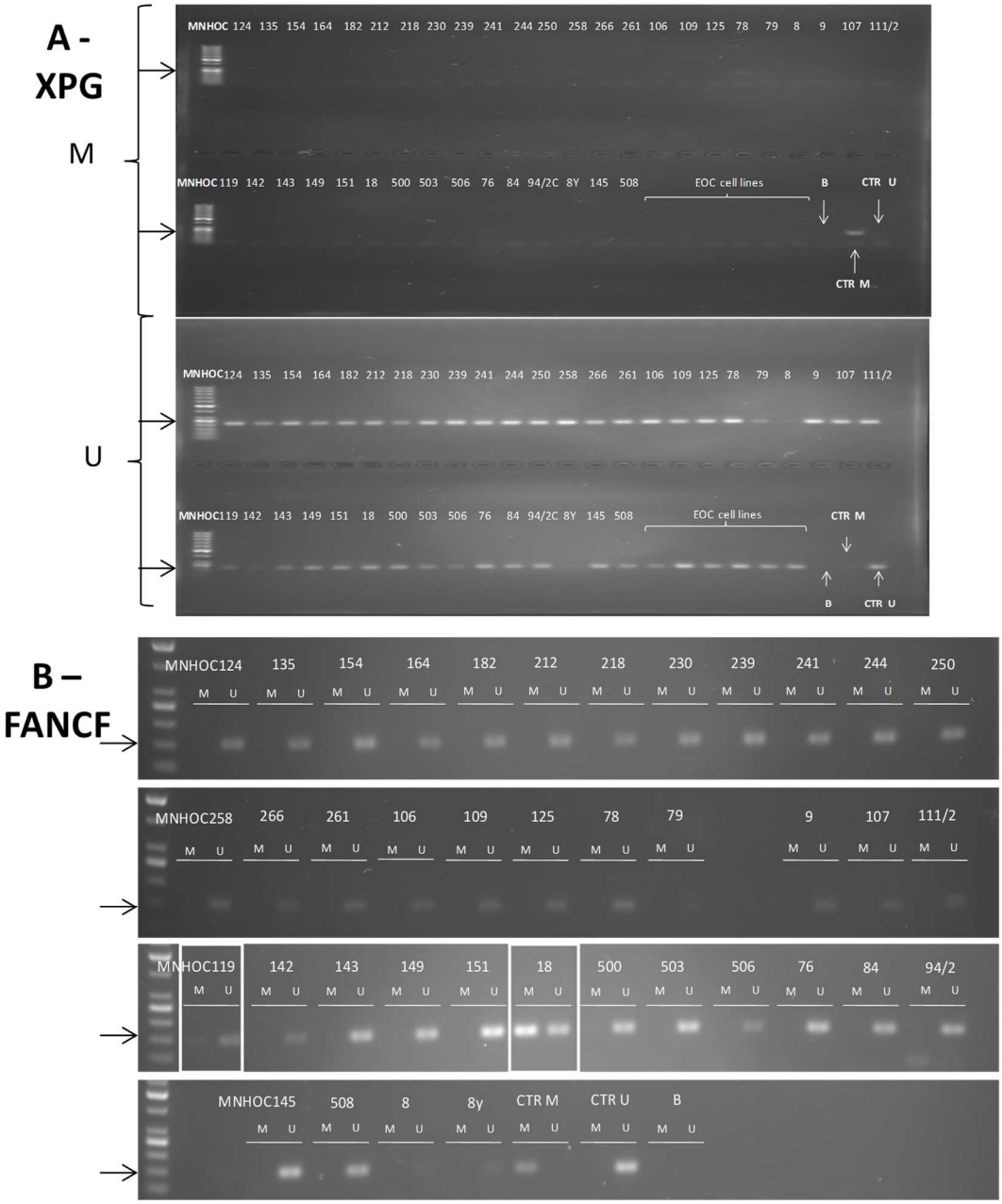

Figure 4.5 Methylation status of *XPG* and *FANCF* promoters

EOC-PDXs analysed by MS-PCR with couples of primers designed for the methylated (M) or unmethylated (U) region. **A)** ***XPG*** **methylation status by MS PCR**. The upper gel shows the MS-PCR with M primers; the lower panel shows the MS-PCR with U primers. **B**) ***FANCF*** **methylation status by MS PCR**. In this gel samples amplified with primer for M or U region have been loaded alternatively. EpiTect PCR Control DNA set (Qiagen) was used as PCR internal control (CTR M: methylated DNA and CTR U: unmethylated DNA). B: blank. PDXs resulted methylated are surrounded.

4.1.5 Pharmacological characterization of the EOC-PDXs

I will focus here on the antitumor activity of the two drugs, DDP and olaparib, that are the focus of my thesis: 48 EOC-PDXs have been characterized for their response to cisplatin and 26 for olaparib.

The efficacy of the treatment has been expressed as the best tumour growth inhibition (T/C%) for subcutaneous tumours and increase in lifespan (ILS%) for intraperitoneal xenografts. The T/C value represents the magnitude of tumour growth inhibition after treatment (the lower the value, the higher the antitumor effect) for s.c. growing tumours and ILS represents the increase in life span over untreated/control group (the higher the value, the higher the antitumor effect) for i.p. transplanted tumours. Best T/C% and ILS% are not the only parameters used to evaluate the tumour response to therapy in vivo. In the clinical setting, response to cancer treatment in solid tumours follows the Response Evaluation Criteria in Solid Tumours (RECIST) (Eisenhauer et al., 2009; Schwartz et al., 2016; Therasse et al., 2000) that classifies response in: complete response (CR), partial response (PR), stable disease (SD) and progressive disease (PD), mainly based in the modification in tumour diameter after treatment over baseline pre-treatment condition. For s.c. tumours, in which a quantification of the change in tumour dimensions can be done, we could apply a modified RECIST (mRECIST) criteria, as recently described (Castroviejo-Bermejo et al., 2018a; Cruz et al., 2018) and compared the two different metrics. **Table 4.4** reports a heat-map representation of EOC-PDXs response to therapy calculated with the different parameters. A good concordance could be observed between the mRECIST method and T/C value for olaparib (Cohen's k= 0.86), with only one case misclassified; while lower concordance was found when considering DDP response to therapy (Cohen's k= 0.33), probably due to the wider range of DDP antitumor effect (**figure 4.6**). Not being able to apply the RECIST method to orthotopically transplanted tumours, we decided to express the data as T/C and

ILS, as this allowed, in aggregate, classifying tumour drug response in three types: very sensitive (VS), sensitive (S) and resistant (R), as specified in Materials and Methods.

Remarkably, 73% of the PDXs present in the xenobank are VS/ S to DDP treatment, while only one third (31%) of the xenografts are responsive to olaparib treatment. This platinum sensitivity pattern reflects the % of response in the clinical setting (Lheureux et al., 2019b). Among the biomarkers of olaparib response, DDP response has been advocated (D'Andrea, 2018). In the 26 PDXs characterized for both drug sensitivity, we observed that all the olaparib responsive tumours (n=8) were sensitive to DDP and all the DDP resistant tumours did not respond to olaparib (n=8). However, 10 PDXs classified as very sensitive/sensitive to DDP were resistant to olaparib (**table 4.4 and figure 4.6**). These data showed a low concordance between cisplatin and olaparib response (Cohen's k= 0.33).

Table 4.4 Classification of EOC-PDXs based on their response to DDP and olaparib therapy

Based on the maximal percentage of tumour growth inhibition (T/C%) calculated for subcutaneous tumours (s.c.) or increase in life span (ILS%) for intraperitoneal PDXs (i.p.), PDXs were classified into three groups: VS= very sensitive; S= sensitive; R= resistant to therapy. Following mRECIST metric (only for s.c. PDXs) tumours were divided into four groups: CR= complete response; PR= partial response; SD= stable disease; PD= progressive disease.

		Best T/C% or ILS%		mRECIST	
	#ID EOC-PDXs	DDP	OLA	DDP	OLA
s.c.	MNHOC218	VS	VS	CR	PR
	MNHOC508	VS	VS	PR	PR
	MNHOC511	VS	VS	PR	PR
	MNHOC513	VS	VS	PR	PR
	MNHOC500	VS	VS	PR	PR
	MNHOC124	VS	R	PR	PD
	MNHOC316	VS	R	PR	PD
	MNHOC271	S	S	PD	PD
	MNHOC239	S	R	SD	
	MNHOC18	S	R	PD	PD
	MNHOC84	S	R	PD	PD
	MNHOC143	S	R	PD	PD
	MNHOC94/2C	R	R	PD	PD
	MNHOC94/2TR	R	R		
	MNHOC124 DDPR	R	R	PD	PD
	MNHOC182	R	R	PD	
	MNHOC239 DDPR	R	R	PD	PD
	MNHOC315	R	R	PD	PD
	MNHOC261	VS		CR	
	MNHOC212	VS		CR	
	MNHOC230	VS		CR	
	MNHOC241	VS		PR	
	MNHOC9	S			
	MNHOC106	S			
	MNHOC107	S			
	MNHOC109	S			
	MNHOC125	S			
	MNHOC135	S		PD	
	MNHOC154	S		PD	
	MNHOC164	S		PD	
	MNHOC258	S		PD	
	MNHOC503	S			
	MNHOC119	R			
i.p.	MNHOC10	R			
	MNHOC111/2C	R			
	MNHOC79	R			
	MNHOC8Y	R			
	MNHOC8R	S			
	MNHOC78	S			
	MNHOC142	S			
	MNHOC76	R	R		
	MNHOC266 DDPR	R	R		
	MNHOC520	S	R		
	MNHOC506	VS	R		
	MNHOC22	VS	R		
	MNHOC266	VS	R		
	MNHOC518	VS	VS		
	MNHOC8	VS	VS		

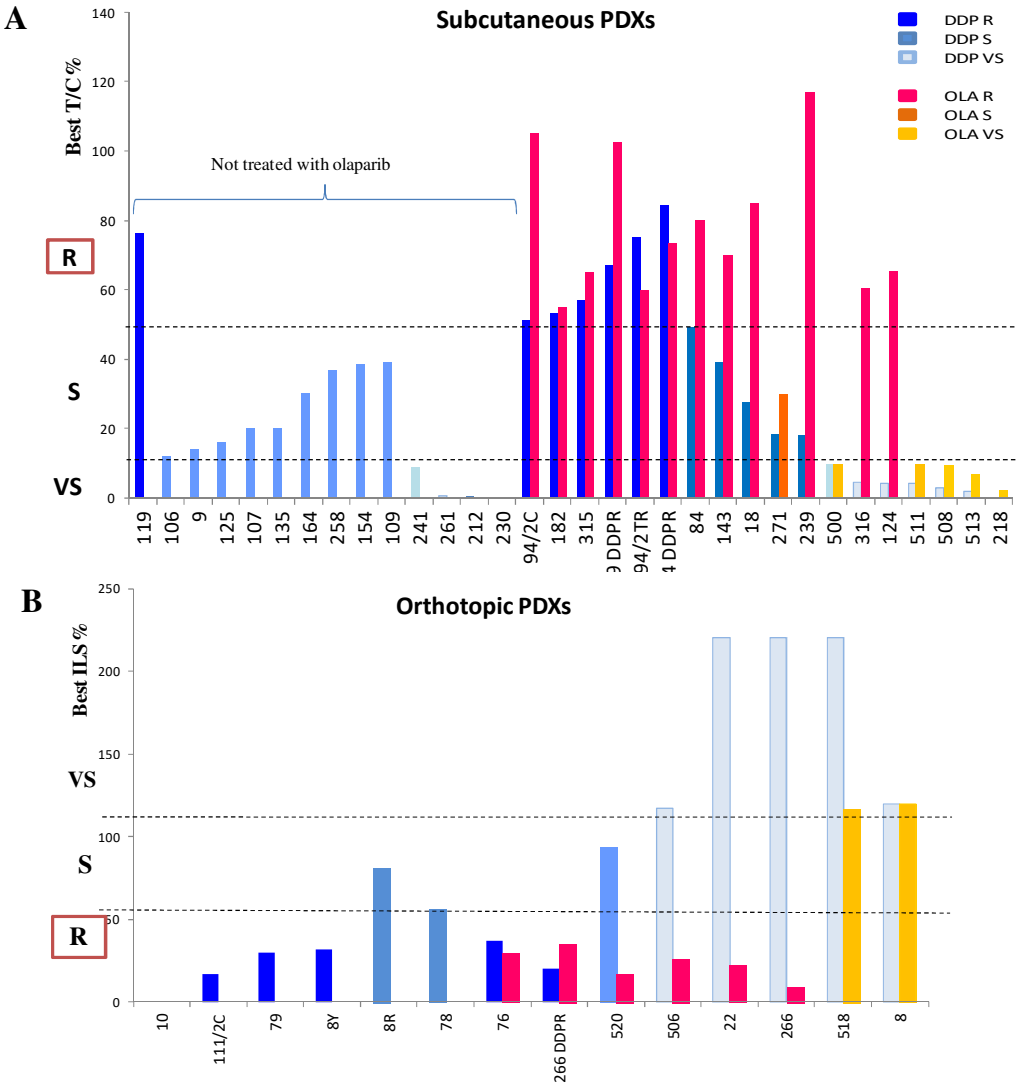

Figure 4.6 Best treatment response to DDP and olaparib of EOC-PDXs pharmacologically characterized

A) For tumours grown subcutaneously the best T/C% has been evaluated for DDP and for olaparib. As detailed in Materials and Methods, tumours were classified as resistant (R) to therapy with T/C% ≥ 50%; sensitive (S) 10%<T/C<50% and very sensitive (VS) T/C% ≤10%. The dashed lines indicate the T/C% thresholds that divide the response into the three categories. Different coloured bars are associated with DDP (blue/light blue) and olaparib (red/yellow) treatment.

B) Similarly, for orthotopic PDXs the best ILS% has been evaluated for each treatment. As detailed in Materials and Methods, tumours were classified as resistant (R) with ILS% ≤ 40%; sensitive (S) 40%< ILS%<100% and very sensitive (VS) ILS%≥100%. The dashed lines indicate the ILS% thresholds that divide the response into the three categories. Different coloured bars are associated with DDP (blue/light blue) and olaparib (red/yellow) treatment.

4.1.6 Discussion I

A collection of EOC-PDXs has been established in the Department of Oncology of the Mario Negri Institute, where I undertook the PhD course. The xenobank presented in this section, includes all the main histological subtypes of EOC: high grade serous and endometrioid, low grade serous, mucinous, clear cell, mixed müllerian, carcinosarcoma and undifferentiated tumours, reflecting the heterogeneity of EOC and the prevalence of these subtypes, with about 80% of high grade tumours present in the xenobank. Ricci *et al*., demonstrated the consistency of these models, which maintain the main characteristics of the patient's tumour from which they derived, both at histological and molecular levels regardless of the site of injection (subcutaneous or intraperitoneal) (Ricci et al., 2014). The PDXs are constantly monitored to avoid phenotypic drift by histopathological analyses, and we check that the STR regions are similar to those of the original tumour, regardless of the number of in vivo passages.

I contributed to PDXs molecular characterization by performing the mutational profiling and the analysis of promoter methylation status in some genes of interest. Regarding the mutational profile, all the high grade tumours harbour mutations in the DNA binding domain of *TP53*, in line with data reported in the literature (Ahmed et al., 2010; Cancer Genome Atlas Research Network, 2011; Cole et al., 2016). For *BRCA1* and *BRCA*2, as well as other HR genes, mutational status is still under investigation. Up to date, we have analysed 33 selected PDXs through genomic sequencing (whole genome sequencing and RNAseq), and then validated in Sanger (Bizzaro, Francesca, 2018) (and present thesis). 14 PDXs harboured a *BRCA1/BRCA2* mutation, even in two of them no LOH or non-pathogenic mutation could be observed and were considered to have a functional protein, so, wild type tumours (MNHOC182 and MNHOC18).

The analysis of HR gene mutational profile helped us to identify those PDXs that could have a *BRCAness* phenotype, a condition associated with a good response to DDP and olaparib therapy (Lord and Ashworth, 2016; O'Connor, 2015; Turner et al., 2004). Since not

only mutations in *BRCA1* but also epigenetic alterations may induce the *BRCAness* phenotype, the promoter methylation status of *BRCA1* has been analysed, together with other DNA repair genes involved in FA, NER and MMR pathways, whose methylation status can be found altered in EOC with consequences on gene transcription and response to chemotherapy (Chen et al., 2010; Lahtz and Pfeifer, 2011; Olopade and Wei, 2003; Sabatino et al., 2010). We used the pyrosequencing method to analyse 3 different regions of *BRCA1* promoter, *ERCC1*, *XPA*, and *MLH1*, while a MS-PCR with primers designed *ad hoc* and already reported in literature (D'Andrea, 2003; Sabatino et al., 2010; Ter Brugge et al., 2016) was performed to evaluate a region of *BRCA1* promoter, besides *FANCF* and *XPG*. We observed for *BRCA1* promoter regions analysed by pyrosequencing with pre-custom assays, a wider hypermethylation status, with 51% of the PDXs having high % of CpG sites methylated in all the three areas analysed, leading us to suspect that these regions were not those involved in the regulation of gene transcription. In fact, when we used validated primers, which amplify another promoter region, 8% of the PDXs were strong methylated in line with the frequency of cases reported for EOC (Cancer Genome Atlas Research Network, 2011; Konstantinopoulos et al., 2015). Regarding the other genes investigated, only sporadic PDXs were methylated, with different % of CpG islands interested, while none showed *XPG* hypermethylation.

The pharmacological characterization was essential to define our EOC-PDXs and their response to the most used chemotherapy drugs involved in ovarian cancer treatment. The majority of the PDXs have been characterized for DDP, paclitaxel and trabectedin, a drug historically studied in our Department of Oncology. Recently, with the introduction of PARPi in EOC management, we began to characterize the sensitivity of PDXs to olaparib. In this thesis I will focus on PDXs response to DDP and olaparib.

A correct and reproducible classification of these PDXs based on their response to therapy, is essential for studies looking at biomarkers of response. There are different ways to

evaluate the best therapy response of tumours and we compared our standard method with mRECIST parameters, adapted to evaluate the drug response of our PDXs (Castroviejo-Bermejo et al., 2018a; Cruz et al., 2018). We found a clear association between mRECIST criteria and the T/C method regards the evaluation of olaparib antitumor activity (Cohen's k= 0.86), because in both cases we could similarly classified the drug antitumor effect. This association was even lower (Cohen's k = 0.33) when considering DDP antitumor activity, probably due to the wider range of antitumour activity observed. On top of this, the main limit in applying the mRECIST criteria was the exclusion of all the non-solid/intraperitoneal PDXs present in our xenobank, which cannot be evaluated by mRECIST. Thus, considering our method, we divided the PDXs into three response groups: very sensitive to treatment (in these cases we usually observed tumour regression or complete response), sensitive and resistant. The majority of our PDXs (73%) are responsive to DDP therapy, as observed in the clinic (Lheureux et al., 2019b) and DDP showed a wide range of response, while for olaparib we have 31% of the PDXs very responsive to therapy and the others resistant, confirming that PARPi are extremely active only in a subgroup of EOC cases.

This overview of the xenobank was necessary to introduce the models used to investigate the role of DNA repair in determining response and resistance to platinum and PARPi therapy, which is the final aim of the thesis.

4.2 EXPRESSION OF DNA REPAIR GENES AND HR MUTATIONAL STATUS OF THE EOC-PDXs IN RESPONSE TO THERAPY

Impairment of DNA repair is a common oncogenic event in most human cancers, including EOC, that has been exploited to enhance the anti-tumour activity of DNA damaging agents and more recently, by PARPi, which have been shown to be particularly active in HR deficient tumours. However, if DNA repair defects are associated with great sensitivity to DDP and PARPi (Bryant et al., 2005; Damia et al., 1996; Farmer et al., 2005; Lehmann, 2003) it is not completely clear whether increased DNA repair activity can be associated with resistance to therapy and there are still no validated biomarkers associated with DNA repair efficiency in tumour cells.

In the EOC-PDXs available in our xenobank, we explored the expression of genes involved in different DNA repair pathways and the mutational status of HR genes as possible biomarkers of DDP and olaparib treatment response. We quantified through real time-PCR the number of mRNA copies of 35 genes involved in different DNA repair pathways and in other mechanisms described in preclinical studies to have a role in DDP and/or PARPi response (**table 4.5**). We also evaluated the *BRCA1/BRCA2* mutational status in some PDXs by using a whole genome sequencing-based test, which allows the application of the HRDetect algorithm and the definition of a HR score.

In addition, we verified if the methylation promoter status of *BRCA1, FANCF, XPA, XPG, ERCC1* and *MLH1* was associated with a reduction of the transcription levels of the genes controlled by the promoter. Then, we analysed all these molecular features in relation with PDXs response to therapy.

4.2.1 Gene expression levels

Initially, a panel of 42 EOC-PDXs was chosen including all the histotypes and in these models we analysed the mRNA levels of 20 selected DNA repair genes (**table 4.5, A**), including *CDK12*, which is not properly involved in the DNA repair mechanism, but it regulates the transcription of several DNA repair genes and is found mutated in 3% of HGSOC (Cancer Genome Atlas Research Network, 2011).

Table 4.5 Lists of genes analysed and pathways in which they are involved

A

DNA repair pathway	Genes investigated
Base excision repair (BER)	*PARP1, OGG1, POLβ*
Nucleotide excision repair (NER)	*XPA, XPD, XPG, XPF, ERCC1*
Homologous recombination (HR)	*BRCA1, RAD51, PALB2, 53BP1*
Fanconi anemia (FA)	*FANCA, FANCC, FANCD2, FANCF*
Mismatch repair (MMR)	*MLH1*
Microhomology end joining (MMEJ)	*POLQ*
Translesion repair (TLS)	*POLH*
Regulator of DNA repair genes transcription	*CDK12*

B

Pathway	Genes investigated
Base excision repair (BER)	*PARP1, OGG1,*
Homologous recombination (HR) & DNA DSB response	*ARTEMIS, BRCA1, BRCA2, RAD51, PTIP, RAD51C, 53BP1,*
Non-homologous end joining (NHEJ)	*KU70, KU80, DNA PK*
MMEJ	*POLQ*
DNA damage response (DDR)	*SLFN11*
Chromatin organization	*CHD4, ARID1A, CARM1*
Cell cycle regulation	*REV7, CCNE1*
Deubiquitination	*USP28*
Drug transporter	*MDR1*

All the 20 genes analysed by RT-PCR with primers designed *ad hoc* were heterogeneously expressed in the PDXs and cluster analysis did not show specific expression patterns among the histotypes (f**igure 4.7**). Considering that *ERCC1* expresses four isoforms, but only isoform 202 is involved in NER (Friboulet et al., 2013b), we used two couples of primers to amplify a region shared by all the isoforms (ERCC1 tot) and another shared only by the two isoforms 202 and 204 (ERCC1 iso2), because it was not possible to design primers entirely specific for the functional isoform 202 involved in NER. However, data obtained did not show differences between ERCC1 iso2 and ERCC1 total expression levels.

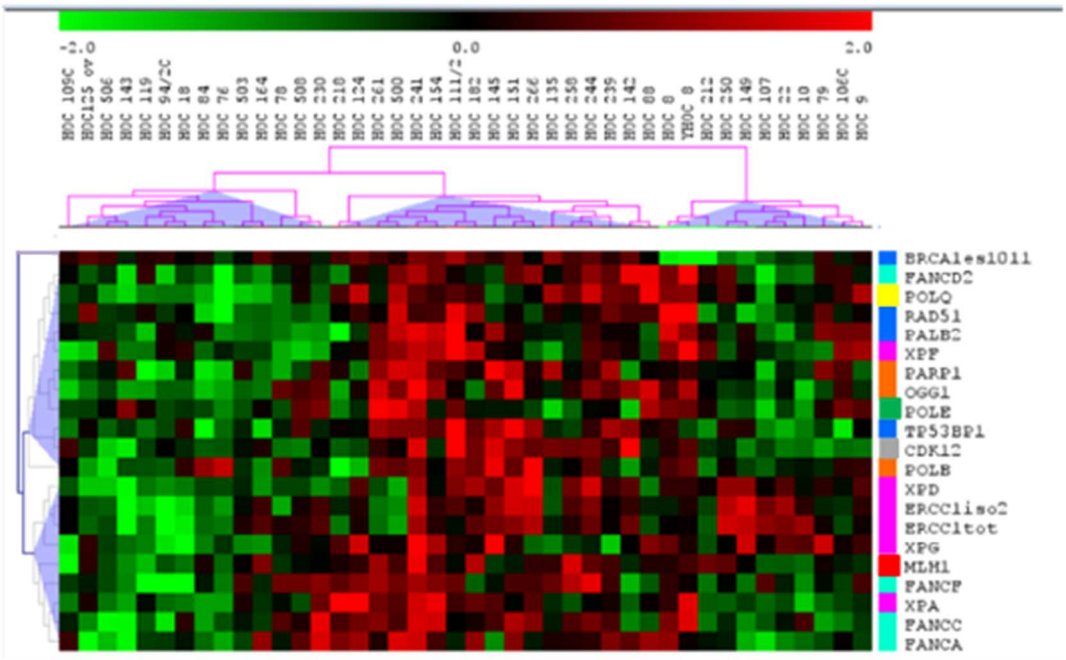

Figure 4.7 Expression pattern of DNA repair genes in all the EOC-PDXs analysed

The heat map represents the mRNA expression levels (low levels in green; high levels in red) of 20 genes involved in different DNA repair pathways (rows) analysed by RT-PCR in 42 EOC-PDXs (columns). Each pathway is associated with a coloured square: blue=HR; light blue=FA; pink=NER; orange=BER; red=MMR; green=TLS; yellow=MMEJ; grey=*CDK12*.

Considering that 80% of the PDXs in the xenobank are high grade tumours, which represent the most diffuse subtype also among patients, we decided to focus the analyses on this homogeneous population. 29 out of 42 PDXs were HGSOC/HGEOC and their gene expression pattern was similar to that of all the PDXs. We decided to investigate the presence of possible correlations between the single genes, since DNA repair pathways are multistep processes and the studies of possible genes association could be important. Dr Maddalena Fratelli, who performed the statistical analyses calculated the Pearson correlation index between each single gene (**table 4.6**)**.** It was observed that *OGG1, FANCD2, XPF*, *FANCD2, PALB2* and CDK12 expression significantly correlated with at least four other genes, and, in particular, *FANCC* correlated with other genes involved in the same pathway (FA pathway).

Table 4.6 Correlations between single gene expressions of DNA repair genes analysed in the high grade EOC-PDXs

gene	MLH1	OGG1	PARP1	POLB	53BP1	BRCA1	RAD51	PALB2	POLQ	POLH	FANCA	FANCC	FANCD2	FANCF	XPA	XPD	XPF	XPG	ERCC1	CDK12
MLH1	1,00	0,35	0,05	-0,14	-0,12	-0,06	0,01	-0,01	0,22	0,11	0,15	0,11	0,26	0,31	0,03	0,07	0,08	-0,06	-0,04	0,12
OGG1	0,35	1,00	**0,41**	0,18	0,16	0,00	**0,41**	**0,41**	**0,52**	**0,49**	**0,45**	**0,65**	**0,69**	**0,53**	0,24	0,18	**0,47**	0,24	0,12	0,25
PARP1	0,05	**0,41**	1,00	0,15	0,32	-0,06	0,25	**0,44**	0,27	**0,44**	0,33	0,18	0,25	0,05	0,01	0,02	0,29	0,23	-0,04	0,29
POLB	-0,14	0,18	0,15	1,00	0,30	-0,10	0,04	0,23	-0,02	0,02	-0,11	0,24	0,21	0,02	-0,15	**0,56**	0,13	0,05	0,18	**0,43**
53BP1	-0,12	0,16	0,32	0,30	1,00	**0,50**	0,24	0,38	0,14	0,18	0,10	0,08	0,09	0,16	-0,04	0,24	0,24	0,03	0,02	**0,62**
BRCA1	-0,06	0,00	-0,06	-0,10	**0,50**	1,00	-0,10	-0,03	0,03	-0,06	0,01	-0,11	-0,24	0,32	0,12	-0,11	-0,07	-0,12	-0,30	0,27
RAD51	0,01	**0,41**	0,25	0,04	0,24	-0,10	1,00	**0,65**	**0,55**	0,22	0,25	**0,44**	**0,72**	0,03	0,31	0,01	**0,72**	0,03	-0,11	0,33
PALB2	-0,01	**0,41**	**0,44**	0,23	0,38	-0,03	**0,65**	1,00	**0,41**	0,28	0,13	0,16	**0,48**	-0,08	-0,06	0,09	**0,79**	0,21	-0,05	**0,45**
POLQ	0,22	**0,52**	0,27	-0,02	0,14	0,03	**0,55**	**0,41**	1,00	0,13	**0,42**	0,37	**0,71**	**0,45**	0,34	0,38	**0,46**	0,28	0,24	0,17
POLH	0,11	**0,49**	**0,44**	0,02	0,18	-0,06	0,22	0,28	0,13	1,00	0,28	0,13	0,16	0,12	-0,04	-0,22	0,24	-0,07	-0,25	-0,07
FANCA	0,15	**0,45**	0,33	-0,11	0,10	0,01	0,25	0,13	**0,42**	0,28	1,00	**0,54**	0,29	0,37	0,34	-0,17	0,07	-0,05	-0,14	-0,01
FANCC	0,11	**0,65**	0,18	0,24	0,08	-0,11	**0,44**	0,16	0,37	0,13	**0,54**	1,00	**0,59**	**0,44**	**0,45**	0,23	0,29	0,16	0,24	0,24
FANCD2	0,26	**0,69**	0,25	0,21	0,09	-0,24	**0,72**	**0,48**	**0,71**	0,16	0,29	**0,59**	1,00	0,26	0,28	0,36	**0,65**	0,04	0,15	0,26
FANCF	0,31	**0,53**	0,05	0,02	0,16	0,32	0,03	-0,08	**0,45**	0,12	0,37	**0,44**	0,26	1,00	0,21	0,29	-0,04	0,06	0,25	0,19
XPA	0,03	0,24	0,01	-0,15	-0,04	0,12	0,31	-0,06	0,34	-0,04	0,34	**0,45**	0,28	0,21	1,00	-0,01	0,24	0,26	-0,10	-0,05
XPD	0,07	0,18	0,02	**0,56**	0,24	-0,11	0,01	0,09	0,38	-0,22	-0,17	0,23	0,36	0,29	-0,01	1,00	0,07	0,33	**0,71**	0,37
XPF	0,08	**0,47**	0,29	0,13	0,24	-0,07	**0,72**	**0,79**	**0,46**	0,24	0,07	0,29	**0,65**	-0,04	0,24	0,07	1,00	0,10	-0,11	**0,42**
XPG	-0,06	0,24	0,23	0,05	0,03	-0,12	0,03	0,21	0,28	-0,07	-0,05	0,16	0,04	0,06	0,26	0,33	0,10	1,00	**0,61**	0,03
ERCC1	-0,04	0,12	-0,04	0,18	0,02	-0,30	-0,11	-0,05	0,24	-0,25	-0,14	0,24	0,15	0,25	-0,10	**0,71**	-0,11	**0,61**	1,00	0,08
CDK12	0,12	0,25	0,29	**0,43**	**0,62**	0,27	0,33	**0,45**	0,17	-0,07	-0,01	0,24	0,26	0,19	-0,05	0,37	**0,42**	0,03	0,08	1,00

The linear correlation between the expression levels of different genes was measured by the *Pearson test*. Significant correlation values are in red.

For *CDK12* significant correlation with *PALB2*, *53BP1* and *XPF* has been reported also in the TCGA databases (yellow).

For *CDK12,* which correlated with *PALB2, 53BP1, XPF* and *POLB* in our xenobank, we analysed the gene expression data reported in the TCGA Affymetrix microarray and RNAseq databases. We found that *CDK12* mRNA levels correlated with *PALB2, 53BP1* and *XPF* transcripts in both the databases, while *POLB* showed a modest significance (p-value ~ 0.05) only in the RNAseq dataset (**table 4.7**). These data seem to support the role of *CDK12* as a transcription regulator protein of some DNA repair genes.

Table 4.7. Correlation of *CDK12* with other DNA repair genes from two TCGA databases

Genes highlighted in grey were found correlated with CDK12 in our experiment.

RNA seq			Affymetrix microarrays		
Gene	**r to CDK12**	**p-value**	**Gene**	**r to CDK12**	**p-value**
BRCA1	0,298019	7,40E-07	*PARP1*	0,26	2,28E-10
53BP1	0,286066	2,10E-06	*MLH1*	0,25	1,14E-09
PARP1	0,262365	1,46E-05	*PALB2*	0,22	9,36E-08
POLH	0,260016	1,75E-05	*XPF*	0,2	1,28E-06
XPF	0,240594	7,37E-05	*53BP1*	0,19	4,31E-06
POLQ	0,218424	3,32E-04	*BRCA1*	0,19	4,31E-06
PALB2	0,187205	0,002169	*POLQ*	0,16	0,000113
POLB	-0,17445	0,00432	*RAD51*	0,15	0,000299
ERCC1	-0,16503	0,00699	*XPA*	0,14	0,000746
FANCC	0,1567	0,010482	*FANCD2*	0,13	0,001753
FANCA	0,146949	0,0166466	*OGG1*	-0,12	0,003893
FANCD2	0,142286	0,02026			

Then, we extended the gene expression characterization to all the PDXs whose response to DDP and olaparib was known (n=46), evaluating the mRNA expression of 21 DNA repair genes and others described in preclinical studies to affect in some extent the response to DDP and olaparib in EOC (**table 4.5, B**).

As in the previous analysis, all the PDXs expressed the genes studied with considerable variability as reported in **figure 4.8**.

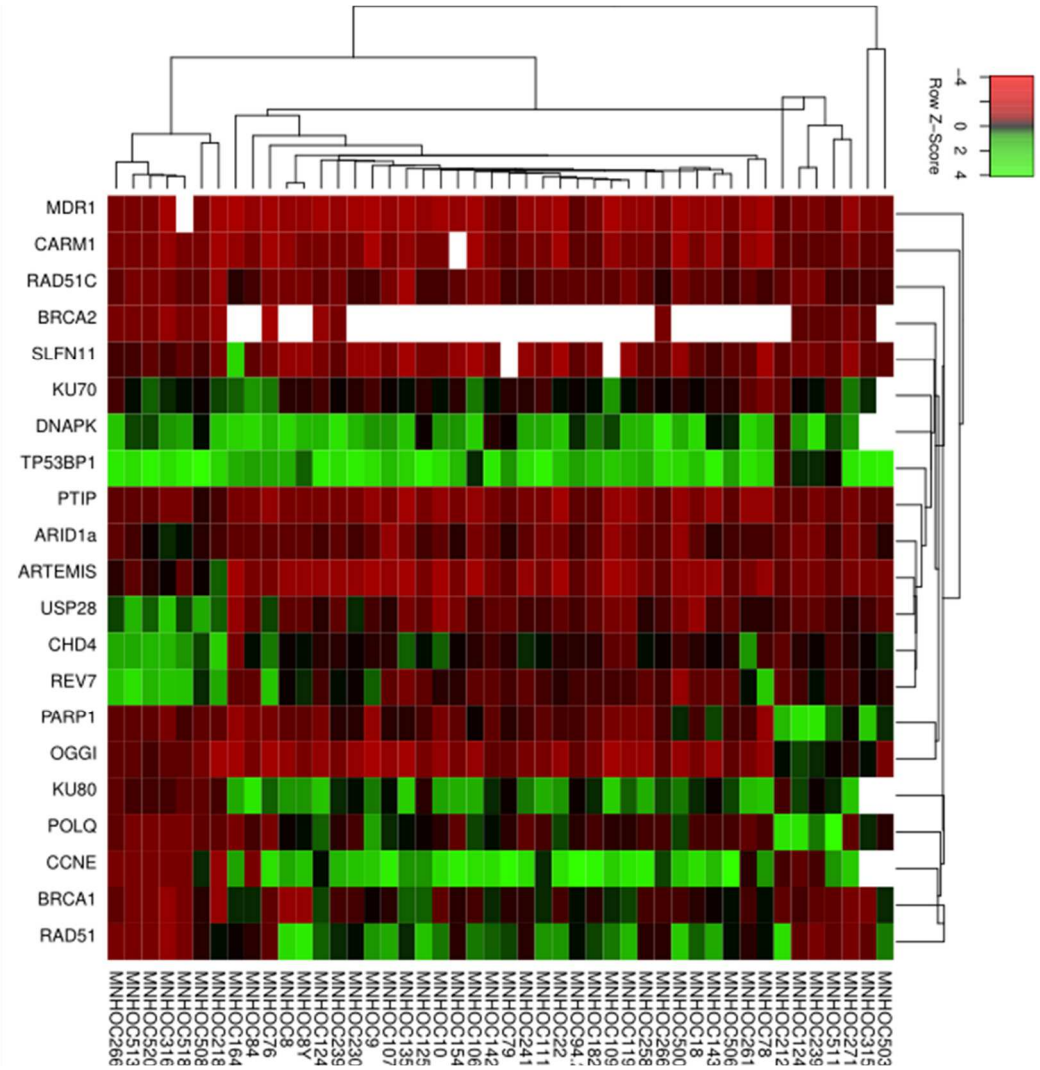

Figure 4.8 Expression pattern of the genes involved in platinum and PARPi response studied in all the EOC-PDXs

The heat map represents the mRNA expression levels (low levels in red; high levels in green) of 21 genes involved in different DNA repair pathways (rows) analysed by RT-PCR in 46 EOC-PDXs (columns). White spaces: the info is not available.

We correlated the expression levels between single genes in all the 46 PDXs. Three strong significant positive correlations were found between *ARTEMIS* and *CHD4* (ρ=0.81, p<0.0001), *ARTEMIS* and *USP28* (ρ=0.82, p<0.0001), and *CHD4* and *REV7* (ρ=0.80, p<0.0001). As in the previous analysis, we then considered the subgroup of high grade PDXs. In this subset, the correlations between *ARTEMIS* and *USP28* (ρ=0.81, p<0.0001) and *CHD4* and *REV7* (ρ=0.82, p<0.0001) have been confirmed, even if, from a preliminary analysis, these correlations have not been observed in the TCGA databases. The detailed correlation indexes and p-values of the significant correlations are reported in **table 4.8**.

Table 4.8 Significant correlations between single gene expression in all the PDXs and in the subgroup of high grade PDXs

	1st gene	2nd gene	ro	p-value	n
all PDXs	*CHD4*	*ARTEMIS*	0.81	<0.0001	46
	USP28	*ARTEMIS*	0.82	<0.0001	
	CHD4	*REV7*	0.80	<0.0001	
High grade PDXs	*USP28*	*ARTEMIS*	0.81	<0.0001	36
	CHD4	*REV7*	0.82	<0.0001	

The linear correlation between the expression levels of different genes was measured by Spearman correlation index (threshold for significance: ro>0.80).

4.2.2 Correlation between gene promoter methylation status and mRNA expression

Pyrosequencing data showed that all the three *BRCA1* promoter regions analysed were hypermethylated in half of our PDXs (**table 4.3**); we did not find any correlation between *BRCA1* promoter methylation status and *BRCA1* mRNA copies. On the contrary, the five PDXs hypermethylated in the region of *BRCA1* promoter analysed by MS-PCR showed a significant reduction of the number of mRNA copies compared with the average number of mRNA copies in all the other not methylated PDXs (t-test p=0.0015) (**table 4.9**).

The *MLH1* promoter was scarcely methylated in our PDXs panel, with few exceptions. MNHOC109 displayed a % of CpG sites in the two promoter regions evaluated close to 100% and associated with a 100-fold less expression level of mRNA as compared to non-methylated PDXs. In MNHOC500 we observed a reduction of *MLH1* expression in line with the low % of CpG sites methylated (11%) (**table 4.9**).

Similar reduction in gene expression has been observed in MNHOC8 and MNHOC124, which displayed 15% and 19% of methylation, respectively, in one of the two *ERCC1* promoter regions analysed (**table 4.9**).

The two PDXs with *FANCF* hypermethylation showed a reduction of mRNA copies, even with 10% of CpG sites methylated (MNOC119) (**table 4.9**).

XPA methylation status seems not to be associated with the gene expression, in fact, the 5 PDXs, which displayed a similar percentage of methylation, ranging from 12% to 22%, differently expressed *XPA*, and in 2 out of 5 PDXs *XPA* was overexpressed (**table 4.9**).

Table 4.9 Comparison between methylation status and gene expression in PDXs resulted hypermethylated in selected genes

Gene	#ID PDXs	%CpG islands methylated	mRNA copies normalized (R1)	Mean mRNA copies normalized in the non-methylated PDXs (R0)	n°	R1/R0
BRCA1	MNHOC212	100%	1,68E-04	4,83E-02	46	0,003
	MNHOC8	84%	7,05E-04			0,015
	MNHOC8Y	100%	2,91E-04			0,006
	MNHOC518	100%	1,05E-03			0,022
	MNHOC520	49%	4,39E-04			0,009
MLH1	MNHOC500	11%	3,94E-01	1,42E+00	42	0,276
	MNHOC109	96%, 87%	1,25E-03			0,001
XPA	MNHOC8Y	13%	7,22E-02	2,70E-02	42	2,679
	MNHOC76	20%	1,55E-02			0,574
	MNHOC239	13%	1,85E-02			0,687
	MNHOC506	22%	1,01E-02			0,374
	MNHOC212	12%	1,18E+00			43,941
ERCC1	MNHOC8	15%	8,95E-01	2,54E+00		0,353
	MNHOC124	19%	7,97E-01			0,314
FANCF	MNHOC18	70%	3,23E-01	2,72E+00	42	0,119
	MNHOC119	10%	2,43E-01			0,089

n°= number of PDXs where mRNA copies have been quantified.

4.2.3 HRDetect score

In collaboration with Dr Nik-Zainal, who set up the HRDetect algorithm (Davies et al., 2017), WGS was performed in 10 EOC-PDXs of the xenobank. The HRDetect algorithm allowed me to assign a HR score to each sample. The HRDetect assay is based on the analysis of a pattern of mutational signatures characteristic of HR deficiency (**figure 4.9, A**) and a HR score >0.7 is indicative of HR deficiency (Davies et al., 2017).

5 out of 10 PDXs had a HR score >0.90, while in the other five PDXs the score was lower than 0.2, indicative of HR proficiency. Considering the positive PDXs (HR score >0.7), MNHOC154 and MNHOC266 harbour a germline *BRCA1* mutation and MNHOC212 shows *BRCA1* promoter hypermethylation, that could explain the *BRCAness* phenotype. MNHOC230 and MNHOC135 had a positive score but no mutations in *BRCA1*, *BRCA2* and other HR genes investigated through WGS, nor *BRCA1* promoter hypermethylation were observed (**figure 4.9, B**).

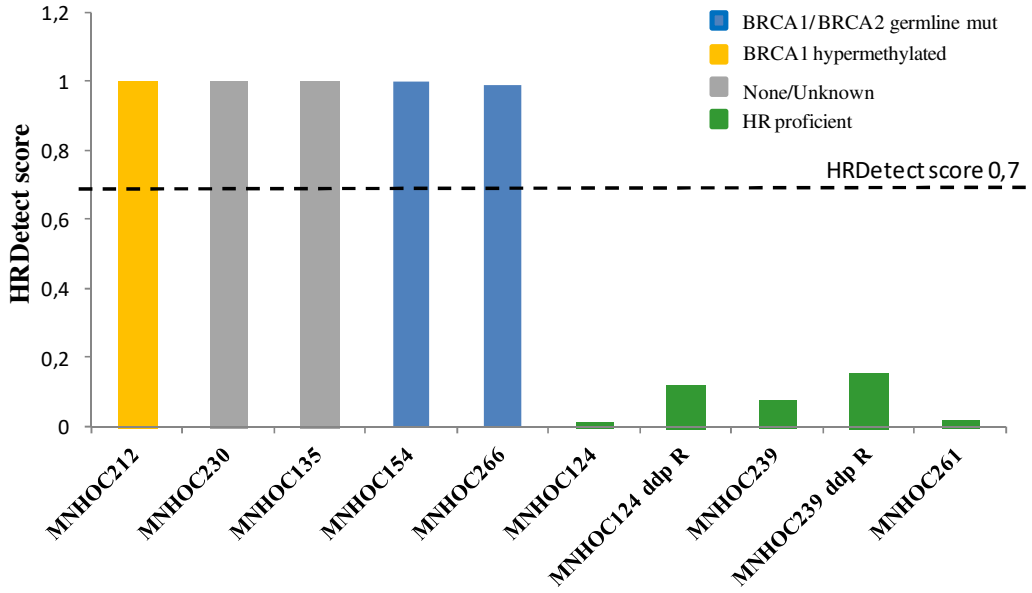

Figure 4.9 HRDetect assay

The HR score calculated in 10 EOC-PDXs, included two with acquired resistance to DDP (MNHOC124 DDPR, MNHOC239 DDPR). HR-positive PDXs (HR score >0.7) were enriched for pathogenic *BRCA1* mutations and showed *BRCA1* promoter hypermethylation compared with HR-negative PDXs. Blue bar: *BRCA1/BRCA2* mutations; yellow bar: *BRCA1* promoter hypermethylation; grey bar: PDXs HR-positive with unknown HR defects; green bar: HR proficient PDXs.

4.2.4 DNA repair gene expression levels and HR mutational status associated with response to therapy in EOC-PDX tumours

The relation between gene expression levels or HR mutational status and antitumour activity of DDP and olaparib were studied in order to find possible biomarkers of therapy response. Firstly, we studied the correlation between DDP response and the expression levels of the 20 DNA repair genes in the high grade PDXs divided into the three response categories: VS, S and R, according to the parameters described in Materials and Methods.

The expression of three genes negatively associated with DDP response, meaning that higher mRNA levels were expressed in resistant xenografts: *XPF* (p=0.016), *PALB2* (p=0.019) and *CDK12* (p=0.017) (**figure 4.10**, **panel A, B, C**). Then, we tried to confirm these data using the independent and public database of the TCGA, where gene expression data and ovarian cancer clinical information are available. Only regarding *CDK12*, we found that patients with higher expression levels of *CDK12* mRNA had a higher risk of relapse (HzR=1.119, 95% CI 0.9188-1.564, p=0.179), even if the difference did not reach statistical significance, while *XPF* and *PALB2* data were not confirmed. However, the analysis included a bias, since the population considered included also those patients with *CDK12* inactivating mutations (Ekumi et al., 2015). We then re-analysed these data considering them as not expressing CDK12 protein and stratifying patients for the residual tumour (RT) after surgery (more or less than 2 cm). We found that patients with higher levels of CDK12, even with a RT< 2 cm (per se a good prognostic indicator) have a worse prognosis than those with low protein levels (HzR=1.295, 95% CI 1.016-1.651, p=0.0367) (**figure 4.10, panel D**). We could not validate the results obtained in our PDXs regarding *PALB2* and *XPF*, because no correlation between the expression levels of these two genes associated with patient prognosis in the TCGA database.

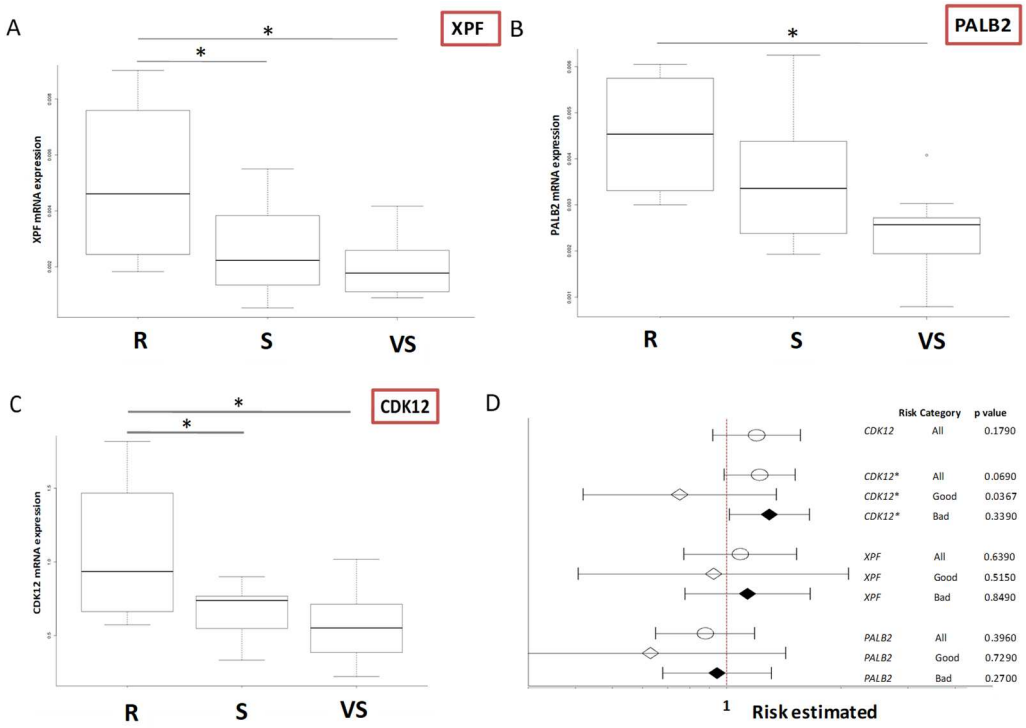

Figure 4.10 DNA repair gene expression levels and DDP response in high grade PDXs

Panels A, B, C: box plots showing the *XPF, PALB2, CDK12* mRNA levels, respectively, in high grade PDXs classified as DDP resistant (R), sensitive (S) and very sensitive (VS). *: p <0.05. **Panel D**: forest plot of the relation between *CDK12* gene expression and ovarian cancer patient survival. The estimated risk of recurrence in patients with different *CDK12*, *XPF* and *PALB2* gene expression levels (I- lower risk, -I higher risk, dot: estimated risk). Risk categories: good: RT <2; bad RT >2.

We then correlated the expression levels of the second panel of 21 genes with DDP and olaparib PDX response.

A significant correlation was observed between *USP28* (p=0.0082), *ARTEMIS* (p=0.0232), *ARID1A* (p=0.0246) and *MDR1* (p=0.0241) and DDP response in all the PDXs (**figure 4.11**). Only *USP*28 was confirmed in the high-grade models (p=0.047). No correlations between olaparib response and gene expression levels in either all the PDXs, or in the high-grade subgroup, were found. Only a trend was also found between *USP 28* and olaparib response, that however, did not reach a statistically significant p-value (p=0.0526).

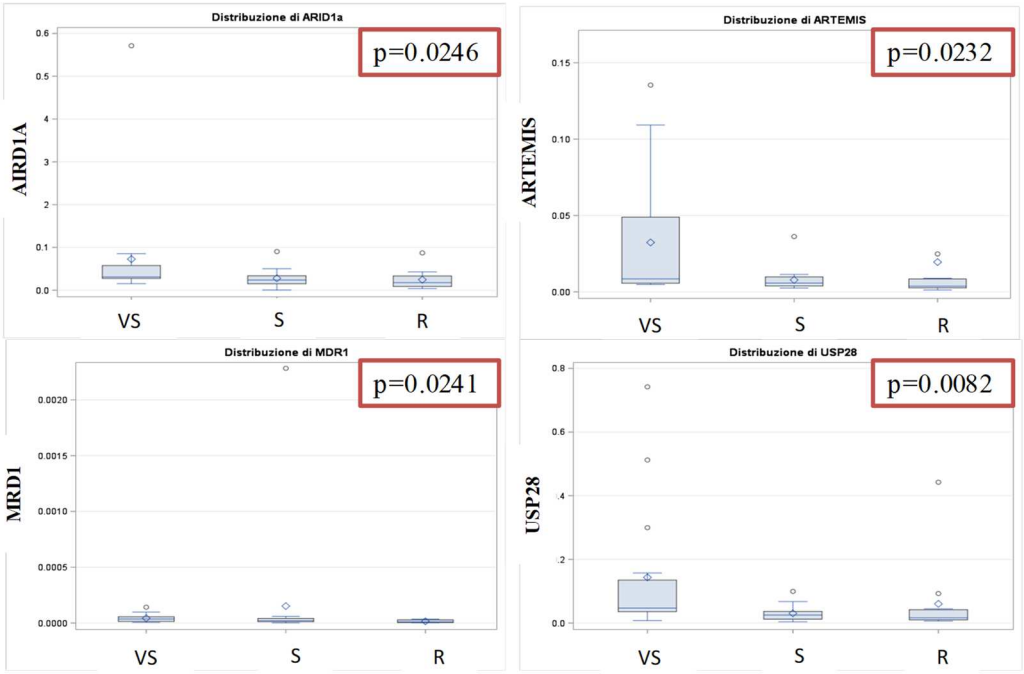

Figure 4.11 mRNA expression levels of genes significantly associated with DDP response in all the EOC-PDXs

Box plots showing the *ARID1A, ARTEMIS, MDR1* and *USP28* mean (diamond) and median (line) of the mRNA copies expressed by all the PDXs classified for their response to DDP in resistant (R), sensitive (S) and very sensitive (VS). $p<0.05$. mRNA copies are calculated as the average of mRNA copies of three different biological replicates normalized. Dots: out layers.

We considered the HR status (deficient/proficient) of the PDXs, based on the presence of *BRCA1/BRCA2* mutations and/or HR ≥0.7 to define PDXs as HR deficient. Conversely, *BRCA1/BRCA2* wt and/or score <0.7 are indicative of HR proficiency. We looked for possible associations with DDP and olaparib response and HR status. The analysis between HR status and response to therapy showed a significant association with both DDP (Jonckheere-Terpstra test: p=0.001, n=34) and olaparib (Jonckheere-Terpstra test: p=0.017, n=19). Figure 4.12 shows the drug response to DDP and/or olaparib in both subcutaneously (**figure 4.12, A**) or orthotopically transplanted PDXs (**figure 4.12, B**), and reports for each PDX *BRCA1/BRCA2* mutational status, HR score positive or negative and the *BRCA1* promoter hypermethylation status.

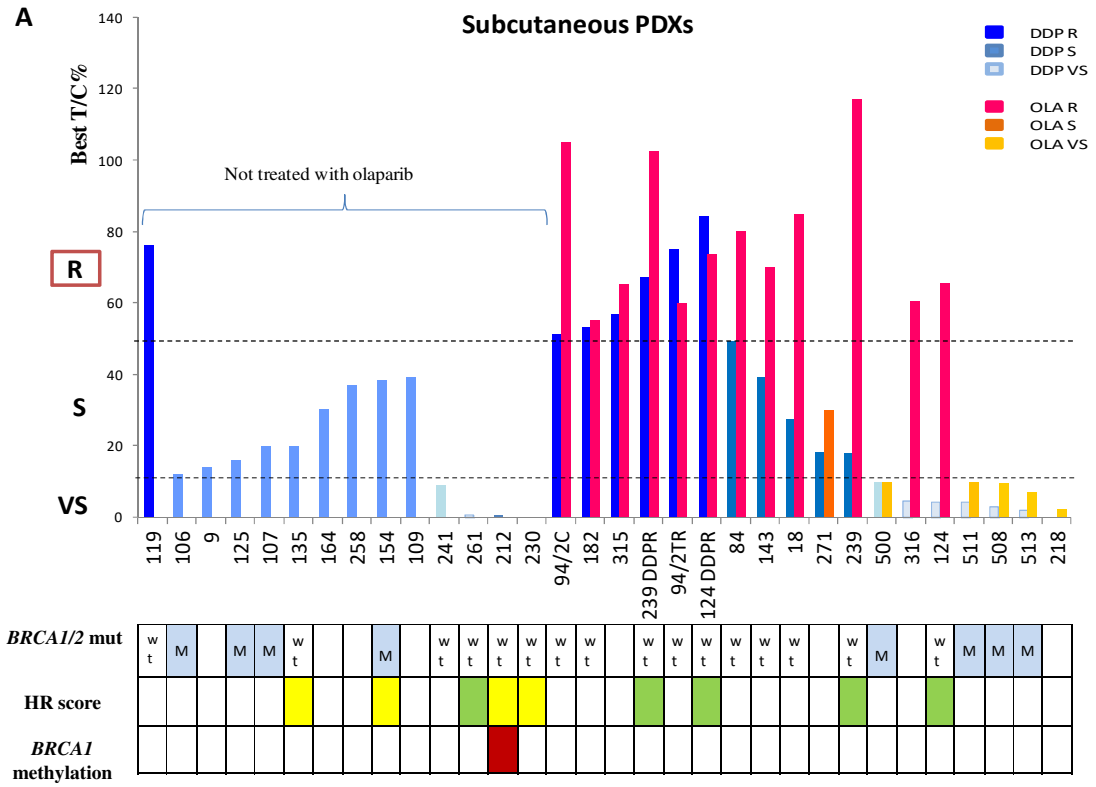

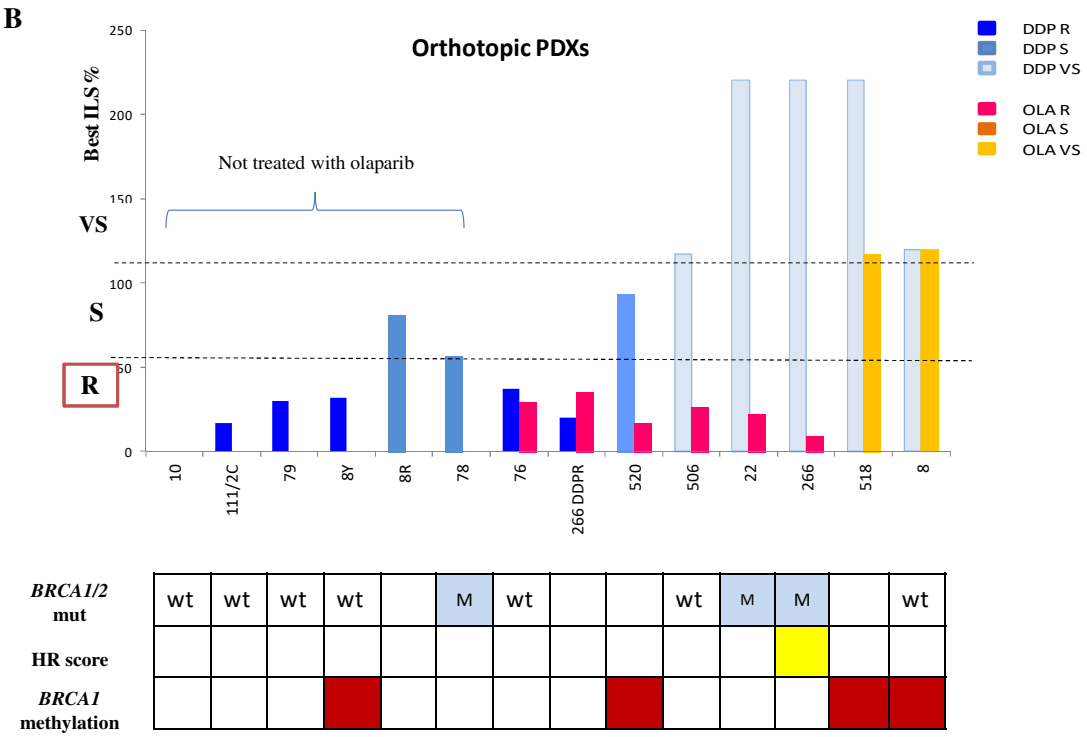

Figure 4.12 Overview of the best treatment response to DDP and olaparib and HR related profile of the EOC-PDXs under study

Response to DDP (blue bars) and olaparib (red bars) in the subcutaneous and intraperitoneal PDX models. *BRCA1/BRCA2* mut= mutated; wt= wild type; HR score: yellow box = positive/ HRD; green box = negative/ HR proficient; *BRCA1* promoter methylation status: red box = hypermethylated.

A) For tumours grown subcutaneously the best T/C% has been evaluated for DDP and for olaparib. As detailed in Materials and Methods, tumours were classified as resistant (R) to therapy with T/C% ≥ 50%; sensitive (S) 10%<T/C%<50% and very sensitive (VS) T/C% ≤10%. The dashed lines indicate the T/C% thresholds that divide the response into the three categories. Different coloured bars are associated with different DDP (blue/light blue) and olaparib (red/yellow) response to treatment.

B) For orthotopic PDXs the best ILS% has been evaluated for each treatment. As detailed in Materials and Methods, tumours were classified as resistant (R) with ILS% ≤ 40%; sensitive (S) 40%< ILS%<100% and very sensitive (VS) ILS% ≥100%. The dashed lines indicate the ILS% thresholds that divide the response into the three categories. Different coloured bars are associated with different DDP (blue/light blue) and olaparib (red/yellow) response to treatment.

4.2.5 Discussion II

DNA repair is an important determinant of the tumour response to DDP and olaparib, and we aimed to explore its potential as a predictive biomarker of chemotherapy response. Using a panel of EOX-PDXs characterized for their response to DDP and olaparib therapy, we selected 35 DNA repair genes and others described to be involved in mechanisms of drug sensitivity/resistance, and quantified by RT-PCR the absolute number of mRNA copies in the PDXs.

All the genes were variably expressed in our models, without showing histotype-specific clusters of expression. This might be explained by the presence of only two cases of mucinous samples, three clear cells, 2 low grade serous/endometrioid and 80% of HGSOC/HGEOC, which reflect the incidence observed in the clinic (Duska and Kohn, 2017). This is the reason why we focused some analyses in this large subgroup. We analysed the correlation between the expression levels of single genes and found significant correlations among genes of the same pathway (i.e. FA genes), which could be explained by the fact that FA DNA repair pathway is a multistep process and their genes should be correlated with each other. We also found that *CDK12,* involved in the regulation of DNA repair gene transcription, positively correlated with *PALB2*, *XPF* and *53BP1*. Besides this role, CDK12 is a kinase involved in chromosome organization, stress induced gene expression and possibly RNA processing factors (Chilà et al., 2016). It has been found mutated in 3% of EOCs (Cancer Genome Atlas Research Network, 2011) and inactivating mutations in the catalytic site of the proteins have been associated with impaired HR and sensitivity to DNA damaging agents (Chilà et al., 2016; Ekumi et al., 2015). Moreover, we found positive correlations also between *USP28*, a deubiquitinase protein, able to modify and stabilize some DSB repair proteins (Knobel et al., 2014), and *ARTEMIS*, an endonuclease of the NHEJ pathway, and between *CHD4* and *REV7*, both involved in the mechanism of resistance to PARPi (Gupta et al., 2018; Pan et al., 2012). A preliminary

search in the literature and in public datasets did not report these correlations and required further investigations.

We investigated whether the promoter hypermethylation status found in some PDXs in selected DNA repair genes (*BRCA1, FANCF, XPA, XPG, ERCC1* and *MLH1*) effectively affected the transcription of the genes. *BRCA1* methylation has been evaluated in 5 different areas of the promoter, but only two have been already described to reduce the transcription levels (Ter Brugge et al., 2016). In fact, the other three regions, found strongly hypermethylated in half of the PDXs, did not correlate with *BRCA1* mRNA levels, while considering the other two regions, 5 PDXs were strongly hypermethylated and showed a significant reduction of *BRCA1* gene expression ($p=0.0015$) compared with the average of mRNA copies expressed in the non-hypermethylated PDXs. Regarding the other genes investigated, they were scarcely hypermethylated, confirming similar results in EOC (Cancer Genome Atlas Research Network, 2011; Sabatino et al., 2010). MNHOC109, hypermethylated in *MLH1* promoter, was also the PDX with the lowest *MLH1* mRNA expression level. The low expression of *MLH1* induced by promoter hypermethylation has been reported to associate with DDP resistance (Strathdee et al., 1999). However, MNHOC109 was sensitive to DDP, and MNHOC500, found scarcely hypermethylated (11%) was very sensitive to DDP (**table 4.4**), suggesting other factors could determine the final response to DDP of the tumour. Similar considerations could be applied to *FANCF*, where the two hypermethylated PDXs showed a reduction of FANCF mRNA, but were not associated with DDP response. ERCC1 was found hypermethylated in two very sensitive PDXs to DDP, and the mRNA was reduced. While XPA methylation status in 5 PDXs did not associate with gene expression, maybe, the 2 regions evaluated, as for *BRCA1*, were not those responsible for the regulation of transcription.

We correlated the gene expression levels with DDP and olaparib response, focusing in particular on the subgroup of the high grade serous and endometrioid PDXs. *CDK12, PALB2, XPF* and *USP28* mRNA levels significantly correlated with DDP response. In

particular, higher mRNA levels of *CDK12, PALB2* and *XPF* have been expressed in DDP resistant PDXs tumours and we could corroborate the potential role of *CDK12* as prognostic factor in the TCGA dataset, while *PALB2* and *XPF* expression did not correlate with patient prognosis in the same database. It has been observed that ovarian cancer patients expressing higher levels of CDK12 protein have a worse prognosis, even if they had a residual tumour < 2 cm after surgery, which is generally considered a good prognostic marker. Conversely, higher mRNA levels of *USP28* have been expressed in DDP very sensitive tumours, and this significant correlation was reported in all the PDXs and it was maintained also in the high grade PDXs. Regarding olaparib, none of the selected genes significantly correlated with response to therapy, even if a trend of association was also found between *UPS28* and olaparib response, suggesting other biomarkers are necessary to predict olaparib response.

The deficiency in HR has been associated with sensitivity to both DDP and olaparib (Konstantinopoulos et al., 2015; Vollebergh et al., 2014). However, as already discussed in the introduction, the functional HR status (proficient/deficient) is not easily determined in tumours. Inactivating germline and somatic mutations of genes involved in HR (i.e. *BRCA1/BRCA2, PALB2, FANCD2, RAD51C*), low/absent protein level (due to do promoter hypermethylation or mutations) could all contribute to a deficiency in HR. In addition, different genomic tests, such as Myriad Choice or Foundation Medicine test have been described able to capture, even if not entirely, the *BRCAness* phenotype (Coleman et al., 2017; Stronach et al., 2018). We analysed 10 of our PDXs with the HRDetect assay, which uses an algorithm to analyse different genomic mutational signatures related to the *BRCAness* phenotype, besides the presence of *BRCA1/2* mutations, and elaborates a final HR score indicative of HR status, suggesting that HRDetect test could enlarge the population that could benefit from DNA damaging therapies (Chopra et al., 2020; Davies et al., 2017). We observed that 5 PDXs were HR deficient, having a HR score ≥0.7. Among them, two were effectively *BRCA1* mutated and one had *BRCA1* promoter hypermethylation, while in the other two the causes of HRD are unknown.

We analysed the association between HR deficient status (based on HR score and *BRCA1/2* mutational profile of the PDXs) and DDP and olaparib response, and a significant association has been found between HRD and both the drugs. These data corroborate the role of HRD in determining sensitivity to cross linking agents and PARPi.

4.3 STUDY OF RAD51 FOCI AS PREDICTIVE BIOMARKER FOR RESPONSE TO PLATINUM AND PARPI THERAPY

Evidence from PARPi preclinical and clinical studies suggest that their activity extends beyond *BRCA1/BRCA2* germline and/or somatic mutated tumours (Pilié et al., 2019). In addition, it has been reported that platinum sensitive or *BRCA1/2* mutated tumours don't always benefit from PARPi (Ceccaldi et al., 2015; D'Andrea, 2018), as suggested also by our previous data, where some PDXs even extremely sensitive to DDP, or *BRCA*-mutated, were resistant to olaparib, suggesting an intricate scenario. Tests able to predict HR status based on genomic signatures and mutational profiling of the tumour are not completely successful in predicting response to therapy. Tests able to capture the functionality of different DNA repair pathways would help.

Having available a xenobank of PDXs, whose sensitivity to DDP and olaparib is known, we explored if functional surrogates of HR (i.e. RAD51 foci) and NER (i.e. ERCC1/XPF complex) pathways could correlate/associate with drug response.

4.3.1 Quantitative immunofluorescence assay to evaluate RAD51 foci in a tissue microarray representative of the xenobank

We have available in our laboratory a tissue microarray (TMA) from FFPE EOC-PDX tumours, which includes 60 PDXs samples, representing all the EOC histotypes and the wide spectrum of tumour sensitivity to DDP and olaparib (**table 4.10**). From each donor, two different areas of the tumours were selected by the pathologist and included into the TMA as two different cores.

Table 4.10 List of the EOC-PDXs included in the TMA

#ID EOC-PDXs	Histotype	DDP sensitivity	Olaparib sensitivity
MNHOC22	HGSOC	VS	R
MNHOC125	HGSOC	VS	
MNHOC212	HGSOC	VS	
MNHOC266	HGSOC	VS	R
MNHOC500	HGSOC	VS	VS
MNHOC506	HGSOC	VS	R
MNHOC508	HGSOC	VS	VS
MNHOC511	HGSOC	VS	VS
MNHOC124	HGS/ HGE OC	VS	R
MNHOC218	HGEOC	VS	VS
MNHOC230	HGEOC	VS	
MNHOC261	HGEOC	VS	
MNHOC8	HGSOC	VS	VS
MNHOC84	HGSOC	S	R
MNHOC106	HGSOC	S	
MNHOC107	HGSOC	S	
MNHOC143	HGSOC	S	R
MNHOC239	HGSOC	S	R
MNHOC258	HGSOC	S	
MNHOC271	HGSOC	S	S
MNHOC18	HGEOC	S	R
MNHOC78	HGEOC	S	
MNHOC154	HGEOC	S	
MNHOC503	HGEOC	S	
MNHOC8Y	HGSOC	R	
MNHOC10	HGSOC	R	
MNHOC76	HGSOC	R	R
MNHOC111/2C	HGSOC	R	
MNHOC79	HGEOC/CCC	R	
MNHOC149	HGSOC		
MNHOC130	HGSOC		
MNHOC244	HGSOC		
MNHOC8R	HGSOC	S	
MNHOC94/2TR	HGSOC	R	R
MNHOC247	HGSOC		
MNHOC249	HGSOC		
MNHOC250	HGSOC		
MNHOC253	HGSOC		
MNHOC254	HGSOC		
MNHOC263	HGSOC		
MNHOC268	HGSOC		
MNHOC276	HGSOC		
MNHOC280	HGSOC		
MNHOC283	HGSOC		
MNHOC232	HGS/ HGE OC		
MNHOC241	LGSOC	VS	
MNHOC109	LGEOC	S	
MNHOC135	Mixed müllerian	S	
MNHOC195	Mixed müllerian		
MNHOC151	Carcinosarcoma		
MNHOC213	Undifferentiated		
MNHOC88	Undifferentiated	S	
MNHOC164	MC	S	
MNHOC182	MC	R	R
MNHOC94/2C	CCC	S	R
MNHOC142	CCC	S	
MNHOC119	CCC	R	
MNHOC296	Endometrial tumour		
MNHOC110	not classified		
MNHOC9	not classified	S	

Legend: VS= very sensitive; S= sensitive; R= resistant.

In collaboration with Dr Deborah Wilsker of the Frederick National Laboratory for Cancer Research (MD, USA), who set up a multiplex immunofluorescent (IF) assay to stain and quantify RAD51 foci in FFPE tumours (Wilsker et al., 2019), we performed the quantification of RAD51 foci in our TMA.

RAD51 nuclear foci, along with β-catenin (as tumour tissue marker), were evaluated through immunofluorescence (IF). Only tumours positive for β-catenin, with at least 2900 nuclei available for the analysis, an intact tissue and specific fluorescent signal were included in the analysis. With these criteria, 37 different PDXs and 5 control tissues (i.e. human EOC samples, murine EOC, murine ovarian tissue) were analysed. More than 2500 images were acquired with confocal microscopy and the analysis was performed with Definiens image analysis software, reporting the percentage of cells per core having ≥5 RAD51 foci per nucleus (**figure 4.13, A**). The results showed that 98% of the samples had less and 2% of RAD51 positive cells (**figure 4.13, B**), even removing the cut-off of 2900 nuclei available for the analysis, the results did not change. In addition, we observed a great variability of RAD51 positive cells in the two cores of the same PDXs.

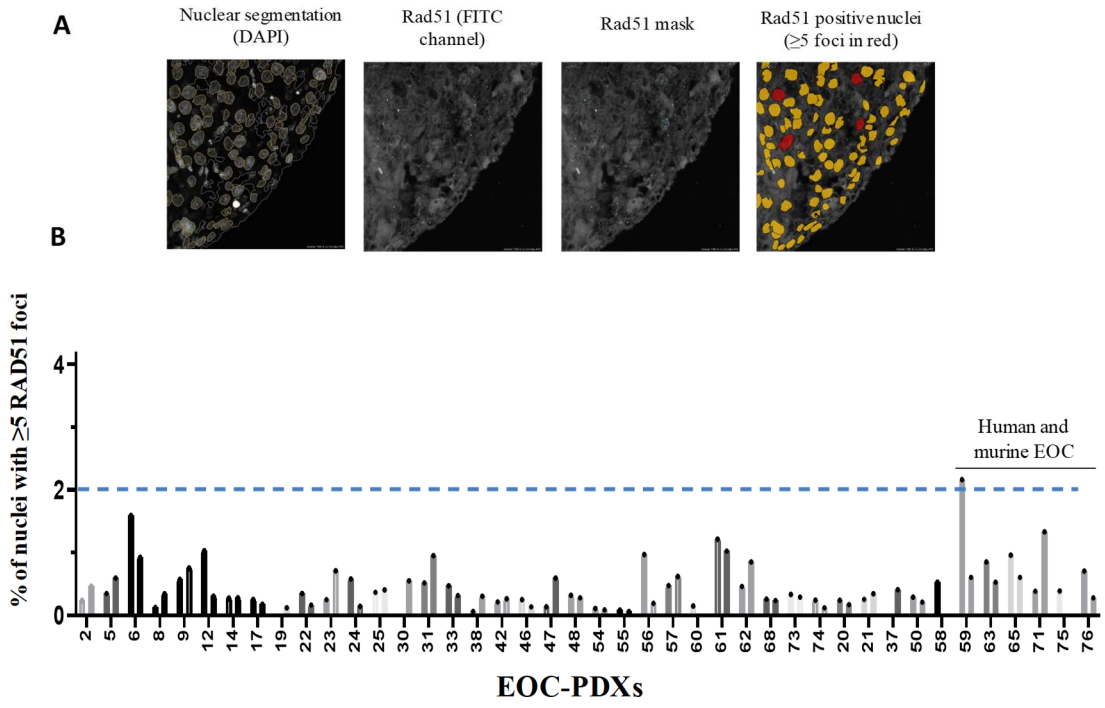

Figure 4.13 RAD51 foci at baseline in EOC-PDXs

A) Representative images of MNHOC18 and the pipeline of software analysis. MNHOC18, core a, expresses 0.6% of RAD51 positive cells (≥5 foci per nucleus). **B)** Baseline expression of RAD51 foci in the tumour cores analysed in the TMA with at least 2900 nuclei per core available for the analysis. Data are expressed as the % of nuclei with ≥5 foci per nucleus per core. For almost all of the PDXs, two different cores were available for the analysis.

Considering the response to DDP and olaparib and dividing the PDXs into the three categories: resistant, sensitive and very sensitive, the % of cells positive for RAD51 foci was not different among the three groups, as shown in **figure 4.14** (**A**, DDP response; **B**, olaparib response). In detail, the group of DDP R PDXs expressed an average of 0.463 ± 0.155 (mean ± SD) (n=3) RAD51-foci positive cells, PDXs DDP S 0.336 ±0.175 (n=12) and PDXs DDP VS 0.380 ±0.110 (n=8) (one way ANOVA, p=0.444) ; while PDXs OLA R had 0.504 ±0.210 (n=5) RAD51-foci positive cells, OLA S 0.41 RAD51-foci positive cells (one sample, MNHOC271) and OLA VS had 0.230 ±0.075 (n=4) (p=0.112).

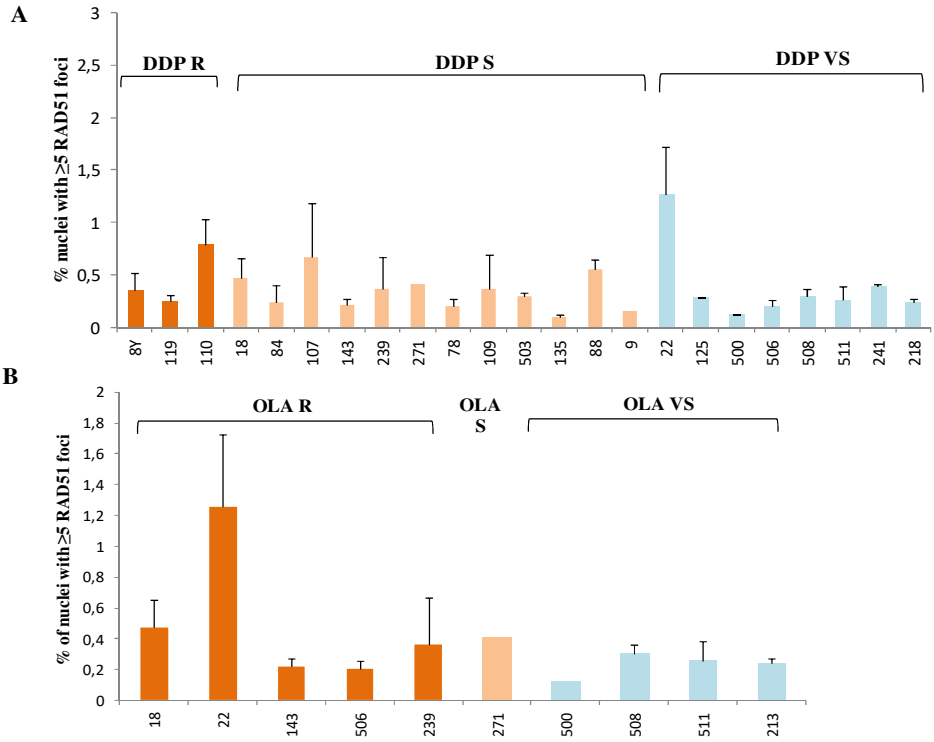

Figure 4.14 RAD51 foci expression at the basal level and response to therapy

A) The upper histogram shows the % of nuclei expressing ≥5 RAD51 foci (mean, SD) in the PDXs analysed, divided into three groups based on their response to DDP therapy: resistant (DDP R), sensitive (DDP S) and very sensitive (DDP VS). **B)** The lower histogram shows the

% of nuclei expressing ≥5 RAD51 foci (mean, SD) in all the PDXs analysed, clustered for their response to olaparib (Ola R, resistant; Ola S, sensitive; Ola VS, very sensitive).

4.3.2 Evaluation of RAD51, BRCA1 and γH2AX nuclear foci in geminin positive FFPE EOC-PDX tumours

Recently, an assay has been set up evaluating RAD51 foci in FFPE tumour samples specifically in cells in S/G2 phase of the cell cycle (where HR takes place), using geminin (GEM) as a marker of cellular proliferation, and it has been reported that low % of RAD51+/GEM+ cells in tumours predict sensitivity to olaparib in a panel of breast cancer PDXs (Castroviejo-Bermejo et al., 2018a; Cruz et al., 2018). Applying this protocol to our EOC-PDXs, we analysed and scored the % of proliferating cells positive for RAD51 foci. We also considered and analysed the expression of BRCA1 foci and γH2AX foci in GEM+ cells, as markers for BRCA1 activity, and DNA DSB and apoptosis, respectively.

As detailed in Materials and Methods, for all the three proteins, we considered positive cells those were ≥5 RAD51 foci per nucleus were observed (**figure 4.15,** representative images). Only geminin positive cells were considered and at least 100 geminin positive cells had to be counted. The cut off of 10% RAD51+/GEM+ cells discriminated between RAD51 positive and negative tumours (Castroviejo-Bermejo et al., 2018a), while the cut off for BRCA1 and for γH2AX were respectively 35% (based on the median of positive cells in the entire xenobank) and 25% (Castroviejo-Bermejo et al., 2018a).

The % of positive cells among the PDXs varied from 0% to 78% for RAD51 (mean 26% ± SD 0.23, median 26%) (**figure 4.15, A**), from 0% to 100% for γH2AX (mean 69% ± SD 0.22, median 74%) (**figure 4.15, B**), and from 0% to 93% for BRCA1 foci (mean 39% ± SD 0.3, median 35%) (**figure 4.15, C**).

Differently from what observed in breast cancer PDXs, in EOC-PDXs several cells showed a pan-γH2AX staining in the nucleus, besides

cells with γH2AX foci, suggesting a higher degree of apoptosis and basal DNA damage compatible with the higher chromosomal instability of this malignancy (Cancer Genome Atlas Research Network, 2011; Tamura et al., 2020).

We observed that 9 out of 10 PDXs *BRCA1* mutated were also negative for BRCA1 foci expression, except MNHOC125 which displayed 51% of positive cells for BRCA1 foci (**figure 4.15, C**).

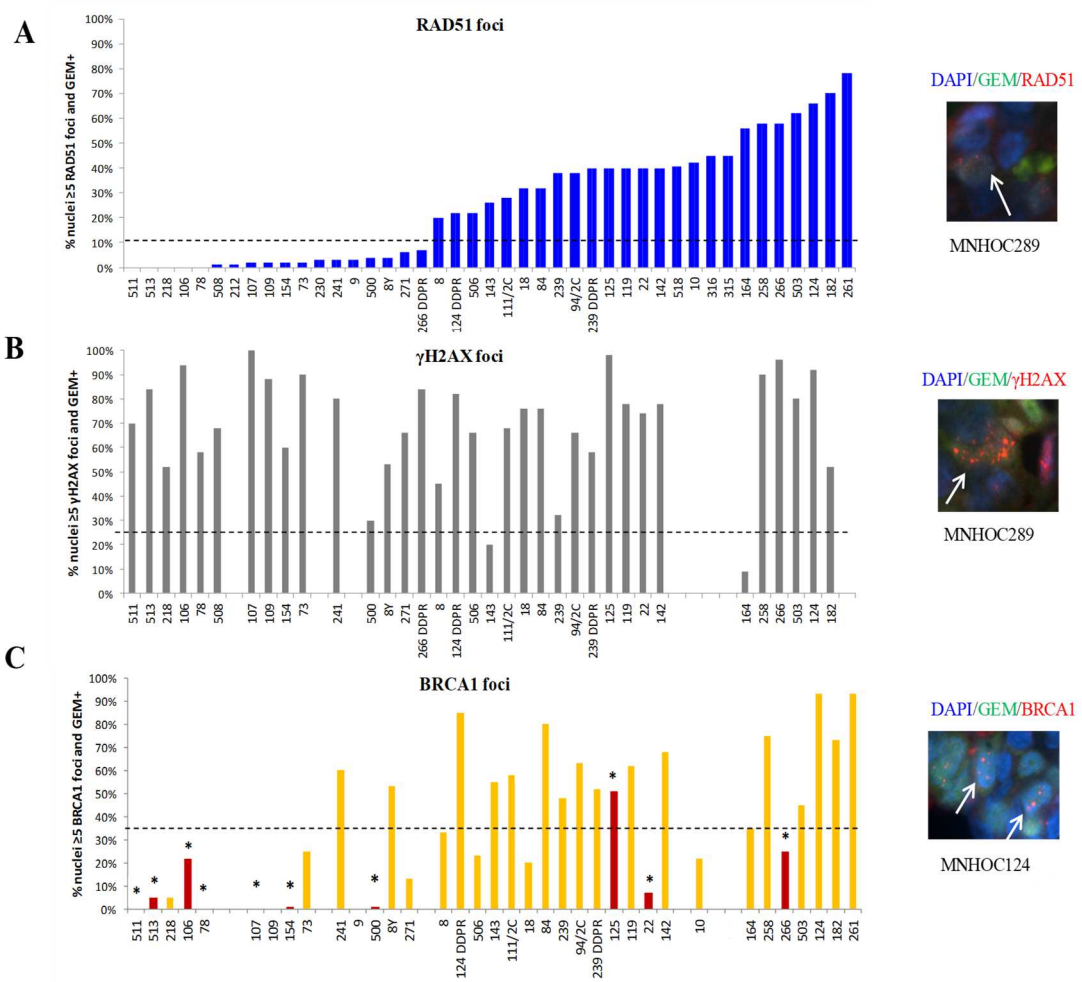

Figure 4.15. Percentage of cells positive for both nuclear foci and geminin in all the PDXs studied

RAD51 foci (**panel A**), γH2AX foci (**panel B**) and BRCA1 foci (**panel C**) have been quantified by IF co-staining with geminin, marker of S/G2 cell cycle phase. Each bar represents the % of cells evaluated in each tumour, having ≥5 foci and positive for geminin. In the histogram **C** relative to BRCA1 foci, ***** red bars indicate *BRCA1* mutated PDXs. Dashed lines are the cut-off that divide tumours in negative (% of positive cells lower than the threshold) or positive. On the right, representative IF images of different PDXs; nuclei are stained in blue (DAPI), geminin in green (FITC) and foci in red (m-Cherry). White arrows indicate positive nuclei.

We explored the correlation between RAD51 and BRCA1 and we observed a positive correlation between RAD51 and BRCA1 foci (Spearman correlation index 0.656, $p<0.0001$, n=35), where tumours with low number of RAD51 positive cells mainly displayed low number of BRCA1 foci positive cells (**figure 4.16**).

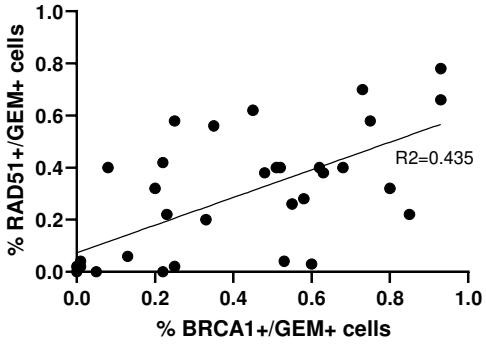

Figure 4.16 Correlation between RAD51 and BRCA1 foci

Distribution of RAD51 and BRCA1 foci in the EOC-PDXs and linear regression.

We studied the correlation between RAD51 and BRCA1 foci expression and the response to therapy. In **figure 4.17** are reported the % of RAD51+/GEM+ cells (**figure 4.17, A**) and the % of BRCA1+/GEM+ cells (**figure 4.17, B**) in the FFPE PDXs divided for their sensitivity to DDP in the three groups of response. We did not find any correlation with DDP response and the % of RAD51+/GEM+ cells (Kruskal-Wallis test p=0.486) (**figure 4.17, C**), not even clustered PDXs in RAD51 positive (positive have >10% of RAD51 positive cells) or negative tumours (Jonckheere-Terpstra test p=0.3164). The correlation between the % of BRCA1+/GEM+ cells vs DDP response was also not significant considering the expression of foci in continuous (Kruskal-Wallis test p=0.1245) (**figure 4.17, D**), while reach the limit of significance considering tumour positive vs negative (positive have >35% of BRCA1 positive cells) vs DDP response (Jonckheere-Terpstra test p=0.040).

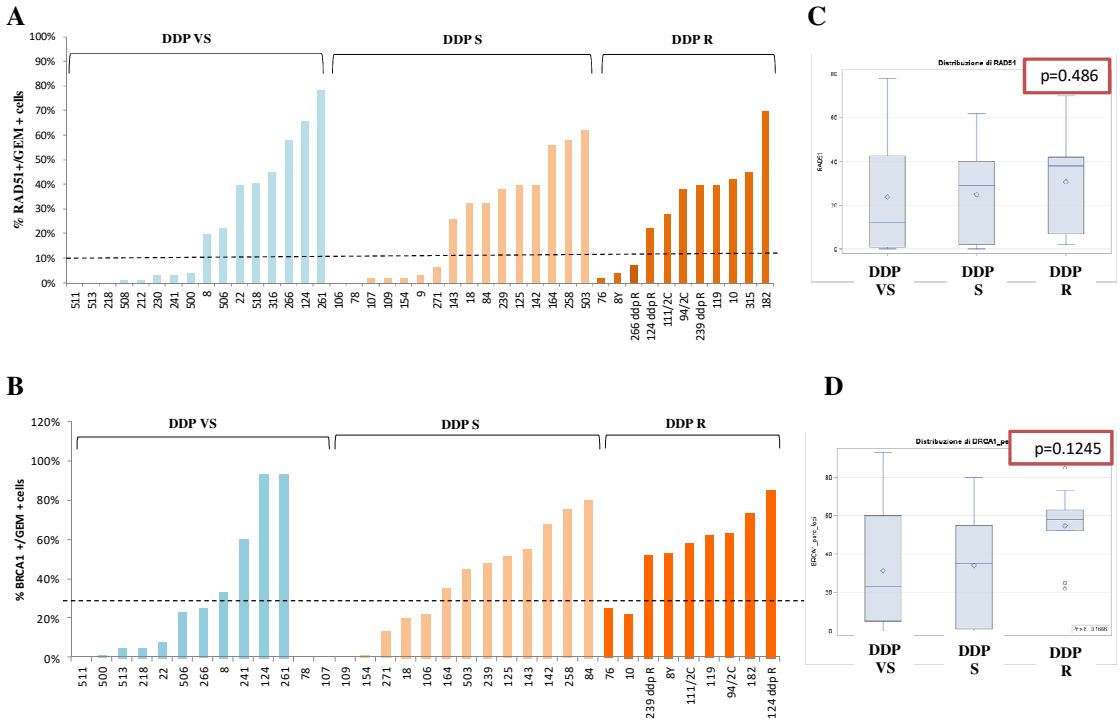

Figure 4.17 RAD51 and BRCA1 foci positive cells and response to DDP treatment in FFPE EOC-PDXs

The histograms show the % of positive cells for RAD51 (**A**) and BRCA1 foci (**B**) among the PDXs studied and clustered for their response to DDP (light blue= very sensitive; pink= sensitive; orange= resistant). The box plots on the right show that no correlation has been found between the distribution of RAD51+/GEM+ and BRCA1+/GEM+ cells and DDP response.

However, the % of RAD51+/GEM+ and BRCA1+/GEM+ cells significantly associated with olaparib response. Indeed, tumours very sensitive to olaparib showed the lowest % of RAD51+/GEM+ positive cells and BRCA1 positive cells than PDXs resistant to olaparib (**figure 4.18, A-B**). In particular, the association between the % of RAD51+/GEM+ positive cells and olaparib response was significant (Kruskal-Wallis test p=0.011) (**figure 4.18, C**), also when considering tumours in RAD51 positive/negative (Jonckheere-Terpstra test: p=0.0047). The association between BRCA1+/GEM+ positive cells and olaparib response was also significant (Kruskal-Wallis test p=0.0144) (**figure 4.18, D**), even dichotomizing tumours in BRCA1 positive and negative vs olaparib response (Jonckheere-Terpstra test: p= 0.022).

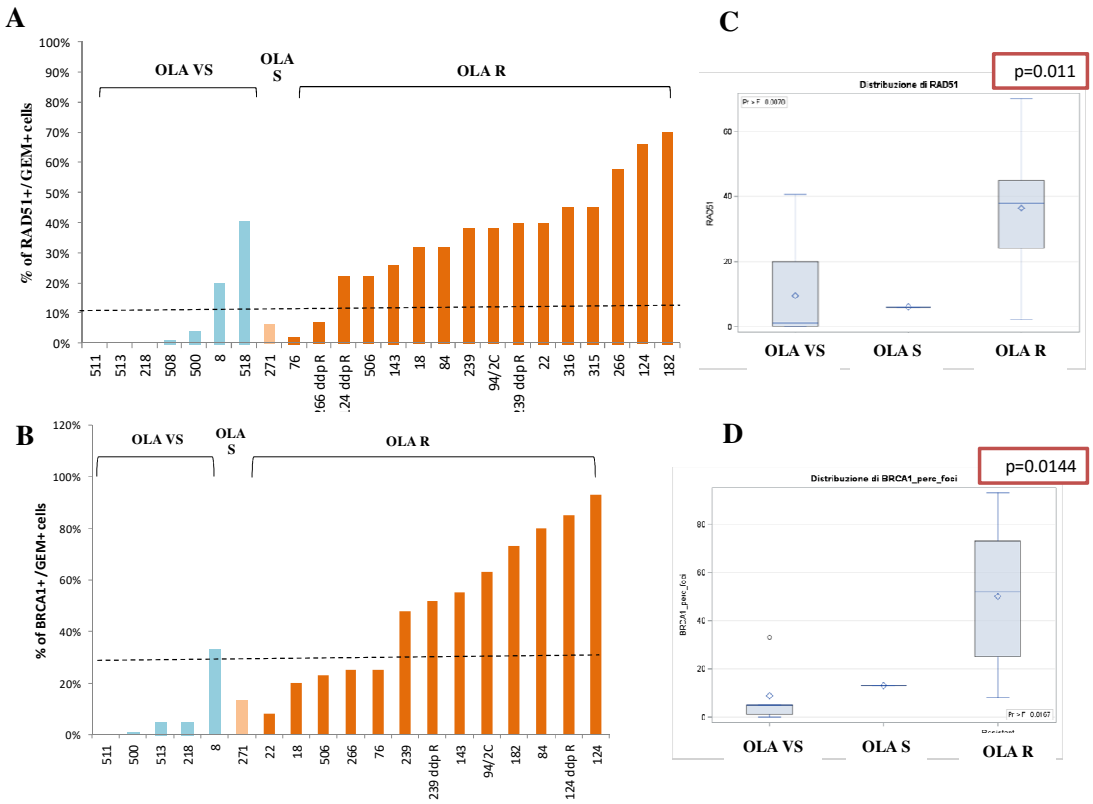

Figure 4.18 RAD51 and BRCA1 foci positive cells and response to olaparib treatment in FFPE EOC-PDXs

The histograms show the % of positive cells for RAD51 (**A**) and BRCA1 foci (**B**) among the PDXs studied and clustered for their response to olaparib (light blue= very sensitive; pink= sensitive; orange= resistant). The box plots show the positive correlation between RAD51 positive cells (**C**) and BRCA1 positive cells (**D**) and olaparib response, where very sensitive tumours to olaparib significantly express lower positive cells.

4.3.3 Discussion III

In this section, we explored the role of RAD51 and BRCA1 foci as potential biomarkers able to predict HRD status and response to therapy in FFPE EOC-PDXs tumours. We studied also the presence of γH2AX foci, markers of DNA DSB and apoptosis, as indicator of the level of endogenous damage. Preclinical evidence support a strong, quantitative correlation between γH2AX foci and DNA DSB, including the ones induced by genetic factors such as DNA repair genes mutations (Rothkamm et al., 2015). However, in our PDXs, we observed a diffuse expression of γH2AX foci in tumour cells and nuclei completely damaged, showing a pan-nuclear γH2AX staining. However, the high expression of γ-H2AX is typical of EOC,

corroborating published data suggesting that EOC is characterized by a high degree of chromosomal instability (Yu et al., 2006).

The induction of RAD51 nuclear foci as biomarker of HR deficiency was firstly described by Graeser *et al.* studying breast cancer biopsies after neoadjuvant chemotherapy (Graeser et al., 2010). The induction of RAD51 foci has been correlated with the ability of cells to repair damage through HR (Ceccaldi et al., 2016; Wilson et al., 2018). However, this method suffers from a poor clinical translatability, because it is not always possible to have fresh tumour specimens or FFPE biopsies at basal and after drug treatment.

We used two different IF-based methods to evaluate RAD51 foci as surrogate marker of HR in FFPE biopsies at the baseline, without the need to induce DNA damage. The first method quantified nuclei expressing at least 5 foci in all the tumour cells of FFPE TMA, while the second method also quantified nuclei expressing at least 5 foci but only in proliferating/geminin positive cells within the FFPE tumours, and it has been described to predict olaparib response in breast cancer PDXs (Castroviejo-Bermejo et al., 2018a; Cruz et al., 2018).

We were able to detect and quantify RAD51 nuclear foci in FFPE ovarian PDXs tumour specimens at baseline (not treated condition). To do this, it is of pivotal importance to use a very sensitive microscope and to be able to establish a discriminating cut off and experimental conditions to have reproducible and reliable results. In addition, we demonstrated that considering only proliferating cells in S/G2 phase of the cell cycle (GEM+) is a determinant factor for RAD51 positivity to be correlated with olaparib response. Indeed, the IF of the total number of tumour cells positive for RAD51 foci was not able to predict olaparib response. This could be due to different reasons: technical and non-technical. The setup of imaging acquisition by confocal microscope and of the software that automatically analyses all the images, is important to avoid loss of information. For instance, the condition to establish whether a cell is positive for RAD51 foci is the presence of at least 5 foci in the nucleus. An automatic acquisition has the advantage of reproducibility, but

when the number of foci is low, it may generate false negative results, as probably happened during the analysis of our TMA, where the number of cells expressing at least 5 foci is very low than in the same PDXs analysed directly by the operator with a good fluorescent microscope during the second test. On the other hand, the analysis made by the operator can suffer from other issues, such as inter-operator reproducibility and the impossibility to analyse rapidly a great number of samples. While, another technical issue could be related with the use of different primary antibodies anti-RAD51 used in the two tests (Castroviejo-Bermejo et al., 2018a; Cruz et al., 2018; Wilsker et al., 2019) that could not have the same specificity. The third factor could be related to the identification of RAD51 foci only in the subgroup of proliferating tumour cells, which is in line with the fact that HR acts during S/G2 phases of the cell cycle. So, the expression of RAD51 foci in proliferating cells should directly depend from HR activation.

The number of RAD51 foci in geminin positive cells determined by IF test significantly correlated with olaparib response of the PDXs studied, but not with DDP, suggesting that platinum anti-tumour activity may be the result of a sum of different factors that need to be clearly identified and taken in consideration together.

4.4 FOCUS ON NER AND BER PATHWAYS AND RESPONSE TO PLATINUM THERAPY

Platinum agents represent the standard therapeutic option for many solid tumours, included EOC. Looking at the mechanism of action of platinum compounds, these drugs mainly determine DNA adducts, which can be repaired or not by the cancer cells determining the anti-tumour activity of the drug. Besides HR, which is the DNA repair pathway most involved in the resolution of ICLs, also NER and BER play crucial roles, particularly involved in the resolution of DDP-induced DNA adducts (Slyskova et al., 2018). For these reasons, we explored the role of some determinant genes and proteins involved in the NER and BER pathways in determining the response to DDP in our EOC-PDXs. The proteins we studied were DNA polymerase β (POLB) and ERCC1. The latter has been investigated both as a single protein and conjugated with XPF, because the formation of ERCC1/XPF complex can be considered a readout of NER activity (Kirschner and Melton, 2010).

4.4.1 Relationship among ERCC1, XPF, POLB and ERCC1/XPF complex expression levels in the xenobank

These experiments have been performed using the TMA available in our laboratory and we analysed 52 EOC-PDXs included in the TMA.

A descriptive analysis is reported in **table 4.11**, which summarises ERCC1 and POLB protein levels expressed as IHC score, the number of ERCC1/XPF complexes per nucleus detected by proximity ligation assay (PLA), and *ERCC1*, *XPF* and *POLB* absolute number of mRNA copies normalized quantified by RT-PCR in all the PDXs and in the subgroup of high grade PDXs.

Table 4.11 Descriptive analysis of ERCC1 and POLB IHC, ERCC1/XPF foci (PLA) and *ERCC1, XPF* and *POLB* mRNA expression levels in the EOC-PDXs studied

		IHC score		ERCC1/XPF foci-number per nucleus (PLA)	Normalized gene expression levels (mRNA copies)		
		ERCC1	DNA pol β	ERCC1/XPF	ERCC1	XPF	POLB
All PDXs (N=52)	Mean (SD)	1.4 (0.9)	5.5 (4.2)	5.0 (2.0)	1.1 (0.8)	0.0025 (0.0016)	0.0448 (0.0336)
	Median (Q1 - Q3)	1.3 (0.8 - 2.0)	6.0 (1.5 - 9.0)	4.9 (3.6 - 6.3)	0.8 (0.6-1.5)	0.0023 (0.0013 - 0.003)	0.036 (0.0258 - 0.0576)
	Min - Max	0.0 - 3.5	0.0 - 12.0	0.9 - 8.8	0.2 - 3.1	0.0005 - 0.009	0.004 - 0.1619
	Missing	3	1	3	16	16	16
High Grade PDXs (N=41)	Mean (SD)	1.2 (1.0)	5.3 (4.0)	5.1 (2.2)	1.2 (0.8)	0.0027 (0.0018)	0.0498 (0.0374)
	Median (Q1 - Q3)	1.0 (0.5 - 2.0)	6.0 (0.8 - 8.5)	5.3 (3.7 - 6.6)	0.8 (0.5 - 1.5)	0.0023 (0.0014 - 0.0033)	0.0430 (0.0272 - 0.0590)
	Min - Max	0.0 - 3.5	0.0 - 12.0	0.9 - 8.8	0.2 - 3.1	0.0009 - 0.0090	0.0040 - 0.1619
	Missing	1	1	2	2	2	2

Legend: n: number of samples; SD: standard deviation; Min-Max: range; missing= number of PDXs were the data is not available.

POLB and ERCC1 protein expression has been determined by IHC using primary antibodies reported in other published studies (Alvisi et al., 2020; Arbogast et al., 2011; Friboulet et al., 2013b). IHC analyses have been done in collaboration with Prof Eugenio Scanziani, an expert pathologist. The calculated IHC score is based on signal intensity and the percentage of positive cells (as detailed in Materials and Methods). The ERCC1 IHC score assigned to the analysed PDXs has been found ranging from 0 (negative signal) to a maximum of 3.5 (median 1.3, mean 1.4 ± SD 0.9) (**figure 4.19, D**), while POLB ranges from 0 to 12 (median 6, mean 5.5 ± SD 4.2) (**figure 4.19, E**). For ERCC1, some samples showed a cytoplasmic staining, much lower than the nuclear, which likely reflects the presence of one of the four isoforms of ERCC1 (the isoform 203), not involved in the NER and reported to be cytoplasmic (Friboulet et al., 2013b). Only the nuclear stain was considered for this analysis (**figure 4.19, A, B, C**).

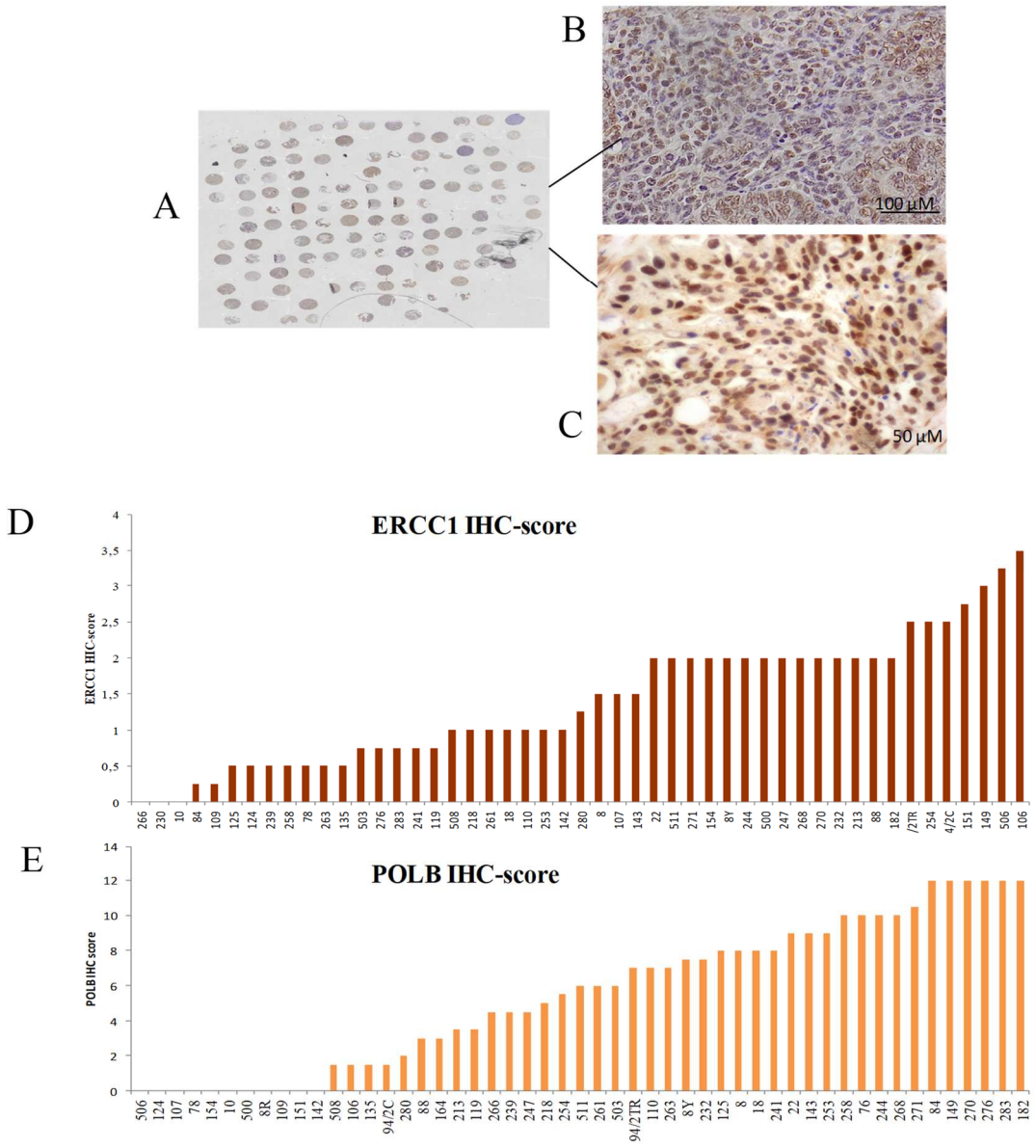

Figure 4.19 ERCC1 and POLB proteins expression on the TMA visible in IHC

A) Representative image of the FFPE-TMA including the 52 EOC-PDXs under study, stained with antibody anti-ERCC1 (Santa Cruz Biotechnology, sc-10785). Magnification 2X. **B)** Representative MNHOC506, ERCC1 positive sample (IHC score= 3.25). ERCC1 dots are present both in the cell nucleus and in the cytoplasm. Magnification 20X, brightfield microscopy. **C)** Representative MNHOC182, POLB positive sample (IHC score=12). Magnification 40X, brightfield microscopy. **D-E)** Distribution of ERCC1 and POLB IHC score assigned to each EOC-PDXs analysed. The IHC score is based on the antibody signal intensity and the % of positive cells evaluated in different areas of the tumour.

ERCC1/XPF complexes have been detected and quantified in 49 PDXs by proximity ligation assay (PLA), a technique used to detect proteins which closely interact and that has been previously reported to be applied to ERCC1/XPF, which are visible as nuclear foci (Friboulet et al., 2013b; Kuo et al., 2018) (**figure 4.20, A-B**). We quantified the average number of ERCC1/XPF foci per nucleus expressed in the PDX tumours, present in duplicate in the TMA, evaluating at least three different areas in each core. ERCC1/XPF complexes were expressed at different levels ranging from 0.9 to 8.8 foci per nucleus (**figure 4.20, C**).

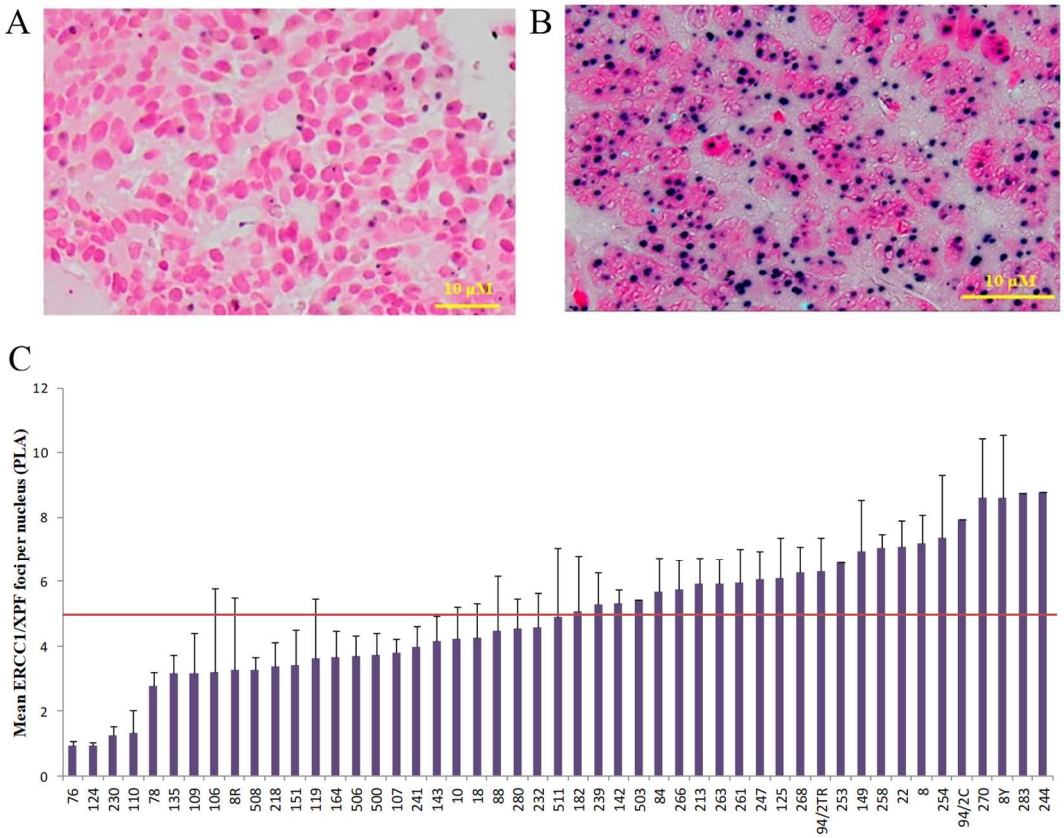

Figure 4.20 ERCC1/XPF protein complexes detected by PLA in IHC in FFPE EOC-PDXs

A) Negative control. PLA was done without primary antibodies. It is possible to observe nuclei counterstained with Nuclear Fast Red (pink nuclei). **B)** The same FFPE EOC-PDX sample after PLA technique. ERCC1/XPF foci are visible as violet dots within epithelial cancer cells nuclei (pink nuclei). Magnification 40X, brightfield microscopy. **C)** Mean of ERCC1/XPF foci per nucleus expressed in the EOC-PDXs under study.

We analysed different correlations between ERCC1 and POLB IHC score, ERCC1/XPF foci number per nucleus and *ERCC1*, *XPF* and *POLB* mRNA number of copies (**table 4.12**). The ERCC1 IHC score positively correlated with the *XPF* mRNA (p>0.0001) and ERCC1/XPF foci number (p=0.05), but interestingly, not with *ERCC1* mRNA.

As regards ERCC1/XPF complex, all the PDXs expressed ERCC1/XPF foci per nucleus (median 4.9; mean 5.0 ± SD 2; range: 3.6-6.3) and no differences among the various EOC subtypes (p=0.392) could be observed. Besides ERCC1 IHC score, ERCC1/XPF foci number significantly correlated POLB IHC score (p<0.0001). *XPF* and *ERCC1* mRNA both correlated with *POLB* mRNA (p=0.02 and p=0.05, respectively).

The same correlations have been then repeated in the high grade EOC-PDXs and in this subgroup were maintained for the correlations between POLB IHC score and ERCC1/XPF foci number (p>0.0001) and ERCC1 IHC score and *XPF* mRNA (p>0.0001).

Table 4.12 Correlations between ERCC1 and POLB IHC score, ERCC1/XPF foci and *ERCC1, XPF* and *POLB* gene expression data in the EOC-PDXs under study

		IHC score		**ERCC1/XPF foci-number per nucleus (PLA)**	**Normalized gene expression levels (mRNA copies)**		
		ERCC1	**POLB**	**ERCC1/XPF**	***ERCC1***	***XPF***	***POLB***
IHC score	**ERCC1**	1 49					
	POLB	0,03 0,85 48	1 51				
ERCC1/XPF foci-number per nucleus (PLA)	**ERCC1/XPF**	0,29 **0,05** 46	0,58 **< 0,0001** 48	1 49			
Normalized gene expression levels (mRNA copies)	***ERCC1***	-0,01 0,96 34	-0,11 0,53 35	0,04 0,82 35	1 36		
	XPF	0,65 **< 0,0001** 34	0,11 0,54 35	0,32 0,06 35	0,15 0,4 36	1 36	
	POLB	0,14 0,43 34	0,17 0,33 35	0,09 0,6 35	0,32 **0,05** 36	0,4 **0,02** 36	1 36

Legend. In each box: first line reports the Spearman correlation index, the second line is the p-value (grey when significant, p≤0.05), the third is the number of observations.

4.4.2 Analysis of ERCC1, XPF, POLB and ERCC1/XPF complex as possible predictive biomarkers for platinum response in EOC-PDX TMA

The pharmacological response to DDP was available for 25 of the PDXs under study, including 10 very sensitive, 12 sensitive and 3 resistant high grade PDXs, in which we focused for this analysis. ERCC1 IHC score did not significantly associate with DDP response (Kruskal-Wallis p=0.847) (**figure 4.21, A**), neither did the POLB IHC score (Kruskal-Wallis p=0.664) (**figure 4.21, B**).

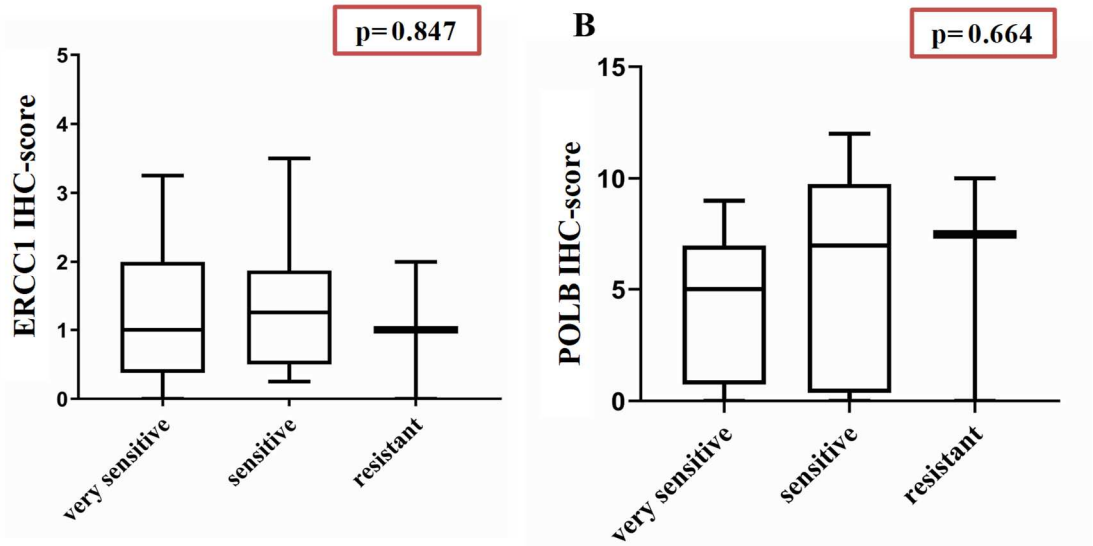

Figure 4.21 ERCC1 IHC score, POLβ IHC score and DDP response in high grade EOC PDXs

A) Distribution of ERCC1 IHC score in PDXs very sensitive (n=10), sensitive (n=12) and resistant (n=2) to DDP. **B)** Distribution of POLB IHC score in PDXs very sensitive (n=9) sensitive (n=12) and resistant (n=3) to DDP. The box plots express data as mean ± standard deviation. p-value (not statistically significant) is reported above the two box plots.

In addition, ERCC1/XPF foci number per nucleus has not been found differently expressed among the three groups of DDP response (Kruskal-Wallis p=0.909) (**figure 4.22, A**), neither when we tried to consider ERCC1/XPF foci number in very sensitive vs sensitive plus resistant tumours (Kruskal-Wallis p=0.710) (**figure 4.22, B**).

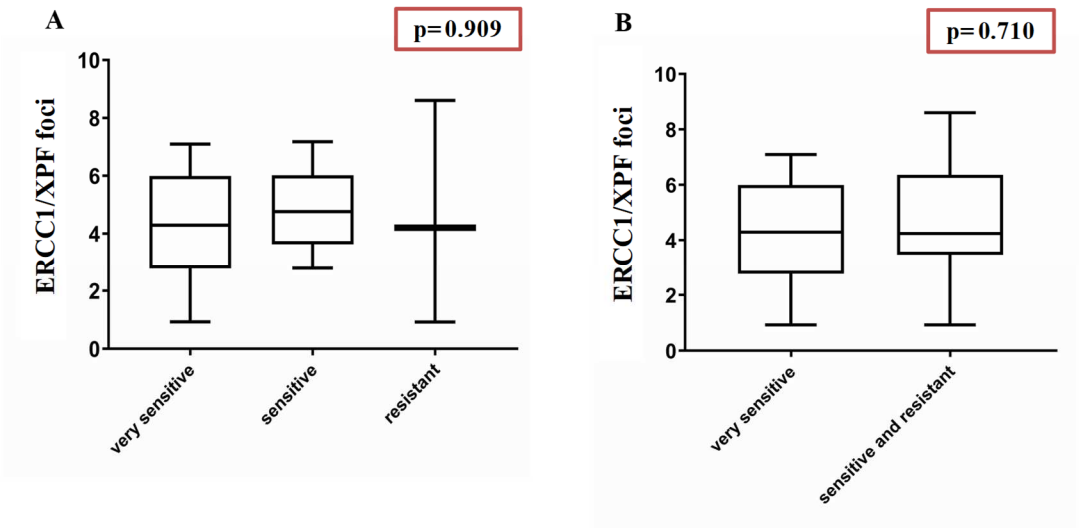

Figure 4.22 ERCC1/XPF foci number per nucleus and response to DDP in high grade EOC-PDXs

A) Distribution of ERCC1/XPF foci per nucleus in the three groups of response to DDP: very sensitive (n=10), sensitive (n=10) and resistant (n=3). **B)** Distribution of ERCC1/XPF foci per nucleus in the PDXs clustered in two groups of response to DDP: very sensitive (n=10) vs sensitive and resistant (n=13). The box plots express data as mean ± standard deviation. p-value (not statistically significant) is reported above the two box plots.

Our preliminary hypothesis that the number of ERCC1/XPF foci expressed at the basal level in the tumour could be a readout of the NER activity and thus, a determinant for platinum response, has not been proved by these data.

To clarify these results, we tested whether DDP treatment could affect the formation of the functional complex ERCC1/XPF in cancer cells using a cell line model. A2780 ovarian cancer cells were treated with cytotoxic doses of DDP and cells were fixed at different time points after drug exposure. We could detect and quantify the ERCC1/XPF nuclear foci in untreated cells (at the baseline) and observed a significant increment of the foci number per nucleus in cells 24 hrs and 48 hrs after DDP treatment at the dose of 10 μM (drug IC_{50} of A2780) (p=0.03 and p=0.02, respectively) (**figure 4.23**). We also treated A2780 cells with the DDP dose of 20 μM, but ERCC1/XPF were not significantly augmented even if a trend towards increment was observed (p=0.12 at 24 hrs; p=0.18 at 48 hrs) (**figure 4.23**). The lack

of significant increment of foci number at the higher dose of DDP could be explained by the enhanced number of apoptotic nuclei observed already 24 hrs after treatment.

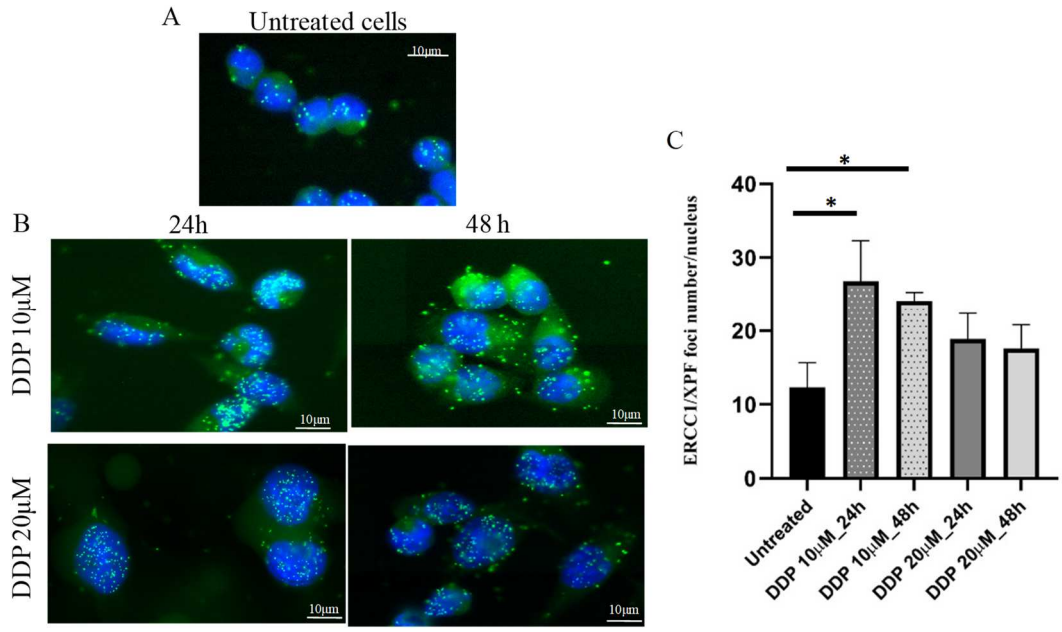

Figure 4.23 Detection by IF and quantification of ERCC1/XPF foci per nucleus in A2780 ovarian cancer cells at the baseline and after DDP treatment

A) IF picture of ERCC1/XPF nuclear foci (green dots, FITC, in blue nuclei, DAPI) expressed in untreated A2780 cells. **B)** Expression of ERCC1/XPF foci at 24 hrs and 48 hrs post-DDP treatment at 10 µM dose (IC_{50}) and 20 µM**. C)** Quantification of ERCC1/XPF number of foci per nucleus in untreated A2780 cells (black bar) and after DDP treatment with 10 µM and 20 µM**,** and fixed at two different time points (different shadows of grey bars). Histograms show the average number of ERCC1/XPF foci and standard deviation of three replicates, where at least 50 nuclei in different tumour areas have been quantified. Unpaired t-test was used to compare untreated vs treated cells at different conditions. * $p \leq 0.05$.

4.4.3 Discussion IV

Besides the 50% of high grade ovarian cancer patients who harbour HR defects associated with the extreme sensitivity to DDP and PARPi therapy, it has been reported that 4-8% of cases have mutations or promoter hypermethylation in NER genes (Konstantinopoulos et al., 2015), which associated with response to platinum treatment and might explain the different therapeutic response to platinum agents and PARPi sometimes observed (Ceccaldi et al.,

2015; Mouw et al., 2015). The role of HR and NER in supporting the antitumour effect of DDP has been proved in preclinical experiments (Damia et al., 1996; Tavecchio et al., 2008) and in the clinic, where patients with NER or HR deficiency were associated with long-lasting response to chemotherapy and increased PFS and OS respect those with NER and HR proficient (Ceccaldi et al., 2015; Mouw et al., 2015). An increase in NER and BER activities in tumours was described to associate with DDP resistance (Bergoglio et al., 2001; Caiola et al., 2015; Damia et al., 1996; Wang et al., 2019). However, the clinical validation of these results was difficult for different reasons: the choice of valid biomarkers able to associate DNA repair activity and DDP response, the choice of the technique used, as well as intra-tumour and intra-patient heterogeneity (Friboulet et al., 2013a; Macerelli et al., 2016).

ERCC1 is one of the most studied NER players as a determinant of therapy response and prognostic marker, but contrasting results have been reported in different solid cancers (Rubatt et al., 2012; Steffensen et al., 2014, 2009) and its role is still to be clarified. DNA POLB is a protein involved in different DNA repair pathways, mainly BER, NER and FA, and high levels of POLB have been associated with resistance to DDP, possibly explained by the capacity to bypass DDP induced intra-strand crosslinks allowing cell replication (Bergoglio et al., 2001), and it was observed in in vitro non-small cell lung cancer cells overexpressing POLB, that the pharmacological inhibition of the protein could revert the DDP resistant phenotype of the cells (Caiola et al., 2015). Based on this evidence, we studied the role of ERCC1 and POLB as potential predictive biomarkers for DDP response in a platform of EOC-PDXs, considering their gene expression levels, as well as protein levels and the functional complex ERCC1/XPF by PLA. Surprisingly, we did not find significant correlation between ERCC1 protein and its mRNA levels, but only between ERCC1 and XPF mRNA ($p<0.0001$). A possible explanation for the lack of correlation between *ERCC1* mRNA and protein expression may be explained by the fact that the ERCC1 mRNA evaluated included all the four isoforms, while in IHC we only considered the nuclear

staining, where the isoform 203 is not localized. This could also explain the lack of association between ERCC1 protein and DDP response of high grade PDXs that has been observed, as well as the contrasting results present in literature, and pinpoints the necessity to find alternative approaches to validate biomarkers (Olaussen and Postel-Vinay, 2016). With this aim, we studied the expression by PLA of ERCC1/XPF functional complex, a limiting step for NER activity during the resolution of DDP adducts (Friboulet et al., 2013a, 2013b). We detected the complex expressed at the baseline in all the PDXs analysed, but the value of ERCC1/XPF foci per nucleus did not associate with DDP response in the high grade EOC-PDXs. As we observed in vitro that ERCC1/XPF complex amount significantly increased after DDP treatment, we may hypothesize that the up-regulation of ERCC1/XPF could be a better predictor for NER activity, rather than its basal expression, similar to RAD51 foci induction upon DSBs for HR, which indicates HR proficiency (Graeser et al., 2010; Waks et al., 2020). In fact, ERCC1 higher levels have been also observed in HGSOC biopsies after neoadjuvant chemotherapy compared with primary untreated tumours, suggesting an up-regulation of ERCC1 after treatment, even if the number of observations was small (Scurry et al., 2018). Another possible reason is that DDP response to therapy is the results of a sum of mechanisms, included NER, which differently contribute to determine the antitumor activity of treatment, and maybe a combinatorial approach might be more indicative.

Regarding POLB, we did not observe a significant correlation between mRNA, protein and DDP response, but we found a significant correlation between POLB protein and ERCC1/XPF foci per nucleus ($p<0.0001$). BER and NER pathways are both involved in the repair of DDP-induced DNA lesions, so this correlation may suggest that these two pathways might cooperate in order to better resolve the DNA damage.

5. GENERAL DISCUSSION

Despite recent improvements in surgical and pharmacological therapy achieved in the treatment of EOC, this malignancy remains the deadliest gynaecological tumour in the Western countries (Bray et al., 2018). Vague symptoms in the early phases of the disease and the lack of effective screening methods allow 75% of cases to be diagnosed at an advanced/metastatic stage (FIGO III/IV), when the chances of surviving are lower (Reid et al., 2017). The third major clinical impediment causing the low survival of EOC patients is the high incidence of relapsing tumours resistant to platinum-based chemotherapy, which occurs in two-thirds of patients (Bowtell et al., 2015; Lheureux et al., 2019b). Platinum-based chemotherapy is the cornerstone of systemic therapy in the treatment of EOC, which is generally, initially very sensitive to platinum agents, i.e. carboplatin and cisplatin (Galluzzi et al., 2012; Lheureux et al., 2019b). These compounds are alkylating agents that exert their cytotoxic effect mainly forming DNA-platinum adducts, such as inter and intra-strand crosslinks between purine bases (Chaney et al., 2005; Dasari and Tchounwou, 2014). DDP-induced DNA damage is repaired by several DNA repair pathways, involving different proteins and cooperating with each other to repair the lesions: NER, BER, TLS, MMR, FA and HR. The great susceptibility to platinum therapy observed in high grade ovarian cancers is in part due to the presence of defects in proteins involved in these pathways, which enhance the anti-tumour activity of DNA damaging agents and led us to hypothesize that, at the contrary, increased DNA repair activity could be associated with resistance to therapy. Half of HGSOC harbours alterations in HR (i.e. *BRCA1/BRCA2* germline or somatic mutations, *BRCA1* hypermethylation, mutations in other HR genes), which impairs HR function, a condition named *BRCAness* phenotype (Konstantinopoulos et al., 2015; Lord and Ashworth, 2016; Turner et al., 2004).

The introduction of PARPi revolutionized the therapeutic strategies of EOC and potentially of all the solid tumours with a *BRCAness* phenotype. In fact, PARPi were found in synthetic lethality with *BRCA1/BRCA2* mutated cancer cells (Bryant et al., 2005; Farmer et al., 2005).

Numerous preclinical and clinical studies have then established that PARPi therapeutic potential exceeds germline *BRCA1/BRCA2* mutated tumours, and may potentially involve all the HRD tumours (Mirza et al., 2016a; Pilié et al., 2019; Pujade-Lauraine et al., 2017). Unfortunately, with the widespread use of PARPi, cases of acquired resistance have been reported in the clinic. Resistance to platinum and PARPi therapy, in a contest lacking valid therapeutic alternatives, is a critical and unmet clinical issue. There is the need to both elucidate the determinants of drug resistance and identify predictive biomarkers of response. With this background, the aim of my thesis was to study the role of different DNA repair pathways, genes and proteins in response to DDP and olaparib and to find potential biomarkers and functional assays able to predict the response to therapy in in vivo EOC models.

The use of suitable and robust preclinical models is of pivotal importance in translational cancer research and in the Department of Oncology, where I undertook this PhD, a collection of more than sixty ovarian cancer PDXs is available. These in vivo models well recapitulate the biological features of the original patient tumour, are stable after several in vivo passages, and in aggregate, represent the complex clinical tumour heterogeneity and molecular diversity of EOC. In fact, all the histotypes of EOC are represented (80% are high grade serous and/or endometrioid tumours, as in the clinic) and pharmacologically the PDX xenobank shows a wide range of response to olaparib and DDP (Ricci et al., 2014). The pharmacological characterization of the PDXs to DDP and olaparib, allowed their classification into three categories based on their response to therapy: very sensitive, sensitive and resistant based on well-established parameters that fulfilled the response to chemotherapy observed in the clinic, and that could also be applied to orthotopic models. The pharmacological characterization has permitted the use of this PDX platform to study the mechanisms of drug resistance and to test biomarkers to possibly predict response to therapy.

I contributed to the characterization of the PDX platform for the mutational profile, observing that all the HGOC models carry *TP53* mutations, as described in the literature (Ahmed et al., 2010; Cancer Genome Atlas Research Network, 2011; Cole et al., 2016). Then, I focused on DNA repair genes, which are the object of my thesis, evaluating the mutational status of HR, FA and DDR genes. I observed that 11 out of 33 PDXs had *BRCA1* mutations, and 2 PDXs were mutated in *BRCA2*, while non-pathogenic or unknown mutations were observed in the other HR genes (i.e. *PALB2*, FA genes, *ATM, ATR*). In order to explore the HRD condition in our PDXs, not only the mutational profiles of HR and FA genes were characterized, but also epigenetic alterations that frequently occur in HGOC, such as the hypermethylation promoter status of *BRCA1* and *FANCF* (D'Andrea, 2003; Konstantinopoulos et al., 2015), as well of other NER and MMR genes. Different CpG islands-enriched promoter regions have been evaluated in the genes of interest with two techniques, pyrosequencing with pre-custom primers and MS-PCR with primers designed *ad hoc*, already reported in literature (Sabatino et al., 2010; Ter Brugge et al., 2016). We also verified that the expression levels of the genes analysed were effectively reduced in the PDXs found hypermethylated, confirming *BRCA1* hypermethylation status in 8% of the PDXs evaluated with MS-PCR, while few PDXs have been found hypermethylated in *FANCF*, *ERCC1* and *MLH1* promoter regions with reduction of gene expression. No correlation between *XPA* hypermethylation status and gene expression was found, suggesting that probably the regions considered were not those involved in the regulation of gene transcription.

In order to deepen the study of DNA repair and response to therapy, I evaluated in the xenobank the expression of a wide panel of DNA repair genes involved in different DNA repair pathways. Genes were variably expressed in all the PDXs and no difference was observed among the different histotypes, even if this analysis suffered from the fact that some histotypes (mucinous, clear cells and low grade serous) were under-represented. Analysing the correlations between the single genes, it was observed that genes belonging

to the same pathway correlated with each other (i.e. FA genes). Interestingly, CDK12, a cyclin-dependent kinase described being mutated in 3% of HGOC (Konstantinopoulos et al., 2015) and a transcriptional regulator of several DNA repair genes, correlated with the expression of *PALB2*, *53BP1* and *XPF* ($p<0.05$). These data were also corroborated in two different TCGA datasets, supporting a role of CDK12 as transcriptional regulator of DNA repair gene expression.

CDK12 also emerged as one of the four genes found significantly associated with DDP response in the HGOC PDXs, and in particular, DDP resistant PDXs expressed higher levels of *CDK12, XPF* and *PALB2* ($p<0.05$) compared with sensitive and very sensitive PDXs. Conversely, *USP28* was more highly expressed in the very sensitive than in resistant HGOC PDXs ($p<0.05$). The biological significance of these correlations needs to be proven. However, we could corroborate the prognostic values of *CDK12* in the TCGA dataset, where patients with a residual tumour < 2cm, but higher levels of *CDK12* mRNA, had a worse prognosis compared with those expressing low *CDK12* levels.

Regarding olaparib, none of the 21 genes whose expression levels were established in the xenobank significantly correlated with olaparib response, even in the subgroup of HGOC PDXs. Currently, the presence of germline *BRCA1/BRCA2* mutations is one of the biomarkers used in the clinical trials to predict response to PARPi therapy. However, because PARPi sensitivity mostly relies on HR defects, as well as for platinum agents, platinum sensitivity itself has been considered a surrogate marker for HRD and another clinical biomarker of PARPi response (Franzese et al., 2019; Konstantinopoulos et al., 2020; Rafii et al., 2017). Looking at the PDX platform response to DDP and olaparib, we have 26 PDXs characterized for both drugs, and among them all the olaparib responsive tumours are also sensitive to DDP (n=8) and all the DDP resistant tumours do not respond to olaparib (n=8). However, not all the DDP very responsive tumours are also responsive to olaparib (n=5). These data showed a low concordance between cisplatin and olaparib response (Cohen'*s* k= 0.33), suggesting that the response to DDP is a poor predictive factor for

olaparib response in our PDXs. Moreover, PDXs with pathogenic mutations in *BRCA1/BRCA2* are very sensitive/sensitive to DDP, but two out of 6 are resistant to olaparib, suggesting that the mechanisms underlying DDP response do not always overlap with mechanisms that determine olaparib response, as already described (Ceccaldi et al., 2015). Preclinical and clinical evidence suggested that PARPi could be effective in a wider range of tumours than those *BRCA* mutated, including *BRCAness* tumours, whose identification requires methods evaluating multiple molecular events. For this reason, we tested 10 PDXs with a genomic-based test, the HRDetect assay, in collaboration with Dr Nik Zainal. Her group set up an algorithm, based on five distinct HR-associated mutational signatures captured by whole genome sequencing, and elaborated a score indicative of HR deficiency (>0.7) or HR proficient status (<0.7) (Chopra et al., 2020; Davies et al., 2017). 5 PDXs had an HR score >0.9, and two of them harboured *BRCA1* mutations, another showed *BRCA1* promoter hypermethylation, while currently, we do not know the cause for which the other two PDXs were classified as HRD.

We wanted to verify if the HRD status could predict response to both DDP and olaparib response. To this aim, we considered HRD PDXs the ones with a HR score >0.7 and/or *BRCA* mutated. Based on these criteria, a significant association between HRD status and DDP response ($p<0.05$) and olaparib response ($p<0.05$) could be observed corroborating the evidence on the role of the HR status as a determinant of the response to these drugs (Konstantinopoulos et al., 2015).

Relapsing patients with acquired resistance to therapy require functional assays to establish the effective DNA repair activity of the tumour to possibly predict response to therapy and ultimately, to direct patients to therapeutic alternatives. In fact, the available tests for the determination of HDR status (i.e. Myriad and Foundation Medicine's assays) evaluate "genomic scars" based on genomic footprints, that have been accumulating during the historical evolution of the tumour and do not catch the determinants of response in "real-time", such as revertant mutations that restore HR proficiency; this likely explains their low

predictive capacity, proven in clinical trials where they were used (Coleman et al., 2017; Mirza et al., 2016b; Pellegrino et al., 2019).

Starting from these considerations, we explored two possible DNA repair functional readouts: the evaluation of RAD51 foci as a surrogate marker of HR activity and ERCC1/XPF complex in IHC as surrogate markers for NER. Their quantification in our PDX platform was then correlated with both DDP and olaparib sensitivity.

The induction of RAD51 foci after DNA damage has been generally considered a readout of a competent HR repair and indeed these tests have been correlated with HR activity and response to neoadjuvant and PARPi therapy in breast and ovarian fresh tumours or primary cultures or FFPE biopsies, collected close to therapy administration (Graeser et al., 2010; Mukhopadhyay et al., 2010; Shah et al., 2014). However, recently, a method able to quantify RAD51 foci and to predict the response to olaparib has been published, which does not require the induction of DNA damage (Castroviejo-Bermejo et al., 2018a; Cruz et al., 2018). In fact, in this method the number of RAD51 foci was evaluated in tumour cells geminin positive, indicating cells in the S/G2 phase of the cell cycle, where the HR repair takes place. We tried two different approaches. We quantified the basal expression of RAD51 foci (minimum 5 foci per nucleus) in all the β-catenin positive cancer cells of PDX tissues included in a TMA. The imaging acquisition was performed with a confocal microscope and the analysis by dedicated software. In this condition, neither of the evaluable PDXs expressed more than 2% of cells positive to RAD51 foci and there was also a great variability between the duplicates available for each PDX in the TMA. We did not find any significant correlation between RAD51 foci quantified with this method and response to therapy. In parallel, we applied on FFPE PDXs tumour specimens the method described by Cruz *et al*., where RAD51 foci were quantified only in proliferative/geminin positive cancer cells and the evaluation was performed by the operator with a fluorescent microscope. Geminin is a pan nuclear protein expressed during the S/G2 phase of the cell cycle, so, we evaluated the RAD51 foci only in the subgroup of proliferating cells, where the HR is effectively active.

γH2AX nuclear foci have been quantified to verify the presence of endogenous damage, and our PDXs showed high levels of γH2AX foci, in accordance with the genomic instability, which is a hallmark of EOC (Prat et al., 2018; Vanderstichele et al., 2017). Besides RAD51 foci, also BRCA1 foci have been quantified following the same criteria, as an additional marker of HR status. We quantified the % of positive cells in the PDXs analysed (those with ≥5 foci per nucleus and geminin +), and then we divided tumours in RAD51 or BRCA1 positive or negative, based on the % of positive cells quantified in the tumour (i.e. RAD51 positive tumours had ≥10% of RAD51+/GEM+ cells; BRCA1 positive tumours had ≥35% of BRCA1+/GEM+ cells). We then correlated the expression of positive cells with DDP and olaparib response (analysis in continuous), as well as the correlation between tumours classified as RAD51 and BRCA1 positive/negative and response to therapy (analysis per trend). We found that low positivity for RAD51 and BRCA1 foci predicted response to olaparib, but not to DDP, both in continuous and in trend analyses. These data confirmed the importance of evaluating RAD51 foci in the subgroup of proliferating cells with sensitive techniques. In addition, our results demonstrated that this test does not predict the response to DDP. The fact that the % of RAD51+/GEM+ cells was not able to predict DDP response, suggests that the analysis of foci alone is not sufficient to capture the complexity of DDP-induced DNA damages, whose repair does not involve only HR, but many other pathways (Enoiu et al., 2012; Rocha et al., 2018; Slyskova et al., 2018; Wang et al., 2011).

Considering the importance of BER and NER pathways in the repair of DNA damage caused by platinum agents (Galluzzi et al., 2014; Martin et al., 2008; Slyskova et al., 2018), we tried to elucidate the role of POLB, ERCC1 and XPF in response to DDP. These proteins are among the most studied effectors of these two DNA repair pathways, even if their predictive role in DDP response has been reported to be contrasting (Alvisi et al., 2020; Steffensen et al., 2014, 2009). We evaluated these three factors as mRNA and protein expression levels and, for the first time, we analysed the expression of the active ERCC1/XPF complex, a heterodimer acting as endonuclease, whose activity is a critical step in the NER pathway, in

relation with DDP response. Again, the complex was quantified at baseline, not treated conditions, in all the PDXs available in the TMA. Its quantification was performed using the proximity ligation assay (PLA), a technique able to identify the presence of two proteins forming a complex. The levels of ERCC1, XPF and POLB (both mRNA and protein) were not associated with DDP response; in addition, neither the ERCC1/XPF complex expression could predict the sensitivity to platinum treatment. These latter negative data could be partially explained by the fact that an induction of ERCC1/XPF complex was found after treatment of cells in vitro with cytotoxic doses of DDP suggesting that ERCC1/XPF induction could be a better biomarker of DDP response.

All the experiments described in this thesis were done using all the PDXs samples we have available in our xenobank, which currently represents one of the largest collections of EOC-PDXs described in literature. However, we are consciousness that our statistical analyses suffered from the lack of preliminary tests aim to determine the sample size necessary to yield a certain power for a test, given a predetermined Type I error rate α. This aspect will necessary be taken in consideration in the future experiments aimed to validate the results obtained until now, in order to ameliorate the experimental design and to enforce the power of the study.

At present, there is an urgent need for biomarkers and functional assays able to predict the response to therapy of EOC patients and our xenobank represents a valid tool to perform preclinical experiments aimed to elucidate the role of potential biomarkers and to test new predictive assays. For the first time, we evaluated the predictive potential of RAD51 foci expressed in untreated FFPE EOC-PDXs, in relation with olaparib response, confirming previous data reported in breast cancer models (Castroviejo-Bermejo et al., 2018b). These results need to be corroborated using FFPE biopsies of patient tumours and could be easily evaluated in the clinical setting by using standardized techniques. Unfortunately, it was not able to predict DDP response.

It will be certainly interesting in the near future to set up other functional assays to be used as predictive biomarkers as these better represent the DNA repair capacity of the tumour cells. Recently, the fiber assay, that evaluates the replication fork stability, has been associated with carboplatin response in HGSOC organoids (Hill et al., 2018). However, this assay also suffers from the fact that live cells are needed and it cannot be applied in FFPE tumour samples.

DNA repair is an important determinant of tumour response to chemotherapy, but it is not the sole determinant. In addition, ovarian carcinomas present unique and highly variable combinations of copy number aberrations and different cancer clones and it could be that a single IHC analysis could be insufficient to capture the complexity of tumour response to therapy. More specific methodologies, such as single-cell multi-omics and parallel deconvolution of the mutational and epigenetic traits of individual cancer cells (Marusyk et al., 2020) and the setting up of liquid biospies through out the entire patients clinical history (Asante et al., 2020) could help in identifying chemo-resistant subpopulations.

6. REFERENCES

Abbotts, R., Wilson, D.M., 2017. Coordination of DNA single strand break repair. Free Radic. Biol. Med. 107, 228–244. https://doi.org/10.1016/j.freeradbiomed.2016.11.039

Abdel-Fatah, T.M.A., Arora, A., Moseley, P., Coveney, C., Perry, C., Johnson, K., Kent, C., Ball, G., Chan, S., Madhusudan, S., 2014. ATM, ATR and DNA-PKcs expressions correlate to adverse clinical outcomes in epithelial ovarian cancers. BBA Clin. 2, 10–17. https://doi.org/10.1016/j.bbacli.2014.08.001

Achkar, I.W., Abdulrahman, N., Al-Sulaiti, H., Joseph, J.M., Uddin, S., Mraiche, F., 2018. Cisplatin based therapy: the role of the mitogen activated protein kinase signaling pathway. J. Transl. Med. 16, 96. https://doi.org/10.1186/s12967-018-1471-1

Aggarwal, I.M., Lim, Y.H., Lim, T.Y.K., 2016. The fallopian tube as the origin of non-uterine pelvic high-grade serous carcinoma. Obstet. Gynaecol. 18, 143–152. https://doi.org/10.1111/tog.12258

Aggarwal, S.K., 1993. A histochemical approach to the mechanism of action of cisplatin and its analogues. J. Histochem. Cytochem. Off. J. Histochem. Soc. 41, 1053–1073. https://doi.org/10.1177/41.7.8515048

Aghajanian, C., Blank, S.V., Goff, B.A., Judson, P.L., Teneriello, M.G., Husain, A., Sovak, M.A., Yi, J., Nycum, L.R., 2012. OCEANS: a randomized, double-blind, placebo-controlled phase III trial of chemotherapy with or without bevacizumab in patients with platinum-sensitive recurrent epithelial ovarian, primary peritoneal, or fallopian tube cancer. J. Clin. Oncol. Off. J. Am. Soc. Clin. Oncol. 30, 2039–2045. https://doi.org/10.1200/JCO.2012.42.0505

Ahmed, A.A., Etemadmoghadam, D., Temple, J., Lynch, A.G., Riad, M., Sharma, R., Stewart, C., Fereday, S., Caldas, C., Defazio, A., Bowtell, D., Brenton, J.D., 2010. Driver mutations in TP53 are ubiquitous in high grade serous carcinoma of the ovary. J. Pathol. 221, 49–56. https://doi.org/10.1002/path.2696

Akbari, M.R., Zhang, S., Cragun, D., Lee, J.-H., Coppola, D., McLaughlin, J., Risch, H.A., Rosen, B., Shaw, P., Sellers, T.A., Schildkraut, J., Narod, S.A., Pal, T., 2017. Correlation between germline mutations in MMR genes and microsatellite instability in ovarian cancer specimens. Fam. Cancer 16, 351–355. https://doi.org/10.1007/s10689-017-9973-1

Albertella, M.R., Green, C.M., Lehmann, A.R., O'Connor, M.J., 2005. A role for polymerase eta in the cellular tolerance to cisplatin-induced damage. Cancer Res. 65, 9799–9806. https://doi.org/10.1158/0008-5472.CAN-05-1095

Alberts, D.S., Liu, P.Y., Hannigan, E.V., O'Toole, R., Williams, S.D., Young, J.A., Franklin, E.W., Clarke-Pearson, D.L., Malviya, V.K., DuBeshter, B., 1996. Intraperitoneal cisplatin plus intravenous cyclophosphamide versus intravenous cisplatin plus intravenous cyclophosphamide for stage III ovarian cancer. N. Engl. J. Med. 335, 1950–1955. https://doi.org/10.1056/NEJM199612263352603

Alexandrov, L.B., Nik-Zainal, S., Wedge, D.C., Campbell, P.J., Stratton, M.R., 2013. Deciphering signatures of mutational processes operative in human cancer. Cell Rep. 3, 246–259. https://doi.org/10.1016/j.celrep.2012.12.008

Alkema, N.G., Wisman, G.B.A., van der Zee, A.G.J., van Vugt, M.A.T.M., de Jong, S., 2016. Studying platinum sensitivity and resistance in high-grade serous ovarian cancer: Different models for different questions. Drug Resist. Updat. Rev. Comment. Antimicrob. Anticancer Chemother. 24, 55–69. https://doi.org/10.1016/j.drup.2015.11.005

Alvisi, M.F., Ganzinelli, M., Linardou, H., Caiola, E., Lo Russo, G., Cecere, F.L., Bettini, A.C., Psyrri, A., Milella, M., Rulli, E., Fabbri, A., De Maglie, M., Romanelli, P., Murray, S., Ndembe, G., Broggini, M., Garassino, M.C., Marabese, M., 2020. Predicting the Role of DNA Polymerase β Alone or with KRAS Mutations in Advanced NSCLC Patients Receiving Platinum-Based Chemotherapy. J. Clin. Med. 9. https://doi.org/10.3390/jcm9082438

Amable, L., 2016. Cisplatin resistance and opportunities for precision medicine. Pharmacol. Res. 106, 27–36. https://doi.org/10.1016/j.phrs.2016.01.001

Anantha, R.W., Simhadri, S., Foo, T.K., Miao, S., Liu, J., Shen, Z., Ganesan, S., Xia, B., 2017. Functional and mutational landscapes of BRCA1 for homology-directed repair and therapy resistance. eLife 6. https://doi.org/10.7554/eLife.21350

Anglesio, M.S., Kommoss, S., Tolcher, M.C., Clarke, B., Galletta, L., Porter, H., Damaraju, S., Fereday, S., Winterhoff, B.J., Kalloger, S.E., Senz, J., Yang, W., Steed, H., Allo, G., Ferguson, S., Shaw, P., Teoman, A., Garcia, J.J., Schoolmeester, J.K., Bakkum-Gamez, J., Tinker, A.V., Bowtell, D.D., Huntsman, D.G., Gilks, C.B., McAlpine, J.N., 2013. Molecular characterization of mucinous ovarian tumours supports a stratified treatment approach with HER2 targeting in 19% of carcinomas. J. Pathol. 229, 111–120. https://doi.org/10.1002/path.4088

Antoniou, A., Pharoah, P.D.P., Narod, S., Risch, H.A., Eyfjord, J.E., Hopper, J.L., Loman, N., Olsson, H., Johannsson, O., Borg, A., Pasini, B., Radice, P., Manoukian, S., Eccles, D.M., Tang, N., Olah, E., Anton-Culver, H., Warner, E., Lubinski, J., Gronwald, J., Gorski, B., Tulinius, H., Thorlacius, S., Eerola, H., Nevanlinna, H., Syrjäkoski, K., Kallioniemi, O.-P., Thompson, D., Evans, C., Peto, J., Lalloo, F., Evans, D.G., Easton, D.F., 2003. Average risks of breast and ovarian cancer associated with BRCA1 or BRCA2 mutations detected in case Series unselected for family history: a combined analysis of 22 studies. Am. J. Hum. Genet. 72, 1117–1130. https://doi.org/10.1086/375033

Aparicio, S., Hidalgo, M., Kung, A.L., 2015. Examining the utility of patient-derived xenograft mouse models. Nat. Rev. Cancer 15, 311–316. https://doi.org/10.1038/nrc3944

Arbogast, S., Behnke, S., Opitz, I., Stahel, R.A., Seifert, B., Weder, W., Moch, H., Soltermann, A., 2011. Automated ERCC1 immunohistochemistry in non-small cell lung cancer: comparison of anti-ERCC1 antibodies 8F1, D-10, and FL-297. Appl. Immunohistochem. Mol. Morphol. AIMM 19, 99–105. https://doi.org/10.1097/PAI.0b013e3181f1feeb

Armbruster, S., Coleman, R.L., Rauh-Hain, J.A., 2018. Management and Treatment of Recurrent Epithelial Ovarian Cancer. Hematol. Oncol. Clin. North Am. 32, 965–982. https://doi.org/10.1016/j.hoc.2018.07.005

Armstrong, D.K., Bundy, B., Wenzel, L., Huang, H.Q., Baergen, R., Lele, S., Copeland, L.J., Walker, J.L., Burger, R.A., Gynecologic Oncology Group, 2006. Intraperitoneal

cisplatin and paclitaxel in ovarian cancer. N. Engl. J. Med. 354, 34–43. https://doi.org/10.1056/NEJMoa052985

Arnesano, F., Scintilla, S., Natile, G., 2007. Interaction between platinum complexes and a methionine motif found in copper transport proteins. Angew. Chem. Int. Ed Engl. 46, 9062–9064. https://doi.org/10.1002/anie.200703271

Asante, D.-B., Calapre, L., Ziman, M., Meniawy, T.M., Gray, E.S., 2020. Liquid biopsy in ovarian cancer using circulating tumor DNA and cells: Ready for prime time? Cancer Lett. 468, 59–71. https://doi.org/10.1016/j.canlet.2019.10.014

Ashworth, A., Lord, C.J., 2018. Synthetic lethal therapies for cancer: what's next after PARP inhibitors? Nat. Rev. Clin. Oncol. 15, 564–576. https://doi.org/10.1038/s41571-018-0055-6

Assis, J., Pereira, D., Medeiros, R., 2013. Ovarian cancer and DNA repair: DNA ligase IV as a potential key. World J. Clin. Oncol. 4, 14–24. https://doi.org/10.5306/wjco.v4.i1.14

Audebert, M., Salles, B., Calsou, P., 2004. Involvement of poly(ADP-ribose) polymerase-1 and XRCC1/DNA ligase III in an alternative route for DNA double-strand breaks rejoining. J. Biol. Chem. 279, 55117–55126. https://doi.org/10.1074/jbc.M404524200

Backes, F.J., Cohn, D.E., 2011. Lynch syndrome. Clin. Obstet. Gynecol. 54, 199–214. https://doi.org/10.1097/GRF.0b013e3182185a41

Bader, A.G., Kang, S., Zhao, L., Vogt, P.K., 2005. Oncogenic PI3K deregulates transcription and translation. Nat. Rev. Cancer 5, 921–929. https://doi.org/10.1038/nrc1753

Bahamon, B.N., Gao, F., Danaee, H., 2016. Development and Validation of an ERCC1 Immunohistochemistry Assay for Solid Tumors. Arch. Pathol. Lab. Med. 140, 1397–1403. https://doi.org/10.5858/arpa.2016-0006-OA

Barber, L.J., Sandhu, S., Chen, L., Campbell, J., Kozarewa, I., Fenwick, K., Assiotis, I., Rodrigues, D.N., Reis Filho, J.S., Moreno, V., Mateo, J., Molife, L.R., De Bono, J., Kaye, S., Lord, C.J., Ashworth, A., 2013. Secondary mutations in BRCA2 associated with clinical resistance to a PARP inhibitor. J. Pathol. 229, 422–429. https://doi.org/10.1002/path.4140

Bassett, E., Vaisman, A., Havener, J.M., Masutani, C., Hanaoka, F., Chaney, S.G., 2003. Efficiency of extension of mismatched primer termini across from cisplatin and oxaliplatin adducts by human DNA polymerases beta and eta in vitro. Biochemistry 42, 14197–14206. https://doi.org/10.1021/bi035359p

Bassett, E., Vaisman, A., Tropea, K.A., McCall, C.M., Masutani, C., Hanaoka, F., Chaney, S.G., 2002. Frameshifts and deletions during in vitro translesion synthesis past Pt-DNA adducts by DNA polymerases beta and eta. DNA Repair 1, 1003–1016. https://doi.org/10.1016/s1568-7864(02)00150-7

Bast, R.C., Hennessy, B., Mills, G.B., 2009. The biology of ovarian cancer: new opportunities for translation. Nat. Rev. Cancer 9, 415–428. https://doi.org/10.1038/nrc2644

Beard, W.A., Wilson, S.H., 2019. DNA polymerase beta and other gap-filling enzymes in mammalian base excision repair. The Enzymes 45, 1–26. https://doi.org/10.1016/bs.enz.2019.08.002

Becker, J.R., Cuella-Martin, R., Barazas, M., Liu, R., Oliveira, C., Oliver, A.W., Bilham, K., Holt, A.B., Blackford, A.N., Heierhorst, J., Jonkers, J., Rottenberg, S., Chapman, J.R., 2018. The ASCIZ-DYNLL1 axis promotes 53BP1-dependent non-homologous end joining and PARP inhibitor sensitivity. Nat. Commun. 9, 5406. https://doi.org/10.1038/s41467-018-07855-x

Bergoglio, V., Canitrot, Y., Hogarth, L., Minto, L., Howell, S.B., Cazaux, C., Hoffmann, J.S., 2001. Enhanced expression and activity of DNA polymerase beta in human ovarian tumor cells: impact on sensitivity towards antitumor agents. Oncogene 20, 6181–6187. https://doi.org/10.1038/sj.onc.1204743

Bhattacharyya, A., Ear, U.S., Koller, B.H., Weichselbaum, R.R., Bishop, D.K., 2000. The breast cancer susceptibility gene BRCA1 is required for subnuclear assembly of Rad51 and survival following treatment with the DNA cross-linking agent cisplatin. J. Biol. Chem. 275, 23899–23903. https://doi.org/10.1074/jbc.C000276200

Bignami, M., Casorelli, I., Karran, P., 2003. Mismatch repair and response to DNA-damaging antitumour therapies. Eur. J. Cancer Oxf. Engl. 1990 39, 2142–2149. https://doi.org/10.1016/s0959-8049(03)00569-0

Binju, M., Amaya-Padilla, M.A., Wan, G., Gunosewoyo, H., Suryo Rahmanto, Y., Yu, Y., 2019. Therapeutic Inducers of Apoptosis in Ovarian Cancer. Cancers 11. https://doi.org/10.3390/cancers11111786

Birkbak, N.J., Wang, Z.C., Kim, J.-Y., Eklund, A.C., Li, Q., Tian, R., Bowman-Colin, C., Li, Y., Greene-Colozzi, A., Iglehart, J.D., Tung, N., Ryan, P.D., Garber, J.E., Silver, D.P., Szallasi, Z., Richardson, A.L., 2012. Telomeric allelic imbalance indicates defective DNA repair and sensitivity to DNA-damaging agents. Cancer Discov. 2, 366–375. https://doi.org/10.1158/2159-8290.CD-11-0206

Bischof, K., Knappskog, S., Hjelle, S.M., Stefansson, I., Woie, K., Salvesen, H.B., Gjertsen, B.T., Bjorge, L., 2019. Influence of p53 Isoform Expression on Survival in High-Grade Serous Ovarian Cancers. Sci. Rep. 9, 5244. https://doi.org/10.1038/s41598-019-41706-z

Bizzaro, F., Falcetta, F., D'Agostini, E., Decio, A., Minoli, L., Erba, E., Alessandro Peccatori, F., Scanziani, E., Colombo, N., Zucchetti, M., Bani, M.R., Ubezio, P., Giavazzi, R., 2018. Tumor progression and metastatic dissemination in ovarian cancer after dose-dense or conventional paclitaxel and cisplatin plus bevacizumab. Int. J. Cancer 143, 2187–2199. https://doi.org/10.1002/ijc.31596

Bizzaro, Francesca, 2021. Preclinical Models to study the Biology and Therapy of Ovarian Cancer. https://doi.org/10.21954/OU.RO.0000E718

Black, J.O., 2016. Xeroderma Pigmentosum. Head Neck Pathol. 10, 139–144. https://doi.org/10.1007/s12105-016-0707-8

Bookman, M.A., Brady, M.F., McGuire, W.P., Harper, P.G., Alberts, D.S., Friedlander, M., Colombo, N., Fowler, J.M., Argenta, P.A., De Geest, K., Mutch, D.G., Burger, R.A., Swart, A.M., Trimble, E.L., Accario-Winslow, C., Roth, L.M., 2009. Evaluation of

new platinum-based treatment regimens in advanced-stage ovarian cancer: a Phase III Trial of the Gynecologic Cancer Intergroup. J. Clin. Oncol. Off. J. Am. Soc. Clin. Oncol. 27, 1419–1425. https://doi.org/10.1200/JCO.2008.19.1684

Bouwman, P., Aly, A., Escandell, J.M., Pieterse, M., Bartkova, J., van der Gulden, H., Hiddingh, S., Thanasoula, M., Kulkarni, A., Yang, Q., Haffty, B.G., Tommiska, J., Blomqvist, C., Drapkin, R., Adams, D.J., Nevanlinna, H., Bartek, J., Tarsounas, M., Ganesan, S., Jonkers, J., 2010. 53BP1 loss rescues BRCA1 deficiency and is associated with triple-negative and BRCA-mutated breast cancers. Nat. Struct. Mol. Biol. 17, 688–695. https://doi.org/10.1038/nsmb.1831

Bouwman, P., van der Gulden, H., van der Heijden, I., Drost, R., Klijn, C.N., Prasetyanti, P., Pieterse, M., Wientjens, E., Seibler, J., Hogervorst, F.B.L., Jonkers, J., 2013. A high-throughput functional complementation assay for classification of BRCA1 missense variants. Cancer Discov. 3, 1142–1155. https://doi.org/10.1158/2159-8290.CD-13-0094

Bowtell, D.D., Böhm, S., Ahmed, A.A., Aspuria, P.-J., Bast, R.C., Beral, V., Berek, J.S., Birrer, M.J., Blagden, S., Bookman, M.A., Brenton, J.D., Chiappinelli, K.B., Martins, F.C., Coukos, G., Drapkin, R., Edmondson, R., Fotopoulou, C., Gabra, H., Galon, J., Gourley, C., Heong, V., Huntsman, D.G., Iwanicki, M., Karlan, B.Y., Kaye, A., Lengyel, E., Levine, D.A., Lu, K.H., McNeish, I.A., Menon, U., Narod, S.A., Nelson, B.H., Nephew, K.P., Pharoah, P., Powell, D.J., Ramos, P., Romero, I.L., Scott, C.L., Sood, A.K., Stronach, E.A., Balkwill, F.R., 2015. Rethinking ovarian cancer II: reducing mortality from high-grade serous ovarian cancer. Nat. Rev. Cancer 15, 668–679. https://doi.org/10.1038/nrc4019

Brabletz, T., Kalluri, R., Nieto, M.A., Weinberg, R.A., 2018. EMT in cancer. Nat. Rev. Cancer 18, 128–134. https://doi.org/10.1038/nrc.2017.118

Bray, F., Ferlay, J., Soerjomataram, I., Siegel, R.L., Torre, L.A., Jemal, A., 2018. Global cancer statistics 2018: GLOBOCAN estimates of incidence and mortality worldwide for 36 cancers in 185 countries. CA. Cancer J. Clin. 68, 394–424. https://doi.org/10.3322/caac.21492

Broustas, C.G., Lieberman, H.B., 2014. DNA damage response genes and the development of cancer metastasis. Radiat. Res. 181, 111–130. https://doi.org/10.1667/RR13515.1

Brozovic, A., 2017. The relationship between platinum drug resistance and epithelial-mesenchymal transition. Arch. Toxicol. 91, 605–619. https://doi.org/10.1007/s00204-016-1912-7

Bryant, H.E., Schultz, N., Thomas, H.D., Parker, K.M., Flower, D., Lopez, E., Kyle, S., Meuth, M., Curtin, N.J., Helleday, T., 2005. Specific killing of BRCA2-deficient tumours with inhibitors of poly(ADP-ribose) polymerase. Nature 434, 913–917. https://doi.org/10.1038/nature03443

Bunting, S.F., Callén, E., Wong, N., Chen, H.-T., Polato, F., Gunn, A., Bothmer, A., Feldhahn, N., Fernandez-Capetillo, O., Cao, L., Xu, X., Deng, C.-X., Finkel, T., Nussenzweig, M., Stark, J.M., Nussenzweig, A., 2010. 53BP1 inhibits homologous recombination in Brca1-deficient cells by blocking resection of DNA breaks. Cell 141, 243–254. https://doi.org/10.1016/j.cell.2010.03.012

Burotto, M., Chiou, V.L., Lee, J.-M., Kohn, E.C., 2014. The MAPK pathway across different malignancies: a new perspective. Cancer 120, 3446–3456. https://doi.org/10.1002/cncr.28864

Byun, S.-S., Kim, S.W., Choi, H., Lee, C., Lee, E., 2005. Augmentation of cisplatin sensitivity in cisplatin-resistant human bladder cancer cells by modulating glutathione concentrations and glutathione-related enzyme activities. BJU Int. 95, 1086–1090. https://doi.org/10.1111/j.1464-410X.2005.05472.x

Cadoni, E., Valletta, E., Caddeo, G., Isaia, F., Cabiddu, M.G., Vascellari, S., Pivetta, T., 2017. Competitive reactions among glutathione, cisplatin and copper-phenanthroline complexes. J. Inorg. Biochem. 173, 126–133. https://doi.org/10.1016/j.jinorgbio.2017.05.004

Cai, M.-Y., Dunn, C.E., Chen, W., Kochupurakkal, B.S., Nguyen, H., Moreau, L.A., Shapiro, G.I., Parmar, K., Kozono, D., D'Andrea, A.D., 2020. Cooperation of the ATM and Fanconi Anemia/BRCA Pathways in Double-Strand Break End Resection. Cell Rep. 30, 2402-2415.e5. https://doi.org/10.1016/j.celrep.2020.01.052

Caiola, E., Broggini, M., Marabese, M., 2014. Genetic markers for prediction of treatment outcomes in ovarian cancer. Pharmacogenomics J. 14, 401–410. https://doi.org/10.1038/tpj.2014.32

Caiola, E., Porcu, L., Fruscio, R., Giuliani, D., Milani, R., Torri, V., Broggini, M., Marabese, M., 2013. DNA-damage response gene polymorphisms and therapeutic outcomes in ovarian cancer. Pharmacogenomics J. 13, 159–172. https://doi.org/10.1038/tpj.2011.50

Caiola, E., Salles, D., Frapolli, R., Lupi, M., Rotella, G., Ronchi, A., Garassino, M.C., Mattschas, N., Colavecchio, S., Broggini, M., Wiesmüller, L., Marabese, M., 2015. Base excision repair-mediated resistance to cisplatin in KRAS(G12C) mutant NSCLC cells. Oncotarget 6, 30072–30087. https://doi.org/10.18632/oncotarget.5019

Cameron, E.E., Bachman, K.E., Myöhänen, S., Herman, J.G., Baylin, S.B., 1999. Synergy of demethylation and histone deacetylase inhibition in the re-expression of genes silenced in cancer. Nat. Genet. 21, 103–107. https://doi.org/10.1038/5047

Cancer Genome Atlas Research Network, 2011. Integrated genomic analyses of ovarian carcinoma. Nature 474, 609–615. https://doi.org/10.1038/nature10166

Cannistra, S.A., 2004. Cancer of the ovary. N. Engl. J. Med. 351, 2519–2529. https://doi.org/10.1056/NEJMra041842

Cao, L., Xu, X., Bunting, S.F., Liu, J., Wang, R.-H., Cao, L.L., Wu, J.J., Peng, T.-N., Chen, J., Nussenzweig, A., Deng, C.-X., Finkel, T., 2009. A selective requirement for 53BP1 in the biological response to genomic instability induced by Brca1 deficiency. Mol. Cell 35, 534–541. https://doi.org/10.1016/j.molcel.2009.06.037

Carrassa, L., Damia, G., 2017. DNA damage response inhibitors: Mechanisms and potential applications in cancer therapy. Cancer Treat. Rev. 60, 139–151. https://doi.org/10.1016/j.ctrv.2017.08.013

Castroviejo-Bermejo, M., Cruz, C., Llop-Guevara, A., Gutiérrez-Enríquez, S., Ducy, M., Ibrahim, Y.H., Gris-Oliver, A., Pellegrino, B., Bruna, A., Guzmán, M., Rodríguez,

O., Grueso, J., Bonache, S., Moles-Fernández, A., Villacampa, G., Viaplana, C., Gómez, P., Vidal, M., Peg, V., Serres-Créixams, X., Dellaire, G., Simard, J., Nuciforo, P., Rubio, I.T., Dienstmann, R., Barrett, J.C., Caldas, C., Baselga, J., Saura, C., Cortés, J., Déas, O., Jonkers, J., Masson, J.-Y., Cairo, S., Judde, J.-G., O'Connor, M.J., Díez, O., Balmaña, J., Serra, V., 2018a. A RAD51 assay feasible in routine tumor samples calls PARP inhibitor response beyond BRCA mutation. EMBO Mol. Med. 10. https://doi.org/10.15252/emmm.201809172

Castroviejo-Bermejo, M., Cruz, C., Llop-Guevara, A., Gutiérrez-Enríquez, S., Ducy, M., Ibrahim, Y.H., Gris-Oliver, A., Pellegrino, B., Bruna, A., Guzmán, M., Rodríguez, O., Grueso, J., Bonache, S., Moles-Fernández, A., Villacampa, G., Viaplana, C., Gómez, P., Vidal, M., Peg, V., Serres-Créixams, X., Dellaire, G., Simard, J., Nuciforo, P., Rubio, I.T., Dienstmann, R., Barrett, J.C., Caldas, C., Baselga, J., Saura, C., Cortés, J., Déas, O., Jonkers, J., Masson, J.-Y., Cairo, S., Judde, J.-G., O'Connor, M.J., Díez, O., Balmaña, J., Serra, V., 2018b. A RAD51 assay feasible in routine tumor samples calls PARP inhibitor response beyond BRCA mutation. EMBO Mol. Med. 10. https://doi.org/10.15252/emmm.201809172

Ceccaldi, R., Liu, J.C., Amunugama, R., Hajdu, I., Primack, B., Petalcorin, M.I.R., O'Connor, K.W., Konstantinopoulos, P.A., Elledge, S.J., Boulton, S.J., Yusufzai, T., D'Andrea, A.D., 2015. Homologous-recombination-deficient tumours are dependent on Polθ-mediated repair. Nature 518, 258–262. https://doi.org/10.1038/nature14184

Ceccaldi, R., Rondinelli, B., D'Andrea, A.D., 2016. Repair Pathway Choices and Consequences at the Double-Strand Break. Trends Cell Biol. 26, 52–64. https://doi.org/10.1016/j.tcb.2015.07.009

Chaney, S.G., Campbell, S.L., Bassett, E., Wu, Y., 2005. Recognition and processing of cisplatin- and oxaliplatin-DNA adducts. Crit. Rev. Oncol. Hematol. 53, 3–11. https://doi.org/10.1016/j.critrevonc.2004.08.008

Chang, H.H.Y., Pannunzio, N.R., Adachi, N., Lieber, M.R., 2017. Non-homologous DNA end joining and alternative pathways to double-strand break repair. Nat. Rev. Mol. Cell Biol. 18, 495–506. https://doi.org/10.1038/nrm.2017.48

Chang, S.-J., Bristow, R.E., 2012. Evolution of surgical treatment paradigms for advanced-stage ovarian cancer: redefining "optimal" residual disease. Gynecol. Oncol. 125, 483–492. https://doi.org/10.1016/j.ygyno.2012.02.024

Chapman, J.R., Barral, P., Vannier, J.-B., Borel, V., Steger, M., Tomas-Loba, A., Sartori, A.A., Adams, I.R., Batista, F.D., Boulton, S.J., 2013. RIF1 is essential for 53BP1-dependent nonhomologous end joining and suppression of DNA double-strand break resection. Mol. Cell 49, 858–871. https://doi.org/10.1016/j.molcel.2013.01.002

Chen, H.-Y., Shao, C.-J., Chen, F.-R., Kwan, A.-L., Chen, Z.-P., 2010. Role of ERCC1 promoter hypermethylation in drug resistance to cisplatin in human gliomas. Int. J. Cancer 126, 1944–1954. https://doi.org/10.1002/ijc.24772

Chen, S.-H., Chang, J.-Y., 2019. New Insights into Mechanisms of Cisplatin Resistance: From Tumor Cell to Microenvironment. Int. J. Mol. Sci. 20. https://doi.org/10.3390/ijms20174136

Chilà, R., Guffanti, F., Damia, G., 2016. Role and therapeutic potential of CDK12 in human cancers. Cancer Treat. Rev. 50, 83–88. https://doi.org/10.1016/j.ctrv.2016.09.003

Chiva, L.M., Gonzalez-Martin, A., 2015. A critical appraisal of hyperthermic intraperitoneal chemotherapy (HIPEC) in the treatment of advanced and recurrent ovarian cancer. Gynecol. Oncol. 136, 130–135. https://doi.org/10.1016/j.ygyno.2014.11.072

Cho, K.R., Shih, I.-M., 2009. Ovarian cancer. Annu. Rev. Pathol. 4, 287–313. https://doi.org/10.1146/annurev.pathol.4.110807.092246

Choi, Y., Lee, S., Kim, K., Kim, S.-H., Chung, Y.-J., Lee, C., 2018. Studying cancer immunotherapy using patient-derived xenografts (PDXs) in humanized mice. Exp. Mol. Med. 50, 99. https://doi.org/10.1038/s12276-018-0115-0

Chopra, N., Tovey, H., Pearson, A., Cutts, R., Toms, C., Proszek, P., Hubank, M., Dowsett, M., Dodson, A., Daley, F., Kriplani, D., Gevensleben, H., Davies, H.R., Degasperi, A., Roylance, R., Chan, S., Tutt, A., Skene, A., Evans, A., Bliss, J.M., Nik-Zainal, S., Turner, N.C., 2020. Homologous recombination DNA repair deficiency and PARP inhibition activity in primary triple negative breast cancer. Nat. Commun. 11, 2662. https://doi.org/10.1038/s41467-020-16142-7

Christie, E.L., Fereday, S., Doig, K., Pattnaik, S., Dawson, S.-J., Bowtell, D.D.L., 2017. Reversion of BRCA1/2 Germline Mutations Detected in Circulating Tumor DNA From Patients With High-Grade Serous Ovarian Cancer. J. Clin. Oncol. Off. J. Am. Soc. Clin. Oncol. 35, 1274–1280. https://doi.org/10.1200/JCO.2016.70.4627

Cimino, G.D., Pan, C., Henderson, P.T., 2013. Personalized medicine for targeted and platinum-based chemotherapy of lung and bladder cancer. Bioanalysis 5, 369–391. https://doi.org/10.4155/bio.12.325

Clamp, A.R., James, E.C., McNeish, I.A., Dean, A., Kim, J.-W., O'Donnell, D.M., Hook, J., Coyle, C., Blagden, S., Brenton, J.D., Naik, R., Perren, T., Sundar, S., Cook, A.D., Gopalakrishnan, G.S., Gabra, H., Lord, R., Dark, G., Earl, H.M., Hall, M., Banerjee, S., Glasspool, R.M., Jones, R., Williams, S., Swart, A.M., Stenning, S., Parmar, M., Kaplan, R., Ledermann, J.A., 2019. Weekly dose-dense chemotherapy in first-line epithelial ovarian, fallopian tube, or primary peritoneal carcinoma treatment (ICON8): primary progression free survival analysis results from a GCIG phase 3 randomised controlled trial. Lancet Lond. Engl. 394, 2084–2095. https://doi.org/10.1016/S0140-6736(19)32259-7

Clark, C.C., Weitzel, J.N., O'Connor, T.R., 2012. Enhancement of synthetic lethality via combinations of ABT-888, a PARP inhibitor, and carboplatin in vitro and in vivo using BRCA1 and BRCA2 isogenic models. Mol. Cancer Ther. 11, 1948–1958. https://doi.org/10.1158/1535-7163.MCT-11-0597

Clarke-Pearson, D.L., 2009. Clinical practice. Screening for ovarian cancer. N. Engl. J. Med. 361, 170–177. https://doi.org/10.1056/NEJMcp0901926

Cleary, J.M., Aguirre, A.J., Shapiro, G.I., D'Andrea, A.D., 2020. Biomarker-Guided Development of DNA Repair Inhibitors. Mol. Cell 78, 1070–1085. https://doi.org/10.1016/j.molcel.2020.04.035

Clements, K.E., Thakar, T., Nicolae, C.M., Liang, X., Wang, H.-G., Moldovan, G.-L., 2018. Loss of E2F7 confers resistance to poly-ADP-ribose polymerase (PARP) inhibitors in BRCA2-deficient cells. Nucleic Acids Res. 46, 8898–8907. https://doi.org/10.1093/nar/gky657

ClinVar, https://www.ncbi.nlm.nih.gov/clinvar/ [WWW Document], n.d.

Cole, A.J., Dwight, T., Gill, A.J., Dickson, K.-A., Zhu, Y., Clarkson, A., Gard, G.B., Maidens, J., Valmadre, S., Clifton-Bligh, R., Marsh, D.J., 2016. Assessing mutant p53 in primary high-grade serous ovarian cancer using immunohistochemistry and massively parallel sequencing. Sci. Rep. 6, 26191. https://doi.org/10.1038/srep26191

Coleman, R.L., Oza, A.M., Lorusso, D., Aghajanian, C., Oaknin, A., Dean, A., Colombo, N., Weberpals, J.I., Clamp, A., Scambia, G., Leary, A., Holloway, R.W., Gancedo, M.A., Fong, P.C., Goh, J.C., O'Malley, D.M., Armstrong, D.K., Garcia-Donas, J., Swisher, E.M., Floquet, A., Konecny, G.E., McNeish, I.A., Scott, C.L., Cameron, T., Maloney, L., Isaacson, J., Goble, S., Grace, C., Harding, T.C., Raponi, M., Sun, J., Lin, K.K., Giordano, H., Ledermann, J.A., ARIEL3 investigators, 2017. Rucaparib maintenance treatment for recurrent ovarian carcinoma after response to platinum therapy (ARIEL3): a randomised, double-blind, placebo-controlled, phase 3 trial. Lancet Lond. Engl. 390, 1949–1961. https://doi.org/10.1016/S0140-6736(17)32440-6

Collaborative Group on Epidemiological Studies of Ovarian Cancer, Beral, V., Doll, R., Hermon, C., Peto, R., Reeves, G., 2008. Ovarian cancer and oral contraceptives: collaborative reanalysis of data from 45 epidemiological studies including 23,257 women with ovarian cancer and 87,303 controls. Lancet Lond. Engl. 371, 303–314. https://doi.org/10.1016/S0140-6736(08)60167-1

Colombo, P.-E., Fabbro, M., Theillet, C., Bibeau, F., Rouanet, P., Ray-Coquard, I., 2014. Sensitivity and resistance to treatment in the primary management of epithelial ovarian cancer. Crit. Rev. Oncol. Hematol. 89, 207–216. https://doi.org/10.1016/j.critrevonc.2013.08.017

Cook, S.A., Tinker, A.V., 2019. PARP Inhibitors and the Evolving Landscape of Ovarian Cancer Management: A Review. BioDrugs Clin. Immunother. Biopharm. Gene Ther. 33, 255–273. https://doi.org/10.1007/s40259-019-00347-4

Coward, J., Kulbe, H., Chakravarty, P., Leader, D., Vassileva, V., Leinster, D.A., Thompson, R., Schioppa, T., Nemeth, J., Vermeulen, J., Singh, N., Avril, N., Cummings, J., Rexhepaj, E., Jirström, K., Gallagher, W.M., Brennan, D.J., McNeish, I.A., Balkwill, F.R., 2011. Interleukin-6 as a therapeutic target in human ovarian cancer. Clin. Cancer Res. Off. J. Am. Assoc. Cancer Res. 17, 6083–6096. https://doi.org/10.1158/1078-0432.CCR-11-0945

Cruz, C., Castroviejo-Bermejo, M., Gutiérrez-Enríquez, S., Llop-Guevara, A., Ibrahim, Y.H., Gris-Oliver, A., Bonache, S., Morancho, B., Bruna, A., Rueda, O.M., Lai, Z., Polanska, U.M., Jones, G.N., Kristel, P., de Bustos, L., Guzman, M., Rodríguez, O., Grueso, J., Montalban, G., Caratú, G., Mancuso, F., Fasani, R., Jiménez, J., Howat, W.J., Dougherty, B., Vivancos, A., Nuciforo, P., Serres-Créixams, X., Rubio, I.T., Oaknin, A., Cadogan, E., Barrett, J.C., Caldas, C., Baselga, J., Saura, C., Cortés, J., Arribas, J., Jonkers, J., Díez, O., O'Connor, M.J., Balmaña, J., Serra, V., 2018. RAD51 foci as a functional biomarker of homologous recombination repair and PARP inhibitor resistance in germline BRCA-mutated breast cancer. Ann. Oncol. Off. J. Eur. Soc. Med. Oncol. 29, 1203–1210. https://doi.org/10.1093/annonc/mdy099

Curtin, N.J., 2012. DNA repair dysregulation from cancer driver to therapeutic target. Nat. Rev. Cancer 12, 801–817. https://doi.org/10.1038/nrc3399

Dabholkar, M., Bostick-Bruton, F., Weber, C., Bohr, V.A., Egwuagu, C., Reed, E., 1992. ERCC1 and ERCC2 expression in malignant tissues from ovarian cancer patients. J. Natl. Cancer Inst. 84, 1512–1517. https://doi.org/10.1093/jnci/84.19.1512

Dabholkar, M., Vionnet, J., Bostick-Bruton, F., Yu, J.J., Reed, E., 1994. Messenger RNA levels of XPAC and ERCC1 in ovarian cancer tissue correlate with response to platinum-based chemotherapy. J. Clin. Invest. 94, 703–708. https://doi.org/10.1172/JCI117388

Dal Molin, G.Z., Westin, S.N., Coleman, R.L., 2018. Rucaparib in ovarian cancer: extending the use of PARP inhibitors in the recurrent disease. Future Oncol. Lond. Engl. 14, 3101–3110. https://doi.org/10.2217/fon-2018-0215

Damia, G., D'Incalci, M., 2007. Targeting DNA repair as a promising approach in cancer therapy. Eur. J. Cancer Oxf. Engl. 1990 43, 1791–1801. https://doi.org/10.1016/j.ejca.2007.05.003

Damia, G., Imperatori, L., Stefanini, M., D'Incalci, M., 1996. Sensitivity of CHO mutant cell lines with specific defects in nucleotide excision repair to different anti-cancer agents. Int. J. Cancer 66, 779–783. https://doi.org/10.1002/(SICI)1097-0215(19960611)66:6<779::AID-IJC12>3.0.CO;2-Z

Damia, G., Sanchez, Y., Erba, E., Broggini, M., 2001. DNA Damage Induces p53-dependent Down-regulation of hCHK1. J. Biol. Chem. 276, 10641–10645. https://doi.org/10.1074/jbc.M007178200

D'Andrea, A.D., 2018. Mechanisms of PARP inhibitor sensitivity and resistance. DNA Repair 71, 172–176. https://doi.org/10.1016/j.dnarep.2018.08.021

D'Andrea, A.D., 2003. The Fanconi road to cancer. Genes Dev. 17, 1933–1936. https://doi.org/10.1101/gad.1128303

Dasari, S., Tchounwou, P.B., 2014. Cisplatin in cancer therapy: molecular mechanisms of action. Eur. J. Pharmacol. 740, 364–378. https://doi.org/10.1016/j.ejphar.2014.07.025

Davies, H., Glodzik, D., Morganella, S., Yates, L.R., Staaf, J., Zou, X., Ramakrishna, M., Martin, S., Boyault, S., Sieuwerts, A.M., Simpson, P.T., King, T.A., Raine, K., Eyfjord, J.E., Kong, G., Borg, Å., Birney, E., Stunnenberg, H.G., van de Vijver, M.J., Børresen-Dale, A.-L., Martens, J.W.M., Span, P.N., Lakhani, S.R., Vincent-Salomon, A., Sotiriou, C., Tutt, A., Thompson, A.M., Van Laere, S., Richardson, A.L., Viari, A., Campbell, P.J., Stratton, M.R., Nik-Zainal, S., 2017. HRDetect is a predictor of BRCA1 and BRCA2 deficiency based on mutational signatures. Nat. Med. 23, 517–525. https://doi.org/10.1038/nm.4292

De Picciotto, N., Cacheux, W., Roth, A., Chappuis, P.O., Labidi-Galy, S.I., 2016. Ovarian cancer: Status of homologous recombination pathway as a predictor of drug response. Crit. Rev. Oncol. Hematol. 101, 50–59. https://doi.org/10.1016/j.critrevonc.2016.02.014

Deans, A.J., West, S.C., 2011. DNA interstrand crosslink repair and cancer. Nat. Rev. Cancer 11, 467–480. https://doi.org/10.1038/nrc3088

Deniz, M., Holzmann, K., Wiesmüller, L., 2013. Functional analysis-make or break for cancer predictability. Mutat. Res. 743–744, 132–141. https://doi.org/10.1016/j.mrfmmm.2013.03.009

Deniz, M., Romashova, T., Kostezka, S., Faul, A., Gundelach, T., Moreno-Villanueva, M., Janni, W., Friedl, T.W.P., Wiesmüller, L., 2017. Increased single-strand annealing rather than non-homologous end-joining predicts hereditary ovarian carcinoma. Oncotarget 8, 98660–98676. https://doi.org/10.18632/oncotarget.21720

Dev, H., Chiang, T.-W.W., Lescale, C., de Krijger, I., Martin, A.G., Pilger, D., Coates, J., Sczaniecka-Clift, M., Wei, W., Ostermaier, M., Herzog, M., Lam, J., Shea, A., Demir, M., Wu, Q., Yang, F., Fu, B., Lai, Z., Balmus, G., Belotserkovskaya, R., Serra, V., O'Connor, M.J., Bruna, A., Beli, P., Pellegrini, L., Caldas, C., Deriano, L., Jacobs, J.J.L., Galanty, Y., Jackson, S.P., 2018. Shieldin complex promotes DNA end-joining and counters homologous recombination in BRCA1-null cells. Nat. Cell Biol. 20, 954–965. https://doi.org/10.1038/s41556-018-0140-1

Dianov, G.L., Hübscher, U., 2013. Mammalian base excision repair: the forgotten archangel. Nucleic Acids Res. 41, 3483–3490. https://doi.org/10.1093/nar/gkt076

Dijk, M., Typas, D., Mullenders, L., Pines, A., 2014. Insight in the multilevel regulation of NER. Exp. Cell Res. 329, 116–123. https://doi.org/10.1016/j.yexcr.2014.08.010

Dilruba, S., Kalayda, G.V., 2016. Platinum-based drugs: past, present and future. Cancer Chemother. Pharmacol. 77, 1103–1124. https://doi.org/10.1007/s00280-016-2976-z

Dobrzycka, B., Terlikowski, S.J., Kowalczuk, O., Niklińska, W., Chyczewski, L., Kulikowski, M., 2009. Mutations in the KRAS gene in ovarian tumors. Folia Histochem. Cytobiol. 47, 221–224. https://doi.org/10.2478/v10042-009-0039-6

Domchek, S.M., 2017. Reversion Mutations with Clinical Use of PARP Inhibitors: Many Genes, Many Versions. Cancer Discov. 7, 937–939. https://doi.org/10.1158/2159-8290.CD-17-0734

Dong, Q., Du, Y., Li, H., Liu, C., Wei, Y., Chen, M.-K., Zhao, X., Chu, Y.-Y., Qiu, Y., Qin, L., Yamaguchi, H., Hung, M.-C., 2019. EGFR and c-MET Cooperate to Enhance Resistance to PARP Inhibitors in Hepatocellular Carcinoma. Cancer Res. 79, 819–829. https://doi.org/10.1158/0008-5472.CAN-18-1273

Doubeni, C.A., Doubeni, A.R., Myers, A.E., 2016. Diagnosis and Management of Ovarian Cancer. Am. Fam. Physician 93, 937–944.

Dougherty, B.A., Lai, Z., Hodgson, D.R., Orr, M.C.M., Hawryluk, M., Sun, J., Yelensky, R., Spencer, S.K., Robertson, J.D., Ho, T.W., Fielding, A., Ledermann, J.A., Barrett, J.C., 2017. Biological and clinical evidence for somatic mutations in BRCA1 and BRCA2 as predictive markers for olaparib response in high-grade serous ovarian cancers in the maintenance setting. Oncotarget 8, 43653–43661. https://doi.org/10.18632/oncotarget.17613

Drost, R., Bouwman, P., Rottenberg, S., Boon, U., Schut, E., Klarenbeek, S., Klijn, C., van der Heijden, I., van der Gulden, H., Wientjens, E., Pieterse, M., Catteau, A., Green, P., Solomon, E., Morris, J.R., Jonkers, J., 2011. BRCA1 RING function is essential for tumor suppression but dispensable for therapy resistance. Cancer Cell 20, 797–809. https://doi.org/10.1016/j.ccr.2011.11.014

du Bois, A., Reuss, A., Pujade-Lauraine, E., Harter, P., Ray-Coquard, I., Pfisterer, J., 2009. Role of surgical outcome as prognostic factor in advanced epithelial ovarian cancer: a combined exploratory analysis of 3 prospectively randomized phase 3 multicenter trials: by the Arbeitsgemeinschaft Gynaekologische Onkologie Studiengruppe Ovarialkarzinom (AGO-OVAR) and the Groupe d'Investigateurs Nationaux Pour les Etudes des Cancers de l'Ovaire (GINECO). Cancer 115, 1234–1244. https://doi.org/10.1002/cncr.24149

Du, Y., Yamaguchi, H., Wei, Y., Hsu, J.L., Wang, H.-L., Hsu, Y.-H., Lin, W.-C., Yu, W.-H., Leonard, P.G., Lee, G.R., Chen, M.-K., Nakai, K., Hsu, M.-C., Chen, C.-T., Sun, Y., Wu, Y., Chang, W.-C., Huang, W.-C., Liu, C.-L., Chang, Y.-C., Chen, C.-H., Park, M., Jones, P., Hortobagyi, G.N., Hung, M.-C., 2016. Blocking c-Met-mediated PARP1 phosphorylation enhances anti-tumor effects of PARP inhibitors. Nat. Med. 22, 194–201. https://doi.org/10.1038/nm.4032

Dubeau, L., 1999. The cell of origin of ovarian epithelial tumors and the ovarian surface epithelium dogma: does the emperor have no clothes? Gynecol. Oncol. 72, 437–442. https://doi.org/10.1006/gyno.1998.5275

Duska, L.R., Kohn, E.C., 2017. The new classifications of ovarian, fallopian tube, and primary peritoneal cancer and their clinical implications. Ann. Oncol. Off. J. Eur. Soc. Med. Oncol. 28, viii8–viii12. https://doi.org/10.1093/annonc/mdx445

Eastman, A., 1987. The formation, isolation and characterization of DNA adducts produced by anticancer platinum complexes. Pharmacol. Ther. 34, 155–166. https://doi.org/10.1016/0163-7258(87)90009-x

Ediriweera, M.K., Tennekoon, K.H., Samarakoon, S.R., 2019. Role of the PI3K/AKT/mTOR signaling pathway in ovarian cancer: Biological and therapeutic significance. Semin. Cancer Biol. 59, 147–160. https://doi.org/10.1016/j.semcancer.2019.05.012

Eisenhauer, E.A., Therasse, P., Bogaerts, J., Schwartz, L.H., Sargent, D., Ford, R., Dancey, J., Arbuck, S., Gwyther, S., Mooney, M., Rubinstein, L., Shankar, L., Dodd, L., Kaplan, R., Lacombe, D., Verweij, J., 2009. New response evaluation criteria in solid tumours: revised RECIST guideline (version 1.1). Eur. J. Cancer Oxf. Engl. 1990 45, 228–247. https://doi.org/10.1016/j.ejca.2008.10.026

Eitan, R., Levine, D.A., Abu-Rustum, N., Sonoda, Y., Huh, J.N., Franklin, C.C., Stevens, T.A., Barakat, R.R., Chi, D.S., 2005. The clinical significance of malignant pleural effusions in patients with optimally debulked ovarian carcinoma. Cancer 103, 1397–1401. https://doi.org/10.1002/cncr.20920

Ekumi, K.M., Paculova, H., Lenasi, T., Pospichalova, V., Bösken, C.A., Rybarikova, J., Bryja, V., Geyer, M., Blazek, D., Barboric, M., 2015. Ovarian carcinoma CDK12 mutations misregulate expression of DNA repair genes via deficient formation and function of the Cdk12/CycK complex. Nucleic Acids Res. 43, 2575–2589. https://doi.org/10.1093/nar/gkv101

Elias, K.M., Guo, J., Bast, R.C., 2018. Early Detection of Ovarian Cancer. Hematol. Oncol. Clin. North Am. 32, 903–914. https://doi.org/10.1016/j.hoc.2018.07.003

El-Khamisy, S.F., Masutani, M., Suzuki, H., Caldecott, K.W., 2003. A requirement for PARP-1 for the assembly or stability of XRCC1 nuclear foci at sites of oxidative

DNA damage. Nucleic Acids Res. 31, 5526–5533. https://doi.org/10.1093/nar/gkg761

Enoiu, M., Jiricny, J., Schärer, O.D., 2012. Repair of cisplatin-induced DNA interstrand crosslinks by a replication-independent pathway involving transcription-coupled repair and translesion synthesis. Nucleic Acids Res. 40, 8953–8964. https://doi.org/10.1093/nar/gks670

Erez, N., Truitt, M., Olson, P., Arron, S.T., Hanahan, D., 2010. Cancer-Associated Fibroblasts Are Activated in Incipient Neoplasia to Orchestrate Tumor-Promoting Inflammation in an NF-kappaB-Dependent Manner. Cancer Cell 17, 135–147. https://doi.org/10.1016/j.ccr.2009.12.041

Esquivel, J., 2016. Cytoreductive surgery and hyperthermic intraperitoneal chemotherapy for colorectal cancer: survival outcomes and patient selection. J. Gastrointest. Oncol. 7, 72–78. https://doi.org/10.3978/j.issn.2078-6891.2015.114

Estrela, J.M., Ortega, A., Obrador, E., 2006. Glutathione in cancer biology and therapy. Crit. Rev. Clin. Lab. Sci. 43, 143–181. https://doi.org/10.1080/10408360500523878

Eustermann, S., Wu, W.-F., Langelier, M.-F., Yang, J.-C., Easton, L.E., Riccio, A.A., Pascal, J.M., Neuhaus, D., 2015. Structural Basis of Detection and Signaling of DNA Single-Strand Breaks by Human PARP-1. Mol. Cell 60, 742–754. https://doi.org/10.1016/j.molcel.2015.10.032

Fabregat, I., Malfettone, A., Soukupova, J., 2016. New Insights into the Crossroads between EMT and Stemness in the Context of Cancer. J. Clin. Med. 5. https://doi.org/10.3390/jcm5030037

Faridounnia, M., Folkers, G.E., Boelens, R., 2018. Function and Interactions of ERCC1-XPF in DNA Damage Response. Mol. Basel Switz. 23. https://doi.org/10.3390/molecules23123205

Farmer, H., McCabe, N., Lord, C.J., Tutt, A.N.J., Johnson, D.A., Richardson, T.B., Santarosa, M., Dillon, K.J., Hickson, I., Knights, C., Martin, N.M.B., Jackson, S.P., Smith, G.C.M., Ashworth, A., 2005. Targeting the DNA repair defect in BRCA mutant cells as a therapeutic strategy. Nature 434, 917–921. https://doi.org/10.1038/nature03445

Fathalla, M.F., 1971. Incessant ovulation--a factor in ovarian neoplasia? Lancet Lond. Engl. 2, 163. https://doi.org/10.1016/s0140-6736(71)92335-x

Feng, L., Fong, K.-W., Wang, J., Wang, W., Chen, J., 2013. RIF1 counteracts BRCA1-mediated end resection during DNA repair. J. Biol. Chem. 288, 11135–11143. https://doi.org/10.1074/jbc.M113.457440

Fiori, M.E., Di Franco, S., Villanova, L., Bianca, P., Stassi, G., De Maria, R., 2019. Cancer-associated fibroblasts as abettors of tumor progression at the crossroads of EMT and therapy resistance. Mol. Cancer 18, 70. https://doi.org/10.1186/s12943-019-0994-2

Fleszar, A.J., Walker, A., Porubsky, V., Flanigan, W., James, D., Campagnola, P.J., Weisman, P.S., Kreeger, P.K., 2018. The Extracellular Matrix of Ovarian Cortical Inclusion Cysts Modulates Invasion of Fallopian Tube Epithelial Cells. APL Bioeng. 2. https://doi.org/10.1063/1.5022595

Fong, P.C., Yap, T.A., Boss, D.S., Carden, C.P., Mergui-Roelvink, M., Gourley, C., De Greve, J., Lubinski, J., Shanley, S., Messiou, C., A'Hern, R., Tutt, A., Ashworth, A., Stone, J., Carmichael, J., Schellens, J.H.M., de Bono, J.S., Kaye, S.B., 2010. Poly(ADP)-ribose polymerase inhibition: frequent durable responses in BRCA carrier ovarian cancer correlating with platinum-free interval. J. Clin. Oncol. Off. J. Am. Soc. Clin. Oncol. 28, 2512–2519. https://doi.org/10.1200/JCO.2009.26.9589

Franzese, E., Centonze, S., Diana, A., Carlino, F., Guerrera, L.P., Di Napoli, M., De Vita, F., Pignata, S., Ciardiello, F., Orditura, M., 2019. PARP inhibitors in ovarian cancer. Cancer Treat. Rev. 73, 1–9. https://doi.org/10.1016/j.ctrv.2018.12.002

Friboulet, L., Olaussen, K.A., Pignon, J.-P., Shepherd, F.A., Tsao, M.-S., Graziano, S., Kratzke, R., Douillard, J.-Y., Seymour, L., Pirker, R., Filipits, M., André, F., Solary, E., Ponsonnailles, F., Robin, A., Stoclin, A., Dorvault, N., Commo, F., Adam, J., Vanhecke, E., Saulnier, P., Thomale, J., Le Chevalier, T., Dunant, A., Rousseau, V., Le Teuff, G., Brambilla, E., Soria, J.-C., 2013a. ERCC1 isoform expression and DNA repair in non-small-cell lung cancer. N. Engl. J. Med. 368, 1101–1110. https://doi.org/10.1056/NEJMoa1214271

Friboulet, L., Postel-Vinay, S., Sourisseau, T., Adam, J., Stoclin, A., Ponsonnailles, F., Dorvault, N., Commo, F., Saulnier, P., Salome-Desmoulez, S., Pottier, G., André, F., Kroemer, G., Soria, J.-C., Olaussen, K.A., 2013b. ERCC1 function in nuclear excision and interstrand crosslink repair pathways is mediated exclusively by the ERCC1-202 isoform. Cell Cycle Georget. Tex 12, 3298–3306. https://doi.org/10.4161/cc.26309

Friedlander, M., Gebski, V., Gibbs, E., Davies, L., Bloomfield, R., Hilpert, F., Wenzel, L.B., Eek, D., Rodrigues, M., Clamp, A., Penson, R.T., Provencher, D., Korach, J., Huzarski, T., Vidal, L., Salutari, V., Scott, C., Nicoletto, M.O., Tamura, K., Espinoza, D., Joly, F., Pujade-Lauraine, E., 2018. Health-related quality of life and patient-centred outcomes with olaparib maintenance after chemotherapy in patients with platinum-sensitive, relapsed ovarian cancer and a BRCA1/2 mutation (SOLO2/ENGOT Ov-21): a placebo-controlled, phase 3 randomised trial. Lancet Oncol. 19, 1126–1134. https://doi.org/10.1016/S1470-2045(18)30343-7

Fu, S., Naing, A., Fu, C., Kuo, M.T., Kurzrock, R., 2012. Overcoming platinum resistance through the use of a copper-lowering agent. Mol. Cancer Ther. 11, 1221–1225. https://doi.org/10.1158/1535-7163.MCT-11-0864

Fusco, N., Lopez, G., Corti, C., Pesenti, C., Colapietro, P., Ercoli, G., Gaudioso, G., Faversani, A., Gambini, D., Michelotti, A., Despini, L., Blundo, C., Vaira, V., Miozzo, M., Ferrero, S., Bosari, S., 2018. Mismatch Repair Protein Loss as a Prognostic and Predictive Biomarker in Breast Cancers Regardless of Microsatellite Instability. JNCI Cancer Spectr. 2, pky056. https://doi.org/10.1093/jncics/pky056

Galluzzi, L., Senovilla, L., Vitale, I., Michels, J., Martins, I., Kepp, O., Castedo, M., Kroemer, G., 2012. Molecular mechanisms of cisplatin resistance. Oncogene 31, 1869–1883. https://doi.org/10.1038/onc.2011.384

Galluzzi, L., Vitale, I., Michels, J., Brenner, C., Szabadkai, G., Harel-Bellan, A., Castedo, M., Kroemer, G., 2014. Systems biology of cisplatin resistance: past, present and future. Cell Death Dis. 5, e1257. https://doi.org/10.1038/cddis.2013.428

Gan, A., Green, A.R., Nolan, C.C., Martin, S., Deen, S., 2013. Poly(adenosine diphosphate-ribose) polymerase expression in BRCA-proficient ovarian high-grade serous carcinoma; association with patient survival. Hum. Pathol. 44, 1638–1647. https://doi.org/10.1016/j.humpath.2013.01.015

Ganai, R.A., Johansson, E., 2016. DNA Replication-A Matter of Fidelity. Mol. Cell 62, 745–755. https://doi.org/10.1016/j.molcel.2016.05.003

Ganzinelli, M., Mariani, P., Cattaneo, D., Fossati, R., Fruscio, R., Corso, S., Ricci, F., Broggini, M., Damia, G., 2011. Expression of DNA repair genes in ovarian cancer samples: biological and clinical considerations. Eur. J. Cancer Oxf. Engl. 1990 47, 1086–1094. https://doi.org/10.1016/j.ejca.2010.11.029

Gaona-Luviano, P., Medina-Gaona, L.A., Magaña-Pérez, K., 2020. Epidemiology of ovarian cancer. Chin. Clin. Oncol. 9, 47. https://doi.org/10.21037/cco-20-34

Garcia, J., Hurwitz, H.I., Sandler, A.B., Miles, D., Coleman, R.L., Deurloo, R., Chinot, O.L., 2020. Bevacizumab (Avastin®) in cancer treatment: A review of 15 years of clinical experience and future outlook. Cancer Treat. Rev. 86, 102017. https://doi.org/10.1016/j.ctrv.2020.102017

Garsed, D.W., Alsop, K., Fereday, S., Emmanuel, C., Kennedy, C.J., Etemadmoghadam, D., Gao, B., Gebski, V., Garès, V., Christie, E.L., Wouters, M.C.A., Milne, K., George, J., Patch, A.-M., Li, J., Arnau, G.M., Semple, T., Gadipally, S.R., Chiew, Y.-E., Hendley, J., Mikeska, T., Zapparoli, G.V., Amarasinghe, K., Grimmond, S.M., Pearson, J.V., Waddell, N., Hung, J., Stewart, C.J.R., Sharma, R., Allan, P.E., Rambau, P.F., McNally, O., Mileshkin, L., Hamilton, A., Ananda, S., Grossi, M., Cohen, P.A., Leung, Y.C., Rome, R.M., Beale, P., Blomfield, P., Friedlander, M., Brand, A., Dobrovic, A., Köbel, M., Harnett, P., Nelson, B.H., Bowtell, D.D.L., deFazio, A., Nadia Traficante, for the Australian Ovarian Cancer Study Group, 2018. Homologous Recombination DNA Repair Pathway Disruption and Retinoblastoma Protein Loss Are Associated with Exceptional Survival in High-Grade Serous Ovarian Cancer. Clin. Cancer Res. Off. J. Am. Assoc. Cancer Res. 24, 569–580. https://doi.org/10.1158/1078-0432.CCR-17-1621

Gavande, N.S., VanderVere-Carozza, P.S., Hinshaw, H.D., Jalal, S.I., Sears, C.R., Pawelczak, K.S., Turchi, J.J., 2016. DNA repair targeted therapy: The past or future of cancer treatment? Pharmacol. Ther. 160, 65–83. https://doi.org/10.1016/j.pharmthera.2016.02.003

Gee, M.E., Faraahi, Z., McCormick, A., Edmondson, R.J., 2018. DNA damage repair in ovarian cancer: unlocking the heterogeneity. J. Ovarian Res. 11, 50. https://doi.org/10.1186/s13048-018-0424-x

Gelmon, K.A., Tischkowitz, M., Mackay, H., Swenerton, K., Robidoux, A., Tonkin, K., Hirte, H., Huntsman, D., Clemons, M., Gilks, B., Yerushalmi, R., Macpherson, E., Carmichael, J., Oza, A., 2011. Olaparib in patients with recurrent high-grade serous or poorly differentiated ovarian carcinoma or triple-negative breast cancer: a phase 2, multicentre, open-label, non-randomised study. Lancet Oncol. 12, 852–861. https://doi.org/10.1016/S1470-2045(11)70214-5

Geyer, J.T., López-García, M.A., Sánchez-Estevez, C., Sarrió, D., Moreno-Bueno, G., Franceschetti, I., Palacios, J., Oliva, E., 2009. Pathogenetic pathways in ovarian

endometrioid adenocarcinoma: a molecular study of 29 cases. Am. J. Surg. Pathol. 33, 1157–1163. https://doi.org/10.1097/PAS.0b013e3181a902e1

Gheorghe-Cetean, S., Cainap, C., Oprean, L., Hangan, A., Virag, P., Fischer-Fodor, E., Gherman, A., Cainap, S., Constantin, A.-M., Laszlo, I., Vlad, C., Oprean, R., 2017. Platinum derivatives: a multidisciplinary approach. J. BUON Off. J. Balk. Union Oncol. 22, 568–577.

Giudice, L.C., 2010. Clinical practice. Endometriosis. N. Engl. J. Med. 362, 2389–2398. https://doi.org/10.1056/NEJMcp1000274

Goff, B.A., Mandel, L.S., Melancon, C.H., Muntz, H.G., 2004. Frequency of symptoms of ovarian cancer in women presenting to primary care clinics. JAMA 291, 2705–2712. https://doi.org/10.1001/jama.291.22.2705

Gogola, E., Duarte, A.A., de Ruiter, J.R., Wiegant, W.W., Schmid, J.A., de Bruijn, R., James, D.I., Guerrero Llobet, S., Vis, D.J., Annunziato, S., van den Broek, B., Barazas, M., Kersbergen, A., van de Ven, M., Tarsounas, M., Ogilvie, D.J., van Vugt, M., Wessels, L.F.A., Bartkova, J., Gromova, I., Andújar-Sánchez, M., Bartek, J., Lopes, M., van Attikum, H., Borst, P., Jonkers, J., Rottenberg, S., 2018. Selective Loss of PARG Restores PARylation and Counteracts PARP Inhibitor-Mediated Synthetic Lethality. Cancer Cell 33, 1078-1093.e12. https://doi.org/10.1016/j.ccell.2018.05.008

Gomes, L.R., Rocha, C.R.R., Martins, D.J., Fiore, A.P.Z.P., Kinker, G.S., Bruni-Cardoso, A., Menck, C.F.M., 2019. ATR mediates cisplatin resistance in 3D-cultured breast cancer cells via translesion DNA synthesis modulation. Cell Death Dis. 10, 459. https://doi.org/10.1038/s41419-019-1689-8

Goodall, J., Mateo, J., Yuan, W., Mossop, H., Porta, N., Miranda, S., Perez-Lopez, R., Dolling, D., Robinson, D.R., Sandhu, S., Fowler, G., Ebbs, B., Flohr, P., Seed, G., Rodrigues, D.N., Boysen, G., Bertan, C., Atkin, M., Clarke, M., Crespo, M., Figueiredo, I., Riisnaes, R., Sumanasuriya, S., Rescigno, P., Zafeiriou, Z., Sharp, A., Tunariu, N., Bianchini, D., Gillman, A., Lord, C.J., Hall, E., Chinnaiyan, A.M., Carreira, S., de Bono, J.S., TOPARP-A investigators, 2017. Circulating Cell-Free DNA to Guide Prostate Cancer Treatment with PARP Inhibition. Cancer Discov. 7, 1006–1017. https://doi.org/10.1158/2159-8290.CD-17-0261

Graeser, M., McCarthy, A., Lord, C.J., Savage, K., Hills, M., Salter, J., Orr, N., Parton, M., Smith, I.E., Reis-Filho, J.S., Dowsett, M., Ashworth, A., Turner, N.C., 2010. A marker of homologous recombination predicts pathologic complete response to neoadjuvant chemotherapy in primary breast cancer. Clin. Cancer Res. Off. J. Am. Assoc. Cancer Res. 16, 6159–6168. https://doi.org/10.1158/1078-0432.CCR-10-1027

Griffiths, C.T., 1975. Surgical resection of tumor bulk in the primary treatment of ovarian carcinoma. Natl. Cancer Inst. Monogr. 42, 101–104.

Guffanti, F., Alvisi, M.F., Caiola, E., Ricci, F., De Maglie, M., Soldati, S., Ganzinelli, M., Decio, A., Giavazzi, R., Rulli, E., Damia, G., 2020. Impact of ERCC1, XPF and DNA Polymerase β Expression on Platinum Response in Patient-Derived Ovarian Cancer Xenografts. Cancers 12. https://doi.org/10.3390/cancers12092398

Guffanti, F., Fratelli, M., Ganzinelli, M., Bolis, M., Ricci, F., Bizzaro, F., Chilà, R., Sina, F.P., Fruscio, R., Lupia, M., Cavallaro, U., Cappelletti, M.R., Generali, D., Giavazzi, R., Damia, G., 2018. Platinum sensitivity and DNA repair in a recently established panel of patient-derived ovarian carcinoma xenografts. Oncotarget 9, 24707–24717. https://doi.org/10.18632/oncotarget.25185

Guillemette, S., Serra, R.W., Peng, M., Hayes, J.A., Konstantinopoulos, P.A., Green, M.R., Cantor, S.B., 2015. Resistance to therapy in BRCA2 mutant cells due to loss of the nucleosome remodeling factor CHD4. Genes Dev. 29, 489–494. https://doi.org/10.1101/gad.256214.114

Gupta, R., Somyajit, K., Narita, T., Maskey, E., Stanlie, A., Kremer, M., Typas, D., Lammers, M., Mailand, N., Nussenzweig, A., Lukas, J., Choudhary, C., 2018. DNA Repair Network Analysis Reveals Shieldin as a Key Regulator of NHEJ and PARP Inhibitor Sensitivity. Cell 173, 972-988.e23. https://doi.org/10.1016/j.cell.2018.03.050

Han, Y., Chen, M.-K., Wang, H.-L., Hsu, J.L., Li, C.-W., Chu, Y.-Y., Liu, C.-X., Nie, L., Chan, L.-C., Yam, C., Wang, S.-C., He, G.-J., Hortobagyi, G.N., Tan, X.-D., Hung, M.-C., 2019. Synergism of PARP inhibitor fluzoparib (HS10160) and MET inhibitor HS10241 in breast and ovarian cancer cells. Am. J. Cancer Res. 9, 608–618.

Hanahan, D., Weinberg, R.A., 2000. The hallmarks of cancer. Cell 100, 57–70. https://doi.org/10.1016/s0092-8674(00)81683-9

Harano, K., Terauchi, F., Katsumata, N., Takahashi, F., Yasuda, M., Takakura, S., Takano, M., Yamamoto, Y., Sugiyama, T., 2014. Quality-of-life outcomes from a randomized phase III trial of dose-dense weekly paclitaxel and carboplatin compared with conventional paclitaxel and carboplatin as a first-line treatment for stage II-IV ovarian cancer: Japanese Gynecologic Oncology Group Trial (JGOG3016). Ann. Oncol. Off. J. Eur. Soc. Med. Oncol. 25, 251–257. https://doi.org/10.1093/annonc/mdt527

Hartwell, L.H., Szankasi, P., Roberts, C.J., Murray, A.W., Friend, S.H., 1997. Integrating genetic approaches into the discovery of anticancer drugs. Science 278, 1064–1068. https://doi.org/10.1126/science.278.5340.1064

Hashimoto, S., Anai, H., Hanada, K., 2016. Mechanisms of interstrand DNA crosslink repair and human disorders. Genes Environ. Off. J. Jpn. Environ. Mutagen Soc. 38, 9. https://doi.org/10.1186/s41021-016-0037-9

Haslehurst, A.M., Koti, M., Dharsee, M., Nuin, P., Evans, K., Geraci, J., Childs, T., Chen, J., Li, J., Weberpals, J., Davey, S., Squire, J., Park, P.C., Feilotter, H., 2012. EMT transcription factors snail and slug directly contribute to cisplatin resistance in ovarian cancer. BMC Cancer 12, 91. https://doi.org/10.1186/1471-2407-12-91

Hasty, P., Montagna, C., 2014. Chromosomal Rearrangements in Cancer: Detection and potential causal mechanisms. Mol. Cell. Oncol. 1. https://doi.org/10.4161/mco.29904

Haynes, B., Saadat, N., Myung, B., Shekhar, M.P.V., 2015. Crosstalk between translesion synthesis, Fanconi anemia network, and homologous recombination repair pathways in interstrand DNA crosslink repair and development of chemoresistance. Mutat. Res. Rev. Mutat. Res. 763, 258–266. https://doi.org/10.1016/j.mrrev.2014.11.005

He, Y.J., Meghani, K., Caron, M.-C., Yang, C., Ronato, D.A., Bian, J., Sharma, A., Moore, J., Niraj, J., Detappe, A., Doench, J.G., Legube, G., Root, D.E., D'Andrea, A.D., Drané, P., De, S., Konstantinopoulos, P.A., Masson, J.-Y., Chowdhury, D., 2018. DYNLL1 binds to MRE11 to limit DNA end resection in BRCA1-deficient cells. Nature 563, 522–526. https://doi.org/10.1038/s41586-018-0670-5

Hehir-Kwa, J.Y., Pfundt, R., Veltman, J.A., 2015. Exome sequencing and whole genome sequencing for the detection of copy number variation. Expert Rev. Mol. Diagn. 15, 1023–1032. https://doi.org/10.1586/14737159.2015.1053467

Hennessy, B.T.J., Timms, K.M., Carey, M.S., Gutin, A., Meyer, L.A., Flake, D.D., Abkevich, V., Potter, J., Pruss, D., Glenn, P., Li, Y., Li, J., Gonzalez-Angulo, A.M., McCune, K.S., Markman, M., Broaddus, R.R., Lanchbury, J.S., Lu, K.H., Mills, G.B., 2010. Somatic mutations in BRCA1 and BRCA2 could expand the number of patients that benefit from poly (ADP ribose) polymerase inhibitors in ovarian cancer. J. Clin. Oncol. Off. J. Am. Soc. Clin. Oncol. 28, 3570–3576. https://doi.org/10.1200/JCO.2009.27.2997

Heo, E.J., Cho, Y.J., Cho, W.C., Hong, J.E., Jeon, H.-K., Oh, D.-Y., Choi, Y.-L., Song, S.Y., Choi, J.-J., Bae, D.-S., Lee, Y.-Y., Choi, C.H., Kim, T.-J., Park, W.-Y., Kim, B.-G., Lee, J.-W., 2017. Patient-Derived Xenograft Models of Epithelial Ovarian Cancer for Preclinical Studies. Cancer Res. Treat. 49, 915–926. https://doi.org/10.4143/crt.2016.322

Hidalgo, M., Amant, F., Biankin, A.V., Budinská, E., Byrne, A.T., Caldas, C., Clarke, R.B., de Jong, S., Jonkers, J., Mælandsmo, G.M., Roman-Roman, S., Seoane, J., Trusolino, L., Villanueva, A., 2014. Patient-derived xenograft models: an emerging platform for translational cancer research. Cancer Discov. 4, 998–1013. https://doi.org/10.1158/2159-8290.CD-14-0001

Hill, S.J., Decker, B., Roberts, E.A., Horowitz, N.S., Muto, M.G., Worley, M.J., Feltmate, C.M., Nucci, M.R., Swisher, E.M., Nguyen, H., Yang, C., Morizane, R., Kochupurakkal, B.S., Do, K.T., Konstantinopoulos, P.A., Liu, J.F., Bonventre, J.V., Matulonis, U.A., Shapiro, G.I., Berkowitz, R.S., Crum, C.P., D'Andrea, A.D., 2018. Prediction of DNA Repair Inhibitor Response in Short-Term Patient-Derived Ovarian Cancer Organoids. Cancer Discov. 8, 1404–1421. https://doi.org/10.1158/2159-8290.CD-18-0474

Hinshaw, D.C., Shevde, L.A., 2019. The Tumor Microenvironment Innately Modulates Cancer Progression. Cancer Res. 79, 4557–4566. https://doi.org/10.1158/0008-5472.CAN-18-3962

Hjortkjær, M., Waldstrøm, M., Jakobsen, A., Kanstrup, H., Søgaard-Andersen, E., Dahl Steffensen, K., 2017. The Prognostic Value of BRCA1 and PARP Expression in Epithelial Ovarian Carcinoma: Immunohistochemical Detection. Int. J. Gynecol. Pathol. Off. J. Int. Soc. Gynecol. Pathol. 36, 180–189. https://doi.org/10.1097/PGP.0000000000000310

Ho, G.Y., Woodward, N., Coward, J.I.G., 2016. Cisplatin versus carboplatin: comparative review of therapeutic management in solid malignancies. Crit. Rev. Oncol. Hematol. 102, 37–46. https://doi.org/10.1016/j.critrevonc.2016.03.014

Hodskinson, M.R.G., Silhan, J., Crossan, G.P., Garaycoechea, J.I., Mukherjee, S., Johnson, C.M., Schärer, O.D., Patel, K.J., 2014. Mouse SLX4 is a tumor suppressor that

stimulates the activity of the nuclease XPF-ERCC1 in DNA crosslink repair. Mol. Cell 54, 472–484. https://doi.org/10.1016/j.molcel.2014.03.014

Hojo, N., Huisken, A.L., Wang, H., Chirshev, E., Kim, N.S., Nguyen, S.M., Campos, H., Glackin, C.A., Ioffe, Y.J., Unternaehrer, J.J., 2018. Snail knockdown reverses stemness and inhibits tumour growth in ovarian cancer. Sci. Rep. 8, 8704. https://doi.org/10.1038/s41598-018-27021-z

Hoppe, M.M., Sundar, R., Tan, D.S.P., Jeyasekharan, A.D., 2018. Biomarkers for Homologous Recombination Deficiency in Cancer. J. Natl. Cancer Inst. 110, 704–713. https://doi.org/10.1093/jnci/djy085

Hoppenot, C., Eckert, M.A., Tienda, S.M., Lengyel, E., 2018. Who are the long-term survivors of high grade serous ovarian cancer? Gynecol. Oncol. 148, 204–212. https://doi.org/10.1016/j.ygyno.2017.10.032

Horton, J.K., Gassman, N.R., Dunigan, B.D., Stefanick, D.F., Wilson, S.H., 2015. DNA polymerase β-dependent cell survival independent of XRCC1 expression. DNA Repair 26, 23–29. https://doi.org/10.1016/j.dnarep.2014.11.008

Hsieh, P., Zhang, Y., 2017. The Devil is in the details for DNA mismatch repair. Proc. Natl. Acad. Sci. U. S. A. 114, 3552–3554. https://doi.org/10.1073/pnas.1702747114

http://primer3.ut.ee/ [WWW Document], n.d.

https://biorender.com/ [WWW Document], n.d.

https://tcga-data. nci.nih.gov [WWW Document], n.d.

https://www.aiom.it/wp-content/uploads/2018/10/2018_NumeriCancro-operatori.pdf [WWW Document], n.d.

https://www.aiom.it/wp-content/uploads/2019/09/2019_Numeri_Cancro-operatori-web.pdf [WWW Document], n.d.

http://www.cbioportal.org [WWW Document], n.d.

Hughes-Davies, L., Huntsman, D., Ruas, M., Fuks, F., Bye, J., Chin, S.-F., Milner, J., Brown, L.A., Hsu, F., Gilks, B., Nielsen, T., Schulzer, M., Chia, S., Ragaz, J., Cahn, A., Linger, L., Ozdag, H., Cattaneo, E., Jordanova, E.S., Schuuring, E., Yu, D.S., Venkitaraman, A., Ponder, B., Doherty, A., Aparicio, S., Bentley, D., Theillet, C., Ponting, C.P., Caldas, C., Kouzarides, T., 2003. EMSY links the BRCA2 pathway to sporadic breast and ovarian cancer. Cell 115, 523–535. https://doi.org/10.1016/s0092-8674(03)00930-9

Hunter, S.M., Anglesio, M.S., Ryland, G.L., Sharma, R., Chiew, Y.-E., Rowley, S.M., Doyle, M.A., Li, J., Gilks, C.B., Moss, P., Allan, P.E., Stephens, A.N., Huntsman, D.G., deFazio, A., Bowtell, D.D., Australian Ovarian Cancer Study Group, Gorringe, K.L., Campbell, I.G., 2015. Molecular profiling of low grade serous ovarian tumours identifies novel candidate driver genes. Oncotarget 6, 37663–37677. https://doi.org/10.18632/oncotarget.5438

Hurley, R.M., Wahner Hendrickson, A.E., Visscher, D.W., Ansell, P., Harrell, M.I., Wagner, J.M., Negron, V., Goergen, K.M., Maurer, M.J., Oberg, A.L., Meng, X.W., Flatten, K.S., De Jonge, M.J.A., Van Herpen, C.D., Gietema, J.A., Koornstra, R.H.T., Jager,

A., den Hollander, M.W., Dudley, M., Shepherd, S.P., Swisher, E.M., Kaufmann, S.H., 2019. 53BP1 as a potential predictor of response in PARP inhibitor-treated homologous recombination-deficient ovarian cancer. Gynecol. Oncol. 153, 127–134. https://doi.org/10.1016/j.ygyno.2019.01.015

Ilenkovan, N., Gourley, C., 2018. Pathogenesis, Genetics, and Genomics of Non-High Grade Serous Ovarian Cancers. Hematol. Oncol. Clin. North Am. 32, 929–942. https://doi.org/10.1016/j.hoc.2018.07.004

International Collaborative Ovarian Neoplasm Group, 2002. Paclitaxel plus carboplatin versus standard chemotherapy with either single-agent carboplatin or cyclophosphamide, doxorubicin, and cisplatin in women with ovarian cancer: the ICON3 randomised trial. Lancet Lond. Engl. 360, 505–515. https://doi.org/10.1016/S0140-6736(02)09738-6

Ireno, I.C., Wiehe, R.S., Stahl, A.I., Hampp, S., Aydin, S., Troester, M.A., Selivanova, G., Wiesmüller, L., 2014. Modulation of the poly (ADP-ribose) polymerase inhibitor response and DNA recombination in breast cancer cells by drugs affecting endogenous wild-type p53. Carcinogenesis 35, 2273–2282. https://doi.org/10.1093/carcin/bgu160

Ishida, S., McCormick, F., Smith-McCune, K., Hanahan, D., 2010. Enhancing tumor-specific uptake of the anticancer drug cisplatin with a copper chelator. Cancer Cell 17, 574–583. https://doi.org/10.1016/j.ccr.2010.04.011

Jacobs, I.J., Menon, U., Ryan, A., Gentry-Maharaj, A., Burnell, M., Kalsi, J.K., Amso, N.N., Apostolidou, S., Benjamin, E., Cruickshank, D., Crump, D.N., Davies, S.K., Dawnay, A., Dobbs, S., Fletcher, G., Ford, J., Godfrey, K., Gunu, R., Habib, M., Hallett, R., Herod, J., Jenkins, H., Karpinskyj, C., Leeson, S., Lewis, S.J., Liston, W.R., Lopes, A., Mould, T., Murdoch, J., Oram, D., Rabideau, D.J., Reynolds, K., Scott, I., Seif, M.W., Sharma, A., Singh, N., Taylor, J., Warburton, F., Widschwendter, M., Williamson, K., Woolas, R., Fallowfield, L., McGuire, A.J., Campbell, S., Parmar, M., Skates, S.J., 2016. Ovarian cancer screening and mortality in the UK Collaborative Trial of Ovarian Cancer Screening (UKCTOCS): a randomised controlled trial. Lancet Lond. Engl. 387, 945–956. https://doi.org/10.1016/S0140-6736(15)01224-6

Jaspers, J.E., Kersbergen, A., Boon, U., Sol, W., van Deemter, L., Zander, S.A., Drost, R., Wientjens, E., Ji, J., Aly, A., Doroshow, J.H., Cranston, A., Martin, N.M.B., Lau, A., O'Connor, M.J., Ganesan, S., Borst, P., Jonkers, J., Rottenberg, S., 2013. Loss of 53BP1 causes PARP inhibitor resistance in Brca1-mutated mouse mammary tumors. Cancer Discov. 3, 68–81. https://doi.org/10.1158/2159-8290.CD-12-0049

Jayson, G.C., Kohn, E.C., Kitchener, H.C., Ledermann, J.A., 2014. Ovarian cancer. Lancet Lond. Engl. 384, 1376–1388. https://doi.org/10.1016/S0140-6736(13)62146-7

Jemal, A., Ward, E.M., Johnson, C.J., Cronin, K.A., Ma, J., Ryerson, B., Mariotto, A., Lake, A.J., Wilson, R., Sherman, R.L., Anderson, R.N., Henley, S.J., Kohler, B.A., Penberthy, L., Feuer, E.J., Weir, H.K., 2017. Annual Report to the Nation on the Status of Cancer, 1975-2014, Featuring Survival. J. Natl. Cancer Inst. 109. https://doi.org/10.1093/jnci/djx030

Jiang, X., Li, W., Li, X., Bai, H., Zhang, Z., 2019. Current status and future prospects of PARP inhibitor clinical trials in ovarian cancer. Cancer Manag. Res. 11, 4371–4390. https://doi.org/10.2147/CMAR.S200524

Johnson, N., Johnson, S.F., Yao, W., Li, Y.-C., Choi, Y.-E., Bernhardy, A.J., Wang, Y., Capelletti, M., Sarosiek, K.A., Moreau, L.A., Chowdhury, D., Wickramanayake, A., Harrell, M.I., Liu, J.F., D'Andrea, A.D., Miron, A., Swisher, E.M., Shapiro, G.I., 2013. Stabilization of mutant BRCA1 protein confers PARP inhibitor and platinum resistance. Proc. Natl. Acad. Sci. U. S. A. 110, 17041–17046. https://doi.org/10.1073/pnas.1305170110

Jones, M.R., Kamara, D., Karlan, B.Y., Pharoah, P.D.P., Gayther, S.A., 2017. Genetic epidemiology of ovarian cancer and prospects for polygenic risk prediction. Gynecol. Oncol. 147, 705–713. https://doi.org/10.1016/j.ygyno.2017.10.001

Jones, S., Wang, T.-L., Kurman, R.J., Nakayama, K., Velculescu, V.E., Vogelstein, B., Kinzler, K.W., Papadopoulos, N., Shih, I.-M., 2012. Low-grade serous carcinomas of the ovary contain very few point mutations. J. Pathol. 226, 413–420. https://doi.org/10.1002/path.3967

Jung, Y., Lippard, S.J., 2006. RNA polymerase II blockage by cisplatin-damaged DNA. Stability and polyubiquitylation of stalled polymerase. J. Biol. Chem. 281, 1361–1370. https://doi.org/10.1074/jbc.M509688200

Kais, Z., Rondinelli, B., Holmes, A., O'Leary, C., Kozono, D., D'Andrea, A.D., Ceccaldi, R., 2016. FANCD2 Maintains Fork Stability in BRCA1/2-Deficient Tumors and Promotes Alternative End-Joining DNA Repair. Cell Rep. 15, 2488–2499. https://doi.org/10.1016/j.celrep.2016.05.031

Kamaletdinova, T., Fanaei-Kahrani, Z., Wang, Z.-Q., 2019. The Enigmatic Function of PARP1: From PARylation Activity to PAR Readers. Cells 8. https://doi.org/10.3390/cells8121625

Karakashev, S., Zhang, R.-G., 2021. Mouse models of epithelial ovarian cancer for preclinical studies. Zool. Res. 1–8. https://doi.org/10.24272/j.issn.2095-8137.2020.382

Karst, A.M., Drapkin, R., 2010. Ovarian cancer pathogenesis: a model in evolution. J. Oncol. 2010, 932371. https://doi.org/10.1155/2010/932371

Katabuchi, H. (Ed.), 2017. Frontiers in Ovarian Cancer Science, Comprehensive Gynecology and Obstetrics. Springer Singapore, Singapore. https://doi.org/10.1007/978-981-10-4160-0

Kaufman, B., Shapira-Frommer, R., Schmutzler, R.K., Audeh, M.W., Friedlander, M., Balmaña, J., Mitchell, G., Fried, G., Stemmer, S.M., Hubert, A., Rosengarten, O., Steiner, M., Loman, N., Bowen, K., Fielding, A., Domchek, S.M., 2015. Olaparib monotherapy in patients with advanced cancer and a germline BRCA1/2 mutation. J. Clin. Oncol. Off. J. Am. Soc. Clin. Oncol. 33, 244–250. https://doi.org/10.1200/JCO.2014.56.2728

Kawachi, A., Yamashita, S., Okochi-Takada, E., Hirakawa, A., Tsuda, H., Shimomura, A., Kojima, Y., Yonemori, K., Fujiwara, Y., Kinoshita, T., Ushijima, T., Tamura, K., 2020. BRCA1 promoter methylation in breast cancer patients is associated with

response to olaparib/eribulin combination therapy. Breast Cancer Res. Treat. 181, 323–329. https://doi.org/10.1007/s10549-020-05647-w

Kehoe, S., Hook, J., Nankivell, M., Jayson, G.C., Kitchener, H., Lopes, T., Luesley, D., Perren, T., Bannoo, S., Mascarenhas, M., Dobbs, S., Essapen, S., Twigg, J., Herod, J., McCluggage, G., Parmar, M., Swart, A.-M., 2015. Primary chemotherapy versus primary surgery for newly diagnosed advanced ovarian cancer (CHORUS): an open-label, randomised, controlled, non-inferiority trial. Lancet Lond. Engl. 386, 249–257. https://doi.org/10.1016/S0140-6736(14)62223-6

Keimling, M., Deniz, M., Varga, D., Stahl, A., Schrezenmeier, H., Kreienberg, R., Hoffmann, I., König, J., Wiesmüller, L., 2012. The power of DNA double-strand break (DSB) repair testing to predict breast cancer susceptibility. FASEB J. Off. Publ. Fed. Am. Soc. Exp. Biol. 26, 2094–2104. https://doi.org/10.1096/fj.11-200790

Kelland, L.R., 1993. New platinum antitumor complexes. Crit. Rev. Oncol. Hematol. 15, 191–219. https://doi.org/10.1016/1040-8428(93)90042-3

Kent, T., Chandramouly, G., McDevitt, S.M., Ozdemir, A.Y., Pomerantz, R.T., 2015. Mechanism of microhomology-mediated end-joining promoted by human DNA polymerase θ. Nat. Struct. Mol. Biol. 22, 230–237. https://doi.org/10.1038/nsmb.2961

Keppler, D., 2011. Multidrug resistance proteins (MRPs, ABCCs): importance for pathophysiology and drug therapy. Handb. Exp. Pharmacol. 299–323. https://doi.org/10.1007/978-3-642-14541-4_8

Kim, Y.-J., Wilson, D.M., 2012. Overview of base excision repair biochemistry. Curr. Mol. Pharmacol. 5, 3–13. https://doi.org/10.2174/1874467211205010003

Kinsella, T.J., 2009. Understanding DNA damage response and DNA repair pathways: applications to more targeted cancer therapeutics. Semin. Oncol. 36, S42-51. https://doi.org/10.1053/j.seminoncol.2009.02.004

Kirschner, K., Melton, D.W., 2010. Multiple roles of the ERCC1-XPF endonuclease in DNA repair and resistance to anticancer drugs. Anticancer Res. 30, 3223–3232.

Kitao, H., Iimori, M., Kataoka, Y., Wakasa, T., Tokunaga, E., Saeki, H., Oki, E., Maehara, Y., 2018. DNA replication stress and cancer chemotherapy. Cancer Sci. 109, 264–271. https://doi.org/10.1111/cas.13455

Kiwerska, K., Szyfter, K., 2019. DNA repair in cancer initiation, progression, and therapy-a double-edged sword. J. Appl. Genet. 60, 329–334. https://doi.org/10.1007/s13353-019-00516-9

Kleih, M., Böpple, K., Dong, M., Gaißler, A., Heine, S., Olayioye, M.A., Aulitzky, W.E., Essmann, F., 2019. Direct impact of cisplatin on mitochondria induces ROS production that dictates cell fate of ovarian cancer cells. Cell Death Dis. 10, 851. https://doi.org/10.1038/s41419-019-2081-4

Knobel, P.A., Belotserkovskaya, R., Galanty, Y., Schmidt, C.K., Jackson, S.P., Stracker, T.H., 2014. USP28 is recruited to sites of DNA damage by the tandem BRCT domains of 53BP1 but plays a minor role in double-strand break metabolism. Mol. Cell. Biol. 34, 2062–2074. https://doi.org/10.1128/MCB.00197-14

Knobel, P.A., Kotov, I.N., Felley-Bosco, E., Stahel, R.A., Marti, T.M., 2011. Inhibition of REV3 expression induces persistent DNA damage and growth arrest in cancer cells. Neoplasia N. Y. N 13, 961–970. https://doi.org/10.1593/neo.11828

Kobayashi, H., Ohno, S., Sasaki, Y., Matsuura, M., 2013. Hereditary breast and ovarian cancer susceptibility genes (review). Oncol. Rep. 30, 1019–1029. https://doi.org/10.3892/or.2013.2541

Komiyama, S., Katabuchi, H., Mikami, M., Nagase, S., Okamoto, A., Ito, K., Morishige, K., Suzuki, N., Kaneuchi, M., Yaegashi, N., Udagawa, Y., Yoshikawa, H., 2016. Japan Society of Gynecologic Oncology guidelines 2015 for the treatment of ovarian cancer including primary peritoneal cancer and fallopian tube cancer. Int. J. Clin. Oncol. 21, 435–446. https://doi.org/10.1007/s10147-016-0985-x

Kondrashova, O., Nguyen, M., Shield-Artin, K., Tinker, A.V., Teng, N.N.H., Harrell, M.I., Kuiper, M.J., Ho, G.-Y., Barker, H., Jasin, M., Prakash, R., Kass, E.M., Sullivan, M.R., Brunette, G.J., Bernstein, K.A., Coleman, R.L., Floquet, A., Friedlander, M., Kichenadasse, G., O'Malley, D.M., Oza, A., Sun, J., Robillard, L., Maloney, L., Bowtell, D., Giordano, H., Wakefield, M.J., Kaufmann, S.H., Simmons, A.D., Harding, T.C., Raponi, M., McNeish, I.A., Swisher, E.M., Lin, K.K., Scott, C.L., AOCS Study Group, 2017. Secondary Somatic Mutations Restoring RAD51C and RAD51D Associated with Acquired Resistance to the PARP Inhibitor Rucaparib in High-Grade Ovarian Carcinoma. Cancer Discov. 7, 984–998. https://doi.org/10.1158/2159-8290.CD-17-0419

Kondrashova, O., Topp, M., Nesic, K., Lieschke, E., Ho, G.-Y., Harrell, M.I., Zapparoli, G.V., Hadley, A., Holian, R., Boehm, E., Heong, V., Sanij, E., Pearson, R.B., Krais, J.J., Johnson, N., McNally, O., Ananda, S., Alsop, K., Hutt, K.J., Kaufmann, S.H., Lin, K.K., Harding, T.C., Traficante, N., Australian Ovarian Cancer Study (AOCS), deFazio, A., McNeish, I.A., Bowtell, D.D., Swisher, E.M., Dobrovic, A., Wakefield, M.J., Scott, C.L., 2018. Methylation of all BRCA1 copies predicts response to the PARP inhibitor rucaparib in ovarian carcinoma. Nat. Commun. 9, 3970. https://doi.org/10.1038/s41467-018-05564-z

Konstantinopoulos, P.A., Ceccaldi, R., Shapiro, G.I., D'Andrea, A.D., 2015. Homologous Recombination Deficiency: Exploiting the Fundamental Vulnerability of Ovarian Cancer. Cancer Discov. 5, 1137–1154. https://doi.org/10.1158/2159-8290.CD-15-0714

Konstantinopoulos, P.A., Lheureux, S., Moore, K.N., 2020. PARP Inhibitors for Ovarian Cancer: Current Indications, Future Combinations, and Novel Assets in Development to Target DNA Damage Repair. Am. Soc. Clin. Oncol. Educ. Book Am. Soc. Clin. Oncol. Annu. Meet. 40, 1–16. https://doi.org/10.1200/EDBK_288015

Kottemann, M.C., Smogorzewska, A., 2013. Fanconi anaemia and the repair of Watson and Crick DNA crosslinks. Nature 493, 356–363. https://doi.org/10.1038/nature11863

Kroeger, P.T., Drapkin, R., 2017. Pathogenesis and heterogeneity of ovarian cancer. Curr. Opin. Obstet. Gynecol. 29, 26–34. https://doi.org/10.1097/GCO.0000000000000340

Kuhn, E., Kurman, R.J., Shih, I.-M., 2012. Ovarian Cancer Is an Imported Disease: Fact or Fiction? Curr. Obstet. Gynecol. Rep. 1, 1–9. https://doi.org/10.1007/s13669-011-0004-1

Kunkel, T.A., Erie, D.A., 2015. Eukaryotic Mismatch Repair in Relation to DNA Replication. Annu. Rev. Genet. 49, 291–313. https://doi.org/10.1146/annurev-genet-112414-054722

Kuo, M.-S., Adam, J., Dorvault, N., Robin, A., Friboulet, L., Soria, J.-C., Olaussen, K.A., 2018. A novel antibody-based approach to detect the functional ERCC1-202 isoform. DNA Repair 64, 34–44. https://doi.org/10.1016/j.dnarep.2018.02.002

Kurman, R.J., Shih, I.-M., 2016. The Dualistic Model of Ovarian Carcinogenesis: Revisited, Revised, and Expanded. Am. J. Pathol. 186, 733–747. https://doi.org/10.1016/j.ajpath.2015.11.011

Kurman, R.J., Shih, I.-M., 2011. Molecular pathogenesis and extraovarian origin of epithelial ovarian cancer--shifting the paradigm. Hum. Pathol. 42, 918–931. https://doi.org/10.1016/j.humpath.2011.03.003

Kurman, R.J., Shih, I.-M., 2010. The origin and pathogenesis of epithelial ovarian cancer: a proposed unifying theory. Am. J. Surg. Pathol. 34, 433–443. https://doi.org/10.1097/PAS.0b013e3181cf3d79

Kurman, R.J., Shih, I.-M., 2008. Pathogenesis of ovarian cancer: lessons from morphology and molecular biology and their clinical implications. Int. J. Gynecol. Pathol. Off. J. Int. Soc. Gynecol. Pathol. 27, 151–160. https://doi.org/10.1097/PGP.0b013e318161e4f5

La Vecchia, C., 2017. Ovarian cancer: epidemiology and risk factors. Eur. J. Cancer Prev. Off. J. Eur. Cancer Prev. Organ. ECP 26, 55–62. https://doi.org/10.1097/CEJ.0000000000000217

Lahtz, C., Pfeifer, G.P., 2011. Epigenetic changes of DNA repair genes in cancer. J. Mol. Cell Biol. 3, 51–58. https://doi.org/10.1093/jmcb/mjq053

Lauchlan, S.C., 1972. The secondary Müllerian system. Obstet. Gynecol. Surv. 27, 133–146. https://doi.org/10.1097/00006254-197203000-00001

Lawrie, T.A., Bryant, A., Cameron, A., Gray, E., Morrison, J., 2013. Pegylated liposomal doxorubicin for relapsed epithelial ovarian cancer. Cochrane Database Syst. Rev. CD006910. https://doi.org/10.1002/14651858.CD006910.pub2

Ledermann, J., Harter, P., Gourley, C., Friedlander, M., Vergote, I., Rustin, G., Scott, C., Meier, W., Shapira-Frommer, R., Safra, T., Matei, D., Macpherson, E., Watkins, C., Carmichael, J., Matulonis, U., 2012. Olaparib maintenance therapy in platinum-sensitive relapsed ovarian cancer. N. Engl. J. Med. 366, 1382–1392. https://doi.org/10.1056/NEJMoa1105535

Ledermann, J., Harter, P., Gourley, C., Friedlander, M., Vergote, I., Rustin, G., Scott, C.L., Meier, W., Shapira-Frommer, R., Safra, T., Matei, D., Fielding, A., Spencer, S., Dougherty, B., Orr, M., Hodgson, D., Barrett, J.C., Matulonis, U., 2014. Olaparib maintenance therapy in patients with platinum-sensitive relapsed serous ovarian cancer: a preplanned retrospective analysis of outcomes by BRCA status in a randomised phase 2 trial. Lancet Oncol. 15, 852–861. https://doi.org/10.1016/S1470-2045(14)70228-1

Lee, J.-H., Chae, J.-W., Kim, J.K., Kim, H.J., Chung, J.Y., Kim, Y.-H., 2015. Inhibition of cisplatin-resistance by RNA interference targeting metallothionein using reducible oligo-peptoplex. J. Control. Release Off. J. Control. Release Soc. 215, 82–90. https://doi.org/10.1016/j.jconrel.2015.07.015

Lehmann, A.R., 2003. DNA repair-deficient diseases, xeroderma pigmentosum, Cockayne syndrome and trichothiodystrophy. Biochimie 85, 1101–1111. https://doi.org/10.1016/j.biochi.2003.09.010

Leskela, S., Romero, I., Cristobal, E., Pérez-Mies, B., Rosa-Rosa, J.M., Gutierrez-Pecharroman, A., Caniego-Casas, T., Santón, A., Ojeda, B., López-Reig, R., Palacios-Berraquero, M.L., García, Á., Ibarra, J., Hakim, S., Guarch, R., López-Guerrero, J.A., Poveda, A., Palacios, J., 2020. Mismatch Repair Deficiency in Ovarian Carcinoma: Frequency, Causes, and Consequences. Am. J. Surg. Pathol. 44, 649–656. https://doi.org/10.1097/PAS.0000000000001432

Levanon, K., Crum, C., Drapkin, R., 2008. New insights into the pathogenesis of serous ovarian cancer and its clinical impact. J. Clin. Oncol. Off. J. Am. Soc. Clin. Oncol. 26, 5284–5293. https://doi.org/10.1200/JCO.2008.18.1107

Levine, D.A., Bogomolniy, F., Yee, C.J., Lash, A., Barakat, R.R., Borgen, P.I., Boyd, J., 2005. Frequent mutation of the PIK3CA gene in ovarian and breast cancers. Clin. Cancer Res. Off. J. Am. Assoc. Cancer Res. 11, 2875–2878. https://doi.org/10.1158/1078-0432.CCR-04-2142

Lheureux, S., Braunstein, M., Oza, A.M., 2019a. Epithelial ovarian cancer: Evolution of management in the era of precision medicine. CA. Cancer J. Clin. 69, 280–304. https://doi.org/10.3322/caac.21559

Lheureux, S., Gourley, C., Vergote, I., Oza, A.M., 2019b. Epithelial ovarian cancer. Lancet Lond. Engl. 393, 1240–1253. https://doi.org/10.1016/S0140-6736(18)32552-2

Li, J., Fadare, O., Xiang, L., Kong, B., Zheng, W., 2012. Ovarian serous carcinoma: recent concepts on its origin and carcinogenesis. J. Hematol. Oncol.J Hematol Oncol 5, 8. https://doi.org/10.1186/1756-8722-5-8

Lin, K.K., Harrell, M.I., Oza, A.M., Oaknin, A., Ray-Coquard, I., Tinker, A.V., Helman, E., Radke, M.R., Say, C., Vo, L.-T., Mann, E., Isaacson, J.D., Maloney, L., O'Malley, D.M., Chambers, S.K., Kaufmann, S.H., Scott, C.L., Konecny, G.E., Coleman, R.L., Sun, J.X., Giordano, H., Brenton, J.D., Harding, T.C., McNeish, I.A., Swisher, E.M., 2019. BRCA Reversion Mutations in Circulating Tumor DNA Predict Primary and Acquired Resistance to the PARP Inhibitor Rucaparib in High-Grade Ovarian Carcinoma. Cancer Discov. 9, 210–219. https://doi.org/10.1158/2159-8290.CD-18-0715

Lin, X., Howell, S.B., 1999. Effect of loss of DNA mismatch repair on development of topotecan-, gemcitabine-, and paclitaxel-resistant variants after exposure to cisplatin. Mol. Pharmacol. 56, 390–395. https://doi.org/10.1124/mol.56.2.390

Liptay, M., Barbosa, J.S., Rottenberg, S., 2020. Replication Fork Remodeling and Therapy Escape in DNA Damage Response-Deficient Cancers. Front. Oncol. 10, 670. https://doi.org/10.3389/fonc.2020.00670

Liu, F.W., Tewari, K.S., 2016. New Targeted Agents in Gynecologic Cancers: Synthetic Lethality, Homologous Recombination Deficiency, and PARP Inhibitors. Curr. Treat. Options Oncol. 17, 12. https://doi.org/10.1007/s11864-015-0378-9

Liu, Y., Burness, M.L., Martin-Trevino, R., Guy, J., Bai, S., Harouaka, R., Brooks, M.D., Shang, L., Fox, A., Luther, T.K., Davis, A., Baker, T.L., Colacino, J., Clouthier, S.G., Shao, Z.-M., Wicha, M.S., Liu, S., 2017. RAD51 Mediates Resistance of Cancer Stem Cells to PARP Inhibition in Triple-Negative Breast Cancer. Clin. Cancer Res. Off. J. Am. Assoc. Cancer Res. 23, 514–522. https://doi.org/10.1158/1078-0432.CCR-15-1348

Liu, Y., Chanana, P., Davila, J.I., Hou, X., Zanfagnin, V., McGehee, C.D., Goode, E.L., Polley, E.C., Haluska, P., Weroha, S.J., Wang, C., 2019. Gene expression differences between matched pairs of ovarian cancer patient tumors and patient-derived xenografts. Sci. Rep. 9, 6314. https://doi.org/10.1038/s41598-019-42680-2

Liu, Y., Feng, Y., Liu, H., Wu, J., Tang, Y., Wang, Q., 2018. Real-time assessment of platinum sensitivity of primary culture from a patient with ovarian cancer with extensive metastasis and the platinum sensitivity enhancing effect by metformin. Oncol. Lett. 16, 4253–4262. https://doi.org/10.3892/ol.2018.9223

Lord, C.J., Ashworth, A., 2017. PARP inhibitors: Synthetic lethality in the clinic. Science 355, 1152–1158. https://doi.org/10.1126/science.aam7344

Lord, C.J., Ashworth, A., 2016. BRCAness revisited. Nat. Rev. Cancer 16, 110–120. https://doi.org/10.1038/nrc.2015.21

Loret, N., Denys, H., Tummers, P., Berx, G., 2019. The Role of Epithelial-to-Mesenchymal Plasticity in Ovarian Cancer Progression and Therapy Resistance. Cancers 11. https://doi.org/10.3390/cancers11060838

Lupo, B., Trusolino, L., 2014. Inhibition of poly(ADP-ribosyl)ation in cancer: old and new paradigms revisited. Biochim. Biophys. Acta 1846, 201–215. https://doi.org/10.1016/j.bbcan.2014.07.004

Ma, Y., Pannicke, U., Schwarz, K., Lieber, M.R., 2002. Hairpin opening and overhang processing by an Artemis/DNA-dependent protein kinase complex in nonhomologous end joining and V(D)J recombination. Cell 108, 781–794. https://doi.org/10.1016/s0092-8674(02)00671-2

Macerelli, M., Ganzinelli, M., Gouedard, C., Broggini, M., Garassino, M.C., Linardou, H., Damia, G., Wiesmüller, L., 2016. Can the response to a platinum-based therapy be predicted by the DNA repair status in non-small cell lung cancer? Cancer Treat. Rev. 48, 8–19. https://doi.org/10.1016/j.ctrv.2016.05.004

Makovec, T., 2019. Cisplatin and beyond: molecular mechanisms of action and drug resistance development in cancer chemotherapy. Radiol. Oncol. 53, 148–158. https://doi.org/10.2478/raon-2019-0018

Makvandi, M., Xu, K., Lieberman, B.P., Anderson, R.-C., Effron, S.S., Winters, H.D., Zeng, C., McDonald, E.S., Pryma, D.A., Greenberg, R.A., Mach, R.H., 2016. A Radiotracer Strategy to Quantify PARP-1 Expression In Vivo Provides a Biomarker That Can Enable Patient Selection for PARP Inhibitor Therapy. Cancer Res. 76, 4516–4524. https://doi.org/10.1158/0008-5472.CAN-16-0416

Mallen, A.R., Townsend, M.K., Tworoger, S.S., 2018. Risk Factors for Ovarian Carcinoma. Hematol. Oncol. Clin. North Am. 32, 891–902. https://doi.org/10.1016/j.hoc.2018.07.002

Mandilaras, V., Garg, S., Cabanero, M., Tan, Q., Pastrello, C., Burnier, J., Karakasis, K., Wang, L., Dhani, N.C., Butler, M.O., Bedard, P.L., Siu, L.L., Clarke, B., Shaw, P.A., Stockley, T., Jurisica, I., Oza, A.M., Lheureux, S., 2019. TP53 mutations in high grade serous ovarian cancer and impact on clinical outcomes: a comparison of next generation sequencing and bioinformatics analyses. Int. J. Gynecol. Cancer Off. J. Int. Gynecol. Cancer Soc. https://doi.org/10.1136/ijgc-2018-000087

Maréchal, A., Zou, L., 2013. DNA damage sensing by the ATM and ATR kinases. Cold Spring Harb. Perspect. Biol. 5. https://doi.org/10.1101/cshperspect.a012716

Markman, M., Bundy, B.N., Alberts, D.S., Fowler, J.M., Clark-Pearson, D.L., Carson, L.F., Wadler, S., Sickel, J., 2001. Phase III trial of standard-dose intravenous cisplatin plus paclitaxel versus moderately high-dose carboplatin followed by intravenous paclitaxel and intraperitoneal cisplatin in small-volume stage III ovarian carcinoma: an intergroup study of the Gynecologic Oncology Group, Southwestern Oncology Group, and Eastern Cooperative Oncology Group. J. Clin. Oncol. Off. J. Am. Soc. Clin. Oncol. 19, 1001–1007. https://doi.org/10.1200/JCO.2001.19.4.1001

Marquard, A.M., Eklund, A.C., Joshi, T., Krzystanek, M., Favero, F., Wang, Z.C., Richardson, A.L., Silver, D.P., Szallasi, Z., Birkbak, N.J., 2015. Pan-cancer analysis of genomic scar signatures associated with homologous recombination deficiency suggests novel indications for existing cancer drugs. Biomark. Res. 3, 9. https://doi.org/10.1186/s40364-015-0033-4

Marrero, A., Lawrence, S., Wilsker, D., Voth, A.R., Kinders, R.J., 2016. Translating pharmacodynamic biomarkers from bench to bedside: analytical validation and fit-for-purpose studies to qualify multiplex immunofluorescent assays for use on clinical core biopsy specimens. Semin. Oncol. 43, 453–463. https://doi.org/10.1053/j.seminoncol.2016.06.003

Marth, C., Reimer, D., Zeimet, A.G., 2017. Front-line therapy of advanced epithelial ovarian cancer: standard treatment. Ann. Oncol. Off. J. Eur. Soc. Med. Oncol. 28, viii36–viii39. https://doi.org/10.1093/annonc/mdx450

Martin, L.P., Hamilton, T.C., Schilder, R.J., 2008. Platinum resistance: the role of DNA repair pathways. Clin. Cancer Res. Off. J. Am. Assoc. Cancer Res. 14, 1291–1295. https://doi.org/10.1158/1078-0432.CCR-07-2238

Martinez-Balibrea, E., Martínez-Cardús, A., Musulén, E., Ginés, A., Manzano, J.L., Aranda, E., Plasencia, C., Neamati, N., Abad, A., 2009. Increased levels of copper efflux transporter ATP7B are associated with poor outcome in colorectal cancer patients receiving oxaliplatin-based chemotherapy. Int. J. Cancer 124, 2905–2910. https://doi.org/10.1002/ijc.24273

Marusyk, A., Janiszewska, M., Polyak, K., 2020. Intratumor Heterogeneity: The Rosetta Stone of Therapy Resistance. Cancer Cell 37, 471–484. https://doi.org/10.1016/j.ccell.2020.03.007

Mateo, J., Lord, C.J., Serra, V., Tutt, A., Balmaña, J., Castroviejo-Bermejo, M., Cruz, C., Oaknin, A., Kaye, S.B., de Bono, J.S., 2019. A decade of clinical development of

PARP inhibitors in perspective. Ann. Oncol. Off. J. Eur. Soc. Med. Oncol. 30, 1437–1447. https://doi.org/10.1093/annonc/mdz192

McCormick, A., Donoghue, P., Dixon, M., O'Sullivan, R., O'Donnell, R.L., Murray, J., Kaufmann, A., Curtin, N.J., Edmondson, R.J., 2017. Ovarian Cancers Harbor Defects in Nonhomologous End Joining Resulting in Resistance to Rucaparib. Clin. Cancer Res. Off. J. Am. Assoc. Cancer Res. 23, 2050–2060. https://doi.org/10.1158/1078-0432.CCR-16-0564

McGuire, W.P., Hoskins, W.J., Brady, M.F., Kucera, P.R., Partridge, E.E., Look, K.Y., Clarke-Pearson, D.L., Davidson, M., 1996. Cyclophosphamide and cisplatin versus paclitaxel and cisplatin: a phase III randomized trial in patients with suboptimal stage III/IV ovarian cancer (from the Gynecologic Oncology Group). Semin. Oncol. 23, 40–47.

McMullen, M., Karakasis, K., Madariaga, A., Oza, A.M., 2020. Overcoming Platinum and PARP-Inhibitor Resistance in Ovarian Cancer. Cancers 12. https://doi.org/10.3390/cancers12061607

Meinhold-Heerlein, I., Fotopoulou, C., Harter, P., Kurzeder, C., Mustea, A., Wimberger, P., Hauptmann, S., Sehouli, J., 2016. The new WHO classification of ovarian, fallopian tube, and primary peritoneal cancer and its clinical implications. Arch. Gynecol. Obstet. 293, 695–700. https://doi.org/10.1007/s00404-016-4035-8

Mendes-Pereira, A.M., Martin, S.A., Brough, R., McCarthy, A., Taylor, J.R., Kim, J.-S., Waldman, T., Lord, C.J., Ashworth, A., 2009. Synthetic lethal targeting of PTEN mutant cells with PARP inhibitors. EMBO Mol. Med. 1, 315–322. https://doi.org/10.1002/emmm.200900041

Mesquita, K.A., Alabdullah, M., Griffin, M., Toss, M.S., Fatah, T.M.A.A., Alblihy, A., Moseley, P., Chan, S.Y.T., Rakha, E.A., Madhusudan, S., 2019. ERCC1-XPF deficiency is a predictor of olaparib induced synthetic lethality and platinum sensitivity in epithelial ovarian cancers. Gynecol. Oncol. 153, 416–424. https://doi.org/10.1016/j.ygyno.2019.02.014

Michl, J., Zimmer, J., Tarsounas, M., 2016. Interplay between Fanconi anemia and homologous recombination pathways in genome integrity. EMBO J. 35, 909–923. https://doi.org/10.15252/embj.201693860

Milanesio, M.C., Giordano, S., Valabrega, G., 2020. Clinical Implications of DNA Repair Defects in High-Grade Serous Ovarian Carcinomas. Cancers 12. https://doi.org/10.3390/cancers12051315

Mirza, M.R., Monk, B.J., Herrstedt, J., Oza, A.M., Mahner, S., Redondo, A., Fabbro, M., Ledermann, J.A., Lorusso, D., Vergote, I., Ben-Baruch, N.E., Marth, C., Mądry, R., Christensen, R.D., Berek, J.S., Dørum, A., Tinker, A.V., du Bois, A., González-Martín, A., Follana, P., Benigno, B., Rosenberg, P., Gilbert, L., Rimel, B.J., Buscema, J., Balser, J.P., Agarwal, S., Matulonis, U.A., ENGOT-OV16/NOVA Investigators, 2016a. Niraparib Maintenance Therapy in Platinum-Sensitive, Recurrent Ovarian Cancer. N. Engl. J. Med. 375, 2154–2164. https://doi.org/10.1056/NEJMoa1611310

Mirza, M.R., Monk, B.J., Herrstedt, J., Oza, A.M., Mahner, S., Redondo, A., Fabbro, M., Ledermann, J.A., Lorusso, D., Vergote, I., Ben-Baruch, N.E., Marth, C., Mądry, R.,

Christensen, R.D., Berek, J.S., Dørum, A., Tinker, A.V., du Bois, A., González-Martín, A., Follana, P., Benigno, B., Rosenberg, P., Gilbert, L., Rimel, B.J., Buscema, J., Balser, J.P., Agarwal, S., Matulonis, U.A., ENGOT-OV16/NOVA Investigators, 2016b. Niraparib Maintenance Therapy in Platinum-Sensitive, Recurrent Ovarian Cancer. N. Engl. J. Med. 375, 2154–2164. https://doi.org/10.1056/NEJMoa1611310

Mistry, P., Harrap, K.R., 1991. Historical aspects of glutathione and cancer chemotherapy. Pharmacol. Ther. 49, 125–132. https://doi.org/10.1016/0163-7258(91)90026-i

Mittempergher, L., 2016. Genomic Characterization of High-Grade Serous Ovarian Cancer: Dissecting Its Molecular Heterogeneity as a Road Towards Effective Therapeutic Strategies. Curr. Oncol. Rep. 18, 44. https://doi.org/10.1007/s11912-016-0526-9

Mitxelena, J., Apraiz, A., Vallejo-Rodríguez, J., García-Santisteban, I., Fullaondo, A., Alvarez-Fernández, M., Malumbres, M., Zubiaga, A.M., 2018. An E2F7-dependent transcriptional program modulates DNA damage repair and genomic stability. Nucleic Acids Res. 46, 4546–4559. https://doi.org/10.1093/nar/gky218

Möltgen, S., Piumatti, E., Massafra, G.M., Metzger, S., Jaehde, U., Kalayda, G.V., 2020. Cisplatin Protein Binding Partners and Their Relevance for Platinum Drug Sensitivity. Cells 9. https://doi.org/10.3390/cells9061322

Momenimovahed, Z., Tiznobaik, A., Taheri, S., Salehiniya, H., 2019. Ovarian cancer in the world: epidemiology and risk factors. Int. J. Womens Health 11, 287–299. https://doi.org/10.2147/IJWH.S197604

Monk, B.J., Minion, L.E., Coleman, R.L., 2016. Anti-angiogenic agents in ovarian cancer: past, present, and future. Ann. Oncol. Off. J. Eur. Soc. Med. Oncol. 27 Suppl 1, i33–i39. https://doi.org/10.1093/annonc/mdw093

Morice, P., Gouy, S., Leary, A., 2019. Mucinous Ovarian Carcinoma. N. Engl. J. Med. 380, 1256–1266. https://doi.org/10.1056/NEJMra1813254

Morrison, J.C., Blanco, L.Z., Vang, R., Ronnett, B.M., 2015. Incidental serous tubal intraepithelial carcinoma and early invasive serous carcinoma in the nonprophylactic setting: analysis of a case series. Am. J. Surg. Pathol. 39, 442–453. https://doi.org/10.1097/PAS.0000000000000352

Morse, C.B., Toukatly, M.N., Kilgore, M.R., Agnew, K.J., Bernards, S.S., Norquist, B.M., Pennington, K.P., Garcia, R.L., Liao, J.B., Swisher, E.M., 2019. Tumor infiltrating lymphocytes and homologous recombination deficiency are independently associated with improved survival in ovarian carcinoma. Gynecol. Oncol. 153, 217–222. https://doi.org/10.1016/j.ygyno.2019.02.011

Mortusewicz, O., Leonhardt, H., 2007. XRCC1 and PCNA are loading platforms with distinct kinetic properties and different capacities to respond to multiple DNA lesions. BMC Mol. Biol. 8, 81. https://doi.org/10.1186/1471-2199-8-81

Mouw, K.W., D'Andrea, A.D., Konstantinopoulos, P.A., 2015. Nucleotide excision repair (NER) alterations as evolving biomarkers and therapeutic targets in epithelial cancers. Oncoscience 2, 942–943. https://doi.org/10.18632/oncoscience.283

Muggia, F., 2009. Platinum compounds 30 years after the introduction of cisplatin: implications for the treatment of ovarian cancer. Gynecol. Oncol. 112, 275–281. https://doi.org/10.1016/j.ygyno.2008.09.034

Muggia, F.M., Braly, P.S., Brady, M.F., Sutton, G., Niemann, T.H., Lentz, S.L., Alvarez, R.D., Kucera, P.R., Small, J.M., 2000. Phase III randomized study of cisplatin versus paclitaxel versus cisplatin and paclitaxel in patients with suboptimal stage III or IV ovarian cancer: a gynecologic oncology group study. J. Clin. Oncol. Off. J. Am. Soc. Clin. Oncol. 18, 106–115. https://doi.org/10.1200/JCO.2000.18.1.106

Mukherjee, C., Tripathi, V., Manolika, E.M., Heijink, A.M., Ricci, G., Merzouk, S., de Boer, H.R., Demmers, J., van Vugt, M.A.T.M., Ray Chaudhuri, A., 2019. RIF1 promotes replication fork protection and efficient restart to maintain genome stability. Nat. Commun. 10, 3287. https://doi.org/10.1038/s41467-019-11246-1

Mukhopadhyay, A., Elattar, A., Cerbinskaite, A., Wilkinson, S.J., Drew, Y., Kyle, S., Los, G., Hostomsky, Z., Edmondson, R.J., Curtin, N.J., 2010. Development of a functional assay for homologous recombination status in primary cultures of epithelial ovarian tumor and correlation with sensitivity to poly(ADP-ribose) polymerase inhibitors. Clin. Cancer Res. Off. J. Am. Assoc. Cancer Res. 16, 2344–2351. https://doi.org/10.1158/1078-0432.CCR-09-2758

Murai, J., Feng, Y., Yu, G.K., Ru, Y., Tang, S.-W., Shen, Y., Pommier, Y., 2016. Resistance to PARP inhibitors by SLFN11 inactivation can be overcome by ATR inhibition. Oncotarget 7, 76534–76550. https://doi.org/10.18632/oncotarget.12266

Murai, J., Huang, S.N., Das, B.B., Renaud, A., Zhang, Y., Doroshow, J.H., Ji, J., Takeda, S., Pommier, Y., 2012. Trapping of PARP1 and PARP2 by Clinical PARP Inhibitors. Cancer Res. 72, 5588–5599. https://doi.org/10.1158/0008-5472.CAN-12-2753

Murai, J., Tang, S.-W., Leo, E., Baechler, S.A., Redon, C.E., Zhang, H., Al Abo, M., Rajapakse, V.N., Nakamura, E., Jenkins, L.M.M., Aladjem, M.I., Pommier, Y., 2018. SLFN11 Blocks Stressed Replication Forks Independently of ATR. Mol. Cell 69, 371-384.e6. https://doi.org/10.1016/j.molcel.2018.01.012

Murai, J., Thomas, A., Miettinen, M., Pommier, Y., 2019. Schlafen 11 (SLFN11), a restriction factor for replicative stress induced by DNA-targeting anti-cancer therapies. Pharmacol. Ther. 201, 94–102. https://doi.org/10.1016/j.pharmthera.2019.05.009

Mutch, D.G., Prat, J., 2014. 2014 FIGO staging for ovarian, fallopian tube and peritoneal cancer. Gynecol. Oncol. 133, 401–404. https://doi.org/10.1016/j.ygyno.2014.04.013

Nagaraj, A.B., Joseph, P., Kovalenko, O., Singh, S., Armstrong, A., Redline, R., Resnick, K., Zanotti, K., Waggoner, S., DiFeo, A., 2015. Critical role of Wnt/β-catenin signaling in driving epithelial ovarian cancer platinum resistance. Oncotarget 6, 23720–23734. https://doi.org/10.18632/oncotarget.4690

Naidoo, K., Wai, P.T., Maguire, S.L., Daley, F., Haider, S., Kriplani, D., Campbell, J., Mirza, H., Grigoriadis, A., Tutt, A., Moseley, P.M., Abdel-Fatah, T.M.A., Chan, S.Y.T., Madhusudan, S., Rhaka, E.A., Ellis, I.O., Lord, C.J., Yuan, Y., Green, A.R., Natrajan, R., 2018. Evaluation of CDK12 Protein Expression as a Potential Novel Biomarker for DNA Damage Response-Targeted Therapies in Breast Cancer. Mol. Cancer Ther. 17, 306–315. https://doi.org/10.1158/1535-7163.MCT-17-0760

Naipal, K.A.T., Verkaik, N.S., Ameziane, N., van Deurzen, C.H.M., Ter Brugge, P., Meijers, M., Sieuwerts, A.M., Martens, J.W., O'Connor, M.J., Vrieling, H., Hoeijmakers, J.H.J., Jonkers, J., Kanaar, R., de Winter, J.P., Vreeswijk, M.P., Jager, A., van Gent, D.C., 2014. Functional ex vivo assay to select homologous recombination-deficient breast tumors for PARP inhibitor treatment. Clin. Cancer Res. Off. J. Am. Assoc. Cancer Res. 20, 4816–4826. https://doi.org/10.1158/1078-0432.CCR-14-0571

Nik-Zainal, S., Davies, H., Staaf, J., Ramakrishna, M., Glodzik, D., Zou, X., Martincorena, I., Alexandrov, L.B., Martin, S., Wedge, D.C., Van Loo, P., Ju, Y.S., Smid, M., Brinkman, A.B., Morganella, S., Aure, M.R., Lingjærde, O.C., Langerød, A., Ringnér, M., Ahn, S.-M., Boyault, S., Brock, J.E., Broeks, A., Butler, A., Desmedt, C., Dirix, L., Dronov, S., Fatima, A., Foekens, J.A., Gerstung, M., Hooijer, G.K.J., Jang, S.J., Jones, D.R., Kim, H.-Y., King, T.A., Krishnamurthy, S., Lee, H.J., Lee, J.-Y., Li, Y., McLaren, S., Menzies, A., Mustonen, V., O'Meara, S., Pauporté, I., Pivot, X., Purdie, C.A., Raine, K., Ramakrishnan, K., Rodríguez-González, F.G., Romieu, G., Sieuwerts, A.M., Simpson, P.T., Shepherd, R., Stebbings, L., Stefansson, O.A., Teague, J., Tommasi, S., Treilleux, I., Van den Eynden, G.G., Vermeulen, P., Vincent-Salomon, A., Yates, L., Caldas, C., van't Veer, L., Tutt, A., Knappskog, S., Tan, B.K.T., Jonkers, J., Borg, Å., Ueno, N.T., Sotiriou, C., Viari, A., Futreal, P.A., Campbell, P.J., Span, P.N., Van Laere, S., Lakhani, S.R., Eyfjord, J.E., Thompson, A.M., Birney, E., Stunnenberg, H.G., van de Vijver, M.J., Martens, J.W.M., Børresen-Dale, A.-L., Richardson, A.L., Kong, G., Thomas, G., Stratton, M.R., 2016. Landscape of somatic mutations in 560 breast cancer whole-genome sequences. Nature 534, 47–54. https://doi.org/10.1038/nature17676

Noordermeer, S.M., Adam, S., Setiaputra, D., Barazas, M., Pettitt, S.J., Ling, A.K., Olivieri, M., Álvarez-Quilón, A., Moatti, N., Zimmermann, M., Annunziato, S., Krastev, D.B., Song, F., Brandsma, I., Frankum, J., Brough, R., Sherker, A., Landry, S., Szilard, R.K., Munro, M.M., McEwan, A., Goullet de Rugy, T., Lin, Z.-Y., Hart, T., Moffat, J., Gingras, A.-C., Martin, A., van Attikum, H., Jonkers, J., Lord, C.J., Rottenberg, S., Durocher, D., 2018. The shieldin complex mediates 53BP1-dependent DNA repair. Nature 560, 117–121. https://doi.org/10.1038/s41586-018-0340-7

Noordermeer, S.M., van Attikum, H., 2019. PARP Inhibitor Resistance: A Tug-of-War in BRCA-Mutated Cells. Trends Cell Biol. 29, 820–834. https://doi.org/10.1016/j.tcb.2019.07.008

Norquist, B., Wurz, K.A., Pennil, C.C., Garcia, R., Gross, J., Sakai, W., Karlan, B.Y., Taniguchi, T., Swisher, E.M., 2011. Secondary somatic mutations restoring BRCA1/2 predict chemotherapy resistance in hereditary ovarian carcinomas. J. Clin. Oncol. Off. J. Am. Soc. Clin. Oncol. 29, 3008–3015. https://doi.org/10.1200/JCO.2010.34.2980

Norquist, B.M., Brady, M.F., Harrell, M.I., Walsh, T., Lee, M.K., Gulsuner, S., Bernards, S.S., Casadei, S., Burger, R.A., Tewari, K.S., Backes, F., Mannel, R.S., Glaser, G., Bailey, C., Rubin, S., Soper, J., Lankes, H.A., Ramirez, N.C., King, M.C., Birrer, M.J., Swisher, E.M., 2018. Mutations in Homologous Recombination Genes and Outcomes in Ovarian Carcinoma Patients in GOG 218: An NRG Oncology/Gynecologic Oncology Group Study. Clin. Cancer Res. Off. J. Am. Assoc. Cancer Res. 24, 777–783. https://doi.org/10.1158/1078-0432.CCR-17-1327

O'Connor, M.J., 2015. Targeting the DNA Damage Response in Cancer. Mol. Cell 60, 547–560. https://doi.org/10.1016/j.molcel.2015.10.040

Okamura, H., Katabuchi, H., 2005. Pathophysiological dynamics of human ovarian surface epithelial cells in epithelial ovarian carcinogenesis. Int. Rev. Cytol. 242, 1–54. https://doi.org/10.1016/S0074-7696(04)42001-4

Olaussen, K.A., Dunant, A., Fouret, P., Brambilla, E., André, F., Haddad, V., Taranchon, E., Filipits, M., Pirker, R., Popper, H.H., Stahel, R., Sabatier, L., Pignon, J.-P., Tursz, T., Le Chevalier, T., Soria, J.-C., IALT Bio Investigators, 2006. DNA repair by ERCC1 in non-small-cell lung cancer and cisplatin-based adjuvant chemotherapy. N. Engl. J. Med. 355, 983–991. https://doi.org/10.1056/NEJMoa060570

Olaussen, K.A., Postel-Vinay, S., 2016. Predictors of chemotherapy efficacy in non-small-cell lung cancer: a challenging landscape. Ann. Oncol. 27, 2004–2016. https://doi.org/10.1093/annonc/mdw321

Olopade, O.I., Wei, M., 2003. FANCF methylation contributes to chemoselectivity in ovarian cancer. Cancer Cell 3, 417–420. https://doi.org/10.1016/s1535-6108(03)00111-9

Orr, B., Edwards, R.P., 2018a. Diagnosis and Treatment of Ovarian Cancer. Hematol. Oncol. Clin. North Am. 32, 943–964. https://doi.org/10.1016/j.hoc.2018.07.010

Orr, B., Edwards, R.P., 2018b. Diagnosis and Treatment of Ovarian Cancer. Hematol. Oncol. Clin. North Am. 32, 943–964. https://doi.org/10.1016/j.hoc.2018.07.010

Oza, A.M., Tinker, A.V., Oaknin, A., Shapira-Frommer, R., McNeish, I.A., Swisher, E.M., Ray-Coquard, I., Bell-McGuinn, K., Coleman, R.L., O'Malley, D.M., Leary, A., Chen, L.-M., Provencher, D., Ma, L., Brenton, J.D., Konecny, G.E., Castro, C.M., Giordano, H., Maloney, L., Goble, S., Lin, K.K., Sun, J., Raponi, M., Rolfe, L., Kristeleit, R.S., 2017. Antitumor activity and safety of the PARP inhibitor rucaparib in patients with high-grade ovarian carcinoma and a germline or somatic BRCA1 or BRCA2 mutation: Integrated analysis of data from Study 10 and ARIEL2. Gynecol. Oncol. 147, 267–275. https://doi.org/10.1016/j.ygyno.2017.08.022

Ozols, R.F., Bundy, B.N., Greer, B.E., Fowler, J.M., Clarke-Pearson, D., Burger, R.A., Mannel, R.S., DeGeest, K., Hartenbach, E.M., Baergen, R., Gynecologic Oncology Group, 2003. Phase III trial of carboplatin and paclitaxel compared with cisplatin and paclitaxel in patients with optimally resected stage III ovarian cancer: a Gynecologic Oncology Group study. J. Clin. Oncol. Off. J. Am. Soc. Clin. Oncol. 21, 3194–3200. https://doi.org/10.1200/JCO.2003.02.153

Palmirotta, R., Silvestris, E., D'Oronzo, S., Cardascia, A., Silvestris, F., 2017. Ovarian cancer: Novel molecular aspects for clinical assessment. Crit. Rev. Oncol. Hematol. 117, 12–29. https://doi.org/10.1016/j.critrevonc.2017.06.007

Pan, M.-R., Hsieh, H.-J., Dai, H., Hung, W.-C., Li, K., Peng, G., Lin, S.-Y., 2012. Chromodomain helicase DNA-binding protein 4 (CHD4) regulates homologous recombination DNA repair, and its deficiency sensitizes cells to poly(ADP-ribose) polymerase (PARP) inhibitor treatment. J. Biol. Chem. 287, 6764–6772. https://doi.org/10.1074/jbc.M111.287037

Park, K.J., Patel, P., Linkov, I., Jotwani, A., Kauff, N., Pike, M.C., 2018. Observations on the origin of ovarian cortical inclusion cysts in women undergoing risk-reducing salpingo-oophorectomy. Histopathology 72, 766–776. https://doi.org/10.1111/his.13444

Parmar, M.K.B., Ledermann, J.A., Colombo, N., du Bois, A., Delaloye, J.-F., Kristensen, G.B., Wheeler, S., Swart, A.M., Qian, W., Torri, V., Floriani, I., Jayson, G., Lamont, A., Tropé, C., ICON and AGO Collaborators, 2003. Paclitaxel plus platinum-based chemotherapy versus conventional platinum-based chemotherapy in women with relapsed ovarian cancer: the ICON4/AGO-OVAR-2.2 trial. Lancet Lond. Engl. 361, 2099–2106. https://doi.org/10.1016/s0140-6736(03)13718-x

Patch, A.-M., Christie, E.L., Etemadmoghadam, D., Garsed, D.W., George, J., Fereday, S., Nones, K., Cowin, P., Alsop, K., Bailey, P.J., Kassahn, K.S., Newell, F., Quinn, M.C.J., Kazakoff, S., Quek, K., Wilhelm-Benartzi, C., Curry, E., Leong, H.S., Australian Ovarian Cancer Study Group, Hamilton, A., Mileshkin, L., Au-Yeung, G., Kennedy, C., Hung, J., Chiew, Y.-E., Harnett, P., Friedlander, M., Quinn, M., Pyman, J., Cordner, S., O'Brien, P., Leditschke, J., Young, G., Strachan, K., Waring, P., Azar, W., Mitchell, C., Traficante, N., Hendley, J., Thorne, H., Shackleton, M., Miller, D.K., Arnau, G.M., Tothill, R.W., Holloway, T.P., Semple, T., Harliwong, I., Nourse, C., Nourbakhsh, E., Manning, S., Idrisoglu, S., Bruxner, T.J.C., Christ, A.N., Poudel, B., Holmes, O., Anderson, M., Leonard, C., Lonie, A., Hall, N., Wood, S., Taylor, D.F., Xu, Q., Fink, J.L., Waddell, Nick, Drapkin, R., Stronach, E., Gabra, H., Brown, R., Jewell, A., Nagaraj, S.H., Markham, E., Wilson, P.J., Ellul, J., McNally, O., Doyle, M.A., Vedururu, R., Stewart, C., Lengyel, E., Pearson, J.V., Waddell, Nicola, deFazio, A., Grimmond, S.M., Bowtell, D.D.L., 2015. Whole-genome characterization of chemoresistant ovarian cancer. Nature 521, 489–494. https://doi.org/10.1038/nature14410

Patel, A.G., Sarkaria, J.N., Kaufmann, S.H., 2011. Nonhomologous end joining drives poly(ADP-ribose) polymerase (PARP) inhibitor lethality in homologous recombination-deficient cells. Proc. Natl. Acad. Sci. U. S. A. 108, 3406–3411. https://doi.org/10.1073/pnas.1013715108

Pekarik, V., Gumulec, J., Masarik, M., Kizek, R., Adam, V., 2013. Prostate cancer, miRNAs, metallothioneins and resistance to cytostatic drugs. Curr. Med. Chem. 20, 534–544. https://doi.org/10.2174/0929867311320040005

Pellegrino, B., Mateo, J., Serra, V., Balmaña, J., 2019. Controversies in oncology: are genomic tests quantifying homologous recombination repair deficiency (HRD) useful for treatment decision making? ESMO Open 4, e000480. https://doi.org/10.1136/esmoopen-2018-000480

Peltomäki, P., 2003. Role of DNA mismatch repair defects in the pathogenesis of human cancer. J. Clin. Oncol. Off. J. Am. Soc. Clin. Oncol. 21, 1174–1179. https://doi.org/10.1200/JCO.2003.04.060

Pennington, K.P., Walsh, T., Harrell, M.I., Lee, M.K., Pennil, C.C., Rendi, M.H., Thornton, A., Norquist, B.M., Casadei, S., Nord, A.S., Agnew, K.J., Pritchard, C.C., Scroggins, S., Garcia, R.L., King, M.-C., Swisher, E.M., 2014. Germline and somatic mutations in homologous recombination genes predict platinum response and survival in ovarian, fallopian tube, and peritoneal carcinomas. Clin. Cancer Res. Off. J. Am. Assoc. Cancer Res. 20, 764–775. https://doi.org/10.1158/1078-0432.CCR-13-2287

Penninkilampi, R., Eslick, G.D., 2018. Perineal Talc Use and Ovarian Cancer: A Systematic Review and Meta-Analysis. Epidemiol. Camb. Mass 29, 41–49. https://doi.org/10.1097/EDE.0000000000000745

Pérez-López, F.R., Chedraui, P., 2016. Surgical prevention of epithelial ovary cancer without oophorectomy: changing the future. Climacteric J. Int. Menopause Soc. 19, 417–418. https://doi.org/10.1080/13697137.2016.1202914

Pettitt, S.J., Krastev, D.B., Brandsma, I., Dréan, A., Song, F., Aleksandrov, R., Harrell, M.I., Menon, M., Brough, R., Campbell, J., Frankum, J., Ranes, M., Pemberton, H.N., Rafiq, R., Fenwick, K., Swain, A., Guettler, S., Lee, J.-M., Swisher, E.M., Stoynov, S., Yusa, K., Ashworth, A., Lord, C.J., 2018. Genome-wide and high-density CRISPR-Cas9 screens identify point mutations in PARP1 causing PARP inhibitor resistance. Nat. Commun. 9, 1849. https://doi.org/10.1038/s41467-018-03917-2

Pettitt, S.J., Rehman, F.L., Bajrami, I., Brough, R., Wallberg, F., Kozarewa, I., Fenwick, K., Assiotis, I., Chen, L., Campbell, J., Lord, C.J., Ashworth, A., 2013. A genetic screen using the PiggyBac transposon in haploid cells identifies Parp1 as a mediator of olaparib toxicity. PloS One 8, e61520. https://doi.org/10.1371/journal.pone.0061520

Piek, J.M.J., Verheijen, R.H.M., Kenemans, P., Massuger, L.F., Bulten, H., van Diest, P.J., 2003. BRCA1/2-related ovarian cancers are of tubal origin: a hypothesis. Gynecol. Oncol. 90, 491. https://doi.org/10.1016/s0090-8258(03)00365-2

Pignata, S., Scambia, G., Ferrandina, G., Savarese, A., Sorio, R., Breda, E., Gebbia, V., Musso, P., Frigerio, L., Del Medico, P., Lombardi, A.V., Febbraro, A., Scollo, P., Ferro, A., Tamberi, S., Brandes, A., Ravaioli, A., Valerio, M.R., Aitini, E., Natale, D., Scaltriti, L., Greggi, S., Pisano, C., Lorusso, D., Salutari, V., Legge, F., Di Maio, M., Morabito, A., Gallo, C., Perrone, F., 2011. Carboplatin plus paclitaxel versus carboplatin plus pegylated liposomal doxorubicin as first-line treatment for patients with ovarian cancer: the MITO-2 randomized phase III trial. J. Clin. Oncol. Off. J. Am. Soc. Clin. Oncol. 29, 3628–3635. https://doi.org/10.1200/JCO.2010.33.8566

Pilié, P.G., Tang, C., Mills, G.B., Yap, T.A., 2019. State-of-the-art strategies for targeting the DNA damage response in cancer. Nat. Rev. Clin. Oncol. 16, 81–104. https://doi.org/10.1038/s41571-018-0114-z

Pilla, D., Bosisio, F.M., Marotta, R., Faggi, S., Forlani, P., Falavigna, M., Biunno, I., Martella, E., De Blasio, P., Borghesi, S., Cattoretti, G., 2012. Tissue microarray design and construction for scientific, industrial and diagnostic use. J. Pathol. Inform. 3, 42. https://doi.org/10.4103/2153-3539.104904

Popova, T., Manié, E., Rieunier, G., Caux-Moncoutier, V., Tirapo, C., Dubois, T., Delattre, O., Sigal-Zafrani, B., Bollet, M., Longy, M., Houdayer, C., Sastre-Garau, X., Vincent-Salomon, A., Stoppa-Lyonnet, D., Stern, M.-H., 2012. Ploidy and large-scale genomic instability consistently identify basal-like breast carcinomas with BRCA1/2 inactivation. Cancer Res. 72, 5454–5462. https://doi.org/10.1158/0008-5472.CAN-12-1470

Prakash, R., Zhang, Y., Feng, W., Jasin, M., 2015. Homologous recombination and human health: the roles of BRCA1, BRCA2, and associated proteins. Cold Spring Harb. Perspect. Biol. 7, a016600. https://doi.org/10.1101/cshperspect.a016600

Prat, J., 2012. New insights into ovarian cancer pathology. Ann. Oncol. Off. J. Eur. Soc. Med. Oncol. 23 Suppl 10, x111-117. https://doi.org/10.1093/annonc/mds300

Prat, J., D'Angelo, E., Espinosa, I., 2018. Ovarian carcinomas: at least five different diseases with distinct histological features and molecular genetics. Hum. Pathol. 80, 11–27. https://doi.org/10.1016/j.humpath.2018.06.018

Prat, J., FIGO Committee on Gynecologic Oncology, 2015. FIGO's staging classification for cancer of the ovary, fallopian tube, and peritoneum: abridged republication. J. Gynecol. Oncol. 26, 87–89. https://doi.org/10.3802/jgo.2015.26.2.87

Pujade-Lauraine, E., Ledermann, J.A., Selle, F., Gebski, V., Penson, R.T., Oza, A.M., Korach, J., Huzarski, T., Poveda, A., Pignata, S., Friedlander, M., Colombo, N., Harter, P., Fujiwara, K., Ray-Coquard, I., Banerjee, S., Liu, J., Lowe, E.S., Bloomfield, R., Pautier, P., SOLO2/ENGOT-Ov21 investigators, 2017. Olaparib tablets as maintenance therapy in patients with platinum-sensitive, relapsed ovarian cancer and a BRCA1/2 mutation (SOLO2/ENGOT-Ov21): a double-blind, randomised, placebo-controlled, phase 3 trial. Lancet Oncol. 18, 1274–1284. https://doi.org/10.1016/S1470-2045(17)30469-2

Rabban, J.T., Garg, K., Crawford, B., Chen, L., Zaloudek, C.J., 2014. Early detection of high-grade tubal serous carcinoma in women at low risk for hereditary breast and ovarian cancer syndrome by systematic examination of fallopian tubes incidentally removed during benign surgery. Am. J. Surg. Pathol. 38, 729–742. https://doi.org/10.1097/PAS.0000000000000199

Rafii, S., Gourley, C., Kumar, R., Geuna, E., Ern Ang, J., Rye, T., Chen, L.-M., Shapira-Frommer, R., Friedlander, M., Matulonis, U., De Greve, J., Oza, A.M., Banerjee, S., Molife, L.R., Gore, M.E., Kaye, S.B., Yap, T.A., 2017. Baseline clinical predictors of antitumor response to the PARP inhibitor olaparib in germline BRCA1/2 mutated patients with advanced ovarian cancer. Oncotarget 8, 47154–47160. https://doi.org/10.18632/oncotarget.17005

Ray Chaudhuri, A., Callen, E., Ding, X., Gogola, E., Duarte, A.A., Lee, J.-E., Wong, N., Lafarga, V., Calvo, J.A., Panzarino, N.J., John, S., Day, A., Crespo, A.V., Shen, B., Starnes, L.M., de Ruiter, J.R., Daniel, J.A., Konstantinopoulos, P.A., Cortez, D., Cantor, S.B., Fernandez-Capetillo, O., Ge, K., Jonkers, J., Rottenberg, S., Sharan, S.K., Nussenzweig, A., 2016. Replication fork stability confers chemoresistance in BRCA-deficient cells. Nature 535, 382–387. https://doi.org/10.1038/nature18325

Reade, C.J., McVey, R.M., Tone, A.A., Finlayson, S.J., McAlpine, J.N., Fung-Kee-Fung, M., Ferguson, S.E., 2014. The fallopian tube as the origin of high grade serous ovarian cancer: review of a paradigm shift. J. Obstet. Gynaecol. Can. JOGC J. Obstet. Gynecol. Can. JOGC 36, 133–140. https://doi.org/10.1016/S1701-2163(15)30659-9

Reid, B.M., Permuth, J.B., Sellers, T.A., 2017. Epidemiology of ovarian cancer: a review. Cancer Biol. Med. 14, 9–32. https://doi.org/10.20892/j.issn.2095-3941.2016.0084

Ricci, F., Bizzaro, F., Cesca, M., Guffanti, F., Ganzinelli, M., Decio, A., Ghilardi, C., Perego, P., Fruscio, R., Buda, A., Milani, R., Ostano, P., Chiorino, G., Bani, M.R., Damia, G., Giavazzi, R., 2014. Patient-derived ovarian tumor xenografts recapitulate human clinicopathology and genetic alterations. Cancer Res. 74, 6980–6990. https://doi.org/10.1158/0008-5472.CAN-14-0274

Ricci, F., Fratelli, M., Guffanti, F., Porcu, L., Spriano, F., Dell'Anna, T., Fruscio, R., Damia, G., 2017. Patient-derived ovarian cancer xenografts re-growing after a cisplatinum treatment are less responsive to a second drug re-challenge: a new experimental

setting to study response to therapy. Oncotarget 8, 7441–7451. https://doi.org/10.18632/oncotarget.7465

Rocha, C.R.R., Silva, M.M., Quinet, A., Cabral-Neto, J.B., Menck, C.F.M., 2018. DNA repair pathways and cisplatin resistance: an intimate relationship. Clin. Sao Paulo Braz. 73, e478s. https://doi.org/10.6061/clinics/2018/e478s

Rogakou, E.P., Nieves-Neira, W., Boon, C., Pommier, Y., Bonner, W.M., 2000. Initiation of DNA fragmentation during apoptosis induces phosphorylation of H2AX histone at serine 139. J. Biol. Chem. 275, 9390–9395. https://doi.org/10.1074/jbc.275.13.9390

Rojas, V., Hirshfield, K.M., Ganesan, S., Rodriguez-Rodriguez, L., 2016. Molecular Characterization of Epithelial Ovarian Cancer: Implications for Diagnosis and Treatment. Int. J. Mol. Sci. 17. https://doi.org/10.3390/ijms17122113

Romero, I., Sun, C.C., Wong, K.K., Bast, R.C., Gershenson, D.M., 2013. Low-grade serous carcinoma: new concepts and emerging therapies. Gynecol. Oncol. 130, 660–666. https://doi.org/10.1016/j.ygyno.2013.05.021

Rondinelli, B., Gogola, E., Yücel, H., Duarte, A.A., van de Ven, M., van der Sluijs, R., Konstantinopoulos, P.A., Jonkers, J., Ceccaldi, R., Rottenberg, S., D'Andrea, A.D., 2017. EZH2 promotes degradation of stalled replication forks by recruiting MUS81 through histone H3 trimethylation. Nat. Cell Biol. 19, 1371–1378. https://doi.org/10.1038/ncb3626

Rosenberg, B., Vancamp, L., Krigas, T., 1965. INHIBITION OF CELL DIVISION IN ESCHERICHIA COLI BY ELECTROLYSIS PRODUCTS FROM A PLATINUM ELECTRODE. Nature 205, 698–699. https://doi.org/10.1038/205698a0

Rosenberg, B., VanCamp, L., Trosko, J.E., Mansour, V.H., 1969. Platinum compounds: a new class of potent antitumour agents. Nature 222, 385–386. https://doi.org/10.1038/222385a0

Rothkamm, K., Barnard, S., Moquet, J., Ellender, M., Rana, Z., Burdak-Rothkamm, S., 2015. DNA damage foci: Meaning and significance. Environ. Mol. Mutagen. 56, 491–504. https://doi.org/10.1002/em.21944

Rottenberg, S., Jaspers, J.E., Kersbergen, A., van der Burg, E., Nygren, A.O.H., Zander, S.A.L., Derksen, P.W.B., de Bruin, M., Zevenhoven, J., Lau, A., Boulter, R., Cranston, A., O'Connor, M.J., Martin, N.M.B., Borst, P., Jonkers, J., 2008. High sensitivity of BRCA1-deficient mammary tumors to the PARP inhibitor AZD2281 alone and in combination with platinum drugs. Proc. Natl. Acad. Sci. U. S. A. 105, 17079–17084. https://doi.org/10.1073/pnas.0806092105

Roy, U., Schärer, O.D., 2016. Involvement of translesion synthesis DNA polymerases in DNA interstrand crosslink repair. DNA Repair 44, 33–41. https://doi.org/10.1016/j.dnarep.2016.05.004

Rubatt, J.M., Darcy, K.M., Tian, C., Muggia, F., Dhir, R., Armstrong, D.K., Bookman, M.A., Niedernhofer, L.J., Deloia, J., Birrer, M., Krivak, T.C., 2012. Pre-treatment tumor expression of ERCC1 in women with advanced stage epithelial ovarian cancer is not predictive of clinical outcomes: a Gynecologic Oncology Group study. Gynecol. Oncol. 125, 421–426. https://doi.org/10.1016/j.ygyno.2012.01.008

Sabatino, M.A., Marabese, M., Ganzinelli, M., Caiola, E., Geroni, C., Broggini, M., 2010. Down-regulation of the nucleotide excision repair gene XPG as a new mechanism of drug resistance in human and murine cancer cells. Mol. Cancer 9, 259. https://doi.org/10.1186/1476-4598-9-259

Samimi, G., Fink, D., Varki, N.M., Husain, A., Hoskins, W.J., Alberts, D.S., Howell, S.B., 2000. Analysis of MLH1 and MSH2 expression in ovarian cancer before and after platinum drug-based chemotherapy. Clin. Cancer Res. Off. J. Am. Assoc. Cancer Res. 6, 1415–1421.

Sander Effron, S., Makvandi, M., Lin, L., Xu, K., Li, S., Lee, H., Hou, C., Pryma, D.A., Koch, C., Mach, R.H., 2017. PARP-1 Expression Quantified by [18F]FluorThanatrace: A Biomarker of Response to PARP Inhibition Adjuvant to Radiation Therapy. Cancer Biother. Radiopharm. 32, 9–15. https://doi.org/10.1089/cbr.2016.2133

Sarkar, S., Davies, A.A., Ulrich, H.D., McHugh, P.J., 2006. DNA interstrand crosslink repair during G1 involves nucleotide excision repair and DNA polymerase zeta. EMBO J. 25, 1285–1294. https://doi.org/10.1038/sj.emboj.7600993

Sawers, L., Ferguson, M.J., Ihrig, B.R., Young, H.C., Chakravarty, P., Wolf, C.R., Smith, G., 2014. Glutathione S-transferase P1 (GSTP1) directly influences platinum drug chemosensitivity in ovarian tumour cell lines. Br. J. Cancer 111, 1150–1158. https://doi.org/10.1038/bjc.2014.386

Schlacher, K., Christ, N., Siaud, N., Egashira, A., Wu, H., Jasin, M., 2011. Double-strand break repair-independent role for BRCA2 in blocking stalled replication fork degradation by MRE11. Cell 145, 529–542. https://doi.org/10.1016/j.cell.2011.03.041

Schlacher, K., Wu, H., Jasin, M., 2012. A distinct replication fork protection pathway connects Fanconi anemia tumor suppressors to RAD51-BRCA1/2. Cancer Cell 22, 106–116. https://doi.org/10.1016/j.ccr.2012.05.015

Schoch, S., Gajewski, S., Rothfuß, J., Hartwig, A., Köberle, B., 2020. Comparative Study of the Mode of Action of Clinically Approved Platinum-Based Chemotherapeutics. Int. J. Mol. Sci. 21. https://doi.org/10.3390/ijms21186928

Schwartz, L.H., Litière, S., de Vries, E., Ford, R., Gwyther, S., Mandrekar, S., Shankar, L., Bogaerts, J., Chen, A., Dancey, J., Hayes, W., Hodi, F.S., Hoekstra, O.S., Huang, E.P., Lin, N., Liu, Y., Therasse, P., Wolchok, J.D., Seymour, L., 2016. RECIST 1.1-Update and clarification: From the RECIST committee. Eur. J. Cancer Oxf. Engl. 1990 62, 132–137. https://doi.org/10.1016/j.ejca.2016.03.081

Schwertman, P., Lagarou, A., Dekkers, D.H.W., Raams, A., van der Hoek, A.C., Laffeber, C., Hoeijmakers, J.H.J., Demmers, J.A.A., Fousteri, M., Vermeulen, W., Marteijn, J.A., 2012. UV-sensitive syndrome protein UVSSA recruits USP7 to regulate transcription-coupled repair. Nat. Genet. 44, 598–602. https://doi.org/10.1038/ng.2230

Scurry, J., van Zyl, B., Gulliver, D., Otton, G., Jaaback, K., Lombard, J., Vilain, R.E., Bowden, N.A., 2018. Nucleotide excision repair protein ERCC1 and tumour-infiltrating lymphocytes are potential biomarkers of neoadjuvant platinum resistance

in high grade serous ovarian cancer. Gynecol. Oncol. 151, 306–310. https://doi.org/10.1016/j.ygyno.2018.08.030

Setiaputra, D., Durocher, D., 2019. Shieldin - the protector of DNA ends. EMBO Rep. 20. https://doi.org/10.15252/embr.201847560

Shachar, S., Ziv, O., Avkin, S., Adar, S., Wittschieben, J., Reissner, T., Chaney, S., Friedberg, E.C., Wang, Z., Carell, T., Geacintov, N., Livneh, Z., 2009. Two-polymerase mechanisms dictate error-free and error-prone translesion DNA synthesis in mammals. EMBO J. 28, 383–393. https://doi.org/10.1038/emboj.2008.281

Shah, M.M., Dobbin, Z.C., Nowsheen, S., Wielgos, M., Katre, A.A., Alvarez, R.D., Konstantinopoulos, P.A., Yang, E.S., Landen, C.N., 2014. An ex vivo assay of XRT-induced Rad51 foci formation predicts response to PARP-inhibition in ovarian cancer. Gynecol. Oncol. 134, 331–337. https://doi.org/10.1016/j.ygyno.2014.05.009

Shee, K., Wells, J.D., Jiang, A., Miller, T.W., 2019. Integrated pan-cancer gene expression and drug sensitivity analysis reveals SLFN11 mRNA as a solid tumor biomarker predictive of sensitivity to DNA-damaging chemotherapy. PloS One 14, e0224267. https://doi.org/10.1371/journal.pone.0224267

Siddik, Z.H., 2003. Cisplatin: mode of cytotoxic action and molecular basis of resistance. Oncogene 22, 7265–7279. https://doi.org/10.1038/sj.onc.1206933

Siddiqui, G.K., Maclean, A.B., Elmasry, K., Wong te Fong, A., Morris, R.W., Rashid, M., Begent, R.H.J., Boxer, G.M., 2011. Immunohistochemical expression of VEGF predicts response to platinum based chemotherapy in patients with epithelial ovarian cancer. Angiogenesis 14, 155–161. https://doi.org/10.1007/s10456-010-9199-4

Silwal-Pandit, L., Langerød, A., Børresen-Dale, A.-L., 2017. TP53 Mutations in Breast and Ovarian Cancer. Cold Spring Harb. Perspect. Med. 7. https://doi.org/10.1101/cshperspect.a026252

Silwal-Pandit, L., Vollan, H.K.M., Chin, S.-F., Rueda, O.M., McKinney, S., Osako, T., Quigley, D.A., Kristensen, V.N., Aparicio, S., Børresen-Dale, A.-L., Caldas, C., Langerød, A., 2014. TP53 mutation spectrum in breast cancer is subtype specific and has distinct prognostic relevance. Clin. Cancer Res. Off. J. Am. Assoc. Cancer Res. 20, 3569–3580. https://doi.org/10.1158/1078-0432.CCR-13-2943

Simon, G.R., Sharma, S., Cantor, A., Smith, P., Bepler, G., 2005. ERCC1 expression is a predictor of survival in resected patients with non-small cell lung cancer. Chest 127, 978–983. https://doi.org/10.1378/chest.127.3.978

Simon, R., Norton, L., 2006. The Norton-Simon hypothesis: designing more effective and less toxic chemotherapeutic regimens. Nat. Clin. Pract. Oncol. 3, 406–407. https://doi.org/10.1038/ncponc0560

Simons, M., Simmer, F., Bulten, J., Ligtenberg, M.J., Hollema, H., van Vliet, S., de Voer, R.M., Kamping, E.J., van Essen, D.F., Ylstra, B., Schwartz, L.E., Wang, Y., Massuger, L.F., Nagtegaal, I.D., Kurman, R.J., 2020. Two types of primary mucinous ovarian tumors can be distinguished based on their origin. Mod. Pathol. Off. J. U. S. Can. Acad. Pathol. Inc 33, 722–733. https://doi.org/10.1038/s41379-019-0401-y

Singh, A., Settleman, J., 2010. EMT, cancer stem cells and drug resistance: an emerging axis of evil in the war on cancer. Oncogene 29, 4741–4751. https://doi.org/10.1038/onc.2010.215

Sleeth, K.M., Robson, R.L., Dianov, G.L., 2004. Exchangeability of mammalian DNA ligases between base excision repair pathways. Biochemistry 43, 12924–12930. https://doi.org/10.1021/bi0492612

Slyskova, J., Sabatella, M., Ribeiro-Silva, C., Stok, C., Theil, A.F., Vermeulen, W., Lans, H., 2018. Base and nucleotide excision repair facilitate resolution of platinum drugs-induced transcription blockage. Nucleic Acids Res. 46, 9537–9549. https://doi.org/10.1093/nar/gky764

Song, I.-S., Savaraj, N., Siddik, Z.H., Liu, P., Wei, Y., Wu, C.J., Kuo, M.T., 2004. Role of human copper transporter Ctr1 in the transport of platinum-based antitumor agents in cisplatin-sensitive and cisplatin-resistant cells. Mol. Cancer Ther. 3, 1543–1549.

Soulier, J., 2011. Fanconi anemia. Hematol. Am. Soc. Hematol. Educ. Program 2011, 492–497. https://doi.org/10.1182/asheducation-2011.1.492

Spivak, G., 2015. Nucleotide excision repair in humans. DNA Repair 36, 13–18. https://doi.org/10.1016/j.dnarep.2015.09.003

Sriraksa, R., Chaopatchayakul, P., Jearanaikoon, P., Leelayuwat, C., Limpaiboon, T., 2010. Verification of complete bisulfite modification using Calponin-specific primer sets. Clin. Biochem. 43, 528–530. https://doi.org/10.1016/j.clinbiochem.2009.11.005

Stefanou, D.T., Bamias, A., Episkopou, H., Kyrtopoulos, S.A., Likka, M., Kalampokas, T., Photiou, S., Gavalas, N., Sfikakis, P.P., Dimopoulos, M.A., Souliotis, V.L., 2015. Aberrant DNA damage response pathways may predict the outcome of platinum chemotherapy in ovarian cancer. PloS One 10, e0117654. https://doi.org/10.1371/journal.pone.0117654

Steffensen, K.D., Smoter, M., Waldstrøm, M., Grala, B., Bodnar, L., Stec, R., Szczylik, C., Jakobsen, A., 2014. Resistance to first line platinum paclitaxel chemotherapy in serous epithelial ovarian cancer: the prediction value of ERCC1 and Tau expression. Int. J. Oncol. 44, 1736–1744. https://doi.org/10.3892/ijo.2014.2311

Steffensen, K.D., Waldstrøm, M., Jakobsen, A., 2009. The relationship of platinum resistance and ERCC1 protein expression in epithelial ovarian cancer. Int. J. Gynecol. Cancer Off. J. Int. Gynecol. Cancer Soc. 19, 820–825. https://doi.org/10.1111/IGC.0b013e3181a12e09

Stewart, D.J., 2007. Mechanisms of resistance to cisplatin and carboplatin. Crit. Rev. Oncol. Hematol. 63, 12–31. https://doi.org/10.1016/j.critrevonc.2007.02.001

Stover, E.H., Konstantinopoulos, P.A., Matulonis, U.A., Swisher, E.M., 2016. Biomarkers of Response and Resistance to DNA Repair Targeted Therapies. Clin. Cancer Res. Off. J. Am. Assoc. Cancer Res. 22, 5651–5660. https://doi.org/10.1158/1078-0432.CCR-16-0247

Strathdee, G., MacKean, M.J., Illand, M., Brown, R., 1999. A role for methylation of the hMLH1 promoter in loss of hMLH1 expression and drug resistance in ovarian cancer. Oncogene 18, 2335–2341. https://doi.org/10.1038/sj.onc.1202540

Stronach, E.A., Paul, J., Timms, K.M., Hughes, E., Brown, K., Neff, C., Perry, M., Gutin, A., El-Bahrawy, M., Steel, J.H., Liu, X., Lewsley, L.-A., Siddiqui, N., Gabra, H., Lanchbury, J.S., Brown, R., 2018. Biomarker Assessment of HR Deficiency, Tumor BRCA1/2 Mutations, and CCNE1 Copy Number in Ovarian Cancer: Associations with Clinical Outcome Following Platinum Monotherapy. Mol. Cancer Res. MCR 16, 1103–1111. https://doi.org/10.1158/1541-7786.MCR-18-0034

Swisher, E.M., Lin, K.K., Oza, A.M., Scott, C.L., Giordano, H., Sun, J., Konecny, G.E., Coleman, R.L., Tinker, A.V., O'Malley, D.M., Kristeleit, R.S., Ma, L., Bell-McGuinn, K.M., Brenton, J.D., Cragun, J.M., Oaknin, A., Ray-Coquard, I., Harrell, M.I., Mann, E., Kaufmann, S.H., Floquet, A., Leary, A., Harding, T.C., Goble, S., Maloney, L., Isaacson, J., Allen, A.R., Rolfe, L., Yelensky, R., Raponi, M., McNeish, I.A., 2017. Rucaparib in relapsed, platinum-sensitive high-grade ovarian carcinoma (ARIEL2 Part 1): an international, multicentre, open-label, phase 2 trial. Lancet Oncol. 18, 75–87. https://doi.org/10.1016/S1470-2045(16)30559-9

Taglialatela, A., Alvarez, S., Leuzzi, G., Sannino, V., Ranjha, L., Huang, J.-W., Madubata, C., Anand, R., Levy, B., Rabadan, R., Cejka, P., Costanzo, V., Ciccia, A., 2017. Restoration of Replication Fork Stability in BRCA1- and BRCA2-Deficient Cells by Inactivation of SNF2-Family Fork Remodelers. Mol. Cell 68, 414-430.e8. https://doi.org/10.1016/j.molcel.2017.09.036

Tamura, N., Shaikh, N., Muliaditan, D., Soliman, T.N., McGuinness, J.R., Maniati, E., Moralli, D., Durin, M.-A., Green, C.M., Balkwill, F.R., Wang, J., Curtius, K., McClelland, S.E., 2020. Specific mechanisms of chromosomal instability indicate therapeutic sensitivities in high-grade serous ovarian carcinoma. Cancer Res. https://doi.org/10.1158/0008-5472.CAN-19-0852

Tan, T.Z., Miow, Q.H., Huang, R.Y.-J., Wong, M.K., Ye, J., Lau, J.A., Wu, M.C., Bin Abdul Hadi, L.H., Soong, R., Choolani, M., Davidson, B., Nesland, J.M., Wang, L.-Z., Matsumura, N., Mandai, M., Konishi, I., Goh, B.-C., Chang, J.T., Thiery, J.P., Mori, S., 2013. Functional genomics identifies five distinct molecular subtypes with clinical relevance and pathways for growth control in epithelial ovarian cancer. EMBO Mol. Med. 5, 1051–1066. https://doi.org/10.1002/emmm.201201823

Tanabe, S., Quader, S., Cabral, H., Ono, R., 2020. Interplay of EMT and CSC in Cancer and the Potential Therapeutic Strategies. Front. Pharmacol. 11, 904. https://doi.org/10.3389/fphar.2020.00904

Tang, N., Lyu, D., Zhang, Y., Liu, H., 2017. Association between the ERCC1 polymorphism and platinum-based chemotherapy effectiveness in ovarian cancer: a meta-analysis. BMC Womens Health 17, 43. https://doi.org/10.1186/s12905-017-0393-z

Tang, S.-W., Bilke, S., Cao, L., Murai, J., Sousa, F.G., Yamade, M., Rajapakse, V., Varma, S., Helman, L.J., Khan, J., Meltzer, P.S., Pommier, Y., 2015. SLFN11 Is a Transcriptional Target of EWS-FLI1 and a Determinant of Drug Response in Ewing Sarcoma. Clin. Cancer Res. Off. J. Am. Assoc. Cancer Res. 21, 4184–4193. https://doi.org/10.1158/1078-0432.CCR-14-2112

Taniguchi, T., Tischkowitz, M., Ameziane, N., Hodgson, S.V., Mathew, C.G., Joenje, H., Mok, S.C., D'Andrea, A.D., 2003. Disruption of the Fanconi anemia-BRCA pathway in cisplatin-sensitive ovarian tumors. Nat. Med. 9, 568–574. https://doi.org/10.1038/nm852

Tavecchio, M., Simone, M., Erba, E., Chiolo, I., Liberi, G., Foiani, M., D'Incalci, M., Damia, G., 2008. Role of homologous recombination in trabectedin-induced DNA damage. Eur. J. Cancer Oxf. Engl. 1990 44, 609–618. https://doi.org/10.1016/j.ejca.2008.01.003

Telli, M.L., Timms, K.M., Reid, J., Hennessy, B., Mills, G.B., Jensen, K.C., Szallasi, Z., Barry, W.T., Winer, E.P., Tung, N.M., Isakoff, S.J., Ryan, P.D., Greene-Colozzi, A., Gutin, A., Sangale, Z., Iliev, D., Neff, C., Abkevich, V., Jones, J.T., Lanchbury, J.S., Hartman, A.-R., Garber, J.E., Ford, J.M., Silver, D.P., Richardson, A.L., 2016. Homologous Recombination Deficiency (HRD) Score Predicts Response to Platinum-Containing Neoadjuvant Chemotherapy in Patients with Triple-Negative Breast Cancer. Clin. Cancer Res. Off. J. Am. Assoc. Cancer Res. 22, 3764–3773. https://doi.org/10.1158/1078-0432.CCR-15-2477

Ter Brugge, P., Kristel, P., van der Burg, E., Boon, U., de Maaker, M., Lips, E., Mulder, L., de Ruiter, J., Moutinho, C., Gevensleben, H., Marangoni, E., Majewski, I., Józwiak, K., Kloosterman, W., van Roosmalen, M., Duran, K., Hogervorst, F., Turner, N., Esteller, M., Cuppen, E., Wesseling, J., Jonkers, J., 2016. Mechanisms of Therapy Resistance in Patient-Derived Xenograft Models of BRCA1-Deficient Breast Cancer. J. Natl. Cancer Inst. 108. https://doi.org/10.1093/jnci/djw148

Therasse, P., Arbuck, S.G., Eisenhauer, E.A., Wanders, J., Kaplan, R.S., Rubinstein, L., Verweij, J., Van Glabbeke, M., van Oosterom, A.T., Christian, M.C., Gwyther, S.G., 2000. New guidelines to evaluate the response to treatment in solid tumors. European Organization for Research and Treatment of Cancer, National Cancer Institute of the United States, National Cancer Institute of Canada. J. Natl. Cancer Inst. 92, 205–216. https://doi.org/10.1093/jnci/92.3.205

Tian, H., Gao, Z., Li, H., Zhang, B., Wang, G., Zhang, Q., Pei, D., Zheng, J., 2015. DNA damage response--a double-edged sword in cancer prevention and cancer therapy. Cancer Lett. 358, 8–16. https://doi.org/10.1016/j.canlet.2014.12.038

Topp, M.D., Hartley, L., Cook, M., Heong, V., Boehm, E., McShane, L., Pyman, J., McNally, O., Ananda, S., Harrell, M., Etemadmoghadam, D., Galletta, L., Alsop, K., Mitchell, G., Fox, S.B., Kerr, J.B., Hutt, K.J., Kaufmann, S.H., Australian Ovarian Cancer Study, null, Swisher, E.M., Bowtell, D.D., Wakefield, M.J., Scott, C.L., 2014. Molecular correlates of platinum response in human high-grade serous ovarian cancer patient-derived xenografts. Mol. Oncol. 8, 656–668. https://doi.org/10.1016/j.molonc.2014.01.008

Torre, L.A., Trabert, B., DeSantis, C.E., Miller, K.D., Samimi, G., Runowicz, C.D., Gaudet, M.M., Jemal, A., Siegel, R.L., 2018. Ovarian cancer statistics, 2018. CA. Cancer J. Clin. 68, 284–296. https://doi.org/10.3322/caac.21456

Tothill, R.W., Tinker, A.V., George, J., Brown, R., Fox, S.B., Lade, S., Johnson, D.S., Trivett, M.K., Etemadmoghadam, D., Locandro, B., Traficante, N., Fereday, S., Hung, J.A., Chiew, Y.-E., Haviv, I., Australian Ovarian Cancer Study Group, Gertig, D., DeFazio, A., Bowtell, D.D.L., 2008. Novel molecular subtypes of serous and endometrioid ovarian cancer linked to clinical outcome. Clin. Cancer Res. Off. J. Am. Assoc. Cancer Res. 14, 5198–5208. https://doi.org/10.1158/1078-0432.CCR-08-0196

Trimbos, J.B., 2017. Surgical treatment of early-stage ovarian cancer. Best Pract. Res. Clin. Obstet. Gynaecol. 41, 60–70. https://doi.org/10.1016/j.bpobgyn.2016.10.001

Tumiati, M., Hietanen, S., Hynninen, J., Pietilä, E., Färkkilä, A., Kaipio, K., Roering, P., Huhtinen, K., Alkodsi, A., Li, Y., Lehtonen, R., Erkan, E.P., Tuominen, M.M., Lehti, K., Hautaniemi, S.K., Vähärautio, A., Grénman, S., Carpén, O., Kauppi, L., 2018a. A Functional Homologous Recombination Assay Predicts Primary Chemotherapy Response and Long-Term Survival in Ovarian Cancer Patients. Clin. Cancer Res. Off. J. Am. Assoc. Cancer Res. 24, 4482–4493. https://doi.org/10.1158/1078-0432.CCR-17-3770

Tumiati, M., Hietanen, S., Kauppi, L., 2018b. Time to go functional! Determining tumors' DNA repair capacity ex vivo. Oncotarget 9, 36826–36827. https://doi.org/10.18632/oncotarget.26419

Turner, N., Tutt, A., Ashworth, A., 2004. Hallmarks of "BRCAness" in sporadic cancers. Nat. Rev. Cancer 4, 814–819. https://doi.org/10.1038/nrc1457

Vaidyanathan, A., Sawers, L., Gannon, A.-L., Chakravarty, P., Scott, A.L., Bray, S.E., Ferguson, M.J., Smith, G., 2016. ABCB1 (MDR1) induction defines a common resistance mechanism in paclitaxel- and olaparib-resistant ovarian cancer cells. Br. J. Cancer 115, 431–441. https://doi.org/10.1038/bjc.2016.203

Vaisman, A., Varchenko, M., Umar, A., Kunkel, T.A., Risinger, J.I., Barrett, J.C., Hamilton, T.C., Chaney, S.G., 1998. The role of hMLH1, hMSH3, and hMSH6 defects in cisplatin and oxaliplatin resistance: correlation with replicative bypass of platinum-DNA adducts. Cancer Res. 58, 3579–3585.

van Driel, W.J., Koole, S.N., Sikorska, K., Schagen van Leeuwen, J.H., Schreuder, H.W.R., Hermans, R.H.M., de Hingh, I.H.J.T., van der Velden, J., Arts, H.J., Massuger, L.F.A.G., Aalbers, A.G.J., Verwaal, V.J., Kieffer, J.M., Van de Vijver, K.K., van Tinteren, H., Aaronson, N.K., Sonke, G.S., 2018. Hyperthermic Intraperitoneal Chemotherapy in Ovarian Cancer. N. Engl. J. Med. 378, 230–240. https://doi.org/10.1056/NEJMoa1708618

Vanderstichele, A., Busschaert, P., Olbrecht, S., Lambrechts, D., Vergote, I., 2017. Genomic signatures as predictive biomarkers of homologous recombination deficiency in ovarian cancer. Eur. J. Cancer Oxf. Engl. 1990 86, 5–14. https://doi.org/10.1016/j.ejca.2017.08.029

Vang, R., Shih, I.-M., Kurman, R.J., 2013. Fallopian tube precursors of ovarian low- and high-grade serous neoplasms. Histopathology 62, 44–58. https://doi.org/10.1111/his.12046

Vaupel, P., Multhoff, G., 2018. Hypoxia-/HIF-1α-Driven Factors of the Tumor Microenvironment Impeding Antitumor Immune Responses and Promoting Malignant Progression. Adv. Exp. Med. Biol. 1072, 171–175. https://doi.org/10.1007/978-3-319-91287-5_27

Vazquez, A., Bond, E.E., Levine, A.J., Bond, G.L., 2008. The genetics of the p53 pathway, apoptosis and cancer therapy. Nat. Rev. Drug Discov. 7, 979–987. https://doi.org/10.1038/nrd2656

Vergote, I., Tropé, C.G., Amant, F., Kristensen, G.B., Ehlen, T., Johnson, N., Verheijen, R.H.M., van der Burg, M.E.L., Lacave, A.J., Panici, P.B., Kenter, G.G., Casado, A., Mendiola, C., Coens, C., Verleye, L., Stuart, G.C.E., Pecorelli, S., Reed, N.S., European Organization for Research and Treatment of Cancer-Gynaecological

Cancer Group, NCIC Clinical Trials Group, 2010. Neoadjuvant chemotherapy or primary surgery in stage IIIC or IV ovarian cancer. N. Engl. J. Med. 363, 943–953. https://doi.org/10.1056/NEJMoa0908806

Vollebergh, M.A., Lips, E.H., Nederlof, P.M., Wessels, L.F.A., Wesseling, J., Vd Vijver, M.J., de Vries, E.G.E., van Tinteren, H., Jonkers, J., Hauptmann, M., Rodenhuis, S., Linn, S.C., 2014. Genomic patterns resembling BRCA1- and BRCA2-mutated breast cancers predict benefit of intensified carboplatin-based chemotherapy. Breast Cancer Res. BCR 16, R47. https://doi.org/10.1186/bcr3655

Waks, A.G., Cohen, O., Kochupurakkal, B., Kim, D., Dunn, C.E., Buendia Buendia, J., Wander, S., Helvie, K., Lloyd, M.R., Marini, L., Hughes, M.E., Freeman, S.S., Ivy, S.P., Geradts, J., Isakoff, S., LoRusso, P., Adalsteinsson, V.A., Tolaney, S.M., Matulonis, U., Krop, I.E., D'Andrea, A.D., Winer, E.P., Lin, N.U., Shapiro, G.I., Wagle, N., 2020. Reversion and non-reversion mechanisms of resistance to PARP inhibitor or platinum chemotherapy in BRCA1/2-mutant metastatic breast cancer. Ann. Oncol. Off. J. Eur. Soc. Med. Oncol. 31, 590–598. https://doi.org/10.1016/j.annonc.2020.02.008

Walton, J.B., Farquharson, M., Mason, S., Port, J., Kruspig, B., Dowson, S., Stevenson, D., Murphy, D., Matzuk, M., Kim, J., Coffelt, S., Blyth, K., McNeish, I.A., 2017. CRISPR/Cas9-derived models of ovarian high grade serous carcinoma targeting Brca1, Pten and Nf1, and correlation with platinum sensitivity. Sci. Rep. 7, 16827. https://doi.org/10.1038/s41598-017-17119-1

Wang, D., Xiang, D.-B., Yang, X.-Q., Chen, L.-S., Li, M.-X., Zhong, Z.-Y., Zhang, Y.-S., 2009. APE1 overexpression is associated with cisplatin resistance in non-small cell lung cancer and targeted inhibition of APE1 enhances the activity of cisplatin in A549 cells. Lung Cancer Amst. Neth. 66, 298–304. https://doi.org/10.1016/j.lungcan.2009.02.019

Wang, H., Zhang, G., Zhang, H., Zhang, F., Zhou, B., Ning, F., Wang, H.-S., Cai, S.-H., Du, J., 2014. Acquisition of epithelial-mesenchymal transition phenotype and cancer stem cell-like properties in cisplatin-resistant lung cancer cells through AKT/β-catenin/Snail signaling pathway. Eur. J. Pharmacol. 723, 156–166. https://doi.org/10.1016/j.ejphar.2013.12.004

Wang, M., Li, E., Lin, L., Kumar, A.K., Pan, F., He, L., Zhang, J., Hu, Z., Guo, Z., 2019. Enhanced Activity of Variant DNA Polymerase β (D160G) Contributes to Cisplatin Therapy by Impeding the Efficiency of NER. Mol. Cancer Res. MCR 17, 2077–2088. https://doi.org/10.1158/1541-7786.MCR-19-0482

Wang, Q.-E., Milum, K., Han, C., Huang, Y.-W., Wani, G., Thomale, J., Wani, A.A., 2011. Differential contributory roles of nucleotide excision and homologous recombination repair for enhancing cisplatin sensitivity in human ovarian cancer cells. Mol. Cancer 10, 24. https://doi.org/10.1186/1476-4598-10-24

Wang, Y., Bernhardy, A.J., Cruz, C., Krais, J.J., Nacson, J., Nicolas, E., Peri, S., van der Gulden, H., van der Heijden, I., O'Brien, S.W., Zhang, Y., Harrell, M.I., Johnson, S.F., Candido Dos Reis, F.J., Pharoah, P.D.P., Karlan, B., Gourley, C., Lambrechts, D., Chenevix-Trench, G., Olsson, H., Benitez, J.J., Greene, M.H., Gore, M., Nussbaum, R., Sadetzki, S., Gayther, S.A., Kjaer, S.K., kConFab Investigators, D'Andrea, A.D., Shapiro, G.I., Wiest, D.L., Connolly, D.C., Daly, M.B., Swisher, E.M., Bouwman, P., Jonkers, J., Balmaña, J., Serra, V., Johnson, N., 2016. The

BRCA1-Δ11q Alternative Splice Isoform Bypasses Germline Mutations and Promotes Therapeutic Resistance to PARP Inhibition and Cisplatin. Cancer Res. 76, 2778–2790. https://doi.org/10.1158/0008-5472.CAN-16-0186

Wang, Y., Helland, A., Holm, R., Kristensen, G.B., Børresen-Dale, A.-L., 2005. PIK3CA mutations in advanced ovarian carcinomas. Hum. Mutat. 25, 322. https://doi.org/10.1002/humu.9316

Wang, Z.C., Birkbak, N.J., Culhane, A.C., Drapkin, R., Fatima, A., Tian, R., Schwede, M., Alsop, K., Daniels, K.E., Piao, H., Liu, J., Etemadmoghadam, D., Miron, A., Salvesen, H.B., Mitchell, G., DeFazio, A., Quackenbush, J., Berkowitz, R.S., Iglehart, J.D., Bowtell, D.D.L., Australian Ovarian Cancer Study Group, Matulonis, U.A., 2012. Profiles of genomic instability in high-grade serous ovarian cancer predict treatment outcome. Clin. Cancer Res. Off. J. Am. Assoc. Cancer Res. 18, 5806–5815. https://doi.org/10.1158/1078-0432.CCR-12-0857

Watanabe, Y., Ueda, H., Etoh, T., Koike, E., Fujinami, N., Mitsuhashi, A., Hoshiai, H., 2007. A change in promoter methylation of hMLH1 is a cause of acquired resistance to platinum-based chemotherapy in epithelial ovarian cancer. Anticancer Res. 27, 1449–1452.

Watkins, J.A., Irshad, S., Grigoriadis, A., Tutt, A.N.J., 2014. Genomic scars as biomarkers of homologous recombination deficiency and drug response in breast and ovarian cancers. Breast Cancer Res. BCR 16, 211. https://doi.org/10.1186/bcr3670

Weaver, A.N., Yang, E.S., 2013. Beyond DNA Repair: Additional Functions of PARP-1 in Cancer. Front. Oncol. 3, 290. https://doi.org/10.3389/fonc.2013.00290

Weigelt, B., Comino-Méndez, I., de Bruijn, I., Tian, L., Meisel, J.L., García-Murillas, I., Fribbens, C., Cutts, R., Martelotto, L.G., Ng, C.K.Y., Lim, R.S., Selenica, P., Piscuoglio, S., Aghajanian, C., Norton, L., Murali, R., Hyman, D.M., Borsu, L., Arcila, M.E., Konner, J., Reis-Filho, J.S., Greenberg, R.A., Robson, M.E., Turner, N.C., 2017. Diverse BRCA1 and BRCA2 Reversion Mutations in Circulating Cell-Free DNA of Therapy-Resistant Breast or Ovarian Cancer. Clin. Cancer Res. Off. J. Am. Assoc. Cancer Res. 23, 6708–6720. https://doi.org/10.1158/1078-0432.CCR-17-0544

Wiegand, K.C., Shah, S.P., Al-Agha, O.M., Zhao, Y., Tse, K., Zeng, T., Senz, J., McConechy, M.K., Anglesio, M.S., Kalloger, S.E., Yang, W., Heravi-Moussavi, A., Giuliany, R., Chow, C., Fee, J., Zayed, A., Prentice, L., Melnyk, N., Turashvili, G., Delaney, A.D., Madore, J., Yip, S., McPherson, A.W., Ha, G., Bell, L., Fereday, S., Tam, A., Galletta, L., Tonin, P.N., Provencher, D., Miller, D., Jones, S.J.M., Moore, R.A., Morin, G.B., Oloumi, A., Boyd, N., Aparicio, S.A., Shih, I.-M., Mes-Masson, A.-M., Bowtell, D.D., Hirst, M., Gilks, B., Marra, M.A., Huntsman, D.G., 2010. ARID1A mutations in endometriosis-associated ovarian carcinomas. N. Engl. J. Med. 363, 1532–1543. https://doi.org/10.1056/NEJMoa1008433

Wilsker, D.F., Barrett, A.M., Dull, A.B., Lawrence, S.M., Hollingshead, M.G., Chen, A., Kummar, S., Parchment, R.E., Doroshow, J.H., Kinders, R.J., 2019. Evaluation of Pharmacodynamic Responses to Cancer Therapeutic Agents Using DNA Damage Markers. Clin. Cancer Res. Off. J. Am. Assoc. Cancer Res. 25, 3084–3095. https://doi.org/10.1158/1078-0432.CCR-18-2523

Wilson, A.J., Stubbs, M., Liu, P., Ruggeri, B., Khabele, D., 2018. The BET inhibitor INCB054329 reduces homologous recombination efficiency and augments PARP inhibitor activity in ovarian cancer. Gynecol. Oncol. 149, 575–584. https://doi.org/10.1016/j.ygyno.2018.03.049

Wilson, D.M., Seidman, M.M., 2010. A novel link to base excision repair? Trends Biochem. Sci. 35, 247–252. https://doi.org/10.1016/j.tibs.2010.01.003

Wilson, M.K., Pujade-Lauraine, E., Aoki, D., Mirza, M.R., Lorusso, D., Oza, A.M., du Bois, A., Vergote, I., Reuss, A., Bacon, M., Friedlander, M., Gallardo-Rincon, D., Joly, F., Chang, S.-J., Ferrero, A.M., Edmondson, R.J., Wimberger, P., Maenpaa, J., Gaffney, D., Zang, R., Okamoto, A., Stuart, G., Ochiai, K., participants of the Fifth Ovarian Cancer Consensus Conference, 2017. Fifth Ovarian Cancer Consensus Conference of the Gynecologic Cancer InterGroup: recurrent disease. Ann. Oncol. Off. J. Eur. Soc. Med. Oncol. 28, 727–732. https://doi.org/10.1093/annonc/mdw663

Wiltshaw, E., Kroner, T., 1976. Phase II study of cis-dichlorodiammineplatinum(II) (NSC-119875) in advanced adenocarcinoma of the ovary. Cancer Treat. Rep. 60, 55–60.

Wojtaszek, J.L., Chatterjee, N., Najeeb, J., Ramos, A., Lee, M., Bian, K., Xue, J.Y., Fenton, B.A., Park, H., Li, D., Hemann, M.T., Hong, J., Walker, G.C., Zhou, P., 2019. A Small Molecule Targeting Mutagenic Translesion Synthesis Improves Chemotherapy. Cell 178, 152-159.e11. https://doi.org/10.1016/j.cell.2019.05.028

Wright, W.D., Shah, S.S., Heyer, W.-D., 2018. Homologous recombination and the repair of DNA double-strand breaks. J. Biol. Chem. 293, 10524–10535. https://doi.org/10.1074/jbc.TM118.000372

Wu, R.-C., Wang, P., Lin, S.-F., Zhang, M., Song, Q., Chu, T., Wang, B.G., Kurman, R.J., Vang, R., Kinzler, K., Tomasetti, C., Jiao, Y., Shih, I.-M., Wang, T.-L., 2019. Genomic landscape and evolutionary trajectories of ovarian cancer precursor lesions. J. Pathol. 248, 41–50. https://doi.org/10.1002/path.5219

www.esmo.org/guidelines/gynaecological-cancers/newly-diagnosed-and-relapsed-epithelial-ovarian-carcinoma/eupdate-ovarian-cancer-treatment-recommendations [WWW Document], n.d.

Xu, G., Chapman, J.R., Brandsma, I., Yuan, J., Mistrik, M., Bouwman, P., Bartkova, J., Gogola, E., Warmerdam, D., Barazas, M., Jaspers, J.E., Watanabe, K., Pieterse, M., Kersbergen, A., Sol, W., Celie, P.H.N., Schouten, P.C., van den Broek, B., Salman, A., Nieuwland, M., de Rink, I., de Ronde, J., Jalink, K., Boulton, S.J., Chen, J., van Gent, D.C., Bartek, J., Jonkers, J., Borst, P., Rottenberg, S., 2015. REV7 counteracts DNA double-strand break resection and affects PARP inhibition. Nature 521, 541–544. https://doi.org/10.1038/nature14328

Yan, L., Shu-Ying, Y., Shan, K., Yip, B.H.K., Rong-Miao, Z., Na, W., Hai-Yan, S., 2012. Association between polymorphisms of ERCC1 and survival in epithelial ovarian cancer patients with chemotherapy. Pharmacogenomics 13, 419–427. https://doi.org/10.2217/pgs.11.181

Yu, T., MacPhail, S.H., Banáth, J.P., Klokov, D., Olive, P.L., 2006. Endogenous expression of phosphorylated histone H2AX in tumors in relation to DNA double-strand breaks and genomic instability. DNA Repair 5, 935–946. https://doi.org/10.1016/j.dnarep.2006.05.040

Zeppernick, F., Meinhold-Heerlein, I., 2014. The new FIGO staging system for ovarian, fallopian tube, and primary peritoneal cancer. Arch. Gynecol. Obstet. 290, 839–842. https://doi.org/10.1007/s00404-014-3364-8

Zhai, J., Shen, J., Xie, G., Wu, J., He, M., Gao, L., Zhang, Y., Yao, X., Shen, L., 2019. Cancer-associated fibroblasts-derived IL-8 mediates resistance to cisplatin in human gastric cancer. Cancer Lett. 454, 37–43. https://doi.org/10.1016/j.canlet.2019.04.002

Zhang, J., Shih, D.J.H., Lin, S.-Y., 2019. The Tale of CHD4 in DNA Damage Response and Chemotherapeutic Response. J. Cancer Res. Cell. Ther. 3.

Zhao, L., Washington, M.T., 2017. Translesion Synthesis: Insights into the Selection and Switching of DNA Polymerases. Genes 8. https://doi.org/10.3390/genes8010024

Zhao, M., Li, S., Zhou, L., Shen, Q., Zhu, H., Zhu, X., 2018. Prognostic values of excision repair cross-complementing genes mRNA expression in ovarian cancer patients. Life Sci. 194, 34–39. https://doi.org/10.1016/j.lfs.2017.12.018

Zhao, Y., Biertümpfel, C., Gregory, M.T., Hua, Y.-J., Hanaoka, F., Yang, W., 2012. Structural basis of human DNA polymerase η-mediated chemoresistance to cisplatin. Proc. Natl. Acad. Sci. U. S. A. 109, 7269–7274. https://doi.org/10.1073/pnas.1202681109

Zhou, J., Kang, Y., Chen, L., Wang, H., Liu, J., Zeng, S., Yu, L., 2020. The Drug-Resistance Mechanisms of Five Platinum-Based Antitumor Agents. Front. Pharmacol. 11, 343. https://doi.org/10.3389/fphar.2020.00343

Zimmermann, M., Lottersberger, F., Buonomo, S.B., Sfeir, A., de Lange, T., 2013. 53BP1 regulates DSB repair using Rif1 to control 5' end resection. Science 339, 700–704. https://doi.org/10.1126/science.1231573

Zoppoli, G., Regairaz, M., Leo, E., Reinhold, W.C., Varma, S., Ballestrero, A., Doroshow, J.H., Pommier, Y., 2012. Putative DNA/RNA helicase Schlafen-11 (SLFN11) sensitizes cancer cells to DNA-damaging agents. Proc. Natl. Acad. Sci. U. S. A. 109, 15030–15035. https://doi.org/10.1073/pnas.1205943109

7. APPENDIX

LIST OF PUBLICATIONS

Works by the candidate emanating from the work described in this thesis

Guffanti F, Alvisi MF, Caiola E, Ricci F, De Maglie M, Soldati S, Ganzinelli M, Decio A, Giavazzi R, Rulli E, Damia G. Impact of ERCC1, XPF and DNA Polymerase β Expression on Platinum Response in Patient-Derived Ovarian Cancer Xenografts. Cancers (Basel). 2020 Aug 24;12(9): E2398.

Guffanti F, Fratelli M, Ganzinelli M, Bolis M, Ricci F, Bizzaro F, Chilà R, Sina FP, Fruscio R, Lupia M, Cavallaro U, Cappelletti MR, Generali D, Giavazzi R, Damia G. Platinum sensitivity and DNA repair in a recently established panel of patient-derived ovarian carcinoma xenografts. Oncotarget. 2018 May 15;9(37):24707-24717.

Work not pertaining, or previous, to the work described in this thesis

Ricci F, Fratelli M, Guffanti F, Porcu L, Spriano F, Dell'Anna T, Fruscio R, Damia G. Patient-derived ovarian cancer xenografts re-growing after a cisplatinum treatment are less responsive to a second drug re-challenge: a new experimental setting to study response to therapy. Oncotarget. 2017 Jan 31;8(5):7441-7451.

Guffanti F, Fruscio R, Rulli E, Damia G. The impact of DNA damage response gene polymorphisms on therapeutic outcomes in late stage ovarian cancer. Sci Rep. 2016 Dec 1; 6:38142.

Ricci F, Bizzaro F, Cesca M, Guffanti F, Ganzinelli M, Decio A, Ghilardi C, Perego P, Fruscio R, Buda A, Milani R, Ostano P, Chiorino G, Bani MR, Damia G, Giavazzi R. Patient-derived ovarian tumor xenografts recapitulate human clinicopathology and genetic alterations. Cancer Res. 2014 Dec 1;74(23):6980-90.

Emmanouilidi A, Casari I, Gokcen Akkaya B, Maffucci T, Furic L, Guffanti F, Broggini M, Chen X, Maxuitenko YY, Keeton AB, Piazza GA, Linton KJ, Falasca M. Inhibition of the Lysophosphatidylinositol Transporter ABCC1 Reduces Prostate Cancer Cell

Growth and Sensitizes to Chemotherapy. Cancers (Basel). 2020 Jul 23;12(8): E2022.

Barilani M, Cherubini A, Peli V, Polveraccio F, Bollati V, Guffanti F, Del Gobbo A, Lavazza C, Giovanelli S, Elvassore N, Lazzari L. A circular RNA map for human induced pluripotent stem cells of foetal origin. EBioMedicine. 2020 Jul; 57:102848.

Caiola E, Iezzi A, Tomanelli M, Bonaldi E, Scagliotti A, Colombo M, Guffanti F, Micotti E, Garassino MC, Minoli L, Scanziani E, Broggini M, Marabese M. LKB1 Deficiency Renders NSCLC Cells Sensitive to ERK Inhibitors. J Thorac Oncol. 2020 Mar;15(3):360-370.

Ricci F, Guffanti F, Affatato R, Brunelli L, Roberta P, Fruscio R, Perego P, Bani MR, Chiorino G, Rinaldi A, Bertoni F, Fratelli M, Damia G. Establishment of patient-derived tumor xenograft models of mucinous ovarian cancer. Am J Cancer Res. 2020 Feb 1;10(2):572-580.

Cisse O, Quraishi M, Gulluni F, Guffanti F, Mavrommati I, Suthanthirakumaran M, Oh LCR, Schlatter JN, Sarvananthan A, Broggini M, Hirsch E, Falasca M, Maffucci T. Downregulation of class II phosphoinositide 3-kinase PI3K-C2β delays cell division and potentiates the effect of docetaxel on cancer cell growth. J Exp Clin Cancer Res. 2019 Nov 21;38(1):472.

Ricci F, Guffanti F, Damia G, Broggini M. Combination of paclitaxel, bevacizumab and MEK162 in second line treatment in platinum-relapsing patient derived ovarian cancer xenografts. Mol Cancer. 2017 May 30;16(1):97.

Guffanti F, Chilà R, Bello E, Zucchetti M, Zangarini M, Ceriani L, Ferrari M, Lupi M, Jacquet-Bescond A, Burbridge MF, Pierrat MJ, Damia G. In Vitro and In Vivo Activity of Lucitanib in FGFR1/2 Amplified or Mutated Cancer Models. Neoplasia. 2017 Jan;19(1):35-42.

Chilà R, Guffanti F, Damia G. Role and therapeutic potential of CDK12 in human cancers. Cancer Treat Rev. 2016 Nov; 50:83-88. doi: 10.1016/j.ctrv.2016.09.003.

Rulli E, Guffanti F, Caiola E, Ganzinelli M, Damia G, Garassino MC, Piva S, Ceppi L, Broggini M, Marabese M. The 5'UTR variant of ERCC5 fails to influence outcomes in

ovarian and lung cancer patients undergoing treatment with platinum-based drugs. Sci Rep. 2016 Dec 14; 6:39217.

Pinessi D, Ostano P, Borsotti P, Bello E, Guffanti F, Bizzaro F, Frapolli R, Bani MR, Chiorino G, Taraboletti G, Resovi A. Expression of thrombospondin-1 by tumor cells in patient-derived ovarian carcinoma xenografts. Connect Tissue Res. 2015;56(5):355-63.

Chilà R, Basana A, Lupi M, Guffanti F, Gaudio E, Rinaldi A, Cascione L, Restelli V, Tarantelli C, Bertoni F, Damia G, Carrassa L. Combined inhibition of Chk1 and Wee1 as a new therapeutic strategy for mantle cell lymphoma. Oncotarget. 2015 Feb 20;6(5):3394-408.

Abbreviations

53BP1	TP53 binding protein 1
ΔVt %	% tumour volume change
γH2AX	Gamma H2A Histone Family Member X
ABCB	ATP-binding cassette membrane transporters
APT	Atypical precursor lesion
ANOVA	Analysis of variance
ATM	Ataxia Telangiectasia kinase
ATR	Ataxia Telangiectasia and Rad3-related protein
BCL2	B-Cell Lymphoma2
bp	Base pairs
BER	Base Excision Repair
BRCA1/2	Breast Cancer-Associated protein 1/2
BW	Body weight
CA125	Cancer antigen 125
CAF	Cancer associated fibroblast
CCC	Clear cell carcinoma
CCNE1	Cyclin E1
CDK	Cyclin-dependent-kinase
CDK12	Cyclin Dependent Kinase 12
cfDNA	circulating free DNA
CGH	Complementary genomic hybridization
CI	Confidence interval
CIC	Cortical inclusion cyst
CNV	Copy number variations
CSC	Cancer stem cell
Ct	Threshold cycle

CTR1	Copper Transport 1
DAPI	4',6-DiAmidino-2-PhenylIndole
DDB	DNA damage-binding protein
DDP	Cisplatin
DDR	DNA damage response
DNA-PK	DNA-dependent Protein Kinase
DNMT	DNA methyltransferases
DSB	Double-strand break
EC	Endometrioid carcinoma
EMA	European Medicines Agency
EMSY	EMSY Transcriptional Repressor, BRCA2 Interacting
EMT	Epithelial to Mesenchymal Transition
EOC	Epithelial Ovarian Cancer
ERCC1	Excision repair cross-complementation group 1
FA	Fanconi anemia
FDA	United States Food and Drug Administration
FFPE	Formalin fixed paraffin embedded
FITC	Fluorescein isothiocyanate
GFP	Green fluorescent protein
GGR	Global genome repair pathway
GOG	Gynaecologic Oncology Group
GSH	Glutathione
GST	Glutathione-S-transferase
GTP	Guanosine-5'-triphosphate
HBOC	Hereditary Breast and Ovarian Cancer syndrome
HGEOC	High grade endometrioid ovarian carcinoma
HGOC	High grade ovarian cancer

HGSC	High-grade serous carcinoma
HRD	Homologous Recombination Deficiency
HRP	Horseradish peroxidase
hrs	Hours
H/E	Hematoxylin/eosin
HR	Homologous Recombination
HSP90	Heat Shock Protein 90
HzR	Hazard ratio
IC50	Concentration inhibiting the growth by 50%
ICL	Inter strand crosslink
IDS	Interval debulking surgery
IHC	Immunohistochemistry
IF	Immunofluorescence
i.p.	Intraperitoneal
ILS	Increase in life span
i.v.	Intravenously
JNK	c-Jun N-terminal Kinase
KRAS	Kirsten Rat Sarcoma
KU70	X-Ray Repair Cross Complementing 6
KU80	X-Ray Repair Cross Complementing 5
LGSC	Low-grade serous carcinoma
LOH	Loss of heterozygosity
LSAB	Labelled streptavidin-biotin
LST	Large scale transition
M	Methylated
MAPK	Mitogen-Activated Protein Kinase
MDR1	Multi drug resistance 1

MLH1	MutL Homolog 1
MMEJ	Micro-Homology-Mediated End Joining
MMR	Mismatch Repair
MRN	MRE11, RAD50 and NSB1 complex
MS-PCR	Methylation-specific polymerase chain reaction
mRECIST	Modified Response Evaluation Criteria in Solid Tumours
MRP	Multidrug Resistance-associated Protein
MT	Metallothionein
MUT	Mutation/mutated
NACT	Neoadjuvant chemotherapy
NER	Nucleotide Excision Repair
NF1	Neurofibromin 1
NHEJ	Non-Homologous End Joining
NGS	Next generation sequencing
OGG1	8-oxoguanine DNA glycosylase
ORR	Objective response rate
OS	Overall survival
OSE	Ovarian surface epithelium
PALB2	Partner and Localizer of BRCA2
PARG	Poly (ADP-ribose) glycohydrolase
PARP	Poly (ADP-ribose) polymerase
PARPi	PARP inhibitor
PBS	Phosphate buffer saline
PCNA	Proliferating cell nuclear antigen protein
PCR	Polymerase chain reaction
PDX	Patient-derived xenograft
PFI	Progression free interval or platinum free interval

PFS	Progression free survival
PI3Kα	Phosphatidyl inositol 3-kinase α
POLB	DNA polymerase β
POLH	Polymerase η
PLA	Proximity ligation assay
PTEN	Phosphatase and Tensin Homolog
RAD51	BRCA1/BRCA2-Containing Complex, Subunit 5
RB1	Retino-blastoma protein 1
RF	Replication fork
RFC	Replication factor C
ROC	Recurrent ovarian cancer
ROS	Reactive oxygen species
RPA	Replication protein A
RT	Residual tumour
RT-PCR	Real time polymerase chain reaction
s.c.	Subcutaneous
SCLC	Small cell lung cancer
SD	Standard deviation
SHLD	Shieldin complex
SLFN11	Shlafen protein 11
SNP	Single nucleotide polymorphisms
SSA	Single-strand annealing
SSB	Single-strand break
STIC	Serous tubal intra-epithelium cancer
STR	Short tandem repeat
SV	Structural variants

TAI	Telomeric allelic imbalance
TAM	Tumour associated macrophage
TBS	Tris buffer saline
TCGA	The Cancer Genome Atlas network
TCR	Transcription coupled repair pathway
TFI	Treatment free interval
TIC	Tubal intra-epithelium cancer
TLS	Translesion synthesis
TME	Tumour microenvironment
TVS	Transvaginal sonography
TW	Tumour weight
T/C	Treated over control ratio OR tumour growth inhibition
U	Unmethylated
UV	Ultra-violet
VEGF	Vascular endothelial growth factor
VEGFR	Vascular endothelial growth factor receptor
VUS	Variants of uncertain significance
WES	Whole exome sequencing
WGS	Whole genome sequencing
WT	Wild type
XP	Xeroderma Pigmentosum
XPA	Xeroderma Pigmentosum complementation group A
XPD	Xeroderma Pigmentosum complementation group D
XPF	Xeroderma Pigmentosum complementation group F
XPG	Xeroderma Pigmentosum complementation group G